Personalising Immunotherapy in Early and Advanced Stage Melanoma

A thesis submitted to the University of Manchester for the degree of Doctor of Medicine in the Faculty of Biology, Medicine and Health.

2022

Zena Salih

School of Medical Sciences
Division of Cancer Sciences

Table of Contents

Word Count: 52,576

List of Abbreviations

Ab	Antibody
AE	Adverse event
AJCC	American Joint Committee on Cancer
ALC	Absolute lymphocyte count
ANA	Antinuclear antibody
ANC	Absolute neutrophil count
APC	Antigen presenting cell
BRCA-1	BReast CAncer gene 1
C	Constant
CCL3	C-C Motif Chemokine Ligand 3
CCR3	C-C Motif Chemokine Receptor 3
CCR7	C-C Chemokine Receptor Type 7
CD	Cluster of differentiation
CDR 1-3	Complementarity-determining regions 1-3
CEACAM	Carcinoembryonic antigen-related cell adhesion molecule
CfDNA	Cell free DNA
CI	Confidence interval
CLND	Completion lymph node dissection
CML	Chronic myeloid leukaemia
CNS	Central nervous system
CODEX	Co-detection by indexing
CR	Complete response
CRP	C reactive protein
CRUK MI	Cancer Research UK Manchester Institute
CT	Computerised tomography
CTC	Circulating tumour cells
CTCAE	Common terminology criteria for adverse events
CtDNA	Circulating tumour DNA
CTLA4	Cytotoxic T Lymphocyte Antigen-4
CyTOF	Cytometry by time of flight
D	Diverse
DC	Disease control
DC	Dendritic Cells
ddPCR	Droplet digital polymerase-chain reaction
DeCOG-SLT	Dermatologic Cooperative Oncology Group-selective lymphadenectomy
DFS	Disease free survival
DMFS	Distant metastasis free survival
DMSO	Dimethyl Sulfoxide
DN	Double negative
DNA	Deoxyribonucleic acid
DP	Double positive
DTIC	Dacarbazine
ECOG	Eastern Cooperative Oncology Group
EDTA	Ethylenediaminetetraacetic Acid
EMA	European Medicines Agency
ETE	Early thymic emigrant
ETP	Early thymic progenitor

FACS	Fluorescence-activated cell sorting
FAMM	Familial atypical multiple mole melanoma
FBS	Foetal bovine serum
FDA	Food and Drug Administration
FFPE	Formalin fixed paraffin embedded
FITC	Fluorescein Isothiocyanate
FMO	Fluorescence Minus One
FSC	Forward Scattered Light
G	Grade
GCP	Good Clinical Practice
GEP	Gene expression profiling
GNAL	guanine nucleotide-binding protein G(olf) subunit alpha
GP-100	Glycoprotein 100
H	Hours
HD	Healthy donor
HNSCC	Head and neck squamous cell carcinoma
HLA	Human Leucocyte Antigen
HLA-DR	Human Leucocyte Antigen – DR isotype
HR	Hazard ratio
HSC	Haematopoietic stem cells
ICB	Immune checkpoint blockade
IFNγ	Interferon gamma
IHC	Immunohistochemistry
IDO1	Indoleamine 2,3-dioxygenase 1
I+N	Ipilimumab + Nivolumab
ITT	Intention to treat
IL	Interleukin
irAE	Immune related adverse event
ITM	In-transit metastases
ITM2B	Integral membrane protein 2B
IV	Intravenous
J	Joining
LAG-3	Lymphocyte activating gene 3
LD	Longest diameter
LDH	Lactate dehydrogenase
LN	Lymph node
MAPK	Mitogen activated protein kinase
MCRC	Manchester Cancer Research Centre
MDSC	Myeloid derived suppressor cell
MHC	Major Histocompatibility Complex
Min	Minutes
MiRNA	Micro RNA
MRD	Minimal residual disease
MRI	Magnetic resonance imaging
mRNA	Messenger ribonucleic acid
MSLT	Multicentre Selective Lymphadenectomy Trial
MSS	Melanoma specific survival

n/N	Number of patients
NGS	Next generation sequencing
NK	Natural killer cells
NKT	Natural killer T cells
NLR	Neutrophil to Lymphocyte Ratio
ns	not significant
NSCLC	Non-small cell lung cancer
N/A	Not applicable or not assessed
ORR	Objective Response Rate
OS	Overall Survival
PBMC	Peripheral Blood Mononuclear Cells
PBS	Phosphate Buffered Saline
pCR	Pathological Complete Response
PCR	Polymerase chain reaction
PD	Progressive disease
PD-1	Programmed Death protein 1
PD-L1	Programmed Death Ligand 1
PD-L2	Programmed Death Ligand 2
PE	Phycoerythrin
PE-Cy7	Phycoerythrin-Cyanine 7
PET	Positron emission tomography
PFA	Paraformaldehyde
PFS	Progression Free Survival
PR	Partial Response
PS	Performance status
PTGS2	Prostaglandin-Endoperoxide Synthase 2
QC	Quality control
RAG 1 + 2	Recombination-activating genes 1 + 2
RBC	Red Blood Cell
RECIST	Response evaluation criteria in solid tumours
RES	Rearrangement efficiency score
RF	Rheumatoid factor
RFS	Relapse free survival
RNA	Ribonucleic acid
RPMI	Roswell Park Memorial Institute
RR	Response rate
RSS	Recombination signal sequence
RT	Room temperature
SD	Stable disease
SD	Standard Deviation
SE	Standard Error
Sec	Seconds
SLNB	Sentinel lymph node biopsy
SSC	Side Scattered Light
TCM	Central Memory T cell
TEFF	Effector T cell
TEM	Effector Memory T cell
Th	T helper cell
T_{IE}	Immune effector T cell

T_N	Naïve T cell
T_{ex}	Exhausted phenotype CD8+ T cells
TCR	T Cell Receptor
TCGA	The Cancer Genome Atlas
TET	Thymic epithelial tumour
TG	Thyroglobulin
Th	T helper cell
TIL	Tumour Infiltrating Lymphocyte
TMB	Tumour mutational burden
TME	Tumour microenvironment
TNBC	Triple negative breast cancer
TNF	Tumour necrosis factor
TNFα	Tumour necrosis factor alpha
TNM	Tumour node metastasis
TPO	Thyroid peroxidase
Treg	T regulatory cell
t-SNE	t-distributed stochastic neighbour embedding
T0	Baseline pre-treatment
TVEC	Talimogene laherparepvec
ULN	Upper limit of normal
UMI	Unique molecular index
USS	Ultrasound scan
UVB	Ultraviolet B
UVR	Ultraviolet radiation
V	Variable
VEGF	Vascular Endothelial Growth Factor
Vs	Versus
WCC	White cell count
WLE	Wide local excision
WT	Wild-type
W3	Week 3
W6	Week 6
W9	Week 9
W12	Week 12
μ	Micro

Abstract

Introduction: Melanoma is a paradigm of how the treatment landscape can be revolutionised over a decade. The advent of immune checkpoint blockade (ICB) has dramatically improved the outcomes of patients with both early and advanced stage disease. Nevertheless, patients are still dying of their disease, highlighting the urgent need to identify which patients will respond to therapy, in order to improve patient stratification and avoid unnecessary toxicity risk. Thus, precision immuno-oncology approaches are required to improve cancer care. Therapy decisions need to be made based on patient-specific immunological signatures, but clinically validated biomarkers for this purpose are currently lacking. The primary aim of this work was to explore liquid biopsy as a minimally invasive approach to investigate peripheral T cell evolution early on treatment as a potential predictive biomarker of response to immunotherapy in melanoma. Additionally, the impact of patient clinical variables on peripheral T cell and T cell receptor (TCR) repertoire evolution under the selective pressure of ICB in advanced melanoma was investigated.

Methods: To assess the peripheral T cell compartment of metastatic melanoma patients undergoing first line anti-PD1 based ICB treatment, peripheral blood samples were taken prior to and early on treatment then analysed by flow cytometry. Phenotypic assessment of peripheral T cells and TCR sequencing data were used to correlate changes in peripheral T cell subset dynamics and TCR repertoire to patient clinical variables before treatment (T0) and after the first cycle of ICB at week 3 (W3). A prospective study was set up to investigate whether changes in peripheral T cells early on adjuvant ICB therapy can predict patient response in stage III melanoma.

Results: Flow cytometry revealed expansion of a subset of CD8+ memory immune effector cytotoxic T cells in peripheral blood. At W3 after therapy initiation, expansion of these cells was significantly greater in patients that responded to ICB. An increase of 0.8% in the ratio of this subset of T cells relative to all CD8+ memory cells at W3 was associated with improved survival and separated 6-month responders from non-responders; this was confirmed in a separate validation cohort. Analysis from later W9 treatment time point revealed the presence of the T cell subset, however there was no longer a correlation with response, highlighting the dynamic nature of the immune signature and indicating that these changes occur early and are transient. Evaluation of whether changes in W3 T cell subset expansion were associated with immune related adverse events revealed no correlation between T cell subset expansion and grade of toxicity, suggesting that these cells are not a predictive marker of immunotherapy toxicity in this setting. Notably, expansion of a separate regulatory T cell subset did correlate with grade of toxicity. Investigation of clinical variables associated with the immune signature demonstrated a correlation between the immune effector T cell subset abundance and age at T0 ($r=0.40$), which reduced following treatment at W3 ($r=0.07$). However, at W3 two significantly opposing patterns ($p=0.03$) of TCR repertoire rearrangement were observed in patients who responded to treatment, with patients ≥70 years of age showing an increase in TCR clonality and patients <70 years of age showing an increase in TCR diversity.

Conclusion: This work has identified a peripheral blood early immune signature characterised by turnover of a specific subset of immune effector T cells. The magnitude of immune signature changes following the first cycle of ICB therapy anticipated which patients would go on to respond and ultimately correlated with overall survival. Additionally, a regulatory T cell subset demonstrated a correlation with toxicity grade. Furthermore, investigation of the clinical correlates associated with the immune signature identified a model whereby age does not affect peripheral immune effector T cell subset expansion in response to ICB, but does influence immunotherapy-induced peripheral TCR repertoire evolution. Thus, T cell repertoire analysis should be contextualised by patient age. Finally, the prospective study to assess the feasibility of translating the immune signature findings into the adjuvant setting to identify patients at high risk of relapse and predict response to ICB therapy in stage III melanoma remains undoubtedly clinically relevant.

Declaration

No portion of the work referred to in the thesis has been submitted in support of an application for another degree or qualification of this or any other university or other institute of learning.

Copyright Statement

i. The author of this thesis (including any appendices and/or schedules to this thesis) owns certain copyright or related rights in it (the "Copyright") and s/he has given the University of Manchester certain rights to use such Copyright, including for administrative purposes.

ii. Copies of this thesis, either in full or in extracts and whether in hard or electronic copy, may be made only in accordance with the Copyright, Designs and Patents Act 1988 (as amended) and regulations issued under it or, where appropriate, in accordance with licensing agreements which the University has from time to time. This page must form part of any such copies made.

iii. The ownership of certain Copyright, patents, designs, trademarks and other intellectual property (the "Intellectual Property") and any reproductions of copyright works in the thesis, for example graphs and tables ("Reproductions"), which may be described in this thesis, may not be owned by the author and may be owned by third parties. Such Intellectual Property and Reproductions cannot and must not be made available for use without the prior written permission of the owner(s) of the relevant Intellectual Property and/or Reproductions.

iv. Further information on the conditions under which disclosure, publication and commercialisation of this thesis, the Copyright and any Intellectual Property and/or Reproductions described in it may take place is available in the University IP Policy (see http://documents.manchester.ac.uk/DocuInfo.aspx?DocID=2442 0), in any relevant Thesis restriction declarations deposited in the University Library, the University Library's regulations (see http://www.library.manchester.ac.uk/about/regulations/) and in the University's policy on Presentation of Theses.

Acknowledgements

Firstly, I would like to thank my supervisors Professor Richard Marais, Professor Paul Lorigan, Dr Nathalie Dhomen, Dr Elaine Kilgour and Dr Sara Valpione for giving me the opportunity to conduct this research and for your invaluable guidance and support whilst completing this MD. This is especially true during the COVID-19 pandemic, you helped me to see that any challenge could be turned into an opportunity.

To my dear friend, mentor and supervisor Sara, thank you for being patient with me whilst I navigated my way in the world of science and research. I have learnt so much from you and you have given me an amazing foundation of knowledge on which to build my future career.

A big thanks to everyone in the molecular oncology group, past and present who helped guide, teach and support me through my laboratory work. You all made an alien world infinitely friendlier and more understandable for me. In particular, a special thanks must go to my two fantastic friends that I was lucky enough to meet in the lab, Franzi and Denys – I do not know how I would have kept going without you. Thank you for your friendship, teaching and moral support.

Collaboration with the MCRC biobank, CRUK MI core facilities (particularly flow cytometry and Antonia Banyard), CRUK MI Cancer Biomarker Centre and The Christie Melanoma Clinical Research team has facilitated this MD, thank you all for your support.

Thanks to my funders NIHR Biomedical Research Centre, without you I would not have been able to do this work. I would also like to thank all of the patients who have generously donated their samples to my research, I have learnt so much from your exceptional gift.

Finally, and most importantly, I am incredibly grateful for all of the love and encouragement I have received from my family and friends (and my wonderful dog Boo, who sat with me over countless hours writing this thesis). You have always been there for me and built me up whenever times have been tough, I could not have completed this at times, seemingly insurmountable project without you. Thank you for always believing I could do it!

Chapter 1: Introduction

1.1 Cutaneous Melanoma

Melanoma is a cancer of melanocytes, cells that produce melanin, the pigment that determines skin tone. Cutaneous melanoma is a type of skin cancer that develops when there is malignant transformation of melanocytes that leads to uncontrolled proliferation of and invasion by these cells. Melanoma can start in a pre-existing mole, in a new pigmented skin lesion or even in normal appearing skin. Cutaneous melanoma comprises a relatively small proportion of all skin cancers, approximately 4%, but it accounts for the majority, 80%, of skin cancer related deaths[1,2], due to its ability to rapidly spread to other organs if not identified and treated early.

1.1.1 incidence and prevalence

The incidence of cutaneous melanoma is rising, both in the UK and worldwide. Worldwide, it accounts for 232,100 newly diagnosed cases and 55,000 deaths each year[3]. In the UK, cutaneous melanoma is the 5th most common cancer, with 16,200 people diagnosed each year, that is 44 new cases every day[4]. Despite it being common, mortality remains lower than other cancers, this is likely due to the majority of patients presenting with early stage disease that is easily resected. With increasing incidence, mortality rates have also risen, albeit at a slower rate, likely due to earlier detection and improvements in treatment modalities. At present, there are approximately 2,300 melanoma skin cancer deaths in the UK each year, equating to more than 6 deaths per day[4]. Clinical outcomes are known to correlate with disease stage at time of diagnosis[5]. Prompt detection can result in a good chance of long-term survival and even cure, particularly for those with earlier stage disease.

1.1.2 Risk factors

There are several risk factors that can contribute to the risk of acquiring melanoma, these include environmental and genetic factors. Cutaneous melanoma can occur at any age, although risk increases with advancing age; in the UK more than 25% of those diagnosed are aged 75 and above[6]. However, it is important to note that younger people can also develop

melanoma and it is the second most common cancer in individuals below 50 years of age[6]. Ultraviolet radiation (UVR) exposure, in particular ultraviolet B (UVB) radiation, is the main environmental risk factor for development of cutaneous melanoma and it is also the most modifiable[7,8,9]. UVR comes from the sun or sunbeds and in the UK, 85% of melanomas are caused by over exposure to UVR. The risk increases with increasing episodes of sunburn at any age. Intermittent sun exposure is associated with higher risk than regular sun exposure[6]. Notably, preclinical studies have highlighted that the use of sunscreen during intermittent sun exposure helps delay, but does not prevent melanomagenesis[8]. Individuals that have used sunbeds prior to age 30, have a 75% higher chance of being diagnosed with cutaneous melanoma compared to those with no exposure to artificial UVR[10].

Skin tone also plays a role, with fair skinned, white populations at higher risk[11]. Other host factors contributing to increased risk include, a personal[12] or family history[13] of melanoma and presence of moles, such as melanocytic or dysplastic naevi, in particular in the context of atypical mole syndrome[14]. Those with a previous non-melanoma skin cancer are 3 times more likely than the general population to develop melanoma[6]. Inherited genetic alterations are also important to consider in the susceptibility to melanoma development. These include mutations in *MC1R* (gene regulating pigment production), loss of *CDKN2A* (cell cycle control gene alteration observed in patients with familial atypical multiple mole melanoma, FAMM) or mutations in DNA repair genes *XPC* (genes in nucleotide excision repair pathway, frequently mutated in xeroderma pigmentosum patients).

1.1.3 Diagnosis, staging and risk assessment

Diagnosis should be based on a full thickness excisional biopsy. The histology report should note tumour, node, metastasis (TNM) classification and include: the maximum thickness in millimetres (Breslow) reported to the nearest 0.1 mm, presence of ulceration and clearance of the surgical margins. Melanoma is staged using the American Joint Committee on Cancer (AJCC) staging system and incorporates: primary tumour thickness, presence or absence of ulceration, lymph node involvement, regional and distant metastasis[15]. Accurate staging is vitally important to facilitate optimal use of effective therapies and adequately inform patients about their prognosis and treatment options. In patients with stage IV disease, elevated lactate dehydrogenase (LDH) and brain metastases have been shown to be independent poor prognostic factors[16,17]. Disease presentation at diagnosis will determine further staging and risk assessment procedures. Physical examination should focus on suspicious pigmented lesions, tumour satellites, in-transit metastases (ITM), regional lymph node (LN) and systemic

metastases. In low-risk melanomas (pT1a), no further assessment is required. However, in pT1b – pT4b further investigations in the form of ultrasound scan (USS) for locoregional LN metastasis and/or computed tomography (CT) or positron emission tomography (PET) scans as well as magnetic resonance imaging (MRI) of the brain may be performed to assess for tumour extension prior to surgical treatment and sentinel lymph node biopsy (SLNB). MRI head and PET CT/CT scans should be performed at baseline and as part of follow up protocol only for very high-risk patients (pT3b and higher)[18]. Table 1.1 and Table 1.2 illustrate the pathological and clinical melanoma staging groups respectively. Table 1.3 outlines the definition of distant metastasis and within Appendix A is the full AJCC TNM eighth edition staging system for melanoma[15].

Table 1.1 AJCC 8th edition melanoma pathological stage groups (adapted from Gershenwald et al[15]).

Tumour (T)	Lymph Node (N)	Metastasis (M)	Pathological stage group
Tis	N0	M0	0
T1a	N0	M0	IA
T1b	N0	M0	IA
T2a	N0	M0	IB
T2b	N0	M0	IIA
T3a	N0	M0	IIA
T3b	N0	M0	IIB
T4a	N0	M0	IIB
T4b	N0	M0	IIC
T0	N1b, N1c	M0	IIIB
T0	N2b, N2c, N3b or N3c	M0	IIIC
T1a/b-T2a	N1a or N2a	M0	IIIA
T1a/b-T2a	N1b/c or N2b	M0	IIIB
T2b/T3a	N1a-N2b	M0	IIIB
T1a-T3a	N2c or N3a/b/c	M0	IIIC
T3b/T4a	Any N ≥N1	M0	IIIC
T4b	N1a-N2c	M0	IIIC
T4b	N3a/b/c	M0	IIID
Any T, Tis	Any N	M1	IV

Table 1.2 AJCC 8th edition melanoma clinical stage groups (adapted from Gershenwald et al[15]).

Tumour (T)	Lymph Node (N)	Metastasis (M)	Clinical stage group
Tis	N0	M0	0
T1a	N0	M0	IA
T1b	N0	M0	IB
T2a	N0	M0	IB
T2b	N0	M0	IIA
T3a	N0	M0	IIA
T3b	N0	M0	IIB
T4a	N0	M0	IIB
T4b	N0	M0	IIC
Any T, Tis	≥N1	M0	III
Any T	Any N	M1	IV

Table 1.3 Definition of distant metastasis (adapted from Gershenwald et al[15]).

Metastasis (M)	Anatomic site	LDH level
M0	No evidence of distant metastasis	N/A
M1	Evidence of distant metastasis	
M1a	Distant metastasis to skin, soft tissue, muscle, non-regional lymph node	Not recorded or unspecified
M1a (0)		Not elevated
M1a (1)		Elevated
M1b	Distant metastasis to lung +/- M1a sites of disease	Not recorded or unspecified
M1b (0)		Not elevated
M1b (1)		Elevated
M1c	Distant metastasis to non-CNS visceral sites +/- M1a or M1b sites of disease	Not recorded or unspecified
M1c (0)		Not elevated
M1c (1)		Elevated
M1d	Distant metastasis to CNS +/- M1a, M1b or M1c sites of disease	Not recorded or unspecified
M1d (0)		Not elevated
M1d (1)		Elevated

N/A= not applicable, CNS= central nervous system

1.1.4 Management of local disease

Surgery is the mainstay of treatment and is often curative for localised, early stage primary cutaneous melanoma that has not spread. Patients with 'high risk' disease require close clinical follow up[19]. Surgery is in the form of wide local excision (WLE) and Breslow thickness will determine the extent of the excision margin. A safety margin of 0.5 cm for in situ melanomas, 1 cm for tumours with a thickness of up to 2 mm and 2 cm for thicker tumours is recommended[18].

1.1.5 Management of locoregional disease

There is no proven survival advantage from pursuing elective lymph node dissection, so it is not recommended[3]. SLNB is advised for accurate staging in melanoma where tumour thickness is >0.8mm (pT1b or higher) or in those <0.8mm with ulceration[18]. The Multicentre Selective Lymphadenectomy Trial I (MSLT-I) confirmed that important staging information is obtained from SLNB, however it did not show any survival benefit for this procedure compared to nodal observation in the 10 year follow up[20]. Therefore, SLNB should not be considered as a therapeutic option. Completion lymph node dissection (CLND) for patients with a positive sentinel node was standard of care until 2018. The results of the MSLT-I trial led to a further two studies, MSLT-II and the German Dermatologic Cooperative Oncology Group-selective lymphadenectomy (DeCOG-SLT) trials which were conducted to explore the value of routine CLND in sentinel node positive melanoma. Both studies revealed no increased survival benefit from immediate CLND compared to nodal observation alone[21,22]. However, CLND does offer further staging information, as approximately 20% of sentinel node positive patients have additional non-sentinel node involvement; despite this upstaging is uncommon at approximately 6% of cases[18]. Therefore, given the morbidity associated with routine CLND, it is no longer recommended practice. However, therapeutic lymph node dissection is deemed standard of care for patients with clinically detected, macroscopic, non-sentinel node isolated locoregional disease[3]. Prior to surgery, full staging investigations including high resolution CT/PET scan and MRI are required to exclude distant metastases. Evidence of metastatic disease would rule out surgery and patients would be considered for systemic therapy.

1.1.6 Molecular characterisation

Cutaneous melanomas exhibit a higher mutation load compared to nearly all other cancers[23,24]. This is most likely due to the substantial number of somatic mutations generated by UVR exposure[25]. Based on the analysis of all mutations in The Cancer Genome Atlas (TCGA), cutaneous melanoma can broadly be divided into four major subclasses: *BRAF* mutant, *NRAS* mutant, *NF1* mutant or triple wild type (WT)[26]. Approximately 40-50% of patients diagnosed with melanoma harbour a mutation in *BRAF*, with the V600E somatic mutation being the most common[27]. Approximately 28% of melanomas have a mutation in *NRAS* and 14% have mutations in *NF1*[28]. Other genes such as *KIT*, *CCND1* and *TERT* are also frequently altered in triple WT melanomas[29].

Testing for actionable mutations is advisable in patients with resectable or unresectable stage III/IV disease or high risk resected stage IIC disease, but not in stage I or stage IIA–IIB disease[18]. BRAF testing is compulsory, as it is the most clinically relevant, given the approval of BRAF inhibitors within the treatment paradigm. Although at present no approved targeted therapy options exist for the other drivers, they are important to identify for future opportunities and to aid patient selection for clinical trials. More recently, clinically validated next-generation sequencing (NGS) panels covering all key oncogenic drivers are increasingly being used to investigate the mutational landscape in melanoma.

1.2 Melanoma and the immune system

There are three key means by which the immune system prevents tumour formation within the host: (1) eradicating or halting viral infections that could otherwise lead to formation of virus induced tumours,[30] (2) promptly eliminating pathogens and resolving inflammation, preventing a chronic inflammatory state favourable for tumourignesis,[31] (3) constant surveillance of host tissues for transformed cells and when identified they are removed before they can cause harm, this is known as the cancer immune-surveillance hypothesis[32]. However, tumours can still form in the presence of a functioning immune system and so this hypothesis has been updated to include mechanisms of tumour equilibrium and escape.

Following oncogenic transformation, malignant cells undergo either recognition and elimination by the immune system, or immune equilibrium. In the equilibrium phase, tumour cells become less immunogenic due to immunoediting and are more resistant to immune cell attack. Subsequently, tumour microenvironment (TME) remodelling leads to formation of further mechanisms of immune evasion allowing the malignant cells to expand and escape immunological control, leading to a clinically detectable tumour. These steps are referred to as the immunoediting hypothesis[33] and are depicted in Figure 1.1.

The immune system has evolved to safeguard the host from a wide range of pathogenic threats and imperative to its role in mobilising a response to an invading pathogen is the ability to distinguish between self and non-self antigens[34]. The mechanisms that regulate this process and result in eradication of the threat can be divided into innate and adaptive immunity. Innate immunity encompasses all aspects of immune defence mechanisms, is non-specific i.e. does not activate against particular antigens and is vital in the initial response to an attack on the host. The innate system includes physical epithelial barriers, soluble proteins and small molecules that are either continually present or secreted from cells when activated. The main cellular components are natural killer (NK) cells, natural killer T (NKT) cells, γδ T cells and the antigen presenting cells (APCs): dendritic cells (DC) and macrophages[35]. The innate system promotes anti-tumour responses both directly and indirectly by supporting cytotoxic T cell function. By contrast, the adaptive immune system responds to specific antigenic targets. These responses are a result of antigen specific receptors on the surface of B and T lymphocytes[36]. Melanoma is considered highly immunogenic and is capable of activating the adaptive immune response.

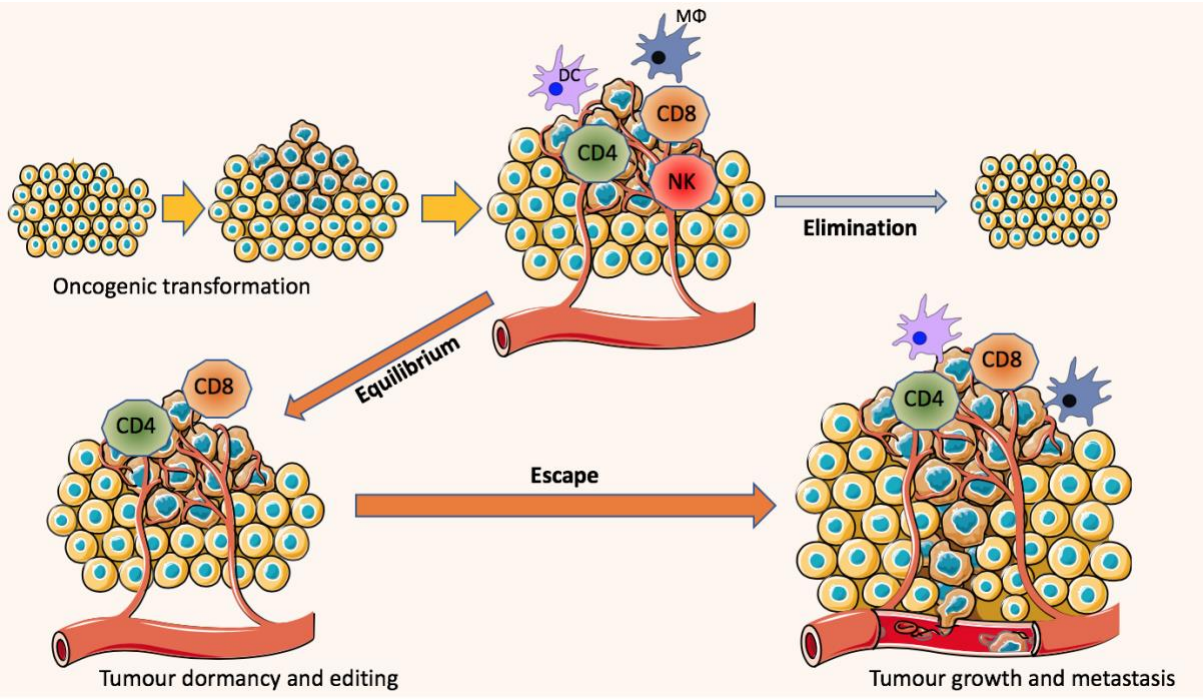

Figure 1.1 Immunoediting hypothesis
The immune system is able to recognise and kill oncogenically transformed cells; this initial phase is known as tumour elimination which results in tumour suppression. However, over time tumour cells are able to first enter a phase of equilibrium by developing mechanisms of immune evasion, resulting in dormancy and then subsequently tumour escape leading to tumour growth and metastasis. Adapted from Cancer Immunosurveillance and Immunoediting: The Roles of Immunity in Suppressing Tumour Development and Shaping Tumour Immunogenicity, by Smyth et al [33].

1.2.1 Immunomodulation and checkpoint blockade

The immune system plays a role in protecting from disease. The T cells of the immune system are able to recognise and kill pathogens, including cancer cells by eliciting a coordinated immune response including innate and adaptive responses. Activated T cells are primary mediators of immune effector functions and as such, they express multiple co-inhibitory receptors such as programmed death 1 (PD-1) and cytotoxic T-lymphocyte-associated protein 4 (CTLA-4)[37]. The CTLA-4 and PD-1 pathways act at different stages of the immune response. PD-1 is recognised to primarily inhibit T cells in the effector phase of a response, in contrast to CTLA-4, which is known to be more important in the early phases of T cell activation. Figure 1.2 demonstrates the co-activatory and inhibitory pathways that have been recognised to regulate T cell function, the so-called immune checkpoint pathways. These immune checkpoint molecules are involved in regulating immune homeostasis and cancer cells are able to exploit these immune checkpoints as a way of evading immune detection and elimination. Tumours can activate suppressive immune checkpoint pathways in order to diminish the immune response to the tumour[38]. Thus, using monoclonal antibodies to block key immune checkpoint pathways could induce effective anti-tumour immunity.

1.2.1.1 CTLA-4 blockade

Early during the process of T cell activation, the checkpoint molecule CD28 transmits activating signals and CTLA-4 transmits inhibitory signals. Naïve T cells highly express CD28 on their surface. When CD28 binds to CD80 (B7.1) or CD86 (B7.2) ligands on APCs, co-stimulatory signals are produced[39]. This co-stimulation that occurs after binding of the T cell receptor (TCR) to the MHC antigen complex on the same cell is essential for activation of the T cell. CD28 ligation leads to phosphorylation of the molecule resulting in promotion of T cell proliferation, cytokine production and cell survival. If the TCR binds to MHC antigen complex in the absence of co-stimulation, T cell anergy and immune tolerance can occur[40]. CTLA-4 is also expressed on the surface of T cells (specifically, CD4+ and CD8+) and is upregulated on activated T cells. It competes with higher affinity than CD28 for binding to CD80 and CD86 on APCs. Once bound, an inhibitory signal is produced that blocks the T cell response and inhibits T cell activation[41]. The anti-CTLA-4 antibody can block this interaction resulting in activated antigen specific T cells that can induce anti-tumour immunity[42]. The monoclonal antibody ipilimumab, a CTLA-4 inhibitor (anti-CTLA-4), was the first treatment to demonstrate a survival advantage in patients with metastatic melanoma[43].

1.2.1.2 PD-1 blockade

While CTLA-4 mainly affects naïve T cells, PD-1 is primarily expressed on mature T cells in peripheral tissues and the TME[42]. PD-1 is a protein more broadly expressed on the surface of activated T cells, B cells, NK cells and DCs. Thus, PD-1 predominantly regulates effector T cell activity within tissues and tumours as opposed to regulating T cell activation in lymphoid organs[44]. PD-1 binds to its ligands PD-L1 and PD-L2 which are widely expressed on the surface of APCs, resting T cells, B cells, NK cells, DCs, macrophages and tumour cells[45]. Upon engagement with PD-L1 and PD-L2, ligation of PD-1 occurs and blocks T cell activation. Thus, T-cell proliferation and cytokine production are inhibited[46]. PD-1 and PD-L1/PD-L2 belong to the family of immune checkpoint proteins that act as co-inhibitory factors that can prevent the development of the T cell response in cancer. Blocking PD-1 signalling with anti-PD-1 monoclonal antibodies has been shown to induce significant anti-tumour immune responses. Anti-PD-1 monoclonal antibodies pembrolizumab and nivolumab have shown clinical efficacy in melanoma and other tumour types such as non-small cell lung cancer (NSCLC), head and neck squamous cell carcinoma and gastric/gastro-oesophageal junction adenocarcinoma[47].

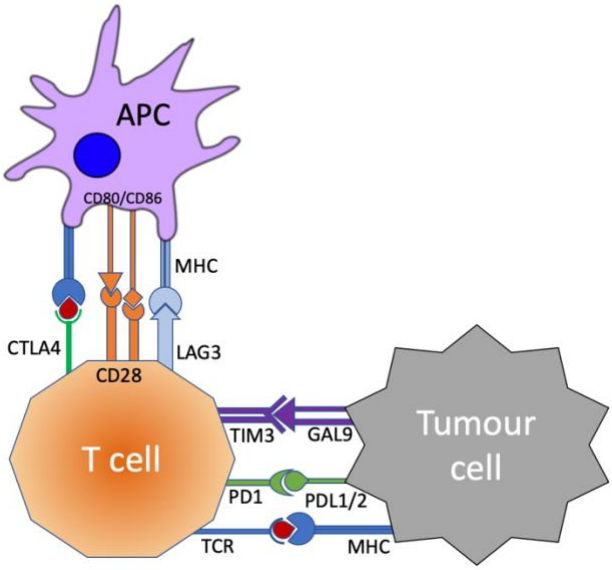

Figure 1.2 T cell function regulatory receptors (immune checkpoints)
T cell activation requires several stimulatory mechanisms, such as recognition of the antigen/major histocompatibility complex (MHC) via T cell receptor (TCR) and CD28 stimulation. In addition, activation of inhibitory receptors on T cell surface such as PD1 or CTLA4 results in inactivation of its function. Current immunotherapies focus on inhibition of these inhibitory receptors with antibodies targeting PD1 or CTLA4.
APC = antigen presenting cell

1.3 The new paradigm of systemic therapies for melanoma

Over the last 20 years there has been an improvement in the understanding of the biology of melanoma and consequently a pivotal change in the treatment landscape of advanced disease over the last decade. Until 2011, no systemic therapy was shown to improve survival in patients with advanced or metastatic melanoma. Dacarbazine (DTIC) chemotherapy was standard of care for many years, however response rates were dismal (7-13%)[48,49]. The identification and characterisation of *BRAF* mutations led to the development of targeted drugs and today, in patients with metastatic disease, survival has improved significantly. Targeted therapy with BRAF and MEK inhibitor combinations were approved for use in patients with metastatic BRAF V600E/K mutated melanoma on the basis of phase III clinical trial data[50,51,52]. Indeed, targeted therapies substantially improved survival from a median survival of 6-9months[53] with chemotherapy to a median of 25.9–33.6 months[54,55]. Since the introduction of immune checkpoint blockade (ICB) as single agent or in combination median survival has increased further to over 5 years[56]. However, despite various studies interrogating different agents, dosing and combinations within these two treatment groups there are still no results from direct prospective comparison of both targeted and immunotherapy approaches. This has meant that all stage IV patients without contra-indications are offered treatment with ICB. For those that are *BRAF* wild-type, this is their only treatment option with proven survival advantage. Those with $BRAF^{V600E}$ mutation are eligible for both targeted and immunotherapy approaches, however, evidence-based standard of care guidance is awaited regarding which strategy to employ first.

1.3.1 Optimum sequencing of systemic therapy

In the advanced melanoma first line setting, an analysis using a comparison of the digitised survival curves from pivotal clinical trials evaluating targeted therapy and ICB is depicted in Figure 1.3[57]. Superiority of combination targeted therapy in the *BRAF* mutant population was observed within the first 6 months of starting treatment and then the survival curve began to drop. Anti-PD-1 with or without anti-CTLA-4 showed an initial drop in survival, however later at 14-16 months, there was a switch to clear superiority of ICB, as the survival curves start to cross the targeted therapy combination. At 2 years and beyond, it appears that the most durable effects are produced by anti-PD-1 based regimens. Overall, there appears to be superiority of combined BRAF plus MEK inhibitor therapy within the first 12 months after treatment initiation, then switching to a clear superiority of anti-PD-1 alone or in combination with anti-CTLA-4 therapy. These findings, although must be considered within the context of

the caveats of cross trial comparison, are extremely relevant as they demonstrate both the acquired resistance with mitogen activated protein kinase (MAPK) inhibitors observed in the clinic, explaining the decline in survival curve at 6 months and the primary resistance frequently encountered with ICB, accounting for the immediate drop in survival curve on starting treatment[58]. As this was a pooled analysis, there is a degree of selection bias within this population, driven by the good prognosis BRAF wild-type patients in the immunotherapy trials.

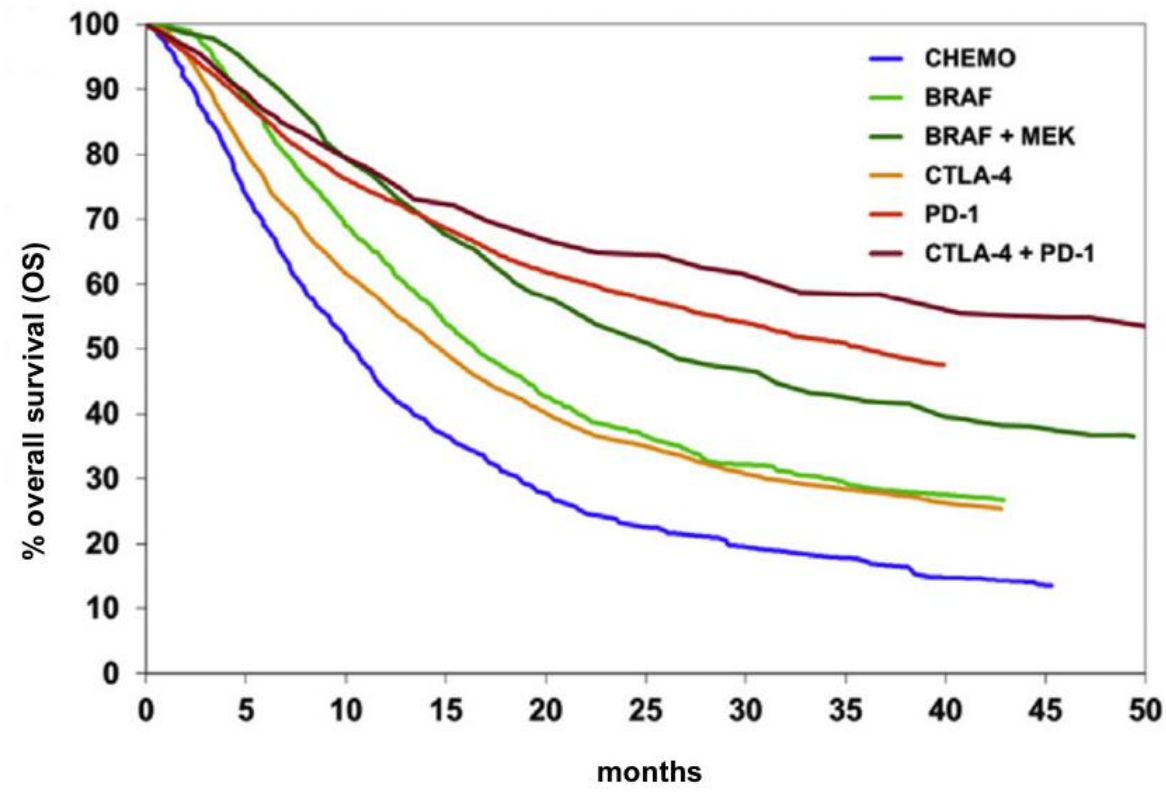

Figure 1.3 Mean overall survival curves created by weighted averaging of digitised Kaplan Meier survival curves of melanoma patients treated in first line setting within selected clinical trials. Figure from: Survival of patients with advanced metastatic melanoma: The impact of MAP kinase pathway inhibition and immune checkpoint inhibition, by Ugurel et al[57].

In patients that harbour a BRAF V600 mutation, the decision between targeted therapies or ICB in the first line setting was investigated in a randomised phase II study, SECOMBIT (NCT02631447), with the primary end point of overall survival (OS). Two hundred and fifty-one patients with untreated metastatic BRAF V600 mutated melanoma were randomised 1:1:1 to; arm A: combination targeted therapy until progression followed by combination ICB; arm B: combination ICB until progression followed by combination targeted therapy, or arm C: combination targeted therapy for 8 weeks followed by combination ICB until progression followed by combination targeted therapy until progression. The study primary endpoint was reached in each arm with at least 30 patients alive at 24 months. The median OS was not reached in any of the treatment arms. The progression free survival (PFS) rate at 2 and 3 years was 46% and 41% in arm A, 65% and 53% in arm B, 57% and 54% in arm C respectively[59]. The OS and total PFS rates at 2 and 3 years indicate a better trend in arm B and C. This study will help to define the optimum sequencing of treatment and data collection is ongoing to provide additional information on the long-term benefit of the three treatment combinations. A similar study, in which recruitment is ongoing, the phase II EBIN trial (NCT03235245) was designed to compare combination BRAF + MEK inhibitor targeted therapy followed by ipilimumab plus nivolumab versus ipilimumab plus nivolumab, to evaluate whether a sequential approach with 12-week induction phase using targeted therapy prior to immunotherapy improves PFS compared to combination ICB alone in patients with BRAF V600 mutant advanced melanoma[60].

Furthermore, the phase III DREAMseq trial (NCT02224781), compared first-line treatment with combination targeted therapy versus ipilimumab plus nivolumab in BRAF V600 mutant metastatic melanoma, with the primary endpoint of 2-year OS and secondary endpoints PFS, objective response rate (ORR) and safety[61]. Two hundred and sixty-five patients were enrolled and randomised to receive step 1 with either ipilimumab and nivolumab (I+N) induction for 12 weeks followed by nivolumab maintenance therapy (Arm A) or continuous combination targeted therapy (Arm B) and at PD were enrolled in step 2 receiving the alternate therapy, combination targeted therapy continuously (Arm C) or induction I+N with subsequent maintenance nivolumab (Arm D), respectively. Interim analysis at median 27.7 month follow up revealed, ORR for step 1 was 46% in I+N arm compared with 43% in the combination targeted therapy arm. For step 2, ORRs were 48% and 30% for patients crossing over to the combination targeted therapy and I+N arms respectively (p =0.136). The median duration of response was not reached in the I+N arm compared to 12.7 months in the targeted therapy arm (p<.001). The 2-year OS rate for patients starting with Arm A was 72% (95% CI: 62-81%) and for Arm B 52% (95% CI: 42-62%) (p= 0.0095). Median PFS among step 1 patients showed a trend in favour of Arm A, 11.8 months (95% CI, 5.9-33.5) in the I+N arm compared with 8.5

months (95% CI, 6.5-11.3) for the targeted therapy arm (p=0.054). Notably, Grade ≥3 toxicity was observed in 60% of patients in I+N arm A, compared to 52% in the targeted therapy arm B. Grade 5 treatment-related AEs included 2 patients on Arm A and 1 patient on Arm C. Although response rates were similar between step 1 regimes and for combination targeted therapy in both steps, I+N appears to be less effective following progression on targeted therapy compared to its utilisation as first line therapy. Thus, the treatment sequence beginning with the immunotherapy combination derived greater clinical benefit in this setting. However, considering the rate of significant toxicity and treatment related deaths with both regimes, the feasibility of a crossover approach will require further investigation.

In view of these studies and the meta-analyses results shown in Figure 1.3, for patients with no clinical evidence of rapidly progressing disease, ICB should be considered in the first instance, preserving targeted therapy for second line treatment. Targeted therapies have limited efficacy in patients with NRAS mutated disease, or those with other drivers such as KIT or NF1 and therefore the first line ICB options of WT disease should be considered[18]. Clinical and laboratory parameters such as Eastern Cooperative Oncology Group (ECOG) performance status (PS), serum LDH level and the number of metastatic sites can act as prognostic and predictive markers for both therapeutic approaches[62,63,64]. Table 1.4 describes the systemic therapies approved for use in melanoma according to stage of disease. This thesis focuses on immunotherapy responses and therefore will concentrate on ICB when considering therapeutic options.

Table 1.4 Immune checkpoint blocker and targeted therapies approved for use in cutaneous melanoma according to stage of disease.

Stage I	No approval in this setting (surgery is mainstay of treatment)
Stage II	At present, no approval in this setting (surgery is current standard of care)
Stage III	Following surgery, up to 12 months of adjuvant therapy with either: • Immune checkpoint blockers - pembrolizumab - nivolumab • Targeted therapy (BRAF +/- MEK inhibitors)
Unresectable stage III Stage IV	Treatment options for metastatic disease: • Immune checkpoint blockers - pembrolizumab - nivolumab - ipilimumab - combination ipilimumab + nivolumab • Targeted therapy (BRAF +/- MEK inhibitors)

1.3.2 Immunotherapy in the metastatic setting

Despite significant progress in the treatment of advanced disease, many questions remain unanswered, and for the majority of melanoma patients prognosis is still poor. Therefore, inclusion in clinical trials is a priority in all settings. The first immunotherapy-based phase III trial in metastatic melanoma (NCT00094653), compared ipilimumab with or without glycoprotein 100 (GP-100) vaccine versus placebo in the second line setting. It reported statistically significant improved OS for both ipilimumab arms, with a median OS of 10 months compared to 6.4 months in the placebo arm. The ipilimumab monotherapy arm had the best overall response rate (ORR) of 10.9% and a disease control rate of 28.5%. Responses in this group were durable, with 60% maintaining objective response for at least 2 years[43]. This study was pivotal in provoking the hope that immunotherapy may change the treatment landscape in a disease with previously much poorer outlook.

With ipilimumab gaining approval for use, the emphasis to test other inhibitors targeting the checkpoint immune regulators such as PD-1 was huge. The phase III CheckMate 066 trial (NCT01721772)[65] randomised previously untreated BRAF wild-type patients to receive either nivolumab or DTIC. Nivolumab was associated with a significant improvement in OS and progression free survival (PFS) compared to chemotherapy. The next step involved a head to head comparison of anti-PD-1 and anti-CTLA4 antibodies. KEYNOTE-006 (NCT01866319) compared pembrolizumab with then standard of care ipilimumab. The study concluded far superior response and survival rates with less high-grade toxicity in the anti-PD-1 pembrolizumab arm[66].

Both of these key studies aided in the identification of the PD-1/PD-L1 axis as clinically relevant for the T cell response to melanoma and ultimately led to the approval of anti-PD-1 antibodies, nivolumab and pembrolizumab.

Ongoing efforts to further improve outcomes with immunotherapy in melanoma led to the hypothesis that a combined approach may have a survival advantage compared to single agent immunotherapy regimens. Dual immune checkpoint blockade with anti-CTLA4 antibody ipilimumab and anti-PD-1 antibody nivolumab was evaluated in the phase III CheckMate 067 trial (NCT01844505)[67]. This study randomised treatment naïve patients to receive combination I+N versus monotherapy with ipilimumab or nivolumab alone. The combination of I+N was significantly superior to both monotherapy regimens in terms of ORR and PFS. The ORR was 57% in the I+N combination arm, 43% in the nivolumab monotherapy arm and 19% in the ipilimumab arm. Median PFS with combination therapy was 11.5 months compared to 6.9

months with nivolumab alone and 2.9 months with ipilimumab[68]. These differences are maintained in the 6.5-year survival update, with median PFS of 34 months for I+N, 29 months for nivolumab monotherapy and 7 months for ipilimumab. Furthermore, the results show durable improved outcomes with median OS of 72.1 months in the combination arm, 36.9 months with nivolumab, and 19.9 months with ipilimumab. Thus, there is a significantly improved outcome for combination I+N over nivolumab or ipilimumab monotherapy[69].

Based on these trials, in the first-line setting ICB is now standard of care for the majority of melanoma patients, regardless of their BRAF status, albeit, there are still many BRAF mutant patients that do require first line targeted therapy based on the fast and high response rates and response in vital organs such as the liver[70]. However, these responses may be limited over time, whereas combination ICB is associated with lower but durable response rates[71]. It is also important to consider that gains in efficacy have come at the expense of toxicity, with 59% of patients treated with combination I+N experiencing grade 3/4 adverse events, 24% with nivolumab and 28% with ipilimumab, which can have a significant impact on quality of life [69]. Therefore, biomarkers are needed to better select patients that benefit from combination immunotherapy and if implemented into clinical practice will avoid patients being given ineffective yet toxic drugs.

1.3.3 Immunotherapy in the adjuvant setting

Adjuvant therapy is indicated in patients at a high risk of recurrence following definitive surgical resection with the aim to treat any residual micro-metastatic disease and reduce the risk of local and distant relapse. Until recently, the lack of effective systemic therapy in the advanced setting had halted the establishment of effective adjuvant therapies in high risk melanoma patients. Over recent years, there has been a remarkable evolution in the management of melanoma. The emergence of active drugs has radically changed the treatment paradigm and a number of randomised clinical trials have been undertaken to evaluate ICB in the adjuvant setting. Several clinical trials have established a role for ICB in melanoma following curative intent surgery and anti-PD-1 therapy has now become a standard of care treatment option in the adjuvant setting[72,73,74].

EORTC 18071 (NCT00636168) was the first study to demonstrate benefit of adjuvant ICB in fully resected stage III melanoma[72]. Patients were randomised to ipilimumab 10mg/kg every 3 weeks for four doses, then 3 monthly for up to 3 years versus placebo. The ipilimumab arm showed superiority with 3 year relapse free survival (RFS) rates of 46.5% versus 34.8%

respectively, (p=0.0013). The OS rate at 5 years was 65% in the ipilimumab cohort, compared to 54% the placebo group, (p=0.001). The OS advantage came at the cost of toxicity, with adverse events leading to 52% of patients in the ipilimumab group discontinuing treatment. Five patients (1%) had treatment related deaths. In view of this, the risk benefit ratio of ipilimumab at the dose and schedule used in this study required additional assessment.

CheckMate 238 (NCT02388906) compared nivolumab (3 mg/kg every 2 weeks) to ipilimumab (10 mg/kg every 3 weeks for 4 doses and every 12 weeks thereafter) in patients with stage IIIB, IIIC or resected stage IV melanoma. Treatment was administered for up to 1 year or until disease recurrence or unacceptable toxicity. Treatment related grade 3/4 adverse events were reported in 14.4% of the patients in the nivolumab arm compared to 45.9% of patients in the ipilimumab arm. With 48 months of follow-up, nivolumab demonstrated superior RFS across all subgroups compared to ipilimumab with 4-year RFS rates of 52% vs 41% and median RFS of 52.4 months vs 24.1 months (p = 0.0003)[73,75]. KEYNOTE-054 (NCT02362594) compared pembrolizumab 200mg every 3 weeks for up to 1 year against placebo in resected stage III melanoma patients. Pembrolizumab had a superior RFS advantage after median follow up of 15 months with RFS rate of 75% compared to 61% in the placebo arm (p<0.001), again with a favourable toxicity profile[74]. The results of these two studies led to European Medicines Agency (EMA) approval of both anti-PD-1 drugs in the adjuvant setting for high risk stage III melanoma in late 2018.

CheckMate 915 (NCT03068455) again sought to explore the role of ipilimumab in high risk stage III or completely resected stage IV melanoma. This study compared the combination of I+N with nivolumab alone. The dose of ipilimumab was lowered to 1mg/kg in an attempt to reduce toxicity previously been seen with this agent. The addition of ipilimumab to nivolumab did not result in a statistically significant improvement in RFS in the all-comer (intention to treat) population[76].

1.3.4 Immunotherapy in the neoadjuvant setting

The neoadjuvant approach is primarily used to rapidly reduce tumour size in order to facilitate surgery. This approach using conventional chemotherapy combinations has been widely used in breast cancer and other solid malignancies[77]. Recently, the role of neoadjuvant immunotherapy in patients with high risk resectable or oligometastatic melanoma prior to surgical resection has been investigated and has demonstrated high response rates[78]. The hypothesis driving the neoadjuvant ICB strategy is that if the tumour remains in situ at the time of ICB administration then the presence of tumour antigens might promote a stronger and more prolonged immune response compared to giving ICB therapy after surgery and this may lead to more robust prevention of disease relapse. It is important to consider, patients benefiting from adjuvant ICB following surgery must have residual microscopic disease that was not eliminated by surgical resection. However, neoadjuvant patients have higher stage disease and thus the risk of micrometastasis is higher than a sentinel node positive patient.

Two studies looked at neoadjuvant ICB in high risk resectable melanoma to explore whether systemic treatment was more effective when administered prior to tumour removal. Both have shown promising results, but with significant toxicity[79,80]. The first study (NCT02519322) investigated neoadjuvant nivolumab (3mg/kg IV every 2 weeks) for up to 4 doses versus combined ipilimumab (3mg/kg IV) and nivolumab (1mg/kg IV) every 3 weeks for up to 3 doses prior to surgery, then after surgery, both arms received nivolumab 3mg/kg IV every 2 weeks for 13 doses. Patients were randomised 1:1, with a planned total accrual of 40 patients. However, the trial closed early after 23 patients were enrolled. Response was assessed using clinical imaging RECIST ORR and pathologic complete response rates (pCR). Combination therapy produced higher response rates (ORR 73%, pCR 45%), but at the cost of significant toxicity (73% [8 out of 11 patients] grade 3 treatment related adverse events). The response rate with single agent nivolumab was modest (ORR 25%, pCR 25%), but with less toxicity (8% grade 3). The trial was closed early due to safety concerns regarding high levels of toxicity and 2 out of 12 patients (17%) experiencing disease progression whilst receiving nivolumab monotherapy, which prevented curative intent surgery from taking place and highlighted clinical concerns with this approach[80]. The second study, OpaCIN (NCT02437279) compared an adjuvant and neoadjuvant approach to combination I+N in stage III melanoma. This study recruited 20 patients who were randomized 1:1 to each arm which consisted of four cycles of adjuvant therapy with ipilimumab 3 mg/kg and nivolumab 1 mg/kg or the same treatment regimen divided into two neoadjuvant treatments followed by two treatments after surgery. Again, toxicity was a significant issue with 90% of patients experiencing grade 3/4 treatment related adverse events in both arms, resulting in 18 out of 20 patients having to discontinue

treatment early. Notably, no delay or complications in surgery were reported. Pathological response in the neo-adjuvant arm was seen in 78% (7 out of 9 patients)[79]. After a median follow up of 36.7 months, none of the 7 patients with a pathological response have relapsed. The estimated 3 year RFS rate was 80% in the neoadjuvant arm compared to 60% in the adjuvant arm and the 3 year OS rates were 90% and 67%, respectively[81].

Subsequently, a multi-centre phase II OpACIN-neo trial (NCT02977052) was undertaken to explore whether alternative scheduling of neoadjuvant I+N might preserve efficacy while reducing toxicity[82]. Eighty-six patients with resectable stage III melanoma were randomised 1:1:1 to either arm A: 2 cycles of ipilimumab 3mg/kg + nivolumab1mg/kg 3 weekly; Arm B: 2 cycles of ipilimumab 1mg/kg + nivolumab 3mg/kg 3 weekly or arm C: 2 cycles of ipilimumab 3mg/kg 3 weekly followed immediately by 2 cycles of nivolumab 3mg/kg 2 weekly. Arm C closed early due to toxicity with 50% affected by grade ≥3 adverse events. Toxicity (grade ≥3) was less in arm A at 40% and lower still in arm B at 20%. In terms of response, both arm A and B had a radiological response rate of 60%, with a pathological response rate of 80% (pCR 43%) in arm A and pathological response rate of 77% (pCR 57%) in arm B. With median follow up of 7.7 months no patients with a pCR relapsed[82]. This study suggests that the lower dose ipilimumab 1mg/kg + nivolumab 3mg/kg regimen has lower rates of toxicity compared to standard dosing, but the response rates remain similar and thus this schedule could be compared to the adjuvant anti-PD1 approach in a phase III study.

Neoadjuvant therapy appears to be feasible, although is associated with significant toxicity. These studies suggest that pCR could be a promising surrogate marker for RFS and OS in the neoadjuvant setting. However, the major issues facing the neoadjuvant immunotherapy approach are the clinical deterioration of non-responders and the onset of severe immune-related adverse events, potentially interfering with curative intent surgery. At present, neoadjuvant treatment of early stage melanoma has not gained approval for use and remains under investigation with ongoing clinical trials. Further work is required to elucidate when this strategy may be preferred over adjuvant treatment.

1.4 Clinical challenges: melanoma immunotherapy

The advent of immune checkpoint inhibitors has dramatically changed the treatment landscape and improved the outcomes of melanoma patients. In contrast to the majority of chemotherapy and targeted therapies, ICB can provide durable responses[83]. Nevertheless, In the advanced setting, although survival has significantly improved, 50% of patients are still dying of their disease[56]. ORR are seen in less than half of patients treated with monotherapy regimens and although combination therapy raises response rates, it inevitably also increases toxicity and cost[84]. Thus, highlighting the urgent need to further refine the appropriate selection of patients for ICB therapy.

As discussed earlier, there is currently no biological rationale underpinning how patients are selected for treatment with immunotherapy. This has meant that the majority of patients with advanced melanoma without contra-indications to ICB are offered treatment with immunotherapy. For those that are BRAF wild-type, this is their only treatment option with proven survival advantage. For those patients with a *BRAF*^{V600E} mutation, knowledge is currently lacking on optimum sequencing and combinations of therapy. There are several clinical trials underway investigating this, with the aim to improve patient stratification and clinical outcomes.

1.4.1 Predictive Biomarkers of response to ICB in melanoma

There are a number of factors that have been suggested as predictive of response and informative for treatment selection. Five-year outcomes from Checkmate 067 (NCT01844505) showed that at a minimum follow-up of 60 months, the nivolumab-containing arms continued to demonstrate improved OS, PFS, and response compared with ipilimumab alone[56]. Furthermore, subgroup analysis identified a number of factors that could aid prediction of long-term responders and inform treatment selection. Those alive at 5 years are an enriched population that were more likely to have had a complete response (CR), normal LDH at baseline, and a lower number of metastatic sites of disease. In addition, of the patients that had an initial CR, 80% remained in CR at 5 years. The 20% of patients that progressed tend to be those with poorer prognostic features at baseline, such as M1c disease with metastases affecting visceral organs. Overall, patients with *BRAF*-mutant disease had better outcomes with combination I+N with OS of 60% compared to 48% for *BRAF* wild-type patients[56].

Tumour PD-L1 expression has been identified as a predictor of response to anti-PD-1 and anti-PD-L1 therapy[85]. It has been shown that a higher proportion of patients with an objective response to these agents have PD-L1 positive disease[86]. Additionally, improved PFS and OS has been observed in patients with metastatic melanoma and NSCLC when comparing PD-L1 positive and PD-L1 negative subgroups[67,87,88]. However, patients with PD-L1 negative tumours can still achieve clinical benefit with anti-PD-1 or anti-PD-L1 therapies[67,86]. PD-L1 status is therefore an unreliable biomarker and this is likely multifactorial. Firstly, PD-L1 expression can be transient, and intrapatient and intratumour heterogeneity in PD-L1 tumour expression can exist[89]. Therefore, tumour sampling at a single timepoint or at one tumour site may not accurately reflect the state of the PD-1 or PD-L1 axis[90]. Secondly, varying thresholds for PD-L1 positivity are accepted, for example, some studies using a cut off ≥1% tumour cells, and others use cut off ≥ 50%[91]. However, no studies have reported a threshold for which the positive or negative predictive value approaches 100%[90].

Immune gene signatures, such as those induced by interferon gamma (IFNγ), have been suggested as predictive biomarkers of response to anti-PD-1/anti-PD-L1 therapies[90]. In melanoma patients treated anti-PD-1/anti-PD-L1, high MHC class II (HLA-DR) expression was associated with improved clinical response, PFS and OS when compared to patients with low MHC class II expression[92]. A further retrospective analysis of an interferon inflammatory immune gene signature and response to anti-PD-1 pembrolizumab in patients with advanced melanoma was undertaken and an IFNγ score developed based on a 10-gene signature, which was subsequently expanded to a 28-gene signature in a validation cohort. The genes included those encoding IFNγ, granzyme A and B, perforin 1 (*PFR1*), Indoleamine 2,3-dioxygenase 1 (*IDO1)*, lymphocyte activation gene 3 (*LAG3)*, as well as other immune-related genes. Both the 10-gene and 28-gene scores demonstrated significant correlation with response and PFS[93].

An important consideration within gene expression profiling is that the predictive utility of the algorithms may be dependent on specific treatments. For example, a phase I study evaluating the efficacy of antihuman glucocorticoid-induced tumour necrosis factor receptor (GITR) antibody MK-4166 as monotherapy or in combination with pembrolizumab in patients with advanced solid malignancies failed to demonstrate the ability of IFNγ gene expression profiles to predict response to treatment[94]. This suggests that IFNγ signalling may correlate only with response to therapy of directly related targets such as downstream PD-1/PD-L1 inhibition. Immune pathways involving targets such as tumour necrosis factor (TNF) may necessitate distinct and individualised gene expression assays. Tumours that are classified as inflamed

have high levels of immune cell infiltrate and proinflammatory cytokines[95]. These tumours are associated with better clinical outcomes and response to immunotherapy. However, not all patients with the inflamed phenotype respond to ICB[90]. In melanoma patients, baseline tumour CD8+ levels correlate with response to anti-PD-1, whereas, with anti-CTLA-4 agent ipilimumab, response is more strongly associated with post-treatment increases in tumour infiltrating lymphocytes (TIL) not baseline levels[90,96,]. This suggests that although the inflamed phenotype may support tumour response to ICB, treatment induced modulation of a less immunogenic tumour could also promote response, thus highlighting opportunities for therapeutic intervention.

TMB can be defined as the total number of mutations present in a tumour specimen and was identified as a potential response biomarker for ICB in melanoma[97]. Further studies have strengthened the potential relevance of TMB in this setting[98,99]. However, at present consensus is lacking regarding the optimal TMB cut off for patient stratification. For example, Foundation Medicine defines high TMB (h- TMB) as >20 mutations/Mb, TMB-Intermediate as 6–19 mutations/Mb, and TMB-Low as <5 mutations/Mb[100]. Yet, a genomic profiling assay of 324 genes validated as an accurate assessment of TMB and approved by the FDA as a companion diagnostic for pembrolizumab defined h-TMB as greater than 10 mutations/Mb[101]. Furthermore, a study of advanced melanoma patients treated with anti-PD-1 monotherapy showed that high TMB correlated with OS, but not response. Thus, suggesting that high TMB might be an important marker of anti-tumour activity and may serve as a prognostic biomarker. However, a larger retrospective study investigating the prognostic impact of TMB across 20 solid tumour types did not report a significant association with TMB as a predictive biomarker for OS across all cancer subtypes[102], suggesting that gene panels tailored to specific cancer types may be necessary.

A strategy that combines two or more methods for capturing the immune status of the TME, such as the incorporation of TMB into a panel that includes other orthogonal biomarkers such as PD-L1 and TIL might prove more effective as a composite predictive biomarker for ICB therapy. However, at present, there are no baseline factors that reliably predict ICB response on an individual patient basis allowing treatment strategies to be tailored and thus, the shift now is to early on treatment assessment.

Gaining further insight and understanding into which factors predict clinical benefit from ICB will undoubtedly enhance selection of patient subsets who will respond, highlight the mechanism of action of novel immunotherapeutic approaches and potentially inform which patients require single agent versus various combination strategies. In patients with

metastatic melanoma, identification of disease progression early on treatment is imperative. Not all patients will exhibit evidence of clinical response initially, however, it is important that patients that are not gaining any benefit are identified promptly, minimising the time spent on ineffective drugs and permitting a switch to second line therapies thereby limiting the time the tumour has to progress and improving the chances of achieving meaningful clinical benefit. At present response assessment is usually not performed until radiographic imaging is carried out at 12 weeks.

1.4.2 Patient selection for adjuvant ICB

Though surgical excision is the mainstay of treatment in stage III melanoma and this approach can be curative, approximately half of patients will suffer loco-regional recurrence or distant relapse with metastatic disease. Recent practice changing studies have shown that adjuvant ICB is likely to have a positive impact on OS, reducing the recurrence rate by eradicating minimal residual disease (MRD)[103]. Keynote-054 (NCT02362594), showed at median follow-up of 15 months, pembrolizumab was associated with significantly longer RFS than placebo in the overall intention-to-treat population (ITT) (Figure 1.4A), with 1-year rate of RFS, 75.4% (95% confidence interval [CI], 71.3-78.9) compared to 61.0% (95% CI, 56.5-65.1); hazard ratio (HR) for recurrence or death, 0.57; 98.4% CI, 0.43-0.74; p<0.001[74]. Additionally, the trial highlighted that following surgical resection, only a proportion of patients have MRD requiring further intervention and 50% of patients do not relapse at 2 years on the placebo arm (Figure 1.4 A), suggesting that a potentially toxic treatment is given to a subgroup of patients that may not require it. In the ITT population, the 3·5-year distant metastasis free survival (DMFS) rate was 65·3% (95% CI 60·9–69·5) in the pembrolizumab group and 49·4% (95% CI 44·8–53·8) in the placebo group (Figure 1.4B). DMFS was significantly longer in the pembrolizumab group compared to the placebo group (HR stratified by stage 0·60 [95% CI 0·49 - 0·73]; p<0·0001)[104].

At present there is no way to identify the subgroup with MRD upfront in order to appropriately select for adjuvant therapy and separate from patients cured by surgery alone. For these patients, the risk of relapse varies greatly and thus far there are no established biomarkers for predicting likelihood of recurrence or response to therapy in this setting. The risk of toxicity and potential for irreversible immune-related adverse events (irAEs) is also an important aspect to consider in a population potentially already cured by surgery. Treating all patients with expensive and potentially toxic treatment is not in every patient's best interest nor is it the most economical approach. The key unmet clinical need in both early and advanced stage

disease is the identification of clinically validated predictive biomarkers to select patients who will benefit from ICB while sparing those who are unlikely to benefit from potential long term or life-threatening toxicity, thus minimising the number of patients exposed to potentially toxic treatment without clinical benefit.

A

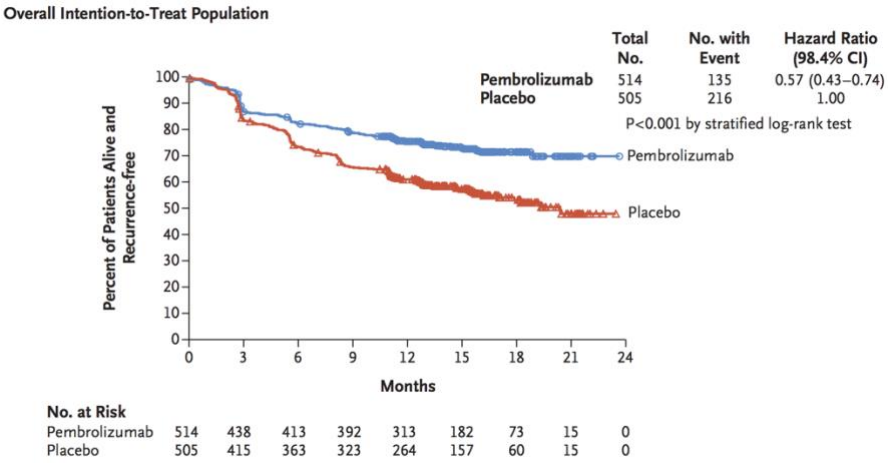

B

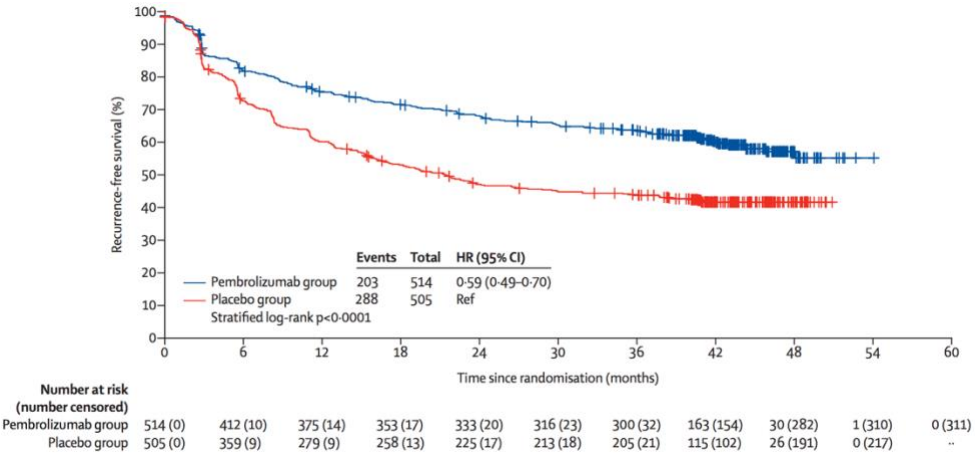

Figure 1.4: Kaplan–Meier estimate of recurrence free and distant metastasis free survival in the overall intention to treat population from KEYNOTE 054, phase III clinical trial of adjuvant pembrolizumab versus placebo in resected stage III melanoma
A: RFS curves at 24 months from KEYNOTE 054 adjuvant pembrolizumab vs placebo[74].
B: Final results for the secondary efficacy endpoint, DMFS from KEYNOTE 054 adjuvant pembrolizumab vs placebo after 3.5 years follow up[104].

1.5 Immunotherapy and toxicity

Activation of the immune system with ICB drugs can result in off target toxicity also referred to as irAEs. The exact pathophysiology underlying irAEs is unknown but is thought to be related to the role that immune checkpoints play in maintaining immunologic homeostasis. Any organ or tissue can be affected, however certain irAEs appear more frequently than others. In particular, skin, colon, endocrine, liver and lung toxicities are the most common. Any irAE can be serious, lead to irreversible outcomes and is potentially life threatening. The clinical characteristics of irAEs can be insidious and may be difficult to determine in the early stages. Therefore, a major clinical challenge is the early identification of patients susceptible to irAEs prior to their onset and monitoring for the development of irAEs. Thus, patient education and clinician's vigilance are paramount.

1.5.1 Toxicity timing of onset and severity

In general, with PD1/PDL1 blockade, irAEs tend to occur within the first few weeks to three months after starting treatment. Some toxicities seem to emerge earlier in the course of treatment. However, most irAEs are not expected to develop prior to the first 4 weeks of treatment. There appears to be a pattern of development of the different immune toxicities with skin and gastrointestinal generally occurring in the first 4-6 weeks, whereas liver and endocrine manifestations tend to occur later[105]. However, irAEs can develop at any time, even after discontinuation of treatment, and may wax and wane over time. It has been observed that in some cases the initial onset of irAEs has been as long as one year after ceasing treatment. While anti-PD1 or anti-PDL1 therapy can be used for months and even years, most studies have indicated that extended treatment does not result in a higher cumulative incidence of irAEs[106].

Treatment related adverse events with CTLA4 inhibitor ipilimumab can arise at any point, but usually present around the third or fourth dose. They are usually more common than in PD-1 inhibitors, occurring in approximately 60%–85% of patients and tend to be more severe[107,108]. Toxicities directly correlate with ipilimumab dose and the incidence of grade 3 or higher is approximately 10%–27%[109]. With combination treatment (I+N), irAEs were observed in 95% of patients and in 55% of patients these were of grade 3 or higher[67]. The onset of grade 3-4 toxicities may develop earlier in combination therapy for example skin toxicity can occur within 24 hours of the first dose, however adverse events can also develop over a prolonged period of time[109].

1.5.2 Organ specific toxicity and management

Patients treated with anti-CTLA-4 therapy experience a spectrum of irAEs that differ from those treated with anti-PD-1 agents[66,110]. For example, colitis and hypophysitis are more commonly observed with anti-CTLA-4 therapy, whereas pneumonitis and thyroiditis are more prevalent with anti-PD-1 therapy[111,112,113,114]. The reason behind the differences in organ specific toxicities observed with each of these agents remains to be fully elucidated. However, cases of hypophysitis report the presence of CTLA-4 on normal pituitary cells, potentially facilitating the toxicity of anti-CTLA-4 therapy[115,116]. Whereas, thyroid disorders develop in patients on anti-PD-1 therapy when anti-thyroid antibodies are present either pre-treatment or become detectable after commencing treatment. It has been postulated that in addition to T cell mediated immunity, anti-PD-1 or anti-PDL-1 therapies also regulate humoral immunity, thus enhancing pre-existing anti-thyroid antibodies[114]. PD-1 may also be associated with preserving self-tolerance, the mechanism that enables the immune system to recognise self-produced antigens as non-threatening and preventing attack[117]. Cytokines have also been implicated in the pathophysiology of irAEs, one study identified increased levels of IL-17 in patients with colitis secondary to ipilimumab[118]. Anti-IL-17 drugs are currently used to treat auto-immune conditions such as psoriasis and ankylosing spondylitis. Reports suggest IL-17 could also be an actionable target for treating ICB induced irAEs such as colitis and dermatologic toxicities[118,119]. To date, the immune biology of ICB associated irAEs has not been fully understood, thus limiting treatment options to broadly immunosuppressive strategies.

Initiation of steroid treatment counteracts lymphocyte activation, resulting in regression of irAEs and is the mainstay of management of toxicity[120]. However, it is important to consider whether the immunosuppression associated with steroids and/or steroid sparing agents may reduce the anti-tumour efficacy of ICB. There are no prospective studies testing immunosuppressive strategies to address this, however retrospective studies have indicated that overall, outcomes were not inferior for patients who received immune-modulatory agents to manage checkpoint inhibitor-related toxicities when compared to outcomes for patients who did not receive immunosuppressive agents for irAEs[121,122]. In the majority of patients, response and durability of response was not adversely affected. There could be distinct exceptions to this, possibly associated specifically with the type of immunosuppressive treatment used[123]. As the number of patients treated with ICB grows and the volume of real-world data increases, the aetiology and characterisation of immunotherapy related toxicities will become clearer, and management more targeted and effective. Since adverse events may occur late, even

after discontinuing active treatment, and there is a potential for long-term chronic complications, constant vigilance and early recognition and treatment of irAEs is paramount.

1.5.3 Toxicity and efficacy of ICB

Some studies propose that patients with irAEs have higher response rates than those patients who do not experience toxicity, however this is yet to be fully validated[124, 125]. In a large, retrospective study of ipilimumab, treatment outcomes were similar in patients with and without irAEs, suggesting that there is no association between irAE onset and anti-CTLA-4 efficacy[121]. In contrast, across disease sites, the onset of irAEs is predictive of anti-PD-1 response, with improved clinical outcomes as measured by ORR, PFS and OS[126,127,128]. However, the overall impression is that toxicity is not required to yield benefit from immune checkpoint inhibitors. A recent study of over 1000 patients with metastatic melanoma that received anti-PD1 monotherapy with pembrolizumab observed no significant association of irAEs with improved PFS or OS[129]. It is proposed that specific irAEs are more directly linked to anti-tumour response than others. For example, multiple studies involving melanoma patients have shown links between vitiligo and positive clinical outcomes[130,131]. As vitiligo is a side effect that is directly related to antigen specific immunity, it may be more strongly correlated with anti-tumour efficacy than other irAEs.

1.5.4 Biomarkers of toxicity

Several biomarkers have been identified as potentially predictive of irAEs, however, none have been prospectively validated. The candidate nonspecific and organ specific predictive and early on treatment biomarkers of irAEs that have been described in studies of melanoma and other tumour types are shown in Table 1.5 and Table 1.6 respectively. There has been limited progress on research into biomarkers of irAEs and the field remains in relative infancy. Biomarkers are not used routinely for clinical diagnosis or treatment of toxicity and their high costs are likely to limit clinical utility. Although ICB have transformed the treatment landscape for patients with advanced melanoma, only 15-60% respond, leaving a significant number of patients who do not derive benefit but risk exposure to potentially life-threatening toxicity[132]. Thus, development of measurable and cost-effective biomarkers of irAEs and identification of biomarkers to optimise identification of patients who will benefit from ICB is vital to personalising patient management in a clinically meaningful way.

Table 1.5: Non-specific biomarkers of irAEs (adapted from Jia et al[133]).

Biomarker	Tumour type	Treatment	Number of patients in study	Correlation between biomarker and irAE
CRP	Melanoma	Anti-PD-1 Anti-CTLA-4	37	Raised CRP at the onset of irAE predictive: CRP rise in 93% of patients to a mean of 52.7 mg/L from 8.4 mg/L at baseline ($P < 0.0001$) in the absence of infection[134].
IL-6	Melanoma	Anti-CTLA-4	140	Low baseline IL6 serum levels were significantly and independently associated with higher risk of development of irAEs[135].
Blood cell count	Melanoma	Anti-PD-1	101	Increase in white blood cell count (WCC) and decrease of relative lymphocyte counts correlated with incidence of grade 3–4 irAEs[136].
Blood count	Lung, melanoma, renal, urothelial, head and neck, merkel cell, colon	Anti-PD-1	167	Elevated baseline and rise in absolute lymphocyte count (ALC) following treatment initiation were associated with development of irAEs[137].
Cytokines	Lung, Renal, Melanoma, bladder, liver, head and neck	Anti-PD-1/L1 Anti-CTLA-4	65	Lower levels of CXCL9, CXCL10, CXCL11 and CXCL19 at baseline and increases in CXCL9 and CXCL10 levels post treatment correlated with the development of irAEs[138].
Cytokines	Melanoma	Anti-PD-1 Anti-CTLA-4	98	Baseline and early on treatment cytokines, including G-CSF, GMCSF, Fractalkine, FGF-2, IFN-2, IL-12p70, IL-1a, IL-3 1B, IL-1RA, IL-2, IL-13, were significantly upregulated in patients with severe irAEs[139].
TMB	19 different solid tumours	Anti-PD-1	16,397	Significant correlation between high TMB and development of irAEs[140].
Soluble CTLA-4	Melanoma	Anti-CTLA-4	113	Higher baseline soluble CTLA-4 levels were associated with the onset of any irAEs[141].

Table 1.6: Organ specific biomarkers of irAEs (adapted from Jia et al[133]).

IrAE	Biomarker	Tumour type	Treatment	Number of patients in study	Correlation between biomarker and irAE
Gastrointestinal	Gut microbiome	Melanoma	Anti-CTLA-4	26	Baseline stool samples enriched with Faecalibacterium and other Firmicutes were more likely to develop immune-related colitis[142].
Gastrointestinal	CD177 and CEACAM1	Melanoma	Anti-CTLA-4	162	Gene expression profiling (GEP) of whole blood identified high expression of CD177 and CEACAM1 at baseline and early on treatment in patients that develop GI toxicity[143].
Gastrointestinal	mRNA expression (CCL3, CCR3, IL-5, IL-8 and PTGS2)	Melanoma	Anti-CTLA-4	210	Peripheral blood gene expression signature (mainly CCL3, CCR3, IL-5, IL-8 and PTGS2) was predictive of immune-related diarrhoea (particularly grade 2–4)[144].
Gastrointestinal	IL-17	Melanoma	Anti-CTLA-4	35	Upregulation of IL-17 level at baseline and 6 weeks after treatment identified a correlation with grade 3 diarrhoea/colitis[118].
Gastrointestinal	HLA allele	Melanoma NSCLC	Anti-PD-1 Anti-CTLA-4	102	Association between HLA type II variant HLA-dqb1 * 03:01 and immune-related colitis[145].
Lung Pneumonitis	CD74	Bladder, prostate	Anti-CTLA-4 Anti-PD-1	8	Development of immune mediated pneumonitis correlated with raised plasma levels of CD74 following ICB therapy[146].

Endocrine Thyroid	Peripheral blood rheumatoid factor (RF), antinuclear antibody (ANA), anti-thyroglobulin (TG) and anti-thyroid peroxidase (TPO)	NSCLC	Anti-PD-1	137	Pre-existing antibodies associated with clinical benefit and with the development of irAEs. Patients with positive RF are more likely to develop dermal irAEs, and thyroid dysfunction is more common in patients with positive TPO Ab[147].
Endocrine Hypophysitis	guanine nucleotide-binding protein G(olf) subunit alpha (anti-GNAL) and integral membrane protein 2B (anti-ITM2B) autoantibodies	Melanoma Prostate Renal cell	ICB	9	Elevated anti-GNAL autoantibody both baseline and on-treatment marker for irAE hypophysitis. Elevated anti-ITM2B autoantibody on-treatment marker for irAE hypophysitis[146].
Skin	HLA alleles	Melanoma NSCLC	Anti-PD-1 Anti-CTLA-4	102	HLA- drb1 *11:01 correlated with itching[145].
Skin	IL-17	Melanoma	Anti-PD-1	1	Psoriasiform dermatologic irAE resolved after treatment with systemic IL-17A blockade[119].

1.6 Refining and personalising the approach to melanoma immunotherapy

Traditional prognostic biomarkers in melanoma are based on immunohistochemical markers such as mitotic rate and rate of proliferation measured by Ki-67 expression, pathological markers such as Breslow thickness (measure of distance between upper layer of epidermis and deepest point of tumour penetration), presence or absence of ulceration and serological markers such as LDH[148]. For ICB in metastatic melanoma, there is an estimated 5-year survival rate of 52% with combination PD-1 and CTLA-4 inhibitors and 44% with PD-1 monotherapy[56]. Although the combination appears to be superior to monotherapy, the higher response rates (58% vs 44%) and improved survival rates are at the expense of significant toxicity (grade 3 and 4: 55% vs 16%)[67]. Therefore, there is a need to identify the patients that will benefit from single agent therapy, those that require the combination approach and those that will not respond to either and require a different treatment approach. Additionally, development of novel treatment strategies and improved prediction of toxicity will be key to improving patient outcomes. Thus, the focus has shifted to improving patient stratification, refining treatment regimens and personalising therapy.

As our understanding of melanoma biology and the interactions between tumour and immune system improves, there has been a shift towards a more individualised approach to the management of patients one which utilises a more tailored approach to enhance patient care and improve clinical outcomes. As such, molecular testing has facilitated the identification of genetic mutations that confer sensitivity of cancer cells to targeted therapies. In this setting, the biomarker is characterised by a binary outcome, i.e. mutation present or absent and is highly predictive of response to treatment. The advent of immunotherapy has led to new challenges to this approach. The durable responses described above tend to be observed only in a small population of patients. Understanding what renders some responsive and others resistant is key to improving patient outcomes. This clinically evident disparity in response to ICB combined with the increasing cost of these drugs has prompted the pursuit of response biomarkers. Thus far, currently available predictive biomarkers that have been identified as potential indicators of response to ICB are lacking precision, so they are more nuanced in their application and are not binary in nature.

1.7 Peripheral blood biomarkers

Tumour tissue is highly sought after for biomarker identification and analysis, due to the importance of the TME. However, access to tumour samples can be challenging for several reasons, including difficulty accessing lesions and heterogeneity of the biopsy site. Tumour biopsies are invasive, associated with increased risk of adverse events and impractical when considering multiple longitudinal tumour sampling. Thus, from a practical perspective the ability to use minimally invasive, easily reproducible liquid biopsy is vital for the development of biomarkers with clinical utility.

Recently, circulating biomarkers in peripheral blood have come to the forefront as a potentially valuable platform for assessing therapeutic responses and predicting early relapse in melanoma. Those linked with early on treatment changes may help guide when to continue or switch treatment regime and the feasibility of longitudinal sampling makes liquid biopsy an attractive prospect. However, at present there are no validated circulating biomarkers in clinical use, although, a number of potential markers have been proposed as predictive of response to ICB in melanoma patients.

1.7.1 Peripheral blood markers

Raised levels of circulating LDH, C-reactive protein (CRP), S100 protein and protein vascular endothelial growth factor (VEGF), have been linked with clinical outcomes for melanoma patients treated with ICB[149,150,151,152]. In particular, serum LDH has been identified as prognostic in pivotal melanoma clinical trials[56,153] and changes in LDH on ICB are likely a surrogate marker for response or progression[154].

Elevated baseline levels of serum LDH have been associated with worse OS in melanoma patients treated with ICB. Baseline serum LDH > twice the upper limit of normal (ULN) in 166 patients treated with ipilimumab was associated with decreased OS and limited long-term benefit from treatment[155]. These findings were validated in an independent cohort of 64 patients. Disease control and survival were found to be significantly associated with decreasing levels of serum LDH and CRP between baseline and end of treatment, at week 12 in another study of 95 patients treated with ipilimumab[156]. The association between serum LDH level, OS and response to ICB was confirmed in a subsequent study. Anti-PD1 treated metastatic melanoma patients with an elevated baseline LDH who had a partial response to treatment had a mean reduction of 27.3% in their serum LDH in contrast to patients with

disease progression who had a mean increase of 39% in serum LDH. Those patients with a relative increase >10% from elevated baseline LDH had a significantly shorter OS compared with patients with ⩽ 10% change. (4.3 vs 15.7 months, p<0.00623)[157].

In melanoma patients receiving ipilimumab, raised serum S100B at baseline in addition to week 3 and week 6 on treatment correlated with poor OS. Furthermore, S100B levels increased 12 weeks after starting ipilimumab in patients who progressed following treatment[158,159]. Although S100B levels were associated with improved PFS and melanoma-specific survival, there was not a significant correlation with overall response[160].

A further retrospective analysis of S100B and LDH serum levels was assessed in 152 melanoma patients treated with anti-PD-1 monotherapy and 86 patients treated with combination anti-PD1 plus anti-CTLA-4 therapy. In the monotherapy group, high baseline S100B or LDH correlated with poor OS compared to those with normal S100B (1-year OS: 51.1% vs 83.1%, p< 0.0001) and normal LDH (1-year OS: 44.4% vs 80.8%, p=0.00022) respectively. An LDH rise >25% and S100B rise of >145% from baseline correlated with worse OS (p < 0.0001). In patients treated with combination therapy, baseline LDH, baseline S100B and rising S100B levels of >145% were associated with worse OS (*p*=0.005, *p*< 0.0001 and p=0.0006, respectively), however LDH rise >25% was not (*p*=0.64)[161]. Baseline S100B levels may act as a prognostic marker in melanoma patients receiving anti-PD-1 monotherapy. Additionally, increasing S100B levels on treatment may reflect patients that require earlier response assessment imaging.

Analysis of peripheral blood from 176 melanoma patients treated with ipilimumab revealed that baseline VEGF ≥ 43 pg/mL correlated with decreased survival rates[162]. Another potential marker for both baseline and early on treatment changes is angiopoietin-2 which is a vascular growth factor known to be pro-tumour and pro-angiogenesis. Angiopoietin-2 is an immune modulator involved in resistance to anti-VEGF therapies[163]. Elevated baseline levels of circulating angiopoietin-2 were found to be associated with decreased OS in metastatic melanoma patients treated with ipilimumab monotherapy or ipilimumab in combination with anti-VEGF agent Bevacizumab (10.9 vs 19.3 months, p=0.0125). Raised angiopoietin-2 levels 3 months post treatment initiation with ipilimumab were also linked to worse OS, (p=0.019). Similarly, in metastatic melanoma patients treated with anti-PD-1 therapy, elevated baseline levels of angiopoietin-2 were associated with decreased OS (p=0.004), and raised angiopoietin-2 at 3 months correlated with reduced response rates, (p=0.002)[164].

Lymphocytes are the most commonly investigated peripheral blood component when evaluating potential predictors of immunotherapy response. Initial lymphopenia and subsequent rebound lymphocytosis is a known haematological side effect of interleukin-2 (IL-2) therapy. One study identified a significant association between clinical response and extent of lymphocytosis in metastatic melanoma patients immediately after treatment with IL-2[165]. Two studies investigating ALC have shown that a baseline ALC > 1000μL prior to commencing therapy and a rise in ALC after two doses of ipilimumab correlate with response[166,167]. Decreasing regulatory CD4+ FoxP3+ T cells and increasing ALC during treatment with ipilimumab were positively associated with response and improved survival in patients with metastatic melanoma[156]. This finding of increasing ALCs correlating with clinical response to ICB has also been noted in another prospective analysis[168]. However, a pooled analysis from several studies identified the rise in ALC among all treated patients irrespective of benefit[169].

Neutrophil to lymphocyte ratio (NLR) has also been examined as a predictor of response to ICB in melanoma. One study identified that a decrease in NLR was associated with improved survival in 27 advanced melanoma patients treated with ipilimumab[170]. Conversely, another study of 720 advanced melanoma patients found that those with both baseline absolute neutrophil counts (ANC) ≥ 7500 and NLR ≥ 3 had a significantly increased risk of death and disease progression[171].

Myeloid derived suppressor cells (MDSCs), a heterogeneic immunoregulatory population of monocytic cells have also been investigated in peripheral blood as predictors of response to ICB therapy. Using flowcytometry, it has been noted that melanoma patients with a higher circulating level of MDSCs during the first 6 months of ICB treatment have a poorer prognosis, whereas those with lower baseline MDSC counts have improved clinical outcomes[172,173]. A further study confirmed a baseline low frequency of MDSCs in melanoma patients treated with ICB was associated with the highest probability of long-term survival[174]. This study proposed a baseline peripheral blood signature of low LDH and absolute monocyte count in combination with elevation in both lymphocyte and eosinophil counts and high levels of regulatory T cells to correlate with improved clinical outcomes, thus highlighting the potential need for monitoring multiple dynamic cell populations to attain predictive power.

1.7.2 MicroRNA

Micro RNAs (MiRNAs) are another emerging class of non-invasive biomarker of disease and therapy response[175,176,177]. MiRNAs are released dynamically into the circulation from dying tumour cells. One group were the first to report the presence of circulating miRNA-21 as predictive of response to ICB[178]. Subsequent studies have investigated this further with larger miRNA panels. Notably, one study of metastatic melanoma patients, identified several miRNAs in the circulation as predictive of resistance to ICB therapy and poor survival[179].

1.7.3 Exosomes

It has been shown that PD-L1 expression correlates with both response and survival rates[180]. However, PD-L1 expression as a biomarker of response to ICB has not been translated into the clinic for several reasons. Firstly, PD-L1 expression within tumours displays significant heterogeneity. This is because PD-L1 expression is a dynamic process, influenced by therapy and inflammation, thus levels of expression can vary[181]. Furthermore, there remains disparity in the antibodies used for immunohistochemical analyses of PD-L1, which requires optimisation to standardise the approach. The optimal level of PD-L1 expression level also remains ambiguous, as some patients deemed PD-L1 negative have responded to anti-PD-1 therapy[182].

This has prompted the study of plasma levels of PD-L1 and their correlation with treatment responses. A novel class of biomarker is represented by exosomes which are micro-vesicles actively released from tumours into the circulation. Exosomes released into the circulation from metastatic melanoma patient tumours carry PD-L1 on their surface. Lower baseline levels and increases in circulating exosomal PD-L1 during treatment positively correlates with response to pembrolizumab[183]. However, in another study of melanoma patients treated with anti-PD1 monotherapy, expression of PD-L1 mRNA in the exosomes was higher at baseline and significantly reduced following treatment in responding patients, remained stable in patients with stable disease and increased in patients with disease progression[184]. Thus, the information gained on response to ICB from transcripts of exosomal PD-L1 may be conflicting with that from direct measurement of PD-L1 proteins within circulating exosomes. Therefore, large prospective studies are required for validation.

1.7.4 Circulating tumour cells

In a prospective study aiming to utilise blood-based monitoring to measure treatment response, peripheral blood samples were collected from 29 metastatic melanoma patients prior to and during ICB therapy. Longitudinal digital measurements of circulating tumour cells (CTCs) score using a quantitative 19-gene digital RNA signature was observed as predictive of clinical outcome. Those with a high number of CTCs had a significantly higher risk of relapse, whereas those with stable or a reducing number of CTCs had better OS. In addition, a decrease in CTC score within 7 weeks of treatment was associated with significant longer PFS and OS. Thus, the ability to serially sample CTCs using a minimally invasive approach during the course of ICB therapy may enable early assessment of response and progression[185]. More recently, CTCs were identified in peripheral blood from 52 patients with metastatic melanoma receiving ICB therapy. High numbers of CTCs correlated with raised LDH levels. This information was used to stratify patients as low-risk or high-risk and those defined as high-risk had worse disease-free survival (DFS) and OS. In addition, serial monitoring of CTCs enabled identification of subclinical disease in patients who went on to develop disease progression[186]. The lack of standardisation and the variety of methodologies used for CTC isolation has hampered the ability to implement analysis into prospective clinical trials to facilitate study of their prognostic and predictive applications in melanoma. Thus, there is a need to standardise protocols for CTC enrichment, detection, and quantification.

1.7.5 Circulating tumour DNA and cell free DNA

Circulating tumour DNA (ctDNA) is an emerging minimally invasive “liquid biopsy” that can be used to monitor patients, facilitating a more dynamic approach to identification of treatment response and relapse, thus informing early therapeutic decision making[187]. Cell free DNA (cfDNA) is DNA that is freely circulating in the blood stream. CfDNA can be found in the blood stream of healthy subjects and the concentration can range between 0-100ng/mL[188]. However, in the setting of cancer, the levels of cfDNA are significantly higher ranging between 0-1000ng/mL which may indicate underlying disease[189]. CtDNA is shed directly from the tumour into the peripheral circulation, therefore contributing to the total cfDNA in the blood. The mechanisms underpinning the release of cfDNA into the circulation have not been fully elucidated, although it is thought to be either a passive byproduct of cell death (i.e. necrosis, apoptosis) or as a result of active secretion from macrophages following cell phagocytosis[190]. In cancer patients, up to 1% of total circulating DNA is ctDNA originating from tumour cells[191]. Tumour-specific mutations such as *BRAF* and *NRAS* that can be tracked in circulation using

ctDNA have been proposed as a biomarker of disease status and for monitoring of immunotherapy response in advanced melanoma[192].

An illustrative study of 7 cases has suggested that BRAF/NRAS ctDNA monitoring of melanoma patients during anti-PD1 therapy can be utilised to monitor clinical benefit[193]. These findings are supported by a larger multi-institutional retrospective study of 229 melanoma patients[194]. To assess how TMB and ctDNA can be used to estimate response to ICB in metastatic melanoma a prospective study of 35 patients treated with combination I+N was undertaken. A panel of 710 tumour-associated genes was used to calculate TMB in liquid biopsies before and during treatment. TMB obtained from ctDNA prior to commencing therapy was significantly higher in responders compared to non-responders. In addition, undetectable ctDNA 3 weeks after treatment initiation was associated with clinical response and longer OS[195].

The predictive power of ctDNA as a response marker to ICB therapy has been evaluated in another prospective study of 85 advanced melanoma patients receiving anti-PD1 therapy. Those with undetectable ctDNA pre-treatment had longer PFS and OS compared to patients with detectable ctDNA. Furthermore, ctDNA levels also accurately reflected tumour burden[196]. Another study exploring the clinical utility of cfDNA as a surrogate biomarker for tumour burden in 38 metastatic melanoma patients supports these findings[189]. Moreover, another group prospectively confirmed ctDNA level correlated with clinical and radiologic outcomes in advanced melanoma[197].

Similarly, a further prospective analysis of 40 metastatic melanoma patients harbouring $BRAF^{V600E/K}$ or $NRAS^{Q61/G12/G13}$ mutations established the role of longitudinal ctDNA monitoring in predicting response to ICB (anti-PD1 monotherapy or in combination with ipilimumab) and clinical outcome. Patients with higher pre-treatment ctDNA levels that remained persistently elevated on treatment had a poorer prognosis with shorter PFS and OS. Undetectable ctDNA at baseline or within 8 weeks from treatment initiation was an independent predictor of response and improved survival[198]. These findings were confirmed in an independent validation cohort of 29 patients[198].

More recently, a prospective phase II clinical trial, INSPIRE (NCT02644369) was undertaken to assess the clinical utility of ctDNA as a prognostic and predictive biomarker in 5 different tumour types including melanoma. Patients were treated with anti-PD1 Pembrolizumab and ctDNA was measured prior to and serially on treatment. Those with better prognosis were

identified by early reduction in ctDNA following 2 cycles of pembrolizumab and on-treatment ctDNA clearance, independent of tumour type, TMB or PDL-1 status[199].

Monitoring response to treatment is essential to determine clinical benefit. Longitudinal tracking of BRAF or NRAS mutations in ctDNA identified that a decrease in ctDNA levels 2-4 weeks following the initial dose of nivolumab accurately predicted response to therapy in advanced melanoma. Whereas, ctDNA levels increased within 2–4 weeks in patients with uncontrolled disease. Furthermore, ctDNA level was a superior indicator of treatment response and the emergence of therapy resistance compared to serum LDH level which lacks sensitivity and specificity[200]. A patient with metastatic KIT mutant vaginal mucosal melanoma that was not amenable to tissue biopsy received sequential targeted, immuno- and chemotherapy. Longitudinal analysis of cfDNA enabled monitoring of the patient's response to therapy and identified the presence of two tumour subclones that responded differently to treatment. Furthermore, cfDNA analysis anticipated response to therapy and progression several weeks prior to radiological confirmation[201].

Interestingly a recent study seeking to evaluate the predictive value of pre-treatment ctDNA relative to line of therapy in advanced melanoma found that in patients receiving first line ICB, baseline ctDNA was a strong predictor of clinical outcome, with longer PFS[202]. This was confirmed in both a discovery cohort of 125 patients and an external validation cohort of 128 patients. In contrast, the predictive value of ctDNA was not maintained in the second line ICB therapy setting, thus highlighting the potential limitation of pre-treatment ctDNA as a predictive biomarker in the second line setting[202].

Altogether these studies demonstrate that ctDNA is a novel minimally invasive strategy to assess response to immunotherapy both at baseline and on treatment and predict long-term survival in advanced melanoma. However, the clinical utility of ctDNA as a biomarker in the metastatic setting remains uncertain. The applicability of ctDNA is currently limited to specific research indications and clinical trials and future interventional studies are required to establish whether ctDNA can be used to guide clinical decision making.

Figure 1.5 depicts the main candidate non-immune based circulating biomarkers predictive of response to ICB in melanoma described within the literature and discussed within this section.

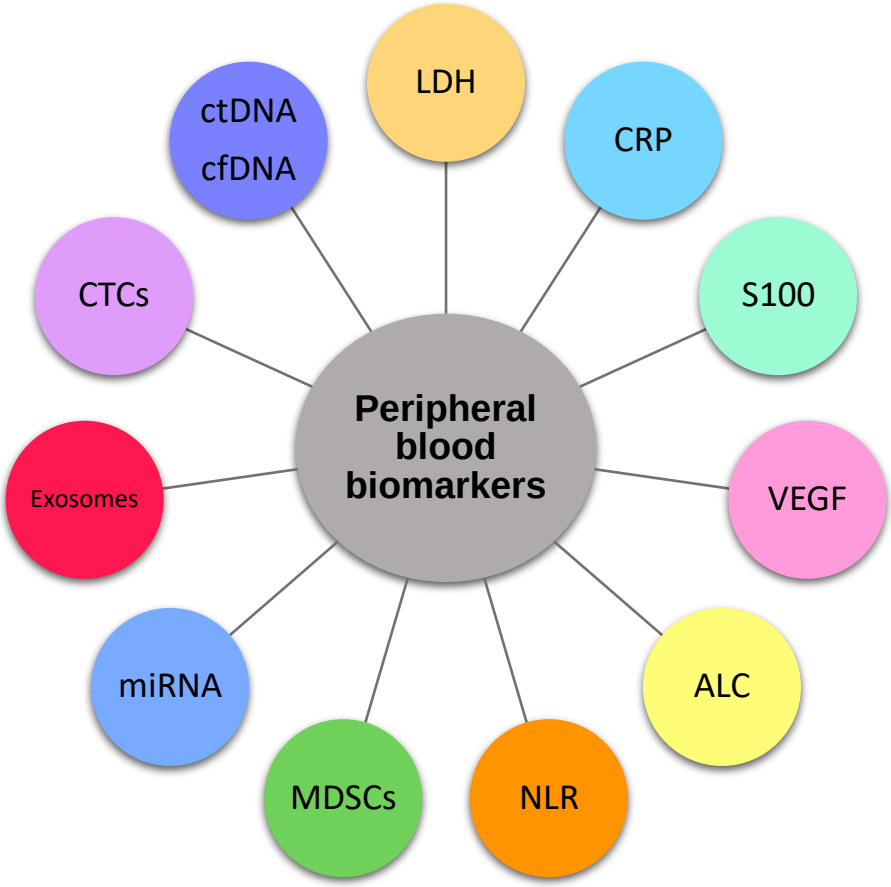

Figure 1.5 Circulating biomarkers predictive of response to ICB in melanoma
Radial chart of the main candidate non-immune based circulating biomarkers predictive of response to ICB in melanoma.

1.7.5.1 Clinical application ctDNA in the post-operative early stage melanoma setting

1.7.5.1.1 Stratification of high-risk patients

Two recent studies, in resected stage III disease, have shown that melanoma patients with detectable ctDNA following surgery have a poorer prognosis[203,204], thus highlighting its potential utility as an additional means of patient stratification. The presence of ctDNA enables identification of a subgroup of patients at high risk of early relapse and inferior survival. The addition of ctDNA to routine clinical practice would facilitate stratification of patients to adjuvant regimens associated with increased risk of toxicity, but greater potential for efficacy. When taken at a single time point following surgery, the detection of ctDNA can provide additional 'personalised' information in addition to current AJCC staging, by informing on individual specific prognosis. This information would facilitate discussion with patients regarding their own specific risks and benefits of adjuvant therapy. Detectable ctDNA would suggest that the patient is more likely to require further treatment as surgery alone has not completely cleared their disease and they are at higher risk of relapse. However, there is no current data to support ctDNA as a predictive biomarker for a particular therapy in this setting. Further research is required to assess post-operative baseline ctDNA detection and response to adjuvant therapy.

1.7.5.1.2 Monitoring for molecular relapse

CtDNA is a valuable surveillance strategy for early relapse of disease. Based on current data, it is unlikely that one time point to sample for ctDNA following surgery is enough to identify all patients that are going to relapse[205]. Longitudinal sampling to monitor ctDNA, on treatment or during clinical follow up has been shown to identify micro-metastatic relapse, not visible on radiological imaging in several cancer types in the adjuvant setting[205,206,207]. These studies provide proof of principle that longitudinal monitoring of ctDNA can identify relapse early. The recent funding of a large multi-centre phase III clinical trial, DETECTION (NCT04901988) reflects the shift towards early detection and treatment to prevent the development of metastatic disease. The primary aim is to assess whether outcomes can be improved in stage II resected melanoma using longitudinal ctDNA monitoring to evaluate whether early diagnosis and treatment of molecular relapse with immunotherapy improves survival.

1.7.5.1.3 Monitoring response to adjuvant treatment

Carrying out longitudinal ctDNA surveillance will enable monitoring of treatment response to adjuvant immunotherapy and early identification of treatment failure. There is limited data regarding the use of ctDNA to monitor response to adjuvant therapy. However, the ability to monitor response to therapy in the stage IV setting has been well documented[208,209].

1.8 Peripheral immune-based biomarkers

The proficiency of the peripheral immune system has been identified in several studies as playing an important role in guiding treatment decisions. At present, there are no peripheral immune based biomarkers validated for use in oncology practice and significant hurdles remain in bridging the gap between identification of immune signatures correlating with response and prospectively validated predictive biomarker selection[210]. Studies of ICB have identified that the evaluation of peripheral blood prior to and on treatment offers insight into patients' immune characteristics and how these relate to response to treatment.

1.8.1 Peripheral T cells

Analysis of peripheral blood mononuclear cells (PBMCs) at baseline and longitudinally during ICB with ipilimumab in 137 metastatic melanoma patients identified that proportions of baseline naïve and memory T-cells correlated with OS. Baseline levels of CD8 effector-memory type 1 (EM1) T-cells >13% correlated with longer OS and better response rates (p=0.01), whereas high baseline levels of late stage-differentiated effector memory CD8 cells were associated with poor OS, but did not correlate with clinical response. This suggests that CD8 EM1 cells may represent surrogate predictive marker candidates and warrant further validation[211].

In a prospective study of pre-treatment PBMCs from 30 patients with advanced melanoma due to commence ICB therapy, it was noted that pre-treatment levels of $CD45RO^{+}CD8^{+}$ T cells varied significantly between patients. Baseline levels of $CD45RO^{+}CD8^{+}$ T-cell were found to be associated with response. Patients with normal baseline levels of $CD45RO^{+}CD8^{+}$ T cells had improved OS with ipilimumab[212].

PBMCs from 29 patients with metastatic melanoma were taken pre and post treatment with pembrolizumab to examine the utility of immune profiling of peripheral blood. Changes in

circulating exhausted-phenotype CD8+ T cells (T_{ex} cells) were examined. Response was assessed in relation to the magnitude of change in T_{ex} cells after pembrolizumab and adjusted for baseline tumour burden. Imbalance between T cell reinvigoration and tumour burden were associated with non-response. Lower pre-treatment tumour burden and higher magnitude change in T_{ex} cell reinvigoration correlated with improved PFS. Thus, inferring T_{ex} cell reinvigoration to tumour burden ratio can reliably distinguish clinical outcomes and predict response[213].

A subsequent pooled analysis of PBMCs from 190 melanoma patients with unresectable disease identified high levels of PD-L1 (and not CTLA-4) on peripheral blood CD4+ and CD8+ T cells predicted resistance to ipilimumab, whereas CD137 expression on circulating CD8+ T cells following lymph node or metastatic lesion resection in stage IIIc and IV melanoma was predictive of longer PFS for combination anti-CTLA-4 + anti-PD1 blockade with I+N[214].

A small prospective study, investigating response to anti-PD-1 monotherapy in advanced melanoma identified a subset of circulating central memory CD4+ T cells harbouring the $CD27^{+}FAS^{-}CD45RA^{-}CCR7^{+}$ phenotype as predictive of long-term survival. This subset of T cells expanded in a higher proportion in responders compared to non-responders to ICB when PBMCs were sampled 6-13 weeks following therapy initiation. These findings were validated in a separate patient cohort[215].

In another recent study, looking at cell-surface markers on host immune cells, high-dimensional single-cell mass cytometry was utilised to characterise immune cell subsets in the peripheral blood of metastatic melanoma patients before and after 12 weeks of anti-PD-1 immunotherapy. During therapy, a reduction in number of CD4+ and CD8+ peripheral T cells was observed in responders compared to non-responders. This was thought to be due to their enhanced ability to migrate to the tumour site. Pre-treatment, they found that the strongest predictor of progression-free and overall survival was the presence of $CD14^{+}CD16^{-}HLA\text{-}DR^{hi}$ monocytes in patients that responded to ICB[216]. Similarly, a separate study identified an ALC increase 2-8 weeks after initiation of ipilimumab and increases in circulating CD4+ and CD8+ T cells 8-14 weeks after first dose of ipilimumab correlated with improved survival in metastatic melanoma patients[217].

In another study utilising mass cytometry, expression of co-stimulatory molecules on peripheral T cells was investigated in 67 melanoma patients, where high pre-treatment frequency of CD4+ and CD8+ memory T cell subsets were a potential marker for response to

anti-CTLA-4 therapy, whereas a higher incidence of distinct NK cell subsets was associated with response to anti-PD1 therapy[218].

1.8.2 T cell receptor on peripheral T cells

T cell diversity is known to play a role in the development of tumour responses in patients receiving ICB therapy. A comparison of melanoma patients PBMCs at baseline and 30-60 days after treatment with anti-CTLA4 agent tremelimumab was undertaken to study the changes in peripheral T cell clonality and diversity. Deep sequencing of the TCR Vβ CDR3 region revealed that 19 out of 21 patients had a median increase of 30% in unique productive sequences of TCR V-beta CDR3. These changes were significant for diversity ($p = 0.04$) and richness ($p = 0.01$). The expansion of the number of TCR V-beta CDR3 sequences reflects a larger T-cell diversity following treatment. There was no significant difference between clinical responders and non-responders. However, PBMCs collected longitudinally over a 12-month period from healthy donors did not show any change in TCR V-beta CDR3 diversity, thus highlighting the pharmacodynamic effect of ICB therapy in relation to modulation of the immune system[219].

Another study assessing changes in TCR repertoire pre-treatment and at 4 weeks on anti-CTLA-4 therapy in 21 melanoma patients confirmed that treatment increased peripheral TCR diversity. This was reflected by a higher number of new TCR clonotypes and reduced loss of existing clonotypes when compared with healthy donors. The number of clonotypes that increased with treatment was not associated with clinical outcome. This is in keeping with the findings from the parallel study described above. However, improved OS was associated with maintenance of the most abundant clones which were present at baseline. Although, patients who survived longer exhibited less clonotypic changes over time and maintained the most abundant clones which were present at baseline, whereas patients with shorter OS had a decrease in the most abundant clones with treatment. These results suggest that CTLA-4 blockade induces T cell repertoire evolution and diversification and that responders at baseline may possess pre-existing peripheral T cells relevant for the anti-tumour immune response[220]. These studies suggest that an increase in diversity of the TCR is associated with improved clinical outcomes in cancer immunotherapy. However, the relevance of TCR repertoire as a predictive biomarker for response to ICB therapy requires further exploration.

One group analysed the pre-treatment peripheral TCR repertoire of 12 patients (4 responders and 8 non-responders), with advanced melanoma due to commence ipilimumab, to assess

the richness (observed V-J rearrangements) and evenness (similarity between the frequencies of specific V-J rearrangements) of the TCR repertoire. It was observed that low richness or evenness of the TCR repertoire significantly correlated with a lack of response to treatment, meaning that a less diverse or more clonal TCR repertoire is predictive of non-response to therapy. There were no significant differences in terms of overall survival. The small sample size and retrospective nature of this study limits its utility and further prospective larger scale studies of peripheral TCR repertoire will be important when seeking to optimise clinical outcomes with ICB[221].

Consistent with these findings, a further retrospective study of metastatic melanoma patients treated with either ipilimumab or anti-PD1 agent pembrolizumab was undertaken with the aim to determine whether baseline TCR repertoire diversity could be used as a predictive biomarker of response to both anti-PD1 and anti-CTLA4 therapy. The results demonstrated that a more clonal (less diverse) repertoire was associated with a poor response to anti-CTLA4 ipilimumab, but correlated with improved response and PFS in patients treated with anti-PD1 therapy[222]. Conversely, in pancreatic ductal adenocarcinoma, low baseline diversity correlates with significantly longer survival after anti-PD1 therapy, but worse survival after anti-CTLA-4 therapy[223]. In NSCLC there are also conflicting findings. Some studies have identified increased peripheral blood TCR diversity after anti-PD-1 treatment and significant overlap between TCR repertoires at pre and post treatment as correlating with better survival[224,225], whereas others have shown that an increase in peripheral TCR clonality following ICB therapy is associated with longer PFS[226].

A study of 29 advanced bladder cancer patients treated with anti-PD-L1 agent atezolizumab identified that patients with a diverse repertoire of circulating T cells at baseline had a longer PFS and OS. Furthermore, expansion of tumour-associated TCR clones in the periphery 3 weeks post treatment initiation was associated with clinical benefit. These findings suggest an important relationship between circulating and intratumoral immunity upon PD-L1 blockade[227]. TCR sequencing of tumour samples has enabled ICB therapy response to be predicted. A higher baseline TCR clonality was observed in the tumours of melanoma patients that responded to pembrolizumab. On treatment samples from responders showed significantly more clonal expansion than non-responders[228]. Furthermore, a study of 24 patients with different solid malignancies treated with anti-PD-1 or anti-PD-L1 therapy revealed that patients with a radiological partial response to treatment had significantly increased peripheral TCR repertoire diversity compared to those with stable disease or progressive disease[224].

These studies suggest that peripheral blood TCR repertoire could accurately guide the personalised approach to immuno-oncology, serving as a predictive biomarker of clinical response to ICB therapy. However, it is important to note that the discordant data suggest that TCR repertoire metrics may be associated with different outcomes dependent on the type of malignancy, mode of immune perturbation with either PD-1/PD-L1 or CTLA-4 agents, the type of sample analysed, peripheral T cells or TILs and if assessment is carried out on fresh or frozen clinical samples.

Sequencing-based quantification of the TCR population offers a unique insight into the immune response. The significant diversity of the TCR repertoire poses a challenge when considering adequate capture and downstream analysis. This has led to the development of in-depth sequencing technologies. At present next generation sequencing based technologies are utilised for high-throughput analysis of the immune cell repertoire, however a gold standard method for the field had not yet been identified.

1.9 T cell biology

1.9.1 T cell maturation

All blood cells are derived from the pluripotent haemopoietic stem cells (HSC) present in the bone marrow and as depicted in Figure 1.6 these stem cells develop into multipotent progenitor cells which have the ability to differentiate into myeloid and lymphoid cells. Further differentiation of the lymphoid cells leads to the formation of a common lymphoid progenitor that can differentiate into T, B or NK cells[229]. T cells are a type of lymphocyte that play an important role in the adaptive immune system and the presence of a TCR on the surface of T cells distinguishes them from other lymphocytes.

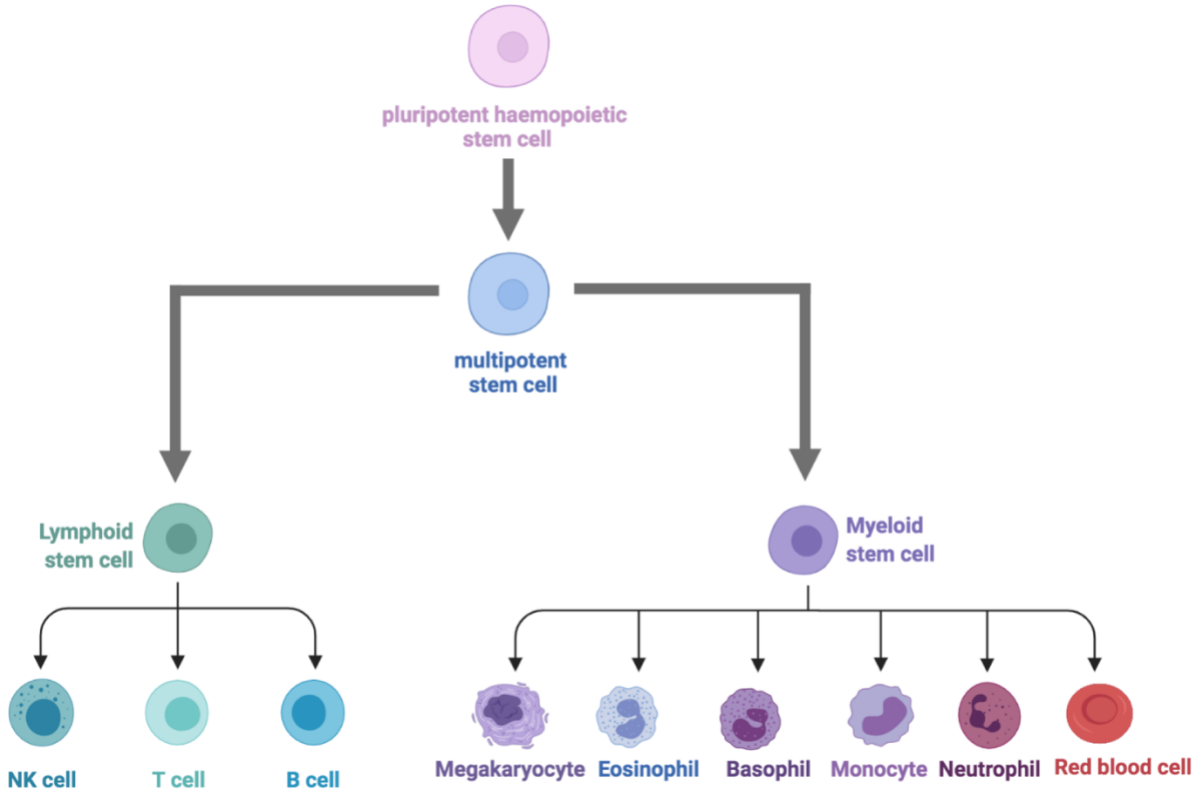

Figure 1.6 Differentiation of haematopoietic stem cells
Schematic representation of haematopoiesis in which pluripotent stem and progenitor cells in the bone marrow divide and differentiate, to give rise to all blood cells. The multipotent stem cells differentiate into the lymphoid and myeloid progenitor lines. The lymphoid lineage differentiates in to NK, T and B cells. The myeloid lineage gives rise to platelets, white blood cells (eosinophil, basophil, monocyte and neutrophil) and red blood cells.

Although T cell development takes place in the bone marrow, they travel in the bloodstream to the thymus to mature. The thymus is made up of an outer cortex and an inner medulla region[230]. The developing progenitors within the thymus, also known as thymocytes, undergo a series of maturation steps that can be identified based on the expression of different cell surface markers. The majority of cells in the thymus develop into αβ T cells, while approximately 4% become γδ T cells[231].

T cells can be either helper T cells or cytotoxic T cells based on whether they express CD4 (helper) or CD8 (cytotoxic) glycoprotein. Immature T cells do not express either the CD4 or CD8 antigen and so are referred to as double-negative (DN) cells (CD4-CD8-). The DN population can be further sub-divided by the expression of CD44 (an adhesion molecule) and CD25 (Interleukin-2 receptor α chain) into 4 stages, DN1-DN4[232]. Figure 1.7 shows the expression of these markers at each stage.

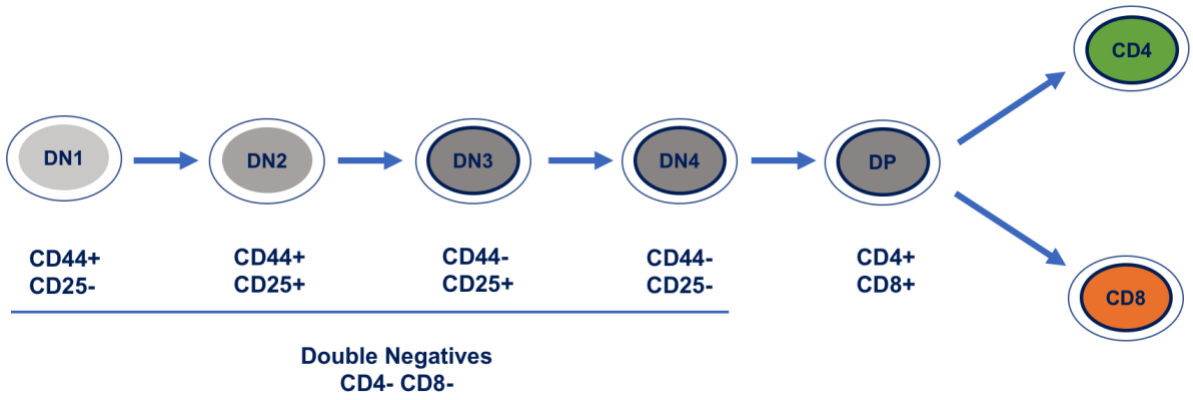

Figure 1.7 αβ T cell development, showing the different cell surface markers (CD44/CD25) expressed at the different stages of T cell development
DN1 cells also known as early thymic progenitor cells (ETPs) are $CD44^{+}CD25^{-}$, DN2 cells are $CD44^{+}CD25^{+}$, DN3 cells lack expression of CD44, but express CD25. DN4 cells lack expression of both CD44 and CD25 and further differentiate into double positive (DP) CD4+ CD8+ thymocytes. Following selection, down-regulation of either co-receptor produces either naïve CD4 or CD8 single positive cells that exit the thymus into peripheral circulation.
Figure Adapted from: A Positive Look at Double Negative Thymocytes, by Ceredig et al[232].

DN1 cells, also known as early thymic progenitor cells (ETPs), are heterogeneous and may give rise to αβ T cells, γδ T cells, NK cells, DC, macrophages, or B cells. DN2 cells migrate through the cortex of the thymus and begin the rearrangement of TCR locus gene segments. They are committed to the T cell lineage after transitioning from DN2 to DN3. Subsequently, DN3 cells undergo a process known as beta-selection, which selects for cells that have successfully rearranged their TCR-β chain locus, leading to T cell maturation and development of αβ T cells[233]. Cells that do not undergo beta-selection i.e. have failed to generate a functional TCR die by apoptosis and their DNA, which encodes the CDR3 unique regions, enters the blood as cfDNA[234]. The next stage in T cell maturation is when the cells then mature into DN4, which are further upregulated into CD4+ and CD8+ cells achieving a double positive (DP) status in the maturation process. This is followed by two distinct processes; positive selection in the cortex and negative selection in the medulla[235].

Positive selection is the process of movement of DP T cells (CD4+ and CD8+) to the cortex, where they encounter self-antigens[236]. The thymic cortical epithelial cells express self-antigens on MHC molecules where the T cells interact with the molecules. The cells that do not interact with the molecules strongly enough die whereas others with high affinity to MHC cells survive[237]. Most thymocytes die in the process of development which lasts a number of days. The remaining 2% become mature T cells[36]. Positive selection results in the development of single positive CD4+ helper, CD8+ cytotoxic lineages or natural killer (NK) cells. T cells with TCRs that bind to MHC class I molecules develop into CD8+ T cells and T cells that bind to MHC class II become CD4+ T cells[237]. The cells that survive the positive selection move into the medulla and undergo negative selection, which eliminates thymocytes with a high affinity for self-antigens[235]. The cells that interact too strongly with the self-antigens receive an apoptotic signal resulting in cell death. During the same process, however, some cells are selected to form regulatory T cells (T_{regs}) which retain their ability to bind to self-antigens in order to suppress overactive immune responses and protect against auto-immunity[238].

The cells that successfully complete the selection process exit the thymus into the bloodstream as mature naïve T cells; they are also known as early thymic emigrants (ETE)[234]. These mature T cells are still referred to as naïve because they have not been presented with an antigen. They travel to sites that contain secondary lymphoid tissue, such as the lymph nodes and tonsils, where antigen presentation takes place[239]. This facilitates the development of antigen-specific adaptive immunity. The process of T cell maturation in the thymus is illustrated in Figure 1.8. With advancing age, the thymus contributes less cells and as it reduces in size by approximately 3% per year for the duration of middle age, there is a

subsequent reduction in thymic output of naive T cells (T_N), thus clonal expansion of immature T cells contributes to a greater extent in protecting older individuals[240].

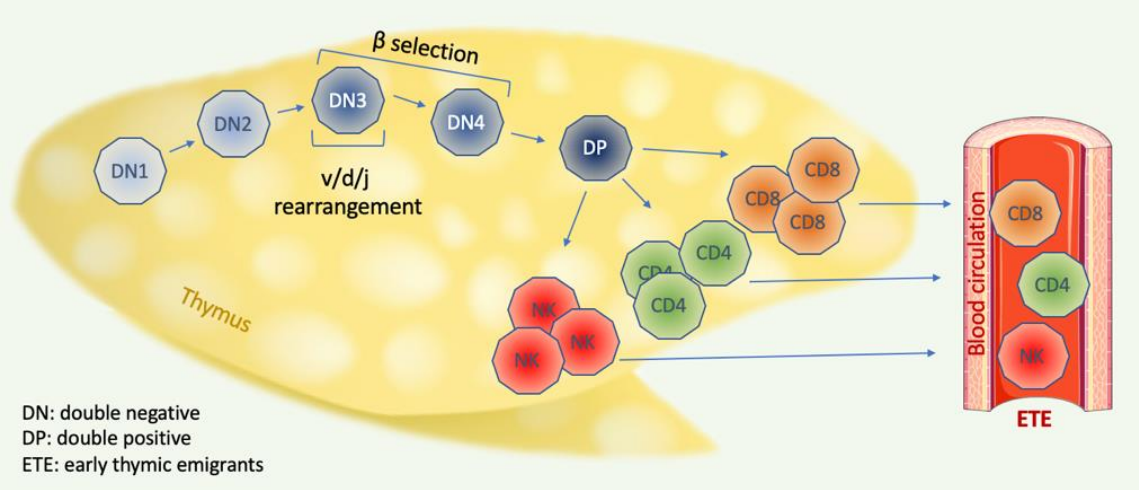

Figure 1.8 T cell maturation in the thymus
In the thymus haematopoietic stem cells differentiate into double negative T cells (DN1), initiating T cell maturation. TCR receptor v/d/j rearrangement occurs in DN3 stage of maturation. DN3 to DN4 transition is marked by β selection and elimination of non-functional or self-recognising T cells. This is followed by differentiation into double positive (DP) cells, expressing both CD8 and CD4, which then differentiate into single positive CD4 or CD8 T cells or into natural killer cells. Naïve T cells exiting the thymus into the circulation are known as early thymic emigrants (ETE).

1.9.2 TCR development

The TCR is a protein complex found on the surface of T cells, that is responsible for antigen recognition. TCRs are able to recognise an antigen when it is presented as a peptide in the MHC on the cell surface[237]. The process of antigen presentation and recognition is illustrated in Figure 1.9. More than 90% of TCR complexes are comprised of an alpha (α) and beta (β) chain and a small subset of T cells express a TCR with gamma (γ) and delta (δ) chains. TCRαβ recognises peptides bound to MHC class I or II, whereas γδ TCRs recognise unprocessed antigens[241].

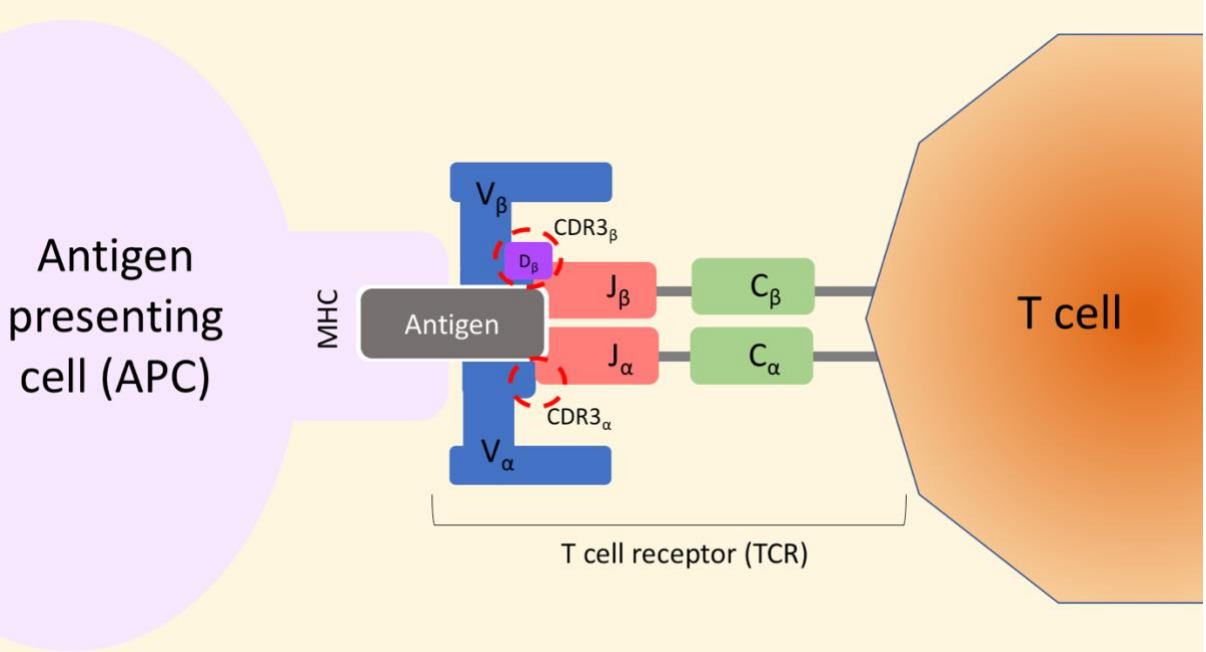

Figure 1.9 αβ T Cell Receptor and antigen presentation and recognition
The TCR is a heterodimeric molecule with a single antigen-binding site. Cells expressing TCRαβ are called αβ T cells. T cell receptors recognise foreign antigens via α and β chains. Each chain is composed of variable (V), junction (J) and constant (C) regions. The antigens that TCRs bind are small peptide fragments, displayed by MHC molecules on the surface of APCs. TCRαβ recognises peptides bound to MHC class I or II. The variable regions of the TCR are responsible for antigen recognition and contain a unique CDR3 which interacts with the peptide and MHC complex. The CDR3β chain is more diverse than CDR3α, because it is encoded by an additional gene segment known as diversity (D).
CDR3= complementarity-determining region 3

TCR development occurs in the thymus through an error-prone process of somatic recombination which constructs a terminal sequence from a vast number of possible segments. In a TCR composed of α and β chains, each chain contains a variable region (V) and constant region (C), joined by a junction region (J). T cells can express one or more types of α chain but will only express one type of β chain[36]. The variable regions are responsible for antigen recognition and contain 3 hypervariable loops termed complementarity-determining regions (CDR1-3) which interact with the MHC complex. CDR1 and CDR2 are encoded by the variable (v) gene segment and influence sensitivity and affinity of the TCR binding to the MHC, whilst CDR3 interacts with the peptide and MHC complex[36]. The CDR3β chain is more diverse than CDR3α, because it is encoded by an additional gene segment known as diversity (D) in addition to the variable (V), and joining (J) segments (Vβ and Jβ segments), whereas the TCRα gene locus contains only variable (V) and joining (J) gene segments (Vα and Jα). Accordingly, the α chain is generated from VJ recombination and the β chain is produced from VDJ recombination[242]. This process of recombination is illustrated in Figure 1.10 and results in a highly diverse repertoire of TCRs, a defining feature of the adaptive immune system.

During T cell maturation TCR recombination is a two-step process. Enzymatic activity encoded by recombination activating gene 1 (*RAG1*) and *RAG2* initiates the rearrangement of first TCR-β and then TCR-α chain genes. *RAG* expression and thus TCR-β gene rearrangement (Dβ Jβ rearrangement followed by Vβ DJβ recombination) is initiated in DN thymocytes. *RAG* re-expression and thus TCR-α gene rearrangement is then initiated in DP thymocytes[243]. Both RAG1 and RAG2 are expressed by all lymphoid progenitors and naive T and B cells. They bind to and introduce double strand breaks at recombination signal sequences (RSS), which flank all TCR gene segments[244].

The TCR α chain comprises 46 variable segments, 8 joining segments and the constant region. The TCR β chain is comprised of over 50 variable segments, 2 diversity segments, 13 joining segments and two constant regions[245]. A vital step in VDJ recombination is the contraction of the locus which produces a looping that allows the different V genes access to the already combined DJ segments with similar frequency[246].

The overall aim of recombination is to ensure a diverse repertoire of CDRs, as the CDRs are the antigen binding portion of the TCRs and thus a diverse capacity for recognition results in effective protection against pathogens and production of successful immune responses. VDJ recombination and the inclusion or removal of nucleotides at the junctions between gene segments give rise to such a substantial amount of TCR diversity, which

is thought to be greater than 10^{15} TCRs[247]. TCR revision is a mechanism whereby CDRs can be re-edited in the lymphoid periphery, causing an alteration in the antigen specificity of the TCR. This results in induction of self-tolerance in mature peripheral T cells and a highly selected but diverse TCR repertoire that protects against invading pathogens[248].

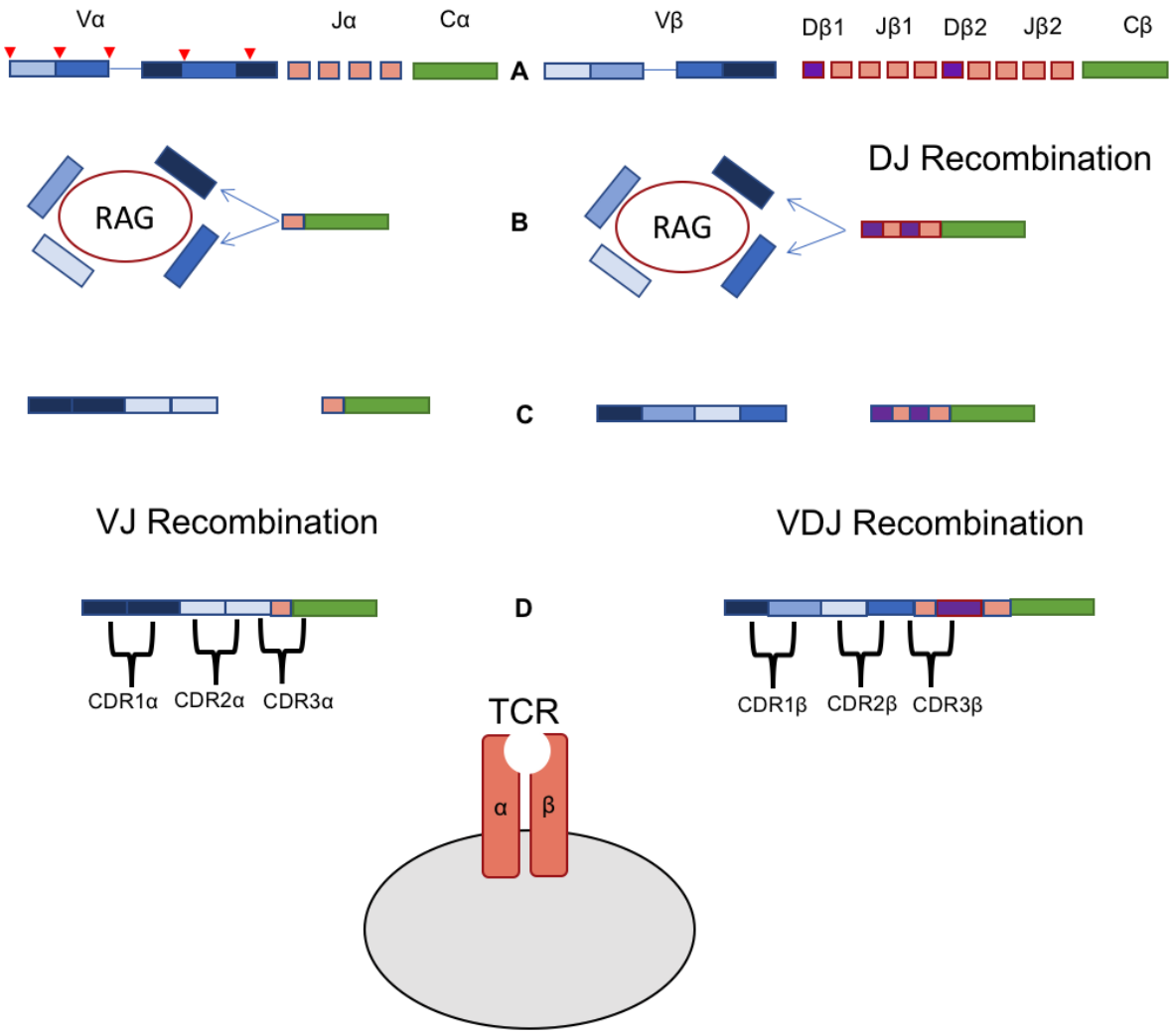

Figure 1.10 VJ and V(D)J recombination of alpha (α) and beta (β) chains of TCRs
A: TCR gene locus showing the (V) variable (blue), (J) joining (pink) and (C) constant regions (green). The red triangles indicate the RSS at the border of each gene segment. Diversity (D) (purple) regions of the beta chain where DJ recombination occurs.
B: After DJ recombination in the precursor cells, enzymatic activity encoded by RAG initiates the rearrangement of the TCR chain genes. The locus has moved to a more central location and V gene segments undergo looping allowing each an opportunity at combination with the DJ segments.
C: Combination of the selected V regions with DJ segment.
D: Mature TCR transcripts showing the location of complementary determining regions (CDRs).
RSS= recombination signal sequences. Figure adapted from: An overview of T cell receptors, by Bio-Rad[245].

1.9.3 T cell priming and activation

Naïve T cells primed by APCs in the lymphatic system undergo clonal expansion. T cell homeostasis is maintained by subsequent contraction (turnover cycles), releasing further CDR3 DNA into the blood. T cell activation occurs after antigen presentation via MHC class I, which are present on the surface of all nucleated cells, or class II which are only present on the surface of 'professional' APCs such as dendritic cells[237]. The quality and nature of the immune response that follows is dependent upon further molecular signalling and cell to cell communication at the immune synapse. A second signal in the form of co-stimulatory molecule ligation is necessary for full T cell activation. This results in intracellular calcium ion release, required for T cell effector functions such as proliferation, differentiation and cytokine production[249]. Absence of this second signal or presence of co-inhibitory signals regulate the degree of calcium ion release and thus T cell activation and can lead to T cell anergy[40].

The most well characterised co-activatory and inhibitory pathways that have been recognised as regulating T cell function are described in section 1.2.1 and Figure 1.2, the so-called immune checkpoint pathways. In normal tissues, following T cell activation, the upregulation of co-inhibitory signals is the gatekeeper that attenuates the immune response and protects against aberrant recognition of self and auto-immunity[250]. However, tumour cells within the TME can overexpress and manipulate these inhibitory pathways, thus down-regulating anti-tumour T cell responses[251]. Over time, this results in tumour equilibrium and ultimately tumour escape.

1.9.4 T cell differentiation

T cells are released form the thymus as T_N which are known to express high levels of lymph node homing receptor CD26L, a cell adhesion molecule that plays a role in T cell trafficking and migration. T_N cells also express the chemokine receptor CCR7 and the CD45RA isoform. Following antigenic stimulation, T_N cells proliferate and differentiate into effector cells which migrate to peripheral tissues to facilitate destruction of infected targets. When the antigen has been cleared, the majority of effector cells die while a small number, approximately 5% develop into memory T cells[252]. T cells show mutually exclusive expression of CD45RA or CD45RO, as the CD45RA isoform is most highly expressed on resting or naïve T cells, whereas CD45RO is expressed on activated memory T cells. Thus, T cell subsets can be isolated by the expression of cluster differentiation markers on the surface of the cells that are linked to their functionality, as illustrated in Figure 1.11.

Memory T cells have the ability to mount a rapid immune response to a second exposure to an antigen. All memory cells express CD95[253,254]. Subsets of CD8+ memory T cells have been phenotypically defined based on their effector functions using a combination of CD27 (a member of the TNF receptor superfamily), CCR7 and CD45RA[255,256]. $CD45RA^{-}CD8^{+}$ memory T cells expressing CD27 produce IL-2 and IFNγ, but do not have immediate cytotoxic capacity, they are therefore termed 'memory', whereas $CD45RA^{-}CD8^{+}$ T cells that are CD27- produce IFNγ and TNF, but not IL-2 and possess immediate killing ability, they are therefore termed 'effectors'. Thus, memory T cells can be further divided into central (T_{CM}) and effector (T_{EM}) memory cells, and can be defined by expression patterns of CCR7 and CD45RA[252].

T_{CM} cells possess a $CCR7^{+}$ $CD45RA^{-}$ phenotype, are capable of homing to secondary lymphoid organs, but have a limited capacity to produce cytokines. T_{EM} cells have a $CCR7^{-}$ $CD45RA^{-}$ phenotype and are able to display immediate effector function. A subset of T_{EM} cells that re-express CD45RA, named effector T (T_{EFF}) cells have been previously activated and primed, therefore downregulate CD62L and CCR7, as such T_{EFF} migration is restricted. These cells have low proliferative and functional capacity, indicating terminal differentiation and their phenotype is $CD8^{+}CD45RA^{+}CCR7^{-}CD26L^{-}$[257].

In contrast to CD8+ T cells, CD4+ T cells can differentiate into several distinct effector phenotypes, these include, but are not limited to T-helper 1 (Th1), T-helper 2 (Th2), T-helper 17 (Th17), and T_{regs}. The effector functions of these cells are mediated by the cytokines secreted by the differentiated cells[252]. Differentiated CD4+ T cells have several functions including regulating B cell and cytotoxic T cell responses within the TME and maintaining homeostasis and tolerance within the immune system[258].

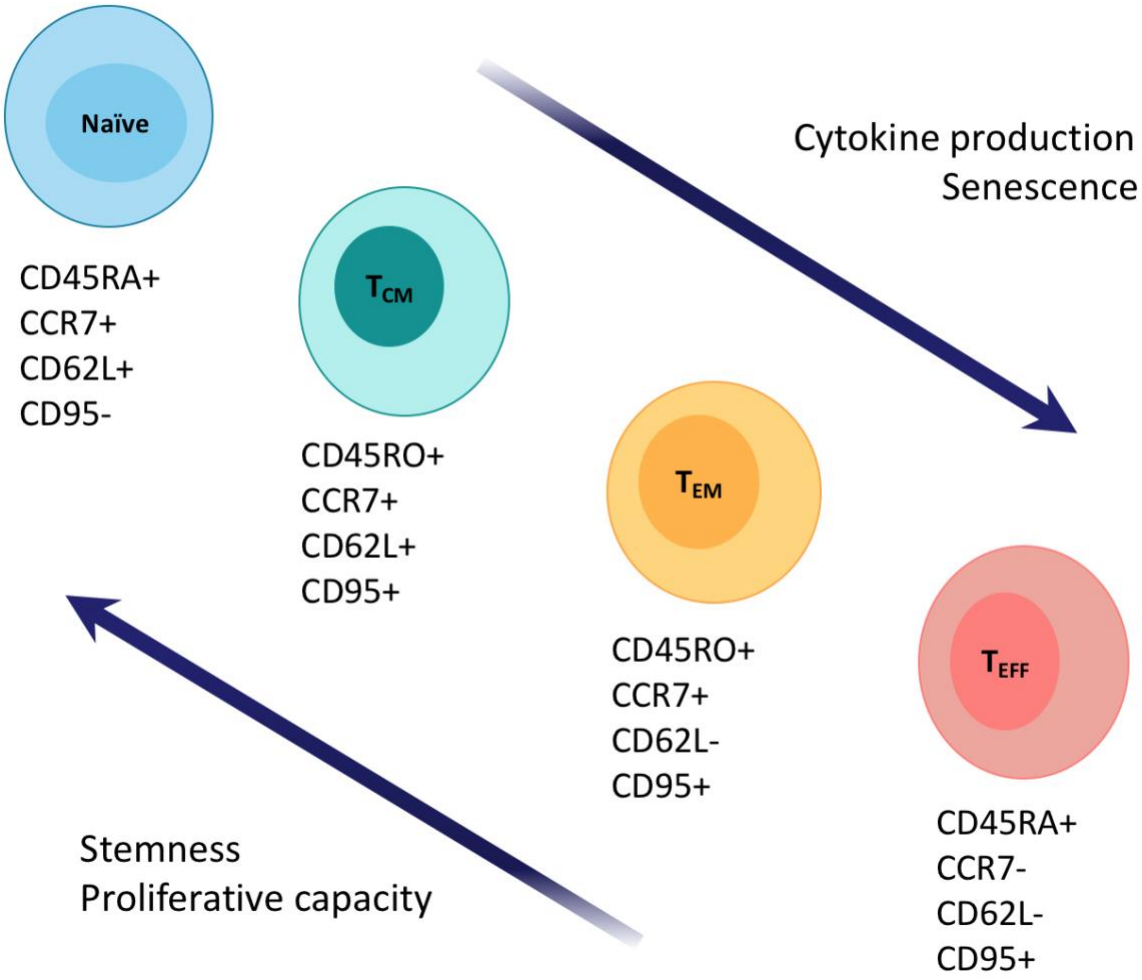

Figure 1.11 T cell differentiation
The stages of T cell differentiation are defined by the cluster differentiation (CD) markers presented. Naïve T cells are the most stem cell like and possess significant proliferative capacity. Naïve T cells give rise to memory T cells which subsequently give rise to the most differentiated effector T cells. These cells are able to produce cytokines, but are also more senescent. Figure adapted from Metabolic Regulation of T Cell Longevity and Function in Tumour Immunotherapy, by Kishton et al[259].
T_{CM} = T central memory, T_{EM} = T effector memory, T_{EFF} = T effector cells

2.0 Project Aims

Despite several candidate circulating markers being suggested as predictive of immune response, these are yet to be prospectively validated for routine clinical use in a standardised and easily reproducible manner. Liquid biopsy represents a minimally invasive approach to monitor dynamic changes in immune responses through immunophenotypic characterisation of subpopulations of PBMCs. In particular, phenotypic investigation of the peripheral T cell compartment early on initiation of ICB treatment in melanoma patients may identify whether peripheral T cells can serve as actionable biomarkers for response to ICB therapy. The TCR is highly relevant in immunotherapeutics as it is here that cancer antigens presented on MHC molecules are identified by host T cells. TCR sequencing facilitates study of clonality and diversity of the receptor. The analysis of TCR repertoire has the potential to act as a predictive tool in order to facilitate patient stratification in the context of ICB therapy in melanoma. To date, this has mainly been exploited in tumour tissue whereas TCR sequencing of peripheral T cells has not been as fully explored and data is limited.

Establishing predictive biomarkers of response to ICB could be instrumental in achieving effective patient stratification as well as tailoring optimal sequencing and scheduling of therapy. The increasing incidence rates of cancer worldwide highlight the ever-growing need to identify novel ways of refining patient care and improving outcomes using precision and personalised immuno-oncology approaches.

My project therefore had the following aims:

1. To determine if peripheral blood T cells can be used to predict response to ICB early after treatment initiation in stage IV melanoma.

2. To identify a candidate biomarker of response to ICB in stage IV melanoma that can be utilised to improve patient care.

3. To ascertain the impact of patient's clinical variables on peripheral T cell and TCR repertoire evolution under the selective pressure of ICB in stage IV melanoma.

4. To identify whether there are changes in circulating T cells early on adjuvant ICB that identify patients with MRD and predict response in stage III melanoma.

Chapter 2: Materials and Methods

2.1 Ethical considerations for collection of patient samples

Ethical approval was obtained and all patient samples were collected with written full-informed patient consent under Manchester Cancer Research Centre (MCRC) Biobank ethics application #07/H1003/161+5 and approval for the work obtained under MCRC Biobank Access Committee application 13_RIMA_01. Healthy volunteers were consented as part of study protocol ethics/12324 given favourable ethical opinion by the University of Manchester Senate Ethics Committee. For the study described in chapter 5, samples were collected under 19_RIMA_08. All clinical investigations were conducted according to the principles expressed in the Declaration of Helsinki and Good Clinical Practice (GCP) guidelines.

2.2 Human Tissue

2.2.1 Tumour samples and matched patient blood

Tumour samples were collected into MACS tissue storage solution (Miltenyi Biotech, Germany), stored at 4°C and processed within 4 hours (h). Blood samples were taken in EDTA coated Vacutainer tubes (Beckton Dickinson, UK), transported and stored at room temperature (RT). They were processed within 4 h of collection.

2.2.2 Peripheral blood samples

Peripheral blood was collected from patients undergoing first line immunotherapy for metastatic melanoma. 30mL of blood was collected in potassium-EDTA coated S-Monovette tubes (Sarstedt, Germany) for the study described in chapter 3. Healthy donor (HD) blood was collected for comparison and for optimisation of flow cytometry experiments. Blood was stored at RT and processed within 4 h.

For the study described in chapter 5, peripheral blood was collected from patients with early stage melanoma undergoing SLNB or CLND surgery followed by adjuvant immunotherapy for stage III disease. For this study, 60mL of blood was collected in total per timepoint, 20mL in

x2 10mL potassium-EDTA coated S-Monovette tubes (Sarstedt, Germany) and 40mL in x 4 10mL Streck tubes (Streck, USA). EDTA blood was stored at RT and processed within 4 h. Streck bloods were stored at RT and processed within 96 h. HD blood was collected and used in other method development work for PBMC and RNA extraction for use in CyTOF and TCR sequencing experiments.

2.3 PBMC isolation from whole blood

2.3.1 Isolation of PBMCs

PBMCs were isolated from whole blood using the SepMate™ (STEMCELL Technologies, Cambridge, UK) protocol and density gradient centrifugation Lymphoprep™ (STEMCELL Technologies, Cambridge, UK) as per manufacturer's instructions. Briefly, to begin, 15mL density gradient medium (Lymphoprep™) was added to the 50mL SepMate™ tube by pipetting it through the central hole of the SepMate™ insert. The top of the density gradient medium was above the insert. Then, the blood sample was diluted with an equal volume of phosphate buffered saline (PBS) + 2% foetal bovine serum (FBS) (1:1) and gently mixed. Keeping the SepMate™ tube vertical, the diluted blood sample was added by gently pipetting it down the side of the tube. The sample was then mixed with the density gradient medium above the insert. The SepMate™ tube was placed in the centrifuge at 1200g for 10 minutes (min) at RT, with the brake applied. After centrifugation, the top layer containing the enriched PBMCs was poured into a fresh sterile 50mL centrifuge tube. To reduce platelet contamination in the enriched PBMCs, some of the supernatant above the PBMC layer was pipetted off before pouring. Cells were then washed with PBS + 2% FBS to make a total volume of 50mL. The samples were then centrifuged at 300g for 8 min at RT with the brake applied, the supernatant discarded, the cell pellet resuspended in PBS + 2% FBS to a total volume of 50mL and a further centrifuge at 300g for 8 min at RT with the brake on was carried out. Supernatant was discarded and cell pellet underwent red blood cell (RBC) lysis followed by cell counting. PBMCs were then used for downstream analysis (section 2.6.2) or cryopreserved in 1mL aliquots (section 2.4.1).

2.3.2 RBC lysis

The 10X RBC Lysis Buffer (BioLegend, UK) was diluted to a 1X working concentration with deionized water. This was done by aliquoting 1mL of 10X lysis buffer into a 50mL falcon tube and adding 9mL of deionized water. The 1X solution was then warmed to RT prior to use. The cell pellet was resuspended in 2mL of 1X RBC Lysis Buffer. The tube was then gently vortexed immediately after adding the lysis solution and incubated at RT, protected from light for 10 min. The sample was then centrifuged at 350g for 5 min with brake applied. Supernatant was then aspirated and the cell pellet was resuspended in PBS + 2% FBS and centrifuged again at 350g for 5 min with brake on. The supernatant was aspirated and the PBMC pellet resuspended in PBS + 2% FBS for cell counting.

2.4 Cell cryopreservation, recovery and counting

2.4.1 Cryopreservation of cells

PBMCs were centrifuged at 250g, after aspiration of the media the cells were washed with PBS, centrifuged again at 250g. The cell pellet was resuspended in cryoprotectant freezing medium made from FBS with 10% Dimethyl sulfoxide (DMSO), (FBS/DMSO). Optimally, $1x10^6$ cells were re-suspended in 1mL FBS/DMSO. Cells were then gradually frozen using 1.8mL Nunc® cryotubes® (Sigma-Aldrich, UK) and a Mr Frosty™ (Thermo Fisher, Altrincham UK), an isopropanol freezing container, and stored at -80°C for at least 24 hours before being transferred to vapour phase liquid nitrogen tanks for long term storage.

2.4.2 Recovery of cryopreserved cells

PBMCs were thawed rapidly by placing cryovials in a water bath at 37°C until some ice crystals remained. Cell suspension was then pipetted into a 15mL falcon tube, 3mL of PBS was added to the cell suspension and then it was centrifuged at 250g and the supernatant discarded. Cells were then resuspended in media, counted and transferred to an appropriate tube for the experiment.

2.4.3 Cell counting

Cells were counted using Trypan Blue exclusion dye (Thermo Fisher, Altrincham UK). 10µl of media/cells was pipetted 1:1 with Trypan Blue into a cell counter slide and then viable cell number per mL estimated using an automated TC20 cell counter (BioRad, Watford, UK).

2.5 Tumour dissociation

Melanoma tumour samples were mechanically and enzymatically dissociated using the gentleMACS system (Miltenyi Biotec, Germany) to disaggregate the tumour. Tissue was first weighed and then cut into small 2-4mm sections using a sterile scalpel. The tissue pieces were then transferred into a C tube with 4.7 mL Roswell Park Memorial Institute 1640 Media (RPMI), 200 µl of enzyme H, 100 µl enzyme R and 25 µl enzyme A as per the manufacturer's instructions (Miltenyi Biotec). The C tube was then subjected to three mechanical disaggregation steps (programs h_tumour_01) separated by two 30 min incubations at 37 °C under continuous rotation using the MACSmix Tube Rotator (Miltenyi Biotec, Germany). Following tumour digest, the sample was passed through 70µm strainer into a fresh sterile 50mL conical tube and washed with 20mL of RPMI. The cell suspension was then centrifuged at 300g for 7 min, supernatant was then aspirated. The cell pellet then underwent red blood cell lysis protocol (section 2.3.2) followed by cell counting and cryopreservation.

2.6 Flow cytometry

2.6.1 Flow cytometry panel design

A summary of the cellular targets chosen and the justification for these is appraised in Table 2.1.

Table 2.1 Summary of cellular targets included in flow cytometry panel

Target	Justification for inclusion
Live/Dead	Dead cells are highly auto-fluorescent and non-specifically bind antibody, staining allows removal from further analysis, reducing false positive events.
CD3	A co-receptor of the TCR complex and plays a role in antigen recognition, signal transduction, and T cell activation.
CD4	A co-receptor of the TCR. Identifies T helper cells. Specific for class II MHC protein.
CD8	A co-receptor of the TCR. Identifies cytotoxic T cells. Specific for class I MHC protein.
CD25	A glycoprotein known as the low-affinity IL-2 receptor (IL-2R), enables T cells to respond to the growth-promoting cytokine IL-2.
CD27	Expressed on mature T cells and is upregulated upon T cell activation.
CD31	An inhibitory co-receptor involved in regulation of T cell homeostasis, effector function and trafficking.
CD45RA	A specific splice variant of the transmembrane tyrosine phosphatase CD45. The CD45RA isoform is most highly expressed on resting/ naïve T cells.
CD45RO	A splice variant of CD45, is expressed on activated memory T cells.
CD127	Also known as the IL-7 receptor is a 60–90kDa type I transmembrane glycoprotein.
CCR7	Both memory ($CD45RO^+$) and naïve ($CD45RA^+$) $CD4^+$ and $CD8^+$ T cells express the CCR7 receptor. Within the memory T cell population, CCR7 expression discriminates between T cells with effector function that can migrate to inflamed tissues ($CCR7^-$) compared to T cells that require a stimulus prior to displaying effector functions ($CCR7^+$).
PD1	Inhibitory immune checkpoint molecule. Binding leads to reduced T cell proliferation.
Ki67	Required for cell proliferation and is commonly used as a marker for proliferating cells.

The flow cytometry panels and antibody conjugates used for the study described in chapter 3 are described in the tables below.

Table 2.2 T cell regulatory panel

Target	Fluorophore	Clone	Antibody Dilution (µl)	Company	Catalogue Number
Live/Dead	Zombie UV		1:200	Thermo Fisher	L23105
CD3	PerCP/Cy5.5	OKT3	1:100	BioLegend	317336
CD4	BV610	OKT4	1:100	BioLegend	317438
CD8	PE-Cy7	HIT8a	1:40	BioLegend	300914
CD25	APC	BC96	1:10	BioLegend	302610
CD127	PE	A019D5	1:40	BioLegend	351304

Table 2.3 T cell maturation panel

Target	Fluorophore	Clone	Antibody Dilution (µl)	Company	Catalogue Number
Live/Dead	Zombie UV		1:200	Thermo Fisher	L23105
CD3	PerCP/Cy5.5	OKT3	1:100	BioLegend	317337
CD4	BV610	OKT4	1:100	BioLegend	317438
CD8	FITC	HIT8a	1:40	BioLegend	300906
CD45RA	BV421	HI100	1:100	BioLegend	304130
CD45RO	APC-Cy7	UCHL1	1:200	BioLegend	304228
CD31	PE-Cy7	WM59	1:40	BioLegend	303118
CD27	APC	M-T271	1:200	BioLegend	356410
CCR7	PE	150503	1:20	BD Pharmingen	560765

Table 2.4 T cell reinvigoration panel

Target	Fluorophore	Clone	Antibody Dilution (µl)	Company	Catalogue Number
Live/Dead	Zombie UV		1:200	Thermo Fisher	L23105
CD3	PerCP/Cy5.5	OKT3	1:100	BioLegend	317337
CD4	BV610	OKT4	1:100	BioLegend	317438
CD8	FITC	HIT8a	1:40	BioLegend	300906
CD45RA	BV421	HI100	1:100	BioLegend	304130
CD45RO	APC-Cy7	UCHL1	1:200	BioLegend	304228
CD27	APC	M-T271	1:200	BioLegend	356410
CCR7	PE	150503	1:20	BD Pharmingen	560765
PD1	PE/Dazzle	EH12.27	1:40	BioLegend	329939
Ki67	Alexa Fluor 488		1:20	BioLegend	350507

2.6.2 Sample preparation for fluorescence-activated cell sorting analysis

Following isolation, PBMCs were kept at 4°C in PBS plus 2% FBS and analysed within 24 h. PBMCs were suspended in fluorescence-activated cell sorting (FACS) buffer (PBS containing 2% FBS, 2mM EDTA and 0.02% sodium azide) plus 50ul of Brilliant Stain Buffer (BD Biosciences, San Diego, CA, USA) and Human TruStain FcX (BioLegend, San Diego, CA, USA) as per manufacturer's instructions, and incubated at RT for 40 min with T cell regulatory (Table 2.2) and T cell maturation (Table 2.3) panels of fluorochrome labelled antibodies. LIVE/DEAD Fixable Blue Dead Cell Stain was added to the final suspension to exclude dead cells. Stained PBMCs were washed once at 300g for 7 min in FACS buffer ready for analysis.

For T cell reinvigoration staining, which was performed for 5 patients, PBMCs previously cryopreserved in FBS/DMSO were thawed in cold RPMI and washed twice. Then, PBMCs were suspended in FACS buffer and Human TruStain FcX (BioLegend, San Diego, CA, USA), as per the manufacturer's instructions, and incubated at RT for 40 min with antibodies targeting the receptors described in Table 2.4. Stained PBMCs were then fixed and permeabilized with a Cytofix/Cytoperm kit (BD Biosciences, San Diego, CA, USA) according to the manufacturer's instructions and stained for Ki67 for 30 min at RT. Stained cells were then resuspended in FACS buffer ready for analysis.

2.6.3 Flow cytometry controls

For FACS analyses, it was necessary to use appropriate controls to record accurate and reliable results from the flow cytometry panel. As the various antibodies were conjugated to different fluorophores, compensation matrices were acquired by using single antibody stained compensation bead controls (Anti-Mouse Comp Beads, BioLegend, UK). Fluorescence minus one (FMO) controls were performed to identify correct gating positions. Biological controls of HD PBMCs were included where necessary to enable normalisation of data.

2.6.3.1 Compensation Matrix

Prior to data acquisition, correction for any fluorophore/fluorescent spectral overlap was performed by creating a compensation matrix that was subsequently applied to data acquisition. The compensation matrix corrects for fluorescence from fluorophore A that is emitted and can be detected in the channel for fluorophore B. This would give a false positive population in the read-out of fluorophore B. Therefore, compensation was performed using single stained antibody compensation beads, to allow for dimly expressed markers and to eliminate autofluorescence from cells.

2.6.3.2 Fluorescence minus one controls

Fluorescence minus one (FMO) control wells exclude one fluorophore from the conjugated antibody fluorophore panel, and were used for each fluorophore in the panel. The purpose of FMO controls was to aid differentiation between specific and non-specific antibody binding and to identify any fluorescence spill-over into incorrect channels. Thus, they were an important gating control to confirm positive population gates were correctly placed and data accurately recorded. Exclusion of the fluorophore to be gated allowed observation of the true spread of the negative population and accounted for the background antibody staining of the remaining fluorophores. This gate was then applied to a sample which contained all fluorophores to identify the positive cells.

2.6.4 Gating strategy

The gating strategy for the identification of T cell subsets, specifically regulatory T cells and T cell maturation in peripheral blood of melanoma patients is illustrated in Figure 2.1. Two panels were designed to identify the aforementioned T cell populations. For both panels, all cells were assessed using the side scatter (SSC) and forward scatter (FSC) to provide information about the granularity and size. As these panels were aimed at identifying single lymphoid cells, FSC area (FSC-A) and width (FSC-W) were used to identify single cells and exclude doublets or multiple cells stuck to each other. Next, use of the live/dead dye distinguished viable cells from dead cells and therefore only viable cells were considered for downstream analysis. To identify regulatory, memory and emerging T cells, two different panels were designed. Panel 1 (Table 2.2) has been used to identify CD3+ and CD4+ lymphoid cells. To identify regulatory T cells CD3+ CD4+ populations simultaneous analysis of CD25 and CD127 of the CD3+ CD4+ population revealed regulatory T cells. The proportion of CD3+ lymphocytes expressing the naïve/memory markers CD45RA and CD45RO were analysed using a second panel. This panel also included antibodies specific for CD4, CD8, CD27, CD31 and CCR7 to assess the phenotypes of differentiated T cells and was termed the maturation panel (Table 2.3). Immune effector T (T_{IE}) cells were quantified as the percentage of $CD27^{-}CCR7^{-}$ cells in the $CD3^{+}CD8^{+}CD45RO^{+}CD45^{-}$ gate.

2.6.5 Data acquisition and analysis

Data acquisition was performed using LSR II, LSR Fortessa, Aria II or Aria III (Special Order Research Product) (BD Biosciences) cytometers and FlowJo v.10 software (Tree Star Inc., USA) was subsequently used to analyse the data.

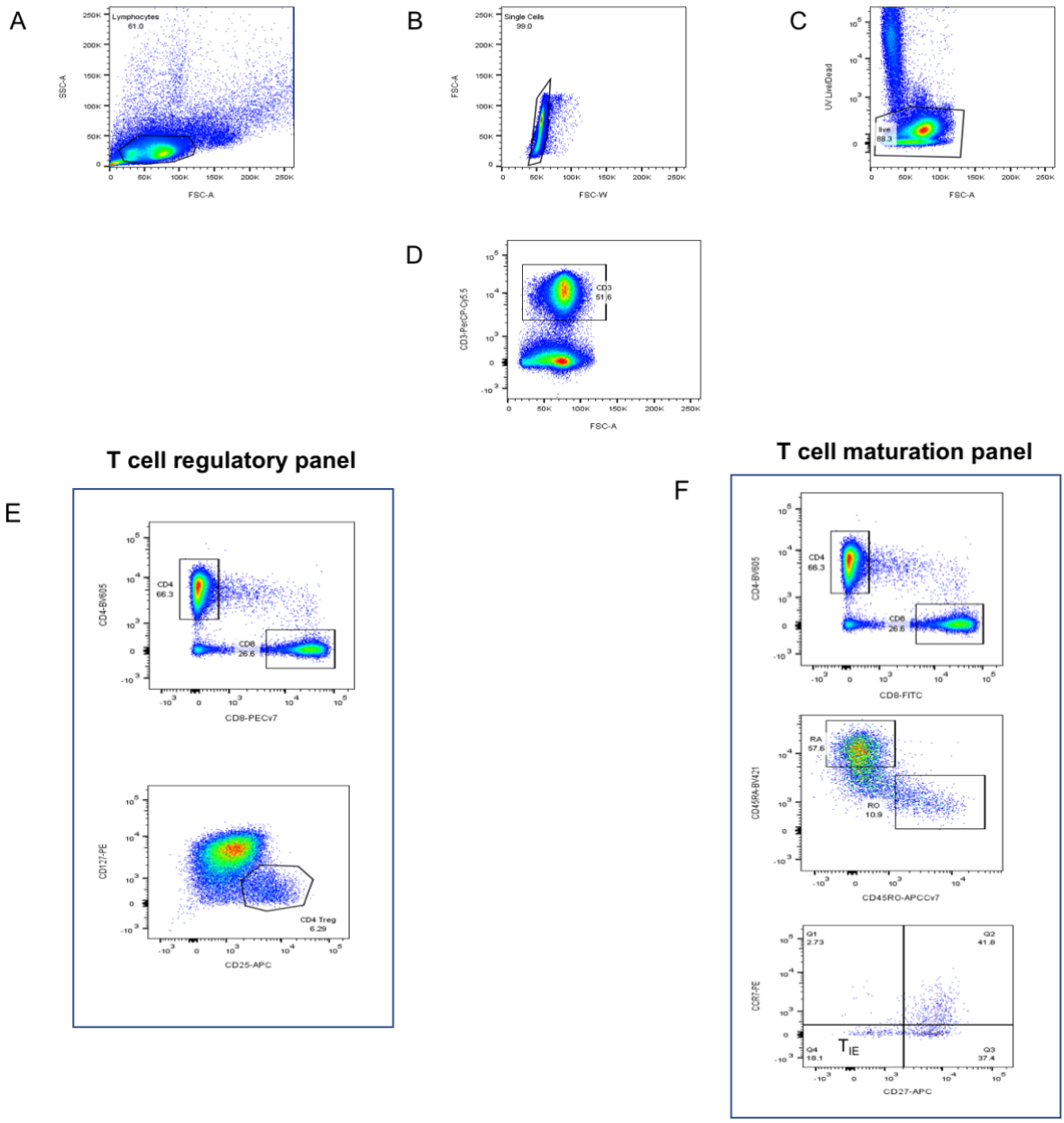

Figure 2.1 Gating strategy for identifying T cell subsets
Single cell suspensions prepared from PBMCs were surface stained with antibodies against T cell markers.
A) Lymphocytes are first identified by size and internal complexity on FSC-A and SSC- A.
B) Doublets are excluded by selecting single cells on FSC-A and FSC-W dot plot.
C) Live cells are selected by gating on cells negative for Zombie UV viability dye to exclude dead cells from subsequent gates.
D) CD3+ gate for T cells.
E) CD4+ and CD8+ gates were defined for “helper” and “killer” T cell subsets, regulatory T cells were identified in the CD4+ CD25+ CD127- population.
F) CD4+ and CD8+ gates were defined for “helper” and “killer” T cell subsets, CD8+ population was used for identifying the mature T cells. CD8+ population was further characterised by CD45RA and CD45RO. CD8+ memory T cell subsets and CCR7- CD27- represents the T_{IE} cells.

2.7 Statistical Analysis

2.7.1 Peripheral T cells as an early biomarker for response and toxicity in melanoma patients treated with immunotherapy (Chapter 3)

Correlation between continuous variables was performed with Spearman test, the Spearman r was reported as a measure of the correlation magnitude. Delta week 3 values (Δ_{W3}), were calculated as the difference between week 3 and baseline T0 values. Delta week 12 values (Δ_{W12}) were calculated as the difference between week 12 and baseline T0 values.

All statistical tests were two tailed and the statistical differences between two groups for numerical variables were assessed using two-tailed Mann-Whitney U test (unpaired comparisons) or Wilcoxon test (paired comparisons). Kaplan-Meier plots with the log-rank test (3-week landmark analysis) were used to analyse the survival data. Univariate Cox regression was used to calculate the hazard of death. P values <0.05 were considered significant. Circulating T cell phenotypic subset analyses was corrected for multiple testing (Bonferroni correction). Analyses were performed using Prism version 7.0.

2.7.2 Clinical correlates of peripheral T cell responses to immunotherapy in melanoma (Chapter 4)

Correlation between continuous variables was performed with Spearman test, the Spearman r was reported as a measure of the correlation magnitude. Delta week 3 values (Δ_{W3}), were calculated as the difference between week 3 and baseline T0 values. Linear discriminant analysis was used to separate Δ_{W3}Renyi index and Δ_{W3}Gini coefficient and categorise the values in classes. Mann-Whitney U test (two-sided) was used for comparison between continuous variables. Comparison between categorial variables was performed with Fisher's exact test. All tests were two-sided and p values <0.05 were considered significant. Analyses were performed using Prism version 7.0.

TCR sequences were analysed using ImmunoSEQ® ANALYZER (Adaptive Biotechnologies, Seattle, USA). Gini coefficient was used as a measure of clonality[260] and calculated with the function *clonality* from LymphoSeq R package. Diversity was calculated using Renyi index (α=1) as per Spreafico et al[261], with time point pairwise analysis for each individual patient.

2.8 Mass Cytometry by time of flight

Mass cytometry by time of flight (CyTOF), is a variation of flow cytometry in which antibodies are labelled with heavy metal ion tags rather than fluorophores. Readout is by time of flight mass spectrometry using Helios (Fluidigm, USA). Conventional flow cytometers, that use fluorescently conjugated antibodies to detect cellular antigens have a limited spectral profile of approximately 14 channels[262]. The number of metals currently available is up to 40. Therefore, CyTOF has advantages over traditional fluorescent flow cytometry as it facilitates a significantly greater number of parameters to be studied per cell and has a higher sensitivity. Key advantages include the lack of spreading errors from fluorophores and no requirement for compensation controls as there is no equivalent to autofluorescence of cells in mass cytometry. The main disadvantage of the CyTOF platform, is that cells are incinerated and therefore there is no capability for cell sorting.

2.8.1 Panel design

Tables 2.5 and 2.6 illustrate the 37-marker custom design CyTOF panel used in the study described in Chapter 5.

Table 2.5 Intracellular markers

Target	Clone	Company	Catalogue Number
*127IdU		Fluidigm	201127
Tbet	4B10	Fluidigm	3161014B
FOXP3	PCH101	Fluidigm	3162024A
Caspase 3 (cleaved)	D3E9	Fluidigm	3142004A
Ki-67	B56	BioLegend	350523
EOMES	644730	R&D Systems	MAB6166
KLRG1	2388C	R&D Systems	MAB70293
TIGIT	MBSA43	Fluidigm	3153019B

*****5-Iodo-2′-deoxyuridine (IdU) incorporates into DNA of proliferating cells and is a marker of S-phase of the cell cycle. It is detected in the 127I (iodine) channel of the CyTOF mass cytometer and bypasses the need for an antibody or DNA denaturation.

Table 2.6 Surface markers

Target	Clone	Company	Catalogue Number
CD45	HI30	Fluidigm	3089003B
CD45RA	HI100	Fluidigm	3169008B
CD45RO	UCHL1	Fluidigm	3164007B
CD3	UCHT1	Fluidigm	3141019B
CD4	RPA-T4	Fluidigm	3145001B
CD14	RMO52	Fluidigm	3148010B
CD25	2A3	Fluidigm	3149010B
CD223/LAG- 3	11C3C65	Fluidigm	3150030B
CD103	Ber-ACT8	Fluidigm	3151011B
CD95/Fas	DX2	Fluidigm	3152017B
CD183/CXCR3	G025H7	Fluidigm	3156004B
CD16	3G8	Fluidigm	3165001B
CD11b/Mac-1	ICRF44	Fluidigm	3167011B
CD8a	SK1	Fluidigm	3146001B
CD152/CTLA-4	14D3	Fluidigm	3170005B
CD185/CXCR5	51505	Fluidigm	3171014B
HLA-DR	L243	Fluidigm	3173005B
CD279/PD-1	EH12.2H7	Fluidigm	3174020B
CD274/PDL1	29E.2A3	Fluidigm	3175017B
CD127/IL-7Ra	A019D5	Fluidigm	3176004B
CD56	NCAM16.2	Fluidigm	3163007B
CD27	L128	Fluidigm	3155001B
CD28	CD28.2	BioLegend	302937

CD62L	DREG-56	BioLegend	304835
TIM-3	F38-2E2	Fluidigm	3154010B
Anti-TCF1 (TCF7)	7F11A10	BioLegend	655202
CD39	A1	Fluidigm	3160004B
CD134/OX40	ACT35	Fluidigm	3158012B
CD197 (CCR7)	G043H7	Fluidigm	3159003A

2.8.2 CyTOF Optimisation: Ficoll-paque PBMC isolation using LeucoSep™

Ficoll-paque PBMC preparation can be performed using LeucoSep™ or SepMate™ protocols. Ficoll contains iodine and is a density gradient medium used to separate mononuclear cells from whole blood. Iodine contamination can affect the CyTOF signal when analyzing samples, thus the PBMC isolation protocol used may affect the extent of iodine contamination and consequently the strength of the cyTOF signal when running samples on Helios. Therefore, a comparison of both the SepMate™ and Leucosep™ protocols was undertaken to assess cell viability and the extent of iodine contamination. The results are described in section 5.6.1 and section 5.6.2. The SepMate™ PBMC isolation protocol is described in section 2.3.1.

The Leucosep ™ protocol consisted of adding 15mL of Ficoll medium (Ficoll-Paque Plus™, Amersham Biosciences) into a 50mL falcon tube by placing the stripette against the tube wall to avoid bubble formation. Next, 10mL of blood was added to a new 50 mL Falcon tube and 10mL of PBS was added (1:1). The blood and PBS were mixed by gently inverting the Falcon tube two to three times. Using a 25mL stripette against the wall of the tube with low speed aspiration, the blood-PBS mix was added on top of Ficoll medium very gently, to avoid mixing of blood with Ficoll medium. The Ficoll-Blood-PBS mix was centrifuged at 1000g for 10 min at RT with no brake applied to create a density gradient. The plasma layer was removed using a Pasteur pipette up to a minimum remnant of 5-10mm above the interphase to prevent contamination of the enriched cells with platelets. The layer containing the PBMCs was then isolated with a fine bore Pasteur pipette and placed into a new 50 mL Falcon tube. The enriched cell fraction was then washed with 10mL PBS and subsequently centrifuged at 250g for 10 min at RT with breaks on. This wash step was repeated twice, supernatant discarded and the cell pellet resuspended in 5mL PBS. Cells were then counted and used for downstream applications or cryopreserved in 1mL aliquots.

2.8.3 CyTOF workflow

The CyTOF workflow comprised of 3 days from receipt of whole blood sample to processing in the laboratory and subsequent analysis of the sample on Helios. On day 1, 20mL EDTA whole blood sample arrived in the laboratory, SepMate^{TM} PBMC isolation protocol was performed. Single cell suspension was stained with cisplatin (198 cisplatin) in PBS for 5 min. Cisplatin is a live/dead stain preferentially labelling non-viable cells resulting in a platinum signal that is quantifiable by mass cytometry. Cells were quenched with MaxPar cell staining buffer and washed with MaxPar PBS then Fc blocking reagent was added to staining buffer for 10 min and cells stained with surface antibodies for 30 min. Following this, cells were washed with MaxPar PBS and stained with intercalator iridium (193Ir DNA2) in MaxPar fix/perm buffer before cryopreservation in cell staining media (CSM)/DMSO. 193Ir DNA2 was used to discriminate dead cells from live cells. This workflow is illustrated in Figure 2.4.

When considering how to batch and run samples, waiting for each patient to undergo surgery and complete 5 cycles of 3 weekly ICB therapy could take approximately 5-6 months causing significant delay before acquisition of all of one patients' samples would be possible. This approach was considered to try and minimize batch effects. However, this was time consuming and limited ability to generate data and assess for signal. Therefore, the optimised workflow involved prospective collection, processing and cryopreservation of each patient's blood sample according to the day 1 work flow.

The first 10 patients pre-operative blood samples were batched together for day 2 work flow, then the next 10 samples and so on for each time point. Figure 2.5 illustrates the steps involved in work flow for day 2. The 10 batched samples will be thawed, barcoded (multiple samples stained together, reducing technical variability) and pooled for intracellular antibody labelling then fixed in 4% paraformaldehyde (PFA) overnight. Prior to iridium labelling and acquiring samples on Helios on day 3 as illustrated in Figure 2.6.

Data analysis performed with clustering algorithms in Bioconductor. These modules are run through R. A t-distributed Stochastic Neighbour Embedding (t-SNE) based clustering algorithm utilised and led by the bioinformatics team at Cancer Research UK Manchester Institute.

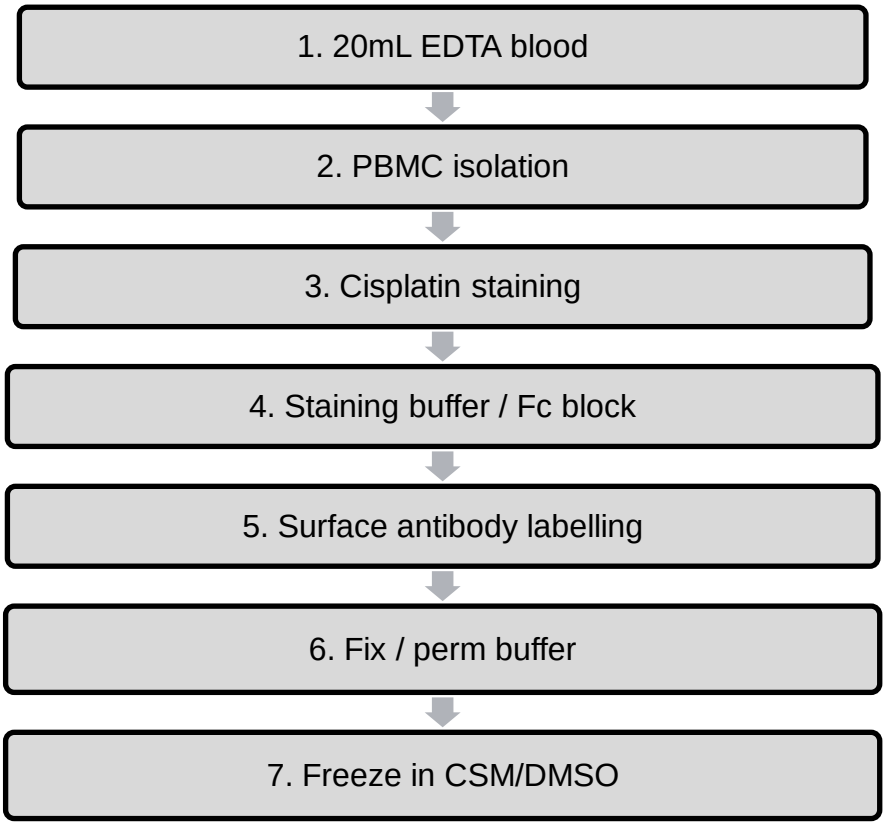

Figure 2.4 CyTOF work flow day 1
Following receipt of whole blood sample to the laboratory the flow diagram illustrates the steps involved in sample processing on day 1 for downstream analysis.

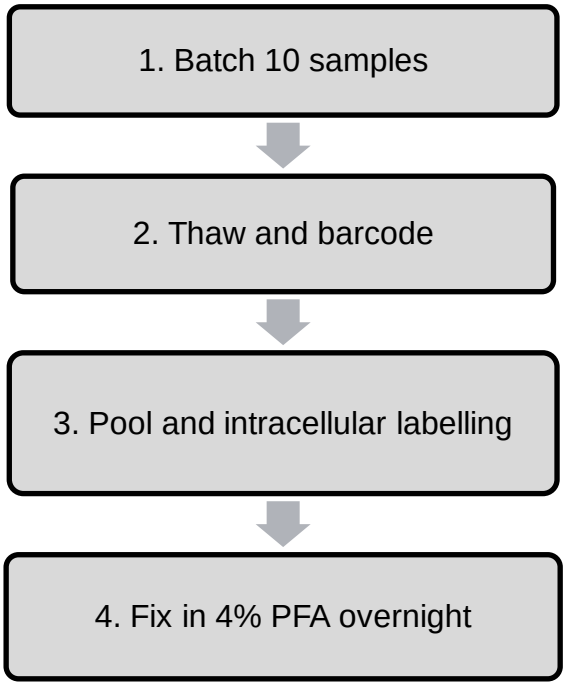

Figure 2.5 CyTOF work flow day 2
When 10 samples have been batched, the flow diagram illustrates the steps involved in sample processing on day 2 for downstream analysis.

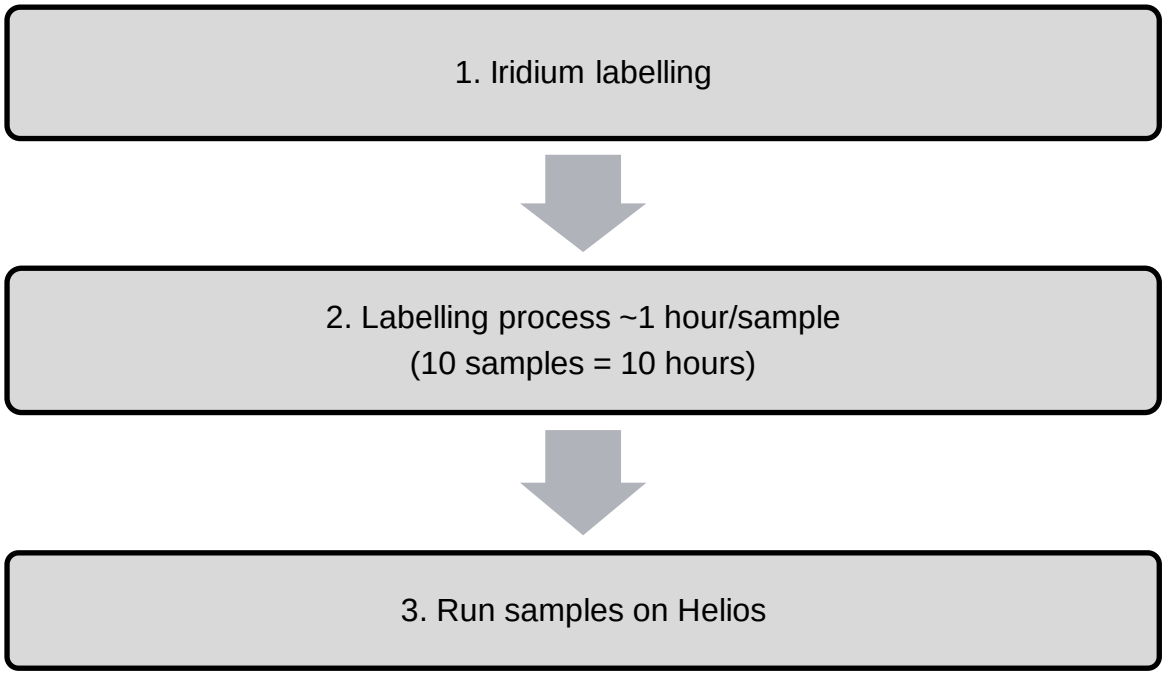

Figure 2.6 CyTOF workflow day 3
The flow diagram illustrates the steps involved in labelling on day 3 for sample acquisition.

2.9 TCR Sequencing

For the study described in Chapter 4, an immunoSEQ® TCRB Assay kit (Adaptive Biotechnologies) was used to amplify and sequence TCR sequences in DNA of PBMCs as per manufacturer instructions. This was carried out by Molecular Biology Core Facility at Cancer Research UK Manchester Institute. Pooled libraries were quantified by quantitative PCR using the KAPA Library Quantification Kit for Illumina platforms (#KK4873, Kapa Biosystems). Sequencing was carried out by clustering 0.6–1.1 pM of pooled libraries on the Illumina NextSeq 500.

For the study described in Chapter 5, the approach for TCR sequencing on RNA extracted from PBMCs and CLND tumour using Qiagen Immune repertoire RNA library is described in section 5.5.1.4 and 5.5.2.2 respectively.

2.10 RNA extraction and quantification

For the study described in Chapter 5, RNA extraction was required for next generation sequencing (NGS) using the Illumina platform to assess the TCR repertoire of patients' PBMCs at longitudinal time points pre-operatively and on ICB therapy. Additionally, there was a plan for TCR repertoire assessment on baseline fresh tumour samples from patients undergoing CLND.

Initially, as part of the optimisation work, PBMCs were isolated from HD and RNA was extracted for fresh analysis of RNA concentration and RNA integrity (RIN) then compared with cryopreserved PBMCs from the same HD, which were subsequently thawed and RNA extracted to assess for significant differences in RNA concentration or RIN value that would affect downstream analysis. This experiment was performed to optimise the work flow for TCR sequencing and the method is described in section 2.10.1.

2.10.1 RNA extraction, concentration and quantification

RNA from cell pellets was extracted using the RNeasy® plus mini kit (Qiagen, Manchester UK). Before starting, add 10µL of β-mercaptoethanol per 1mL of RNeasy Mini Kit lysis buffer (Buffer RLT Plus). The cells were disrupted by adding the appropriate volume of Buffer RLT Plus (350µL for $<5x10^6$ cells, 600µL for $5x10^6$-$1x10_7$ cells) to the sample and mixed thoroughly using a pipette. Next, the lysate was homogenised by pipetting it into a QIAshredder spin column (Qiagen, UK) placed in a 2ml collection tube and centrifuged for 2 min at full speed (17,000g). Then the aliquots were mixed by pipetting with either 350µL or 600 µL of 70% ethanol (in order to keep a 1:1 ethanol: lysate ratio). Subsequently, up to 700µL of the sample was transferred to RNeasy spin column placed in a 2ml collection tube and centrifuged for 15 seconds (s) at 13,500g and the flow through discarded. If the sample volume exceeded 700µL this step was repeated and the collection tube reused.

Contaminating DNA was removed from each RNA extract by means of DNase treatment, which involved performing column DNase digestion. DNase I stock solution was prepared by dissolving lyophilised DNase I (1500KU) in 550µL of RNase free water. This was done by injecting the RNase free water into a vial containing the lyophilised DNase using needle and syringe then mixing gently by inverting the vial. Single use aliquots were then cryopreserved at -20°C and stored for up to 9 months. Next, 350µL Buffer RW1 (Qiagen, UK) was added to the RNeasy spin column placed in a 2ml collection tube and centrifuged for 15 s at 13,500g to wash the spin column membrane, the flow through was discarded and the collection tube reused. Then 10µL DNase I stock solution was added to 70µL Buffer RDD (Qiagen, UK) which was mixed gently by inverting the tube and centrifuged for 15 s at 13,500g to collect residual liquid from the sides of the tube. Next, the DNase I incubation mix (80µL) was added directly to the RNeasy spin column membrane and placed on the benchtop at RT (20-30°C) for 15 min. Then, 350µL Buffer RW1 was added to the RNeasy spin column and centrifuged for 15 s at 13,500g and flow through discarded. Subsequently, 500µL Buffer RPE (Qiagen, UK) was added to the RNeasy spin column placed in 2ml collection tube and centrifuged for 15 s at 13,500g to wash the spin column membrane and flow through discarded and the collection tube reused. Then, 500µL Buffer RPE (Qiagen, UK) was added to the RNeasy spin column and centrifuged for 2 min at 13,500g to wash the spin column membrane. The longer centrifugation dries the spin column membrane, to ensure that no ethanol was carried over during RNA elution as residual ethanol may interfere with downstream analysis. After centrifugation, the RNeasy spin column was carefully removed from the collection tube so that the column did not contact the flow-through, to avoid carry over of ethanol. Then the RNeasy spin column was transferred to a new 2ml collection tube and centrifuged at full speed (17,000g) for 1 min to remove any potential carry over of Buffer RPE, or residual flow through

from the outside of the RNeasy spin column. The RNeasy spin column was then placed into a new 1.5ml collection tube and 30–50µl RNase free water was added directly to the spin column membrane and a timer set for 1 min, before centrifuging for 1 min at 13,500g to elute the RNA. Measurement of RNA concentration was carried out using the Nanodrop 1000 (Thermo Fisher Scientific, UK) and RNA quantified using the Qubit RNA HS Assay (Thermo Fisher Scientific, UK) according to manufacturer's instructions.

2.11 ctDNA

2.11.1 Screening for mutations in primary tumour to track in ctDNA

The DNA mutations tracked in ctDNA were identified in the primary tumour FFPE samples. Primary tumour blocks sent to the Manchester Genomic Medicine Centre (MGMC) using the Royal Mail Safebox system^{TM}, which has been reliably used for a number of clinical trials. DNA was extracted from the formalin fixed and paraffin embedded (FFPE) primary tumours and sequenced using a targeted NGS panel of 34 genes by the MGMC, a UKAS accredited laboratory. The assay is validated to meet ISO15189 standards. The technology does not require germline DNA for analysis and is optimised for use with FFPE derived DNA samples.

Tumour cell content was checked prior to DNA being extracted and the quality of DNA tested prior to NGS testing. Patients who did not have a *BRAF*, *NRAS*, or *TERT* mutation identified in the primary tumour that can be tracked by ctDNA were not enrolled in the study. The assay is capable of detecting single nucleotide variants (SNVs) and indels <40bp in size to at least 5% allele fraction and gene level copy number gain/loss and loss of heterozygosity events. The assay uses Qiaseq primer extension enrichment technology, which incorporates unique molecular indexes 'molecular barcodes' to enhance variant detection. The assay comprises a custom panel of 34 oncogenes which are listed in Table 2.8.

Table 2.8 Genes in validated NGS panel for use in FFPE samples

Genes in validated NGS panel
KRAS, NRAS, BRAF, PIK3CA, KIT, PDGFRA, EGFR, TP53, CDKN2A, HRAS, IDH1, IDH2, H3F3A, TERT, PTEN, H3F3B, ATRX, HIST1H3B, HIST1H3C, HIST2H3C, VHL, MET, CTNNB1, ALK, GNAQ, GNA11, B2M, STK11, ERBB2, AR, MAP2K1, AKT1, DDR2, FGFR3

2.11.2 Blood sample processing

Blood samples were taken in Streck tubes (Streck, USA) at the patient's appointment with the clinical team with a pre-specified 96 h window between the blood being taken and plasma extraction. Streck tubes stabilise ctDNA for up to 14 days. Plasma was processed to double spun plasma at The Christie NHS Foundation Trust and stored in MCRC Biobank until requested to be transferred to the Cancer Biomarker Centre at Cancer Research UK, Manchester Institute for cfDNA isolation and quantification. In order to test for mutations, blood was centrifuged and cell-free DNA extracted from plasma for downstream ctDNA analysis.

2.11.3 ctDNA assay

The ctDNA assay uses droplet digital polymerase chain reaction (ddPCR) technology (BioRad) to analyse for the presence of mutations in cfDNA. The ddPCR assay focuses on mutations that are well characterised in melanoma and have been reproducibly detected at all stages of disease[263,192], *BRAF, NRAS* and *TERT* promoter mutations. They are either driver mutations and/or early events in the evolution of melanoma. Although NGS testing of the primary tumour will identify other mutations e.g. *TP53*, the study only included patients with the following mutations: *BRAF* (V600E, V600K and V600R), *NRAS* (Q61R, Q61K, Q61L and G12D), *TERT* promoter (146 C>T and 124 C>T), which can be tracked in ctDNA with exact point mutation known, as these have been fully validated and cover approximately 80% of patients. A droplet generator is used to partition the ddPCR reaction mix into thousands of nanolitre sized droplets. After PCR on a thermal cycler, droplets from each sample analysed individually using an optical detection system resulting in an absolute quantification of the mutations present. It does not require germline DNA or bioinformatics support, which is an advantage over NGS based ctDNA tests. Currently detectable ctDNA is defined as 1 mutant *BRAF* copy/20mL plasma (equivalent to 40mL of blood/4 tubes) by ddPCR.

2.11.4 Longitudinal ctDNA monitoring

Blood samples were collected from all potentially eligible patients consented into the study pre-operatively on the day of surgery. Recruited patients then had repeat blood sample taken for ctDNA longitudinally at baseline and prior to each cycle of adjuvant ICB therapy or until evidence of clinical/radiological disease progression. Following completion of adjuvant therapy, further longitudinal blood sampling taken at clinic visits every 3 months for up to 24 months or until evidence of clinical/radiological disease progression.

Chapter 3: Peripheral T cells as an early biomarker for response and toxicity in melanoma patients treated with immunotherapy

3.1 Introduction

Over the last decade, melanoma research has driven some of the most significant changes in treatment approaches observed in oncology. The advent of ICB has dramatically changed the treatment landscape and improved the outcomes of melanoma patients. Despite this unprecedented progress, patients are still dying of their disease, indicating the urgent need to identify which patients will respond to therapy, in order to improve patient stratification and avoid unnecessary toxicity risk. In the metastatic setting, an unmet clinical need is the prompt identification of responders and non-responders to immunotherapy, to minimise time patients spend on ineffective drugs and permit a switch to second line therapies, thereby limiting the time the tumour has to progress and improving the chances of achieving meaningful clinical benefit.

The lack of validated biomarkers to monitor immune response following ICB treatment is a key hurdle for the implementation of cancer immunotherapy. Despite ICB revolutionising cancer care, our understanding of T cell evolution on treatment, under the selective pressure of ICB remains incomplete, limiting our ability to acquire full clinical benefit from these drugs. The use of ICB has demonstrated durable responses in several malignancies. However, the response to treatment is variable and currently unpredictable. The immune landscape of host and tumour are integral in determining how patients will respond to ICB therapy. There has been recent emphasis on exploring T cell changes in the circulation during treatment and immunophenotyping has been utilised as a method of measuring these changes. However, in melanoma ICB therapy, attention to date has mainly centred around TILs.

A pivotal study evaluating TIL T cell repertoires has identified that anti-PD-1 therapy enables selective intratumoural expansion of tumour-reactive clonotypes and diversity of the T cell

repertoire is associated with anti-PD-1 induced tumour clonal evolution[228]. The authors also found that changes in T cell repertoire were directly proportional to changes in the fraction of clonal mutations in patients with response to treatment[228]. It is therefore posited that as T cell clones expand within the tumour of responding patients, clonal mutations are targeted and removed. How these TIL T cell repertoire changes are then reflected in the periphery has not yet been fully elucidated.

Furthermore, as immune checkpoints have been shown to modulate T cell responses to self-proteins as well as to infection and tumour antigens[44], it is proposed that the immune response to ICB therapy in melanoma would follow similar dynamics to the T cell response to stimulus such as infection. Within the literature, a specific subset of cytotoxic memory effector T cells ($CD8^+CD4^-CD45RO^+CCR7^-CD27^-$) has been extensively described in the context of effective cytotoxic response to viral infection[252,264]. These cells are characterised by production of IFNγ, perforin and IL-4, with immediate cytotoxic potential ex vivo[265]. Additionally, characterisation of TILs in tumours from melanoma patients revealed an increased infiltration of melanoma metastases by the same cytotoxic memory subset in patients who responded to single agent anti-PD1 therapy[266]. Given the inherent issues with tissue biopsies, blood-based biomarkers have the potential to guide clinical decision making, but have not been widely explored in this setting. Thus far, no immune-monitoring strategies have been validated for routine clinical practice. However, peripheral T cells do hold promise in biomarker research for melanoma, but require further evaluation in prospective studies to ascertain their predictive abilities.

3.2 Hypothesis and Aims

Checkpoint inhibitor drugs awaken the immune system so that it attacks tumours. Sharing features with responses to infectious diseases[267,268,269], tumour control by the immune system requires coordination between systemic and intratumoural immunity[270], and although several studies have investigated intratumoural responses to immunotherapy[214,213,216], few have focused on how ICB therapy affects the peripheral immune system, or whether changes in peripheral T cells are associated with patient responses[213,216,271].

This led to the hypothesis that because immune responses to tumours mirror normal defensive responses to pathogens, it would be possible to study patient responses to ICB by monitoring peripheral T cell evolution during treatment. The following aims were therefore proposed:

1. To collect peripheral blood from a minimum of 30 patients undergoing first line ICB for metastatic melanoma at three time points; baseline, week 3 on treatment and week 9 on treatment.

2. To use an optimised multiparametric flow cytometry panel to characterise the peripheral T cell compartment in detail at these time points.

3. To identify peripheral blood markers of response to immunotherapy early after treatment initiation in stage IV melanoma.

4. To identify peripheral blood markers of toxicity to immunotherapy in stage IV melanoma.

In this chapter, I present my contribution to the manuscript: Immune awakening revealed by peripheral T cell dynamics after one cycle of immunotherapy, by Valpione et al[234], published in Nature Cancer February 2020, see Appendix B for the complete manuscript. I also present here data from: T cell immune awakening in response to immunotherapy is age dependent, by Salih et al[272], (accepted for publication in European Journal of Cancer December 2021), see Chapter 4 for the full study and Appendix C for the manuscript in press. Details of the follow-up study from the work presented in this chapter are described in section 3.5.

3.3 Results

3.3.1 Patient cohort

Patients with confirmed metastatic melanoma on histology report from tissue biopsy and baseline CT scan were enrolled onto the study. Patients with previous systemic oncological treatment in the neoadjuvant, adjuvant or metastatic setting for melanoma or other cancers, concomitant therapy with immunosuppressant drugs at enrolment and synchronous other active malignancies were excluded from the study. Patients were eligible to enrol into the study if they had been consented to commence first line immunotherapy by the responsible clinical treating team. The immunotherapy regime used to treat each patient was decided by the treating physician in line with local guidance, a summary of the immunotherapy patients received and the clinical characteristics of the final patient group is described in Table 3.1.

Peripheral blood samples were collected from a total of 50 patients with a diagnosis of metastatic melanoma. The initial cohort consisted of 30 patients and then a further 20 patients were included as the validation cohort. Written informed consent was then taken from patients who wished to participate in the study. Patient confidentiality was maintained by assigning an anonymous patient number to each sample. Peripheral blood (30mL) was taken from patients at three time points; at baseline prior to any systemic treatment (T0), 3 weeks after the first cycle of treatment, prior to cycle 2 (W3) and at 9 weeks prior to cycle 4 of immunotherapy (W9). The timeline of peripheral blood sample collection is illustrated in Figure 3.1. HD samples were also used as controls within the study.

Response to immunotherapy was assessed on CT scan at 12 weeks post treatment initiation (week 12 response) and recorded using RECIST 1.1[273] as response evaluation criteria. CR was defined as disappearance of all target and non-target lesions. A partial response (PR), was defined as radiological evidence of at least 30% decrease in the sum of the longest diameter (LD) of target lesions compared to baseline. Progression of disease (PD), where there was at least a 20% increase in the sum of the LD of target lesions, taking as reference the smallest sum LD recorded since the treatment started or the appearance of one or more new lesions and/or unequivocal progression of existing non-target lesions. Stable disease (SD) where there was neither sufficient shrinkage to qualify for PR nor sufficient increase to qualify for PD, taking as reference the smallest sum LD since treatment started or persistence of one or more non-target lesions. CR, PR and SD were considered as disease control (DC). For late response evaluation, progression was confirmed or excluded after an additional 12 weeks of treatment (best response).

As a surrogate measure of tumour burden the sum of target lesions on baseline and W12 CT scans were calculated using RECIST 1.1. Measurements from scans at both timepoints were available for 36 patients; the different number of patients included in the sub-studies reflects the availability of detailed target metastatic lesion measurements in the scan reports. Toxicity was measured using the Common Terminology Criteria for Adverse Events (CTCAE) v.4.0.

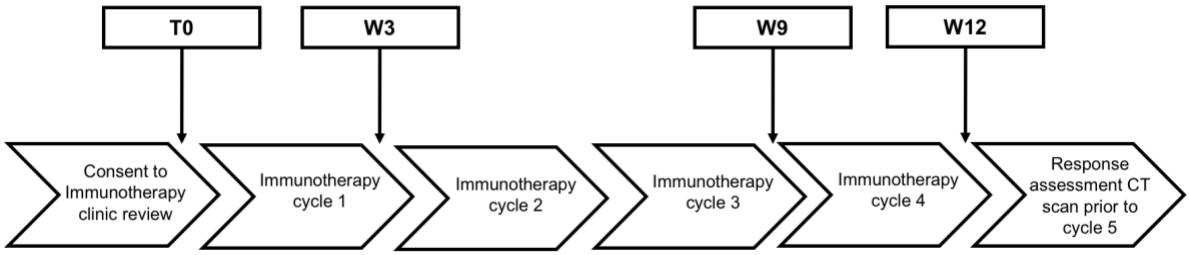

Figure 3.1 Timeline of peripheral blood sampling
The first collection occurred prior to administration of the first cycle of immunotherapy (T0). The second sample was taken immediately prior to cycle 2 of immunotherapy (W3), and the third sample was taken immediately prior to cycle 4 of immunotherapy (W9). Sampling was carried out when patients were attending The Christie NHS Foundation Trust for treatment to reduce inconvenience to study participants.

Table 3.1 Clinical characteristics of the patient cohort

Clinical Characteristics	Number (%)	Median (range)	Total number of patients evaluated
Gender			50
Male	32 (64%)		
Female	18 (36%)		
BRAF V600E/K Mutation Status			50
Mutated	16 (32%)		
Wild-type	34 (68%)		
Stage	10 (20%)		50
IIIC – M1a	13 (26%)		
M1b	27 (54%)		
M1c-d			
Baseline LDH (IU/L)		371 (165-2987)	50
<ULN	42 (84%)		
>ULN	8 (16%)		
Age (years)		70 (35 – 85)	50
Number of organ sites with metastases		2 (1-7)	39*
Immunotherapy Regime			50
Ipilimumab + Nivolumab	21 (42%)		
Pembrolizumab	19 (38%)		
Nivolumab	10 (20%)		
Response to Immunotherapy			50
Complete Response (CR)	7 (14%)		
Partial Response (PR)	23 (46%)		
Stable Disease (SD)	4 (8%)		
Progression of Disease (PD)	16 (32%)		

*The different number of patients included in the sub-study reflects the availability of detailed target metastatic lesion measurements in the scan reports.
ULN=upper limit of normal

3.3.2 Identification of subset of immune effector T cells in the peripheral blood of metastatic melanoma patients undergoing ICB therapy

The surface markers of the subset of cytotoxic memory effector T cells previously described as being involved in immune responses to infection and as also functionally relevant in the tumours of melanoma patients undergoing anti-PD-1 therapy were used as the starting point to explore the behaviour of peripheral T cells expressing those markers at baseline and early on ICB therapy[252,264,266]. To investigate T cell evolution in this setting, high dimensional FACS was utilised to characterise peripheral T cell subsets in the patients' PBMCs (n=50), (panels and gating strategy described in section 2.6). The subset of immune effector T cells with the surface phenotype $CD3^+$ $CD4^-$ $CD8^+$ $CD45RA^-$ $CD45RO^+$ $CD27^-$ $CCR7^-$ which will be referred to as immune effector T (T_{IE}) cells were identified and appeared to show expansion in some patients between T0 and W3. Figure 3.1 illustrates an example of FACS data plots at T0 and W3 from a patient showing expansion of T_{IE} cells, 18.2% at T0 compared to 69.3% at W3.

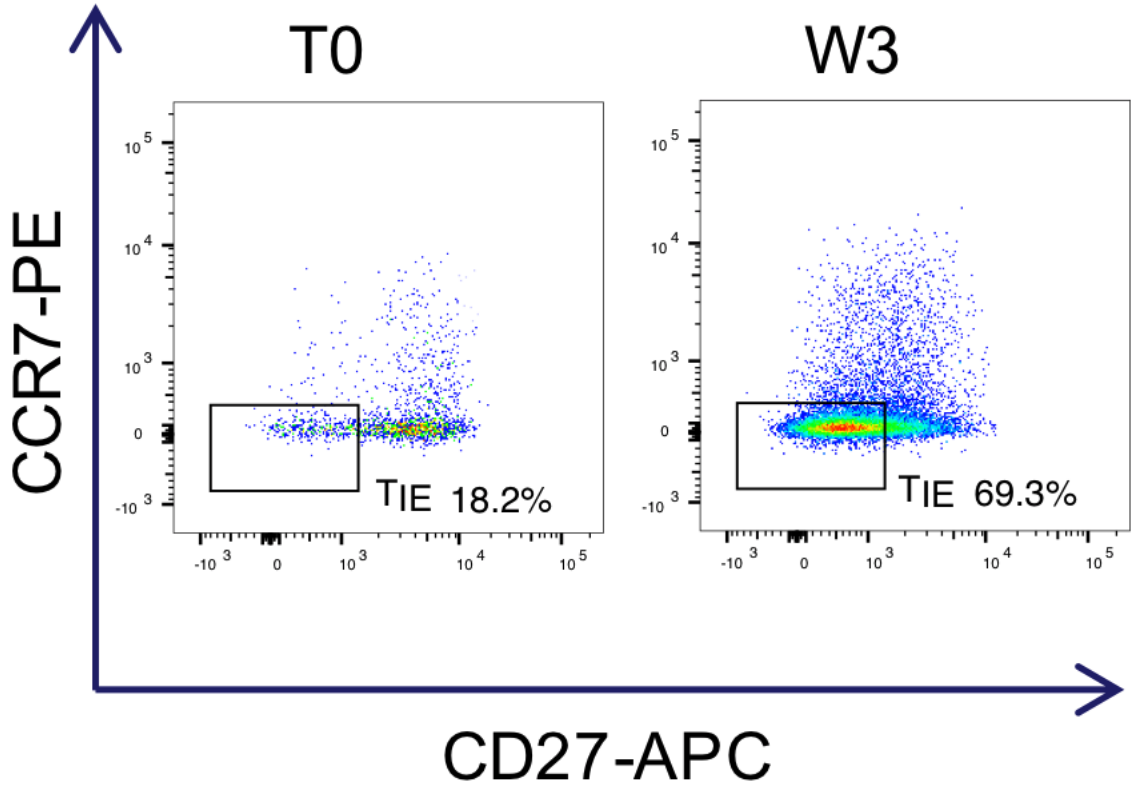

Figure 3.1 Peripheral T_{IE} cell expansion at T0 and W3
Example of gating around cell populations on 2D dot-plot graph. Identification of CCR7 and CD27 negative fraction of the cytotoxic memory effector T cells. Boxes within the plots highlight the gating and expansion of T_{IE} cells from T0 (18.2%) to W3 (69.3%).
Data shown here are the fcs. files acquired by the flow cytometer, n=1 example.

3.3.3 Patient radiological response to ICB correlates with an expansion in peripheral T_{IE} cells

The observation that expansion of peripheral T_{IE} cells was occurring in some patients led to the hypothesis that this expansion may correlate with patients that are responding to ICB therapy. Flow cytometry was used to quantify the percentage of T_{IE} cells in the patients' circulating cytotoxic memory T cells from PBMCs prior to treatment at T0 and after one cycle of ICB at W3. From this, the change in T_{IE} abundance at W3 compared to T0 was calculated (W3[T_{IE}]-T0[T_{IE}]=$\Delta_{W3}T_{IE}$). As a surrogate of tumour burden, the sum of the measured target RECIST lesions were calculated from the patients' scans (T0 RECIST) and then the change at W12 compared to T0 was calculated (W12[RECIST]-T0[RECIST]=Δ_{W12}RECIST)[274,275]. Table 3.2 displays the median sum (including range) of RECIST 1.1 marker lesion diameters at both time points. Notably, patients with a Δ_{W12}RECIST of ≤0 (tumour shrinkage) had a mean $\Delta_{W3}T_{IE}$ of 9.57% (range -2.55-50.62%), whereas patients with a Δ_{W12}RECIST of >0 (tumour growth) had a mean $\Delta_{W3}T_{IE}$ of 0.4% (range -17.5-20.2%) (Figure 3.2A), resulting in a negative correlation between T_{IE} cell subset expansion and tumour burden changes (r=-0.35).

Following activation, many T cells die through the process of turnover, releasing their DNA into the blood as cfDNA. The rearrangement efficiency score (RES) measures the proportion of functional TCR sequences as a product of all TCR sequences[234]. To evaluate T cell turnover (death), the TCR RES were determined from cfDNA in the patients' blood. It was recently demonstrated that the change in cfDNA TCR RES at W3 compared to T0 (W3[RES]-T0[RES]=Δ_{W3}RES) is a surrogate for the dynamic change in peripheral T cell turnover[234]. It was observed that patients with an average Δ_{W3}RES of 0.02 (-0.16-0.17) had a Δ_{W12}RECIST>0, whereas patients with an average Δ_{W3}RES of 0.1 (-0.15-0.30) had a Δ_{W12}RECIST≤0 (Figure 3.2B), indicating a negative correlation between peripheral T cell turnover and tumour size changes (r=-0.50). Thus, the magnitude of the peripheral T_{IE} cell expansion and the magnitude of T cell turnover at W3 are both inversely proportional to tumour burden at W12 (r=-0.35, r=-0.50 respectively) (Figure 3.2A, Figure 3.2B).

Table 3.2 Sum of RECIST 1.1 marker lesion diameters at baseline and W12

	Median (range)	**Total number of patients evaluated**
Sum of RECIST 1.1 marker lesion diameters at Baseline (cm)	4.9 (1.1 – 21.5)	37*
Sum of RECIST 1.1 marker lesion diameters at W12 (cm)	4.5 (0 – 31.1)	36*

***** The different number of patients included in the sub-study reflects the availability of detailed target metastatic lesion measurements in the scan reports.

A

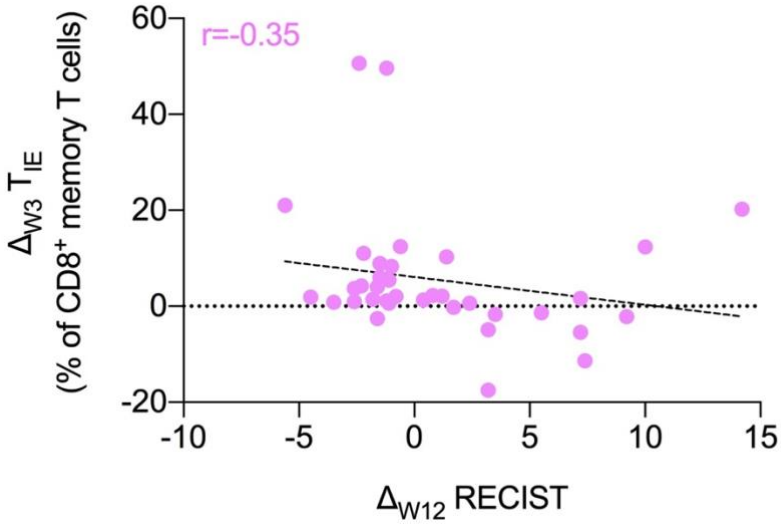

B

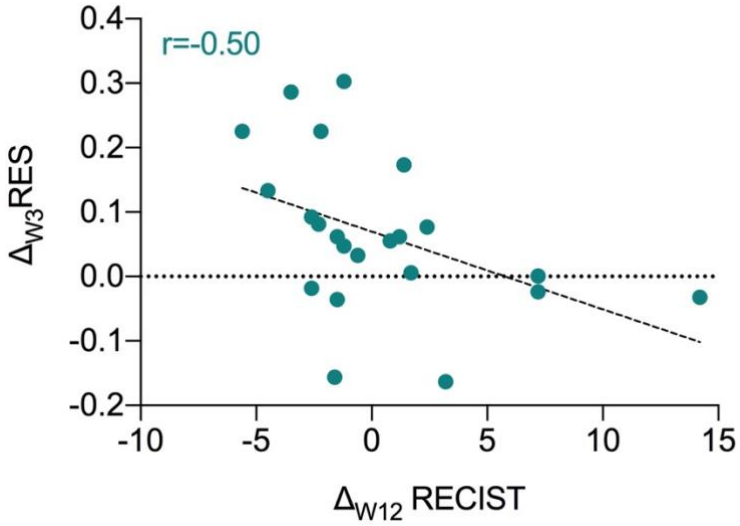

Figure 3.2 Correlation between radiological response and peripheral biomarkers
A: Correlation (r=-0.35) between Δ_{W12}RECIST and $\Delta_{W3}T_{IE}$ in the patient cohort (n=36).
B: Correlation (r=-0.50) between Δ_{W3}RES and Δ_{W12}RECIST in the patient cohort (n=22 patients with both measurements available).
Data points represent individual patients. Dotted line is the linear regression line.

3.3.4 Peripheral T_{IE} cell expansion in metastatic melanoma patients that respond to ICB therapy in the initial cohort

Further analysis revealed that T_{IE} cells expanded at W3 in patients who achieved DC, including late responders, however there was no evidence of T_{IE} cell expansion in patients with PD on radiological response evaluation imaging (p=0.0007) (Figure 3.3A). The finding of T_{IE} expansion at W3 in patients with radiological evidence of disease control was irrespective of whether they were treated with single agent anti-PD1 or combination anti-PD1 and anti-CTLA4 therapy regimes (p=0.20) (Figure 3.3B). An increase of >0.8% in the T_{IE} ratio relative to all CD8+memory T cells at W3 correlated with improved OS and segregated disease control, including late responders from patients with progressive disease, with a sensitivity of 0.94 and a specificity of 0.79 (accuracy = 0.87; area under the curve = 0.85) (Figure 3.3C). The T_{IE} expansion at W3 was associated with significantly increased OS (median survival not reached) compared to patients without T_{IE} expansion (median survival 9.6 months), the HR for patients without W3 T_{IE} expansion was 3.7 (95% CI: 1.12–11.9), (p=0.013) (Figure 3.3D).

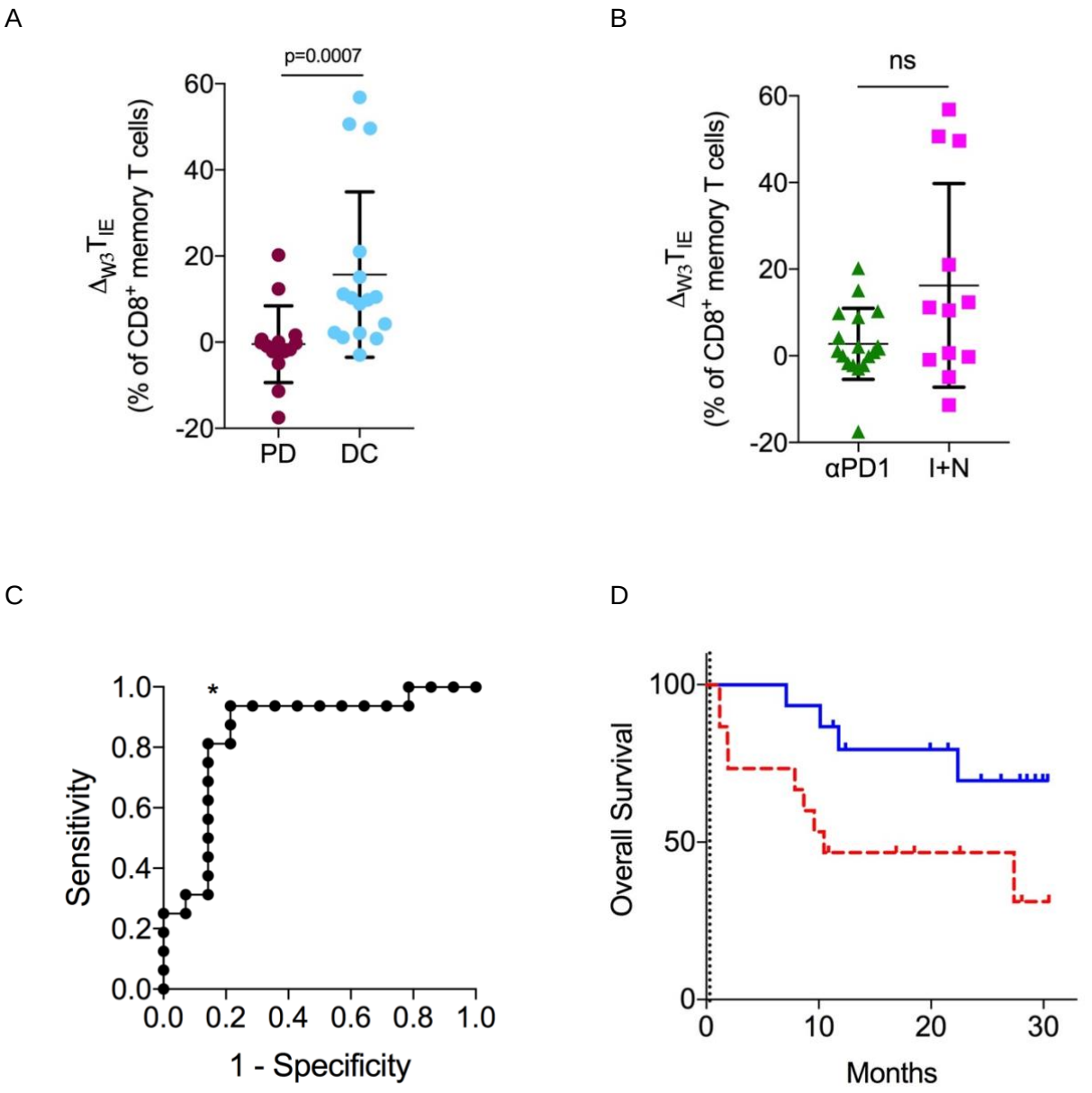

Figure 3.3 Peripheral T_{IE} cell expansion in metastatic melanoma patients that respond to ICB therapy in the initial cohort

A: Δ_{W3} T_{IE} in patients with progressive disease (PD), maroon dots, (n=14; median:−0.58%) or disease control (DC), blue dots (n=16; median:10.04%), p=0.0007 (two-sided Mann–Whitney U-test). Dots represent individual patients; horizontal lines show median values and error bars represent standard deviation.

B: Δ_{W3} T_{IE} in patients receiving anti-PD1 monotherapy pembrolizumab or nivolumab (αPD1; green triangles, n=18; median:1.35%) or a combination of ipilimumab and nivolumab (I + N; pink squares, n=12; median:10.84%). p=0.20 (two-sided Mann–Whitney U-test).

C: Receiver operating curve displaying sensitivity and false positive rate (1 − specificity) of Δ_{W3} T_{IE} values in identifying patients that would achieve disease control. * = maximum accuracy (cut-off=+0.8%).

D: Kaplan–Meier survival curves for patients with T_{IE} expansion ≥ 0.8% (blue; n=12; median survival not reached) at W3 compared with patients with T_{IE} expansion <0.8% (red; n=18; median survival=9.6 months), p=0.013 (log-rank test). The dotted vertical line is landmark at W3.

3.3.5 Peripheral T_{IE} cell expansion in metastatic melanoma patients that respond to ICB therapy in the validation cohort

Following on from the initial cohort findings, these observations were confirmed in a further independent cohort of 20 advanced melanoma patients treated with first line ICB therapy. In this validation cohort, T_{IE} cells also expanded at W3 in patients who achieved DC, including late responders, with no evidence of T_{IE} expansion in patients with PD (p=0.019) (Figure 3.4A). T_{IE} expansion >0.8% at W3 in this cohort was again associated with a significant increase in OS (median survival not reached) compared to those patients with T_{IE} expansion < 0.8% (median survival 4.2 months) (p=0.003) (Figure 3.4B), again separating responders from non-responders with a sensitivity of 0.82 and a specificity of 1 (accuracy=0.90; area under the curve AUC=0.92).

A

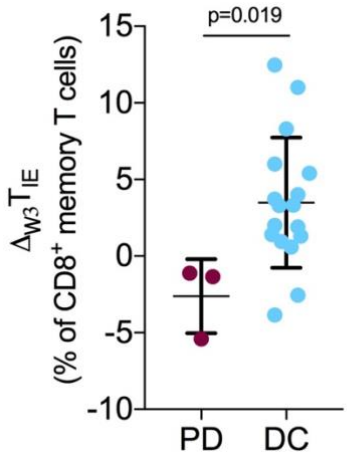

B

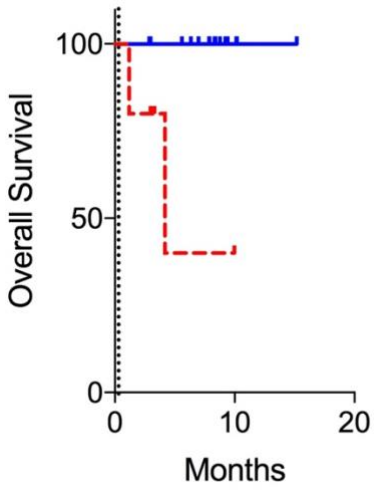

Figure 3.4 Peripheral T_{IE} cell expansion in metastatic melanoma patients that respond to ICB therapy in the validation cohort
A: Δ_{W3} T_{IE} in patients with progressive disease (PD), maroon dots, (n=3; median:−1.3%) or disease control (DC), blue dots, (n=17; median: 3.3%), p=0.019 (two-sided Mann–Whitney U-test). Dots represent individual patients; horizontal lines show median values and error bars represent standard deviation.
B: Kaplan–Meier survival curves for patients with T_{IE} expansion ≥ 0.8% (blue; n=15; median survival not reached) at W3 compared with patients with T_{IE} expansion <0.8% (red; n=5; median survival = 4.2 months), p=0.003 (two-sided log-rank test). The dotted vertical line is landmark at W3.

3.3.6 Peripheral T_{IE} cell expansion in metastatic melanoma patients at W9 and correlation with response to ICB therapy

The next step was to explore the timeframe beyond W3 that T_{IE} cell expansion discriminating responders from non-responders to ICB remained present. This was done by comparison of the percentage difference of T_{IE} cells in the CD8+ memory T cell population in the PBMC of the patients at T0 and W9. By W9, T_{IE} cells no longer discriminated patients with DC from patients with PD. Differences over time were not significant for PD, p=0.375 or DC, p=0.219 and patient values for PD compared to DC did not differ at T0 (p=0.275 or W9; p=0.762) (Figure 3.5). The W9 samples were collected and analysed for an initial pilot of 10 patients and when no signal was detected collection at this time point ceased, hence the difference in patient numbers between T0 (n=30) and W9 (n=10).

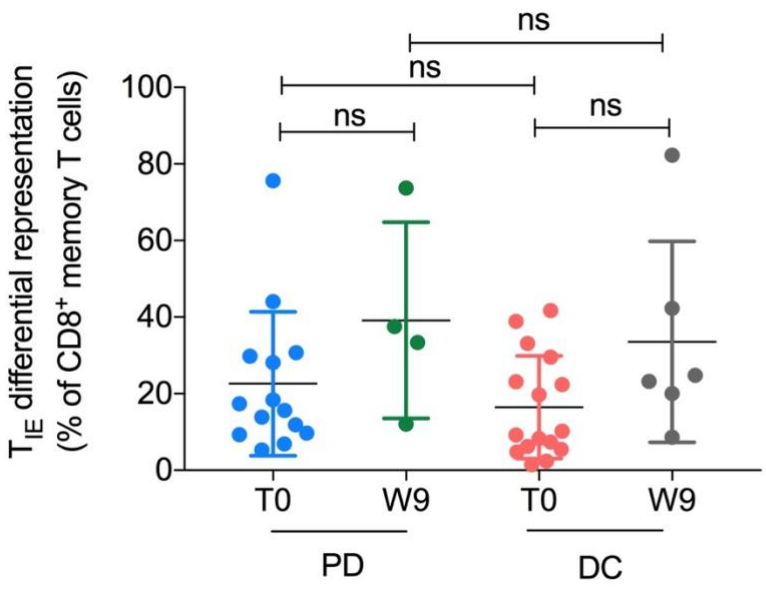

Figure 3.5 Peripheral T_{IE} cell expansion in metastatic melanoma patients at W9 and correlation with response to ICB therapy
Comparison of differential abundance of T_{IE} in CD8+ memory T cells in the PBMCs of patients with progressive disease (PD, n=14) and disease control (DC, n=16) at T0 (n=30) and W9 (n=10, PD, n=4, DC, n=6).
Differences over time were not significant for PD (median=15.2 and 35.5; P=0.375; two-sided Wilcoxon test) or DC (median=7.9 and 24; p=0.219; two-sided Wilcoxon test); PD vs DC patient values did not differ at T0 (p=0.275; two-sided Mann-Whitney U test) or W9 (p=0.762; two-sided Mann-Whitney U test). Error bars represent standard deviation.

3.3.7 Ki67 and PD-1 expression in peripheral T_{IE} cells

The only predictive biomarker of response to ICB currently used in clinical practice is the expression of PD-L1 in tumour tissue as assessed by immunohistochemistry. Despite the use of PD-L1 as a biomarker, it has both technical and biological limitations that are discussed in section 1.4.1. Other tissue-based biomarkers, including tumour mutational burden have comparable predictive power to PD-L1 expression[276]. However, tissue biopsies are invasive, not always accessible and are less likely to represent the whole tumour due to intratumoural heterogeneity. In addition, the dynamic response of the immune system following ICB make serial tissue biopsies an unviable option in clinical practice. Ki67 expression has been utilised as a marker of T cell activation and PD-1 although known as a marker of exhausted T cells, it has also been observed as a marker of continued memory T cell function[277,278]. For this reason, it was beneficial to investigate the expression of Ki-67 and PD-1 in peripheral T_{IE} cells from the study cohort at both time points, T0 before the first cycle of ICB and W3 after the first cycle of ICB. This experiment was limited by the small sample size (frozen PBMC samples from 5 patients), therefore statistical comparison of the outcome groups, $Ki67^{+/-}$ $PD1^{+/-}$ and time points was not possible. However, FACS analysis revealed a propensity for T_{IE} reinvigoration with increased $Ki67^{+}$/$PD\text{-}1^{+}$ expression after one cycle of ICB at W3 (Figure 3.6).

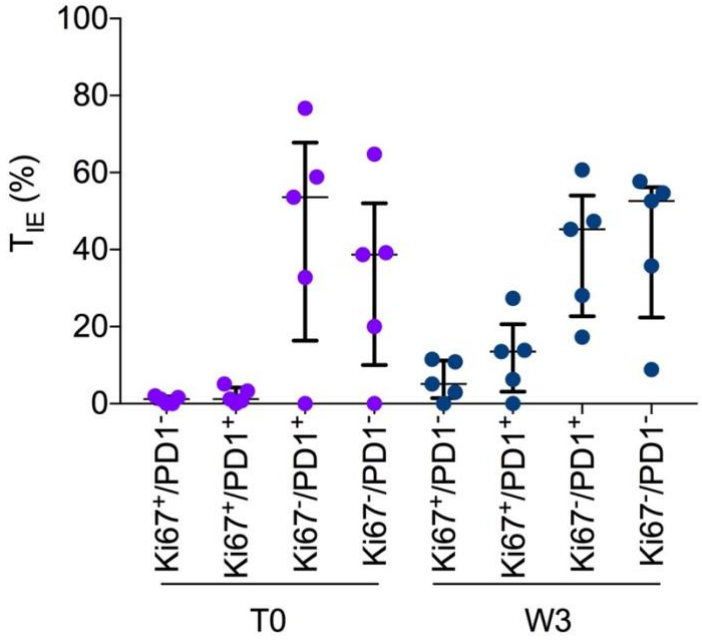

Figure 3.6 Ki-67 and PD-1 expression in peripheral T_{IE} cells at T0 and W3
Frozen samples of PBMCs from patients at T0 and at W3 after first cycle of ICB; expression of Ki67 and PD1 in the peripheral T_{IE} cells as measured by FACS; horizontal line indicates median; error bar indicates standard deviation. n=5, statistical analysis was not possible due to the small sample size.

3.3.8 Correlation between peripheral T cell expansion and toxicity

The growing clinical application of immunotherapy highlights the importance of the recognition and management of its unique toxicity profile. IrAEs, caused by ICB agents can lead to long-term chronic complications and even fatal consequences and thus require early detection and aggressive management. However, at present robust biomarkers of irAEs are lacking. It was therefore of interest to explore whether there was a correlation between T_{IE} cell expansion and toxicity. Within the total study population (n=50), patients were segregated into those with no reported toxicity, or toxicity < grade 3 (G3) and those with toxicity documented ≥ G3 in the clinical notes as per CTCAE v.4.0. Onset of toxicity occurred at any time between 2 weeks and 6 months from therapy initiation. Analysis of the data revealed that T_{IE} expansion at W3 was not associated with toxicity (p=0.347; Figure 3.7). However, expansion of a separate T_{reg} subset did correlate with grade of toxicity (p<0.0001; Figure 3.8A). This subset of T_{reg} is characterised by the surface phenotype $CD3^+CD4^+CD8^-CD25^+CD127^{-/low}$. Figure 3.8B illustrates an example of FACS data plots at T0 and W3 from a patient with grade 3 toxicity, showing expansion of the T_{reg} subset from 6.31% at T0 compared to 13.5% at W3.

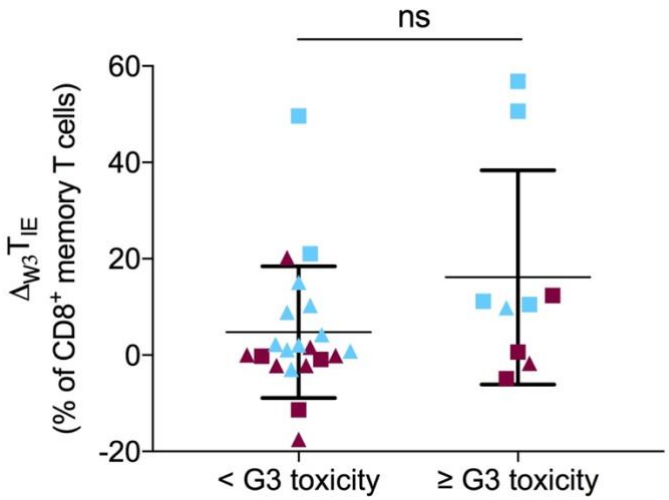

Figure 3.7 T_{IE} cells and immunotherapy related toxicity
Δ_{W3} T_{IE} in patients with less than (<) grade 3 toxicity (i.e. grade 0-2); (median=1.6; n=33) or with greater than or equal to (≥) grade 3 (G3) toxicity (median=3.72; n=17), p=0.347 (two-sided Mann–Whitney U-test). Horizontal lines show median values, error bars represent standard deviation and data points represent individual patients (maroon: progressive disease; blue: disease control; triangles: single-agent anti-PD-1; squares: combination ipilimumab + nivolumab.

A

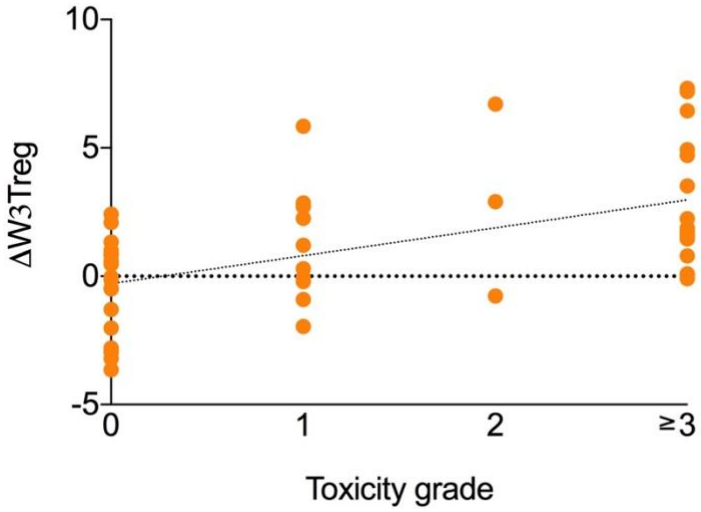

B

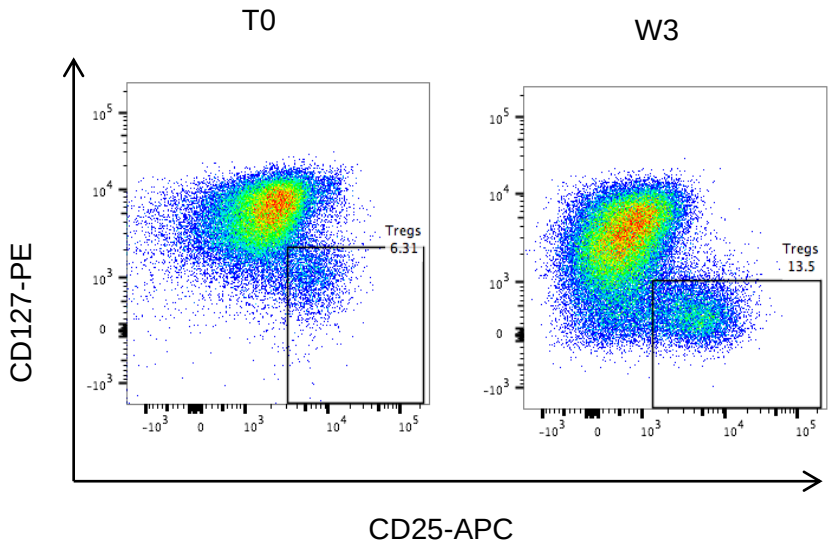

Figure 3.8 Regulatory T cells (T_{reg}) and immunotherapy related toxicity
A: Expansion of $CD25^{+}CD127^{-/low}$ in CD4+ T cells at week 3 ($\Delta_{W3}T_{reg}$) according to toxicity grade. p<0.0001; n=50; two-sided linear regression analysis, R^2=0.29. The dotted line is the linear regression line.
B: Example of 2D dot-plot graph showing expansion of $CD3^{+}CD4^{+}CD8^{-}CD25^{+}CD127^{-/low}$ T_{reg} cells. Boxes within the plots highlighting the gating and expansion of T_{reg} from T0 (6.31%) to W3 (13.5%). Data shown here are the fcs. files acquired by the flow cytometer, n=1 example.

3.4 Discussion

The application of systemic therapy has been largely focussed on patients with stage IV disease. In the advanced setting, patients survive for more than 30 months and some show durable responses since the advent of immunotherapy[279]. However, it is important to note that not all patients respond to treatment, some experience major toxicity and a significant number still die of their disease, highlighting the heterogeneity of response. The mechanisms by which some melanomas escape ICB stimulation while others respond have not yet been fully elucidated. There is a critical need to develop validated assays and provide reliable platforms to stratify and monitor patient response to therapy, as currently there is no biological rationale underpinning how patients are selected for treatment with immunotherapy. To investigate the hypothesis that patient responses to ICB could be studied by monitoring peripheral T cell evolution during treatment the peripheral blood of patients undergoing first line immunotherapy for metastatic melanoma was examined**.** The initial cohort consisted of 30 patients and the study findings were validated in a subsequent independent cohort of 20 patients.

Evaluation of how the selective pressure of the first cycle of ICB affects peripheral T cell evolution in treatment naïve advanced melanoma patients was undertaken. Expansion of a CD8+ cytotoxic memory effector subset that was $CCR7^-/CD27^-$ was observed. This subset of lymphocytes is involved in cytotoxic response to infections and the findings from this study indicate that they are also associated with ICB responses[252,257,264]. Immune effector cells are the cells of the immune system that support anti-cancer immune surveillance[280], and as this data has identified correlation of a specific T cell subset in this network, the term immune-effector T cells, or T_{IE} cells was applied. The data generated enhances knowledge of immune system biology and may have broader implications beyond immuno-oncology. In particular, the downregulation of CCR7 and CD27 in T_{IE} cells, and their association with differentiated effector T cell release from lymph nodes to the periphery[281,282,283,284].

This study aimed to address a clinically relevant question: is it possible to predict patient responses to ICB by monitoring peripheral T cell evolution during treatment. This was achieved by assessing peripheral T cell changes that relate to pre-treatment and early on treatment time points. Early changes at W3 using flow cytometry demonstrated expansion of a subset of $CD8^+$ memory effector cytotoxic T cells ($CD3^+CD4^-CD8^+CD45RA^-CD45RO^+CD27^-CCR7^-$). This expansion was significantly greater in patients with radiological evidence of response to ICB and correlated with subsequent 6 month ongoing responses to ICB therapy. An increase of 0.8% in the ratio of T_{IE} cells to all $CD8^+$ memory cells at W3 following one cycle of ICB was associated with an increase in OS and segregated responders

from non-responders at 6 months, this was upheld with a separate validation cohort. Interestingly, T_{IE} levels at W9 were not able to distinguish patients with DC from those with PD. This highlights the dynamic nature of these responses, indicating that the changes observed at W3 are prognostic for melanoma responses to ICB, but are no longer prognostic by W9. This is consistent with studies showing that the peak of immune activation is at W3[213,271].

Thus, changes in T_{IE} abundance and the RES after the first cycle of immunotherapy identify which patients will achieve disease control at W12[234]. These findings were extended by showing that in melanoma patients receiving ICB, changes in T_{IE} cell abundance inversely correlated with changes in tumour burden determined by RECIST target lesion size in patients' CT scans. This suggests that an increase in T_{IE} abundance 3 weeks after the start of ICB therapy predicts tumour shrinkage at the W12 assessment. Similarly, it has been shown that the peripheral T cell pools undergo dynamic turnover proportional to the magnitude of response, confirming that the immune-signature described is a reliable early biomarker of response to ICB[234].

The ability of unidimensional measurements to accurately represent adequate assessment of total tumour burden has often been questioned. Several studies have compared unidimensional and bi-dimensional measurements in assessment of tumour burden and shown no difference in response and progression rates[285,286,287]. Volumetric measurement of tumour lesions as a more accurate marker of tumour burden has been investigated and shown promise[288,289]. However, there is variability in software platforms used, these are not widely available and have not yet been fully validated. Therefore, unidimensional anatomical assessment of tumour burden is currently the most reliable and accessible surrogate endpoint.

Analysis of anti-tumour reactivity of T_{IE} cells was out of the scope of this study. However, publicly available data demonstrate that peripheral T_{IE} clones infiltrate melanoma and represent an abundant proportion of TILs with high repertoire clonality[290,234]. Additionally, within the literature, a similar cell population of TILs has been identified as correlating with response to ICB in melanoma[266].

To investigate the reliability and utility of T_{IE} cell expansion at W3 in predicting response to ICB in melanoma, comparison with other candidate biomarkers in the published literature was undertaken. The accuracy of W3 T_{IE} expansion in identifying patients who achieved disease control early during treatment in this study was 0.87. This is superior to W3 peripheral T lymphocyte invigoration-to-tumour burden ratio (Ki67/TB), where accuracy was 0.64 (16/24

patients with Ki67/TB > 1.94 had an objective response compared with 3/17 patients with Ki67/TB < 1.94)[213]. Moreover, W3 T_{IE} expansion had greater accuracy than PDL-1 staining in pre-treatment melanoma biopsies, where the accuracy was 0.67 (78/148 patients with PD-L1 positive biopsy had an objective response compared with 89/270 patients with PD-L1 negative biopsy)[65]. The novel observation that T_{IE} expansion could identify which patients benefit from ICB with greater accuracy than standard biopsy PD-L1 staining or Ki67 is noteworthy. However, further research investigating the anti-tumour cytotoxicity and specificity of T_{IE} cells and their potential for clinical development is required. Within this study, the sample size examined was too small to discern a statistically significant trend in increased peripheral Ki67 expression and T_{IE} reinvigoration at W3.

Evaluation of whether W3 T_{IE} expansion was associated with immunotherapy related toxicity was undertaken and no correlation was identified between T_{IE} expansion at W3 and presence or grade of toxicity. However, a linear correlation between toxicity grade and expansion of a separate T_{reg} subset characterised by the surface phenotype $CD3^{+}CD4^{+}CD8^{-}CD25^{+}CD127^{-/low}$ at week 3 was observed. Interestingly, a recent study also investigated baseline and early changes in T_{reg} cells among PBMCs obtained at baseline and 1 week after initiating anti-PD-1 therapy in thymic epithelial tumour (TET) and NSCLC patients. They found that the fold change in effector T_{reg} cells post treatment was associated with the development of irAEs[291]. The impact of irAEs and toxicity are a key factor to consider in the patient centred approach to precision immuno-oncology and the development of reliable biomarkers that predict ICB toxicity could facilitate improved therapeutic decision making and safety monitoring protocols.

In summary**,** to investigate T cell evolution on treatment as a potential predictive biomarker of response to immunotherapy, liquid biopsies were utilised for metastatic melanoma patients undergoing first line treatment with immunotherapy. Expansion of an immune effector subset of peripheral T cells, T_{IE} that correlated with response was identified. These changes occur within 3 weeks of commencing ICB therapy in responding patients and interestingly are no longer detectable at W9, prior to the fourth cycle of treatment. Thus, dynamic and quantifiable changes in peripheral T cells that occur early on treatment using a minimally invasive approach have been identified. This novel approach will require further kinetic analysis and clinical validation, with the potential to provide tractable tools to refine patient care. Treatment may be stopped at an early stage in patients that do not possess the immune cell repertoire necessary for response and could therefore prevent further exposure to costly therapy and risk of toxicity.

These results advance our understanding of the dynamics of immune system evolution after one cycle of ICB. However, the similar responses observed with infection could limit specificity in the immunotherapy setting. In addition, the relatively small size of the study cohort could limit the generalisation of these results, particularly, the lack of a significant difference between single agent and combination immunotherapy. In contrast, within the literature, bulk RNA sequencing with flow cytometry based immunophenotyping of peripheral blood from a cohort of metastatic melanoma patients sampled early on first line ICB indicated similar activation of the CD8+ effector memory T cell population with both monotherapy and combination ICB, although the magnitude of change was significantly higher with combination therapy[292]. If expansion of this CD8+ effector memory T cell population is validated in larger prospective studies as correlating with clinical response to both single agent and combination ICB therapy this could pave the way for treatment escalation studies in order to make more nuanced clinical decisions.

Although further studies are required to determine the mechanisms underpinning the observations from this study and their specificity for ICB-induced response, this approach offers advantages inherent to minimally invasive liquid biopsies and may serve as an actionable biomarker of immune activation generating information in a clinically actionable time frame that could aid treatment decisions with the potential to contribute to the implementation of precision immunotherapy.

3.5 Design of Follow-Up Study Impacted by Global Pandemic

The next step in validating this candidate early response marker is to identify at what time point the maximal differences in T_{IE} cell expansion can be observed. If successful, there is potential to consider a feasibility study to assess whether these tools can be utilised in clinical practice to identify and segregate responders from non-responders early on ICB therapy so that treatment can be tailored to improve outcomes. Importantly, the prediction of response would occur within 3 weeks, significantly earlier than the current clinical response assessments that occur at 12 weeks.

I conceived the rationale for this follow-up study and led on the design and set up of the protocol. Unfortunately, the global pandemic has interrupted study initiation. Section 3.5.1-3.5.4 outlines the hypothesis, aims, research protocol and experimental plan for the study.

3.5.1 Hypothesis and Aims

As demonstrated in this chapter, an increase in T_{IE} expansion at W3 was associated with increased OS and segregated DC, including late responders from patients with PD in the initial study. This work amongst other recently published studies has highlighted that peripheral T cell changes occur early on treatment[213,271,292]. Subsequent focus on earlier time points may give further insight into the kinetics of disease evolution on treatment to identify as early as possible which patients are likely to benefit from therapy and those for which a different combination or treatment regime may be indicated.

Based on the rapid decay of T_{IE} expansion from W3 to W9, I hypothesised that this expansion occurs rapidly and can be detected earlier than the W3 timepoint. In order to test this, the following experimental approach was proposed:

1. To collect weekly blood samples for the first 6 weeks of treatment from a minimum of 12 metastatic melanoma patients undergoing first line ICB therapy.
2. To utilise flow cytometry to assess if the timepoint at which T_{IE} changes occur on ICB can be further refined.

3.5.2 Research Protocol

3.5.2.1 Clinical characteristics

Blood samples from patients collected under the Manchester Cancer Research Centre (MCRC) Biobank ethics application #07/H1003/161+5 with written informed consent from the patients at The Christie NHS Foundation Trust. The study was approved by MCRC Biobank Access Committee application 13_RIMA_01. All clinical investigations conducted in accordance with the principles expressed within the Declaration of Helsinki and GCP guidelines.

A total of 12 patients with metastatic melanoma treated as standard of care with either combination I+N or single agent pembrolizumab in the first line setting will be recruited, with 6 patients recruited to each treatment arm.

Response to treatment assessed at 12 weeks from first cycle of immunotherapy by CT scan, using RECIST 1.1 as response evaluation criteria.

3.5.2.2 Key inclusion criteria

1. Histological confirmation of cutaneous melanoma
2. Stage IV disease confirmed on radiological imaging
3. No previous systemic anti-cancer treatment in the neo-adjuvant, adjuvant or metastatic setting for melanoma or any other cancer
4. No concomitant therapy with immunosuppressive medication at enrolment
5. No synchronous other active malignancy.

3.5.2.3 Feasibility of recruitment

The Christine NHS Foundation Trust, melanoma clinical team were expected to see and commence treatment with immunotherapy, 3-4 patients with metastatic disease per month. Within 6-8 months there was potential to have recruited 12 patients. Total study duration was up to 12 months (3 months from recruitment of the final patient). It was considered that if treatment groups were unbalanced, it may take longer to complete the recruitment phase.

3.5.3 Experimental plan

3.5.3.1 Addressing aim 1: To collect weekly blood samples for the first 6 weeks of treatment from a minimum of 12 metastatic melanoma patients undergoing first line ICB therapy

The sample size required to power this study was assessed by Cancer Research UK statistician Cong Zhou based on analysis of the data generated from 50 patients in the initial study. To consider relevance for clinical trial feasibility design, the cohort can be expanded to explore strength of signal when the time point is refined. Patients recruited to the study should undergo weekly blood sampling during the first two cycles of therapy between T0 and week 6 (W6). The W6 time point was chosen because analysis of data provided from another study informed that T_{IE} expansion was also not present beyond W6[80].

If this study reaches desired initial recruitment of 12 patients, this would equate to 7 blood samples per patient, a total of 84 samples. To maintain the conditions of the initial study, clinical samples will be processed within 4h of collection. The timeline for weekly peripheral blood sampling is illustrated in Figure 3.9. Baseline T0, W3 and W6 sampling would coincide with standard of care time points for phlebotomy prior to administration of each cycle of immunotherapy. Week 1 (W1), week 2 (W2), week 4 (W4) and week 5 (W5) are outside routine clinical follow up and require extra hospital visits. The logistics of phlebotomy taking into consideration what would be deemed acceptable and reasonable to patients was evaluated and an amendment to the pre-existing ethics protocol to incorporate additional phlebotomy was approved. This study is supported by the ‘man in van’ Cancer Research UK initiative, meaning that patients within the catchment area can attend their local pharmacy for phlebotomy. This would be necessary only on the outside standard of care blood sampling timepoints (W1, W2, W4 and W5) that would require extra hospital visits. Otherwise private transport to The Christie NHS Foundation Trust would be arranged for those patients outside of the catchment area willing to participate.

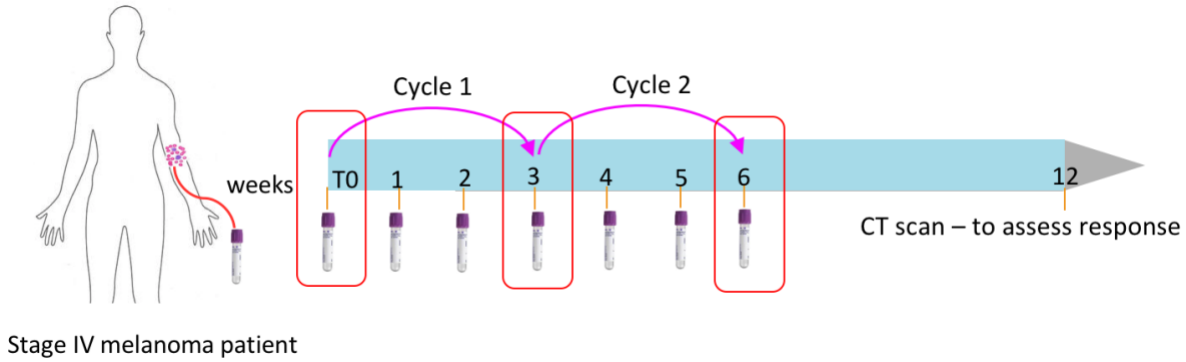

Figure 3.9 Timeline for weekly peripheral blood sample collection
Stage IV melanoma patients commencing first line ICB therapy recruited to the study will undergo weekly bloods for the first 6 weeks of treatment. This is a total of 7 blood samples per patient. Highlighted timepoints in red squares represent immunotherapy cycles.

3.5.3.2 Addressing aim 2: To utilise flow cytometry to assess if the timepoint at which T_{IE} changes occur on ICB can be further refined

The same protocols from the initial study for PBMC isolation and FACS analysis will be used in this follow-on study (method described in section 2.3 and section 2.6). The dynamics of T_{IE} cell behaviour will be monitored longitudinally on a weekly basis to explore whether the maximal differences observed occur earlier or later than the standard of care earliest timepoint of W3 identified in the initial study. The potential timepoints where maximal differences in T_{IE} cell expansion may be observed could be at peak 1 (P1) [week 1 or 2], peak 2 (P2) [week 3] or peak 3 (P3) [week 4 or 5] and are illustrated in Figure 3.10.

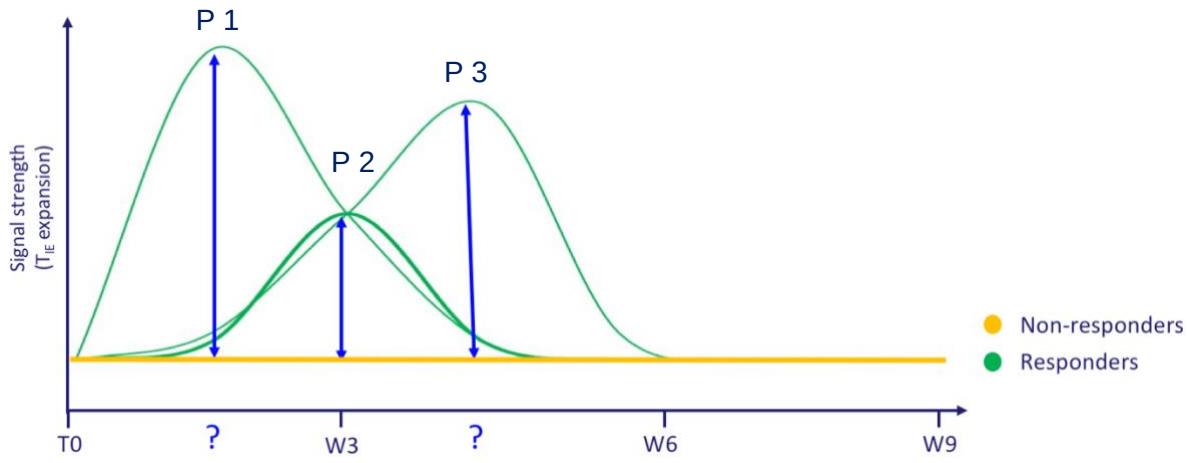

Figure 3.10 Graphical illustration exploring potential signal strength of T_{IE} cell expansion at different timepoints
Green = responders to ICB, disease control. Yellow = non-responders to ICB, progressive disease. Arrows indicate potential variation in signal strength at various timepoints highlighting the need to further refine the timepoint of maximal change in T_{IE} expansion.
P1 = peak 1, P2 = peak 2, P3 = peak 3.

3.5.4 Conclusion

Both the test and validation cohorts from the initial study confirmed that ICB induced measurable changes in peripheral T_{IE} cells that revealed which patients will benefit from treatment. These tools have the potential to be highly clinically relevant in decision making for melanoma treatment and hold promise for exploration of their utility in earlier stage melanoma. It is important to consider that dosing and scheduling of ICB has changed since the global COVID-19 pandemic and so this study, although still relevant and necessary, would need to be adjusted in light of the changes to timing of administration of treatment cycles. The intention is to further validate this candidate biomarker in the stage IV setting and seek to use these tools to aid identification of patients in the stage III resected melanoma setting who will benefit from adjuvant therapy. This will be discussed further in Chapter 5.

Chapter 4: Clinical correlates of peripheral T cell responses to immunotherapy in melanoma

4.1 Introduction

To facilitate the identification of new therapeutic strategies and personalised treatments for melanoma patients, we need to understand the biological mechanisms that underpin why some patients benefit from ICB whereas others do not. Ideally, therapy decisions would be made on the basis of patient-specific cancer or immunological biomarkers. However, clinically validated biomarkers for this purpose are currently lacking although many factors are known to influence response to ICB including: disease stage, serum LDH and organ systems involved. Thus, to deliver effective precision immuno-oncology, assessment of patient specific factors is required to guide clinical decision making.

When considering precision immunological biomarkers of response to immunotherapy in advanced melanoma, the study described in Chapter 3 sought to explore if patient responses to ICB could be predicted by assessing peripheral T cell changes that relate to pre-treatment and early on treatment time points. TCR sequencing in parallel with flow cytometry based immunophenotyping were used to assess T cell evolution in the context of patients undergoing immunotherapy for metastatic melanoma. Analysis of peripheral blood taken from patients prior to treatment and after the first cycle of ICB identified an immune signature that could discriminate, with an accuracy of 0.87, melanoma patients who will go on to respond to immunotherapy from those who will not respond to treatment[234].

Specifically, demonstrating that after one cycle of ICB, responding patients underwent early expansion of a subset of PBMCs, the immune effector T cells, termed T_{IE} cells defined as the $CD27^-/CCR7^-$ fraction of the $CD8^+$ peripheral memory T cells, that were associated with improved OS[234]. In addition, the study explored TCR sequencing as a means of evaluating the peripheral TCR repertoire as a potential biomarker of response and demonstrated that after one cycle of ICB, patients who went on to respond to treatment presented an increase in either the clonality or diversity of the TCR on their circulating T cells. Patients who failed to respond to treatment did not develop this dichotomised evolution in their TCR repertoire[234].

Additionally, changes in RES prior to and following the first cycle of treatment indicated that ICB increased peripheral T cell turnover in responding patients, but not in patients with progressive disease[234]. To further understand the biology underpinning these observations, in this chapter I investigated the clinical correlates associated with this immune signature.

4.2 Hypothesis and Aims

Despite the significant improvement in clinical outcomes since the introduction of immunotherapy to the treatment paradigm in melanoma, durable responses only occur in a minority of patients and treatment is associated with risk of toxicity and high cost. There currently are no definitive biomarkers that facilitate clinical decision making when considering which patients to select for treatment with ICB. Understanding of the dynamic nature of the immune response and the interaction of multiple host factors is required to define the best biomarkers of response to ICB.

It is important to assess the strength of the novel immune biomarkers described in section 4.1 in their ability to predict response to ICB in melanoma. Candidate circulating biomarkers identified in the literature to date have not been validated for clinical use, this is likely in part due to their tendency to be influenced by other clinical variables. It is hypothesised that patient clinical characteristics could affect the robustness of T_{IE} and TCR repertoire changes as predictive biomarkers of response to ICB.

To test this hypothesis, examination of the cohort of metastatic melanoma patients treated with first line immunotherapy (described in Chapter 3) was undertaken to explore whether clinical variables have an impact on the peripheral T cell immune profile prior to and following the first cycle of ICB.

The aims of this study are:

1. To ascertain the impact of clinical variables on peripheral T_{IE} cell evolution and T cell turnover under the selective pressure of immunotherapy.

2. To assess the impact of clinical variables on peripheral TCR repertoire changes under the selective pressure of immunotherapy.

In this chapter I present data from: T cell immune awakening in response to immunotherapy is age dependent, by Salih et al[272], (accepted for publication in European Journal of Cancer December 2021), see Appendix C for manuscript in press.

4.3 Results

4.3.1 Patient samples

Blood samples from patients were collected under MCRC Biobank ethics application #07/H1003/161+5, ethics code 18/NW/0092, with written informed consent from the patients at The Christie NHS Foundation Trust. The study was approved by MCRC Biobank Access Committee application 13_RIMA_01. All clinical investigations were conducted according to the principles expressed in the Declaration of Helsinki and GCP guidelines. The cohort of patients used in this study were the same as those from the study described in Chapter 3, which included a total of 50 patients with metastatic melanoma, treated with either single agent pembrolizumab or combination nivolumab plus ipilimumab as first-line therapy. Inclusion criteria included treatment naïve, inoperable locally advanced or metastatic melanoma. Patients were excluded if they had received any systemic oncological treatment in the neoadjuvant, adjuvant or metastatic setting for melanoma or other cancers, concomitant therapy with immunosuppressant drugs at enrolment, or had synchronous other active malignancies. Data from the previously reported cohort were analysed. Sample collection and processing were performed as previously described. TCR sequence data was retrieved for 29 (PBMC) and 28 (cfDNA) of the 50 patients.

4.3.2 Clinical characteristics of the patient cohort

Fifty (32 male, 18 female), treatment-naïve metastatic melanoma patients attending The Christie NHS Foundation Trust were recruited. Just over half (54%) had stage M1c disease, 16% (8/50) had baseline LDH >ULN, the median age was 70 years (range 35-85), and 68% (34/50) were *BRAF* wild-type (Table 4.1). The number of metastatic sites ranged from 1 to 7, and of the 27 patients (54%) with stage M1c or M1d disease (Table 4.1), 15 had hepatic metastases, 2 in combination with cerebral metastases.

Patients received first-line single agent anti-PD1 drugs (200 mg pembrolizumab 3 weekly, or 480 mg nivolumab 4 weekly; 29 patients) or combination anti-PD1 plus anti-CTLA4 (1 mg/kg nivolumab plus 3 mg/kg ipilimumab 3 weekly for 4 doses, followed by 3 mg/kg nivolumab 2

weekly; 21 patients) as per standard of care. Assessment of tumour response was performed by CT scan at W12 using RECIST 1.1. For late response evaluation, PD was confirmed or excluded after an additional 12 weeks of treatment (best response). DC was defined as CR, PR or SD. The clinical characteristics of the study cohort are further described in Table 4.1 (reproduction of Table 3.1).

Table 4.1 Clinical characteristics of the patient cohort (reproduction of Table 3.1)

Clinical Characteristics	Number (%)	Median (range)	Total number of patients evaluated
Gender			50
Male	32 (64%)		
Female	18 (36%)		
BRAF V600E/K Mutation Status			50
Mutated	16 (32%)		
Wild-type	34 (68%)		
Stage			50
IIIC – M1a	10 (20%)		
M1b	13 (26%)		
M1c-d	27 (54%)		
Baseline LDH (IU/L)		371 (165-2987)	50
<ULN	42 (84%)		
>ULN	8 (16%)		
Age (years)		70 (35 – 85)	50
Number of organ sites with metastases		2 (1-7)	39*
Immunotherapy Regime			50
Ipilimumab + Nivolumab	21 (42%)		
Pembrolizumab	19 (38%)		
Nivolumab	10 (20%)		
Response to Immunotherapy			50
Complete Response (CR)	7 (14%)		
Partial Response (PR)	23 (46%)		
Stable Disease (SD)	4 (8%)		
Progression of Disease (PD)	16 (32%)		

*The different number of patients included in the sub-study reflects the availability of detailed target metastatic lesion measurements in the scan reports.
ULN=upper limit of normal

4.3.3 The impact of patient clinical variables on peripheral T_{IE} cells and T cell turnover

Initially, I sought to understand if clinical factors affected T_{IE} cell expansion and T cell turnover by comparing T_{IE} cell abundance and TCR RES at T0 and W3 across established clinical parameters. The results are summarised in Table 4.2 and described here. Within the study cohort, 32 patients were male (64%) and 18 patients were female (36%). When investigating the relationship between peripheral T_{IE} cells and patient gender, there was no significant association between T_{IE} cell expansion at T0 in males compared to females, (p=0.76) or following one cycle of ICB at W3 (p=0.93) (Figure 4.1A). Additionally, there was no significant association between RES at T0 or W3 and gender (p=0.49 and p=0.75 respectively, Figure 4.2A).

When considering tumour genomics, approximately 40-50% of melanoma patients have an activating point mutation in *BRAF*, most commonly V600E/K mutation (MT) and are therefore more responsive to targeted therapies[27]. In the study cohort 16 patients (32%) had a *BRAF* V600E/K mutation and 34 patients (68%) were *BRAF* wild-type (WT) (Table 4.1). All patients were treatment naïve at baseline having received no prior immune or targeted based therapies. Peripheral T_{IE} cells and RES were examined in relation to *BRAF* mutation status to explore whether presence or absence of BRAF V600E/K mutations impacts T_{IE} expansion or changes in RES in cfDNA pre-treatment T0, and following one cycle of ICB therapy at W3. There was no significant association between T_{IE} cell expansion or RES in *BRAF* MT compared to WT patients at T0 (p=0.68 and p=0.92 respectively) or W3 (p=0.10 and p=0.19 respectively) (Figure 4.1B, Figure 4.2B).

Melanoma staging facilitates reliable assessment of prognosis and rational treatment planning. The study cohort consisted of 10 patients (20%) with unresectable stage III/IV M1a disease, 13 patients (26%) with stage IV M1b disease and 27 patients (54%) with M1c/d disease (Table 4.1). There was no significant association observed between AJCC 8th edition stage of disease and T_{IE} cell expansion at T0 (p=0.07) or W3 (p=0.09) (Figure 4.1C). Additionally, there was no correlation when considering disease stage and RES at T0 (p=0.81) and W3 (p=0.80) (Figure 4.2C). Moreover, peripheral T_{IE} cells and RES were evaluated in relation to the number of organ sites involved with metastasis to ascertain whether the number of organ sites is associated with T_{IE} expansion or changes in RES in the pre-treatment T0 setting and following one cycle of ICB therapy at W3. Within the study cohort of 39 patients with available imaging reports, 27 (70%) had ≤ 3 organ sites and 12 (30%) had ≥ 3 organ sites affected by metastasis (Table 4.2). There was no significant association between T_{IE} cell abundance or TCR RES at T0 in patients with ≤ 3 organ site metastases compared to patients

with ≥ 3 organ sites involved (p=0.49 and p=0.06 respectively) (Figure 4.1D, Figure 4.2D) and this remained non-significant at W3 for RES (p=0.44, Figure 4.2D). However, there was a significant association between W3 T_{IE} and number of organ sites affected by metastasis (p=0.006, Figure 4.1D).

Elevated serum LDH is one of the strongest independent prognostic biomarkers in metastatic melanoma and is the only serum marker that is accepted by the AJCC as a strong prognostic parameter and incorporated into the staging system for use in melanoma[15,293,294]. Furthermore, pivotal studies have shown a poorer outcome for patients with elevated LDH compared to normal LDH level at baseline[54,56,295]. Thus, patients were grouped according to baseline serum LDH below (<) or above (>) ULN and an assessment of association with T_{IE} and TCR RES pre and post one cycle of ICB undertaken. Within the study cohort, 42 patients (84%) had baseline serum LDH levels <ULN and 8 (16%) >ULN (Table 4.1). A significant association was not observed between T_{IE} cell abundance at T0 or W3, or TCR RES at T0 or W3, and LDH (p=0.65, p=0.27, p=0.29, p=0.91) (Figure 4.3A, Figure 4.3B).

When considering ICB therapy options in metastatic melanoma, a key consideration is single agent anti-PD-1 or combination anti-PD-1 plus anti-CTLA4 therapy. The decision regarding choice of treatment regimen is ultimately determined by the treating clinician, whilst considering patient co-morbidities and performance status as the doublet regimen is associated with a significantly higher risk of toxicity, but yields higher response rates, PFS and OS[56]. In the study cohort all patients were treated in the first-line setting, 19 patients (38%) with single agent pembrolizumab, 10 patients (20%) with single agent nivolumab and 21 patients (42%) with combination I+N (Table 4.1). Intriguingly, an apparent association between treatment group and both T_{IE} cell abundance at T0 (p=0.02, Figure 4.4A) and RES at W3 (p=0.01, Figure 4.4B) was observed, although it should be noted that a potential confounding factor here could be selection bias of preferential allocation of combined therapy to younger patients (mean age 58 years; range 35-79) and single agent therapy to older patients (mean age 73 years; range 51-85) (p<0.0001; Figure 4.5).

Table 4.2 Patient cohort clinical variables and their correlation with peripheral T_{IE} cells and RES at T0 and W3

	Gender			**BRAF V600E/K**			**Stage**				**Baseline LDH**			**Treatment**		
	Female n=18	**Male n=32**	**p value**	**mutant n=16**	**wild type n=34**	**p value**	**IIIC/M1a n=10**	**M1b n=13**	**M1c/d n=27**	**p value**	**<ULN n=42**	**>ULN n=8**	**p value**	**αPD1 n=21**	**αPD1 + αCTLA4 n=29**	**p value**
T0 T_n mean (range)	15.19 (1.2-41.7)	17.53 (1.48-75.6)	0.76	16.37 (2.38-39.8)	16.84 (1.2-75.6)	0.68	9.06 (1.2-33.1)	24.58 (2.38-75.6)	15.72 (2.54-44)	0.07	16.94 (1.2-75.6)	15.36 (2.54-44)	0.65	20.83 (2.54-75.6)	10.97 (1.2-38.1)	0.02
W3 T_n mean (range)	21.83 (3.58-79.2)	23.06 (1.2-73.4)	0.93	27.71 (8.97-69.3)	20.22 (1.2-79.2)	0.10	13.75 (4.52-30.1)	33.61 (4.37-79.2)	20.60 (1.2-69.3)	0.09	22.55 (3.58-79.2)	19.68 (0.23-69.3)	0.27	23.30 (1.2-73.4)	21.67 (4.37-79.2)	0.30
	Female n=11	**Male n=17**	**P value**	**Mutant n=7**	**wild type n=21**	**p value**	**IIIC/M1a n=5**	**M1b n=7**	**M1c/d n=16**	**p value**	**<ULN n=23**	**>ULN n=5**	**p value**	**αPD1 n=19**	**αPD1 + αCTLA4 n=9**	**p value**
T0 RES mean (range)	0.61 (0.47-0.71)	0.64 (0.38-0.84)	0.49	0.63 (0.47-0.77)	0.62 (0.38-0.84)	0.92	0.64 (0.51-0.71)	0.65 (0.53-0.78)	0.62 (0.38-0.85)	0.81	0.64 (0.39-0.84)	0.57 (0.48-0.71)	0.29	0.61 (0.38-0.84)	0.65 (0.47-0.84)	0.53
W3 RES mean (range)	0.70 (0.51-0.80)	0.68 (0.52-0.85)	0.75	0.73 (0.58-0.80)	0.67 (0.51-0.84)	0.19	0.68 (0.53-0.77)	0.67 (0.51-0.78)	0.69 (0.52-0.84)	0.80	0.69 (0.51-0.85)	0.66 (0.55-0.80)	0.91	0.65 (0.51-0.85)	0.75 (0.61-0.82)	0.01

The table summarises the values of T immune effector (T_{IE}) cell percental abundance in the peripheral $CD8^+$ memory T cells and rearrangement efficiency score (RES) in cell-free DNA before treatment (T0) and after 3 weeks on treatment (W3) across the clinical factors. αPD1=anti-PD1 therapy (pembrolizumab or nivolumab); αCTLA4=anti-CTLA4 therapy (ipilimumab)**;** ULN=upper limit of normal; p is Mann-Whitney U test two-sided p or non-parametric Analysis of Variance, values in brackets indicate the variable value range.

A

B

C

D

Figure 4.1 Patient cohort clinical variables and correlation with T_{IE} at T0 and W3
A: Correlation between T_{IE} cell abundance and gender at T0 (p=0.76) and W3 (p=0.93).
B: Correlation between T_{IE} cell abundance and *BRAF* V600E/K mutation status at T0 (p=0.68) and W3 (p=0.10).
C: Correlation between T_{IE} cell abundance and disease stage at T0 (p=0.07) and W3 (p=0.09).
D: Correlation between number of organ sites with metastases and T_{IE} cell abundance at T0 (p=0.49) and W3 (p=0.006).
Data points represent individual patients**.** n=50 for all analysis with the exception of D; n=39, error bars show ± SD. Statistical analysis was performed using a Mann-Whitney test two-sided p or non-parametric Analysis of Variance.
ns = not significant, WT = wild-type, MT = mutant, SD = standard deviation.

A

B

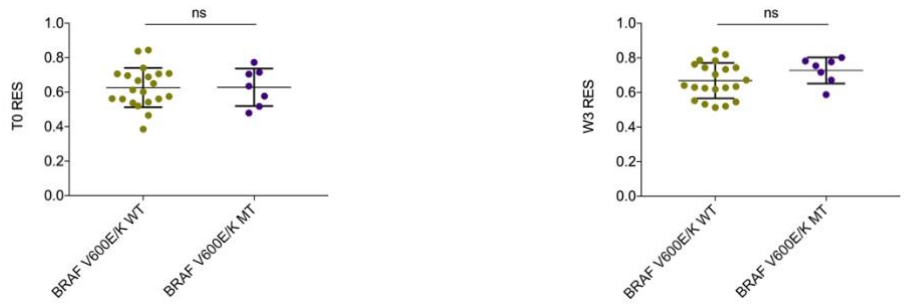

C

D

Figure 4.2 Patient cohort clinical variables and correlation with RES at T0 and W3
A: Correlation between gender and RES at T0 (p=0.49) and W3 (p=0.75).
B: Correlation between BRAF V600E/K mutation status and RES at T0 (p=0.92) and W3 (p=0.19).
C: Correlation between disease stage and RES at T0 (p=0.81) and W3 (p=0.80).
D: Correlation between number of organ sites affected by metastasis and RES at T0 (p=0.06) and W3 (p=0.44).
Data points represent individual patients**.** n=50 for all analysis with the exception of D; n=39, error bars show ± SD. Statistical analysis was performed using a Mann-Whitney test two-sided p or non-parametric Analysis of Variance.
RES = rearrangement efficiency score, ns = not significant, WT = wild-type, MT = mutant, SD = standard deviation.

A

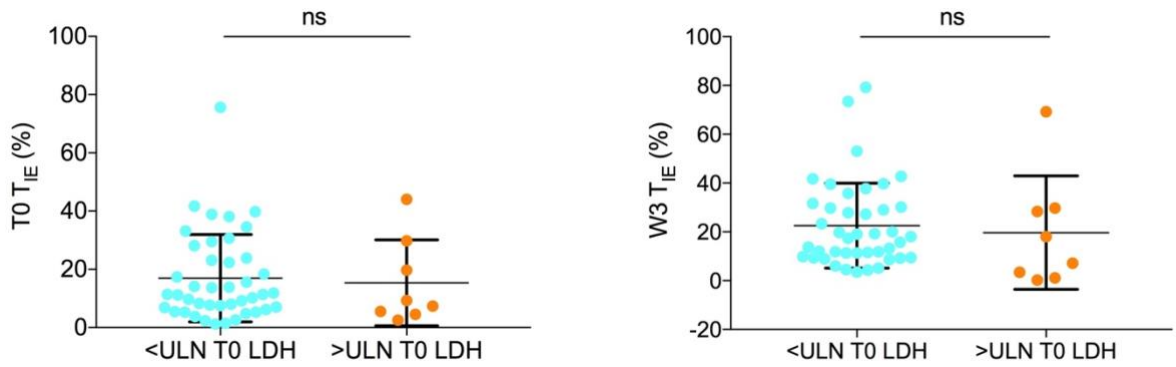

B

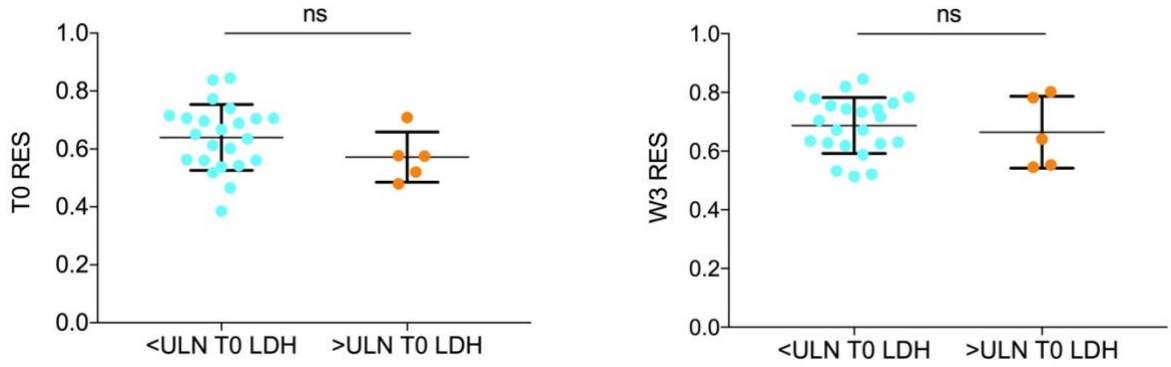

Figure 4.3 T0 ULN LDH and correlation with peripheral T_{IE} cells and RES
A: Baseline, T0 LDH values below (<) and above (>) ULN and their correlation with T_{IE} cells at T0 (p=0.65) and after one cycle of ICB at W3 (p=0.27); n=50.
B: Baseline, T0 LDH values below (<) and above (>) ULN and their correlation with RES at T0 (p=0.29) and after one cycle of ICB at W3 (p=0.91); n=28.
Data points represent individual patients**.** Error bars show ± SD. Statistical analysis was performed using a Mann-Whitney test two-sided p.
ns = not significant, RES = rearrangement efficiency score, ULN = upper limit of normal, SD = standard deviation.

A

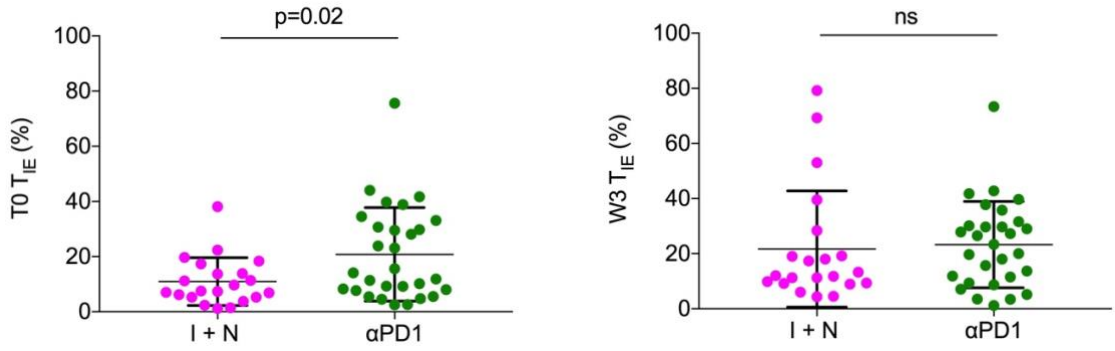

B

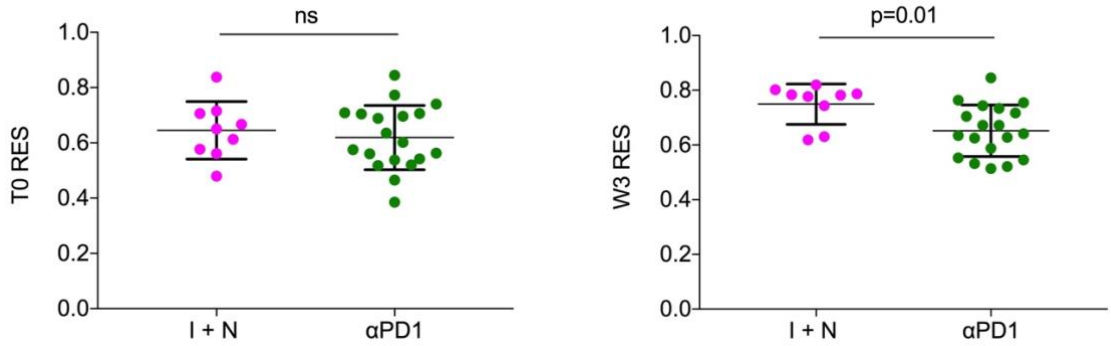

Figure 4.4 Treatment group and their correlation with T_{IE} and RES at T0 and W3
A: Correlation between treatment group and T_{IE} cell abundance at T0 (p=0.02) and W3 (p=0.30); n=50.
B: Correlation between treatment group and RES at T0 (p=0.53) and W3 (p=0.01), n=28.
Data points represent individual patients; error bars show ± SD. Statistical analysis was performed using a Mann-Whitney test two-sided p or non-parametric Analysis of Variance.
RES = rearrangement efficiency score, I + N = ipilimumab + nivolumab; αPD1= nivolumab or pembrolizumab, SD = standard deviation.

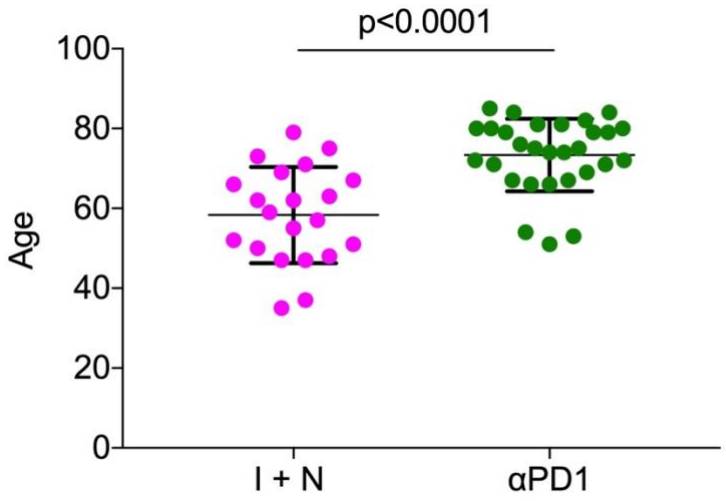

Figure 4.5 Patient age in treatment groups
Age (years) of patients receiving combination anti-CTLA4 plus anti-PD1 drugs (I+N; mean=58, n=21) or single-agent anti-PD1 drugs (αPD1; mean=73, n=29); two-sided Mann-Whitney U test p<0.0001. Data points represent individual patients.
I + N = ipilimumab + nivolumab, αPD1=nivolumab or pembrolizumab.

4.4.4 There is a relationship between T_{IE} abundance, RES and age, but the kinetics of T_{IE} cell expansion and RES increase in response to ICB are not affected by age.

Noting the age-dependent selection bias for treatment protocol, it was important to explore whether age had an impact on the robustness of the immune signature. Using the accepted geriatric oncology definition for the elderly population of 70 years of age[296], it was observed that at T0 the mean T_{IE} cell abundance was 11.2% (range 1.2%-33.1%) of the circulating CD8+ memory T cells in patients of 69 years and less, but 22% (range 2.54%-75.6%) in patients of 70 years and older (Figure 4.6). Thus, as a proportion of the memory T cell pool, the T_{IE} cell subset increased with age (r=0.4), and this finding may underlie the observed association between treatment group and T_{IE} cells abundance at T0 (Figure 4.4A). At W3 a similar pattern was observed, a mean T_{IE} cell abundance of 21% (range 3.47%-79.2%) of the circulating CD8+ memory T cells in patients of 69 years and less, and 24% (range 0.23%-73.4%) in patients of 70 years and older (Figure 4.6). Note that there was an increase in T_{IE} cell abundance in responding patients at all ages as illustrated by the higher regression line at W3 compared to T0.

In addition, it was observed that at T0, the mean RES was 0.62 (range 0.47-0.74) in patients of 69 years and less, and 0.62 (range 0.38-0.84) in patients of 70 years and older, whilst at W3 the mean RES was 0.71(range 0.58-0.80) in patients of 69 years and less, but 0.65 (range 0.51-0.84) in patients of 70 years and older (Figure 4.7). Again, there was an increase in RES in responding patients at all ages as indicated by the upward shift of the line of regression at W3 compared to T0. Although the inverse relationship between RES and age appears to be rather weak (r=-0.12 to -0.32), the slight increase in correlation between RES after treatment and age may underlie the observed association between treatment protocol and TCR RES at W3 (Figure 4.4B).

4.4.4.1 Radiological Response to ICB is not age dependent

Radiological response was evaluated in relation to age to understand if patient age impacts their response to therapy. There was no significant difference identified between patient age and response to therapy (p=0.44) (Figure 4.8). The median age of patients with disease control was 71 years, with a mean age of 65 years (range 35-84 years). In patients with disease progression, both the median and mean age was 69 years (range 47-85 years).

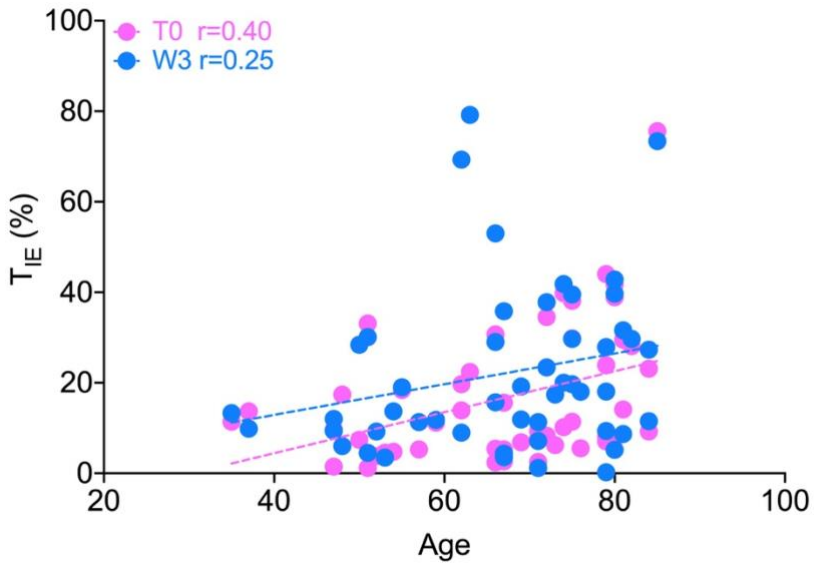

Figure 4.6 Correlation between age and peripheral T_{IE} cells
Correlation between age (years) and T_{IE} cell abundance at baseline (T0, pink, r=0.40; n=50) and after first cycle of immunotherapy (W3, blue, r=0.25; n=50).
Data points represent individual patients, n=50. Statistical analysis was performed using Spearman test. Dotted line is the linear regression line.

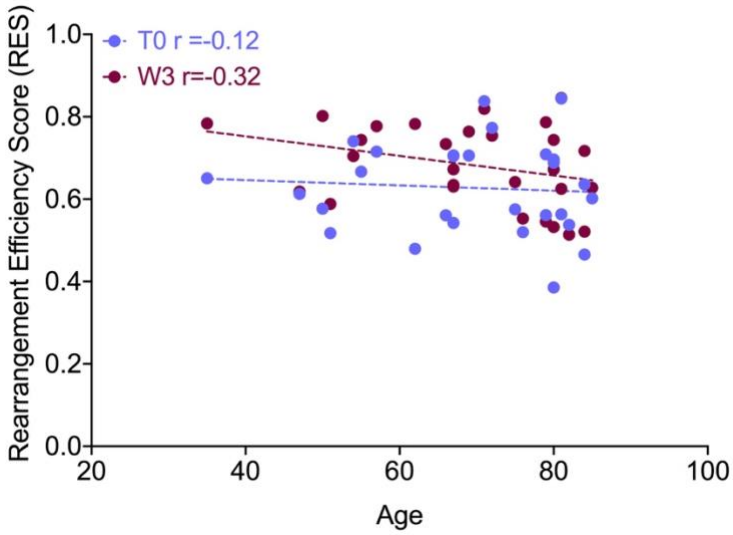

Figure 4.7 Correlation between age and RES
Correlation between age (years) and TCR receptor RES at baseline (T0, purple, r=-0.12; n=28) and after the first cycle of immunotherapy (W3, maroon, r=-0.32; n=28).
Data points represent individual patients. Statistical analysis was performed using Spearman test. Dotted lines represent the linear regression line for each time point.
RES = rearrangement efficiency score.

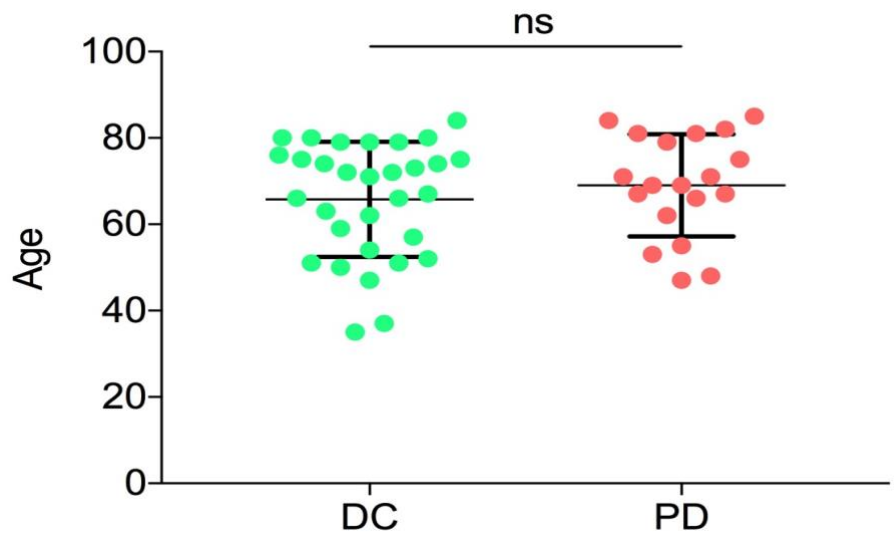

Figure 4.8 Correlation between patient best response and age
Correlation between best response DC (green), n=31 or best response PD (salmon), n= 19 and patient age (years), p=0.44.
Data points represent individual patients. n=50, error bars show ± SD. Statistical analysis was performed using a Mann-Whitney test two-sided p.
ns = not significant, DC = disease control, PD = progressive disease, SD = standard deviation.

4.4.5 The impact of patient clinical variables on TCR repertoire evolution in response to ICB

There was a significant correlation between patients that displayed an increase in either the clonality or diversity of the peripheral TCR repertoire after one cycle of ICB and response to treatment[234]. Therefore, it was important to examine whether peripheral TCR repertoire rearrangements in response to ICB therapy were affected by patient and tumour factors. PBMC TCR sequences were analysed using ImmunoSEQ® as described in section 2.7.2 to calculate clonality (Gini coefficient) and diversity (Renyi index)[234]. No significant association was identified between Gini coefficient, at T0 and W3, or Renyi index, at T0 and W3 and gender (p=0.21, p=0.38, p=0.27, p=0.38, Figure 4.9A), BRAF V600E/K mutation status (p=0.82, p=0.57, p=0.90, p=0.94, Figure 4.9B), AJCC stage of disease (p=0.63, p=0.78, p=0.99, p=0.72, Figure 4.9C), number of organ sites ($\leq$ 3 or >3) affected by metastases (p=0.92, p=0.97, p=0.97, p=0.87, Figure 4.9D) or LDH levels (p=0.52, p=0.89, p=0.76, p=0.72, Figure 4.9E). However, an association was observed between treatment protocol and Gini coefficient at T0 (p=0.03) and W3 (p=0.05) (Figure 4.10A), and between treatment protocol and Renyi index at T0 (p=0.05) and W3 (p=0.03) (Figure 4.10B). The results presented here are displayed in Table 4.3 and include the mean values and range for each analysis.

Table 4.3 Patient cohort clinical variables and their correlation with peripheral TCR repertoire at both T0 and W3

	Gender			**BRAF V600E/K**			**Stage**				**Baseline LDH**			**Treatment**		
	Female n=10	Male n=19	p value	Mutant n=7	wild type n=22	p value	III/M1a n=6	M1b n=7	M1c/d n=16	p value	<ULN n=24	>ULN n=5	p value	αPD1 n=19	αPD1 + αCTLA4 n=10	p value
T0 clonality mean (range)	0.37 (0.13-0.73)	0.30 (0.11-0.61)	0.21	0.32 (0.16-0.55)	0.32 (0.11-0.73)	0.82	0.30 (0.17-0.44)	0.35 (0.19-0.61)	0.32 (0.11-0.73)	0.63	0.33 (0.12-0.74)	0.29 (0.14-0.61)	0.52	0.37 (0.13-0.73)	0.23 (0.11-0.38)	0.03
W3 clonality mean (range)	0.35 (0.12-0.78)	0.30 (0.09-0.60)	0.38	0.33 (0.20-0.60)	0.31 (0.09-0.78)	0.57	0.25 (0.16-0.35)	0.35 (0.16-0.60)	0.33 (0.09-0.78)	0.78	0.33 (0.10-0.79)	0.31 (0.15-0.60)	0.89	0.37 (0.12-0.78)	0.22 (0.09-0.33)	0.05
T0 diversity mean (range)	7.82 (4.98-9.16)	8.17 (4.82-9.73)	0.27	7.93 (4.82-9.25)	8.09 (4.98-9.73)	0.90	8.25 (7.09-9.15)	8.12 (5.78-9.29	7.95 (4.82-9.73)	0.99	8.07 (4.83-9.74)	7.99 (6.23-9.06)	0.76	7.70 (4.82-9.25)	8.72 (7.81-9.73)	0.05
W3 diversity mean (range)	7.92 (4.84-9.06)	8.20 (5.48-9.72)	0.38	8.11 (5.48-9.31)	8.11 (5.48-9.31)	0.94	8.49 (7.42-9.06)	8.17 (5.92-9.35)	7.93 (4.84-9.72)	0.72	8.12 (4.84-9.72)	8.08 (6.47-8.86)	0.72	7.75 (4.84-9.31)	8.79 (7.80-9.72)	0.03

The table summarises the value of peripheral T cell clonality (Gini coefficient) and diversity (Renyi index) before treatment (T0) and after 3 weeks (W3) on treatment across the clinical factors. αPD1=anti-PD1 therapy (pembrolizumab or nivolumab); αCTLA4=anti-CTLA4 therapy (ipilimumab); ULN=upper limit of normal; p is Mann-Whitney U test two-sided p or non-parametric Analysis of Variance; values in brackets are the variable range.

A

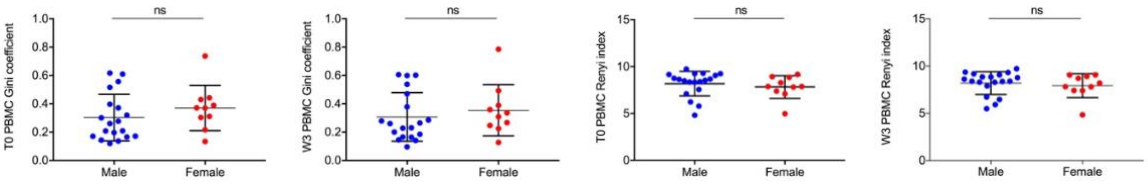
T0 PBMC Gini coefficient
W3 PBMC Gini coefficient
T0 PBMC Renyi index
W3 PBMC Renyi index
ns
Male
Female

B

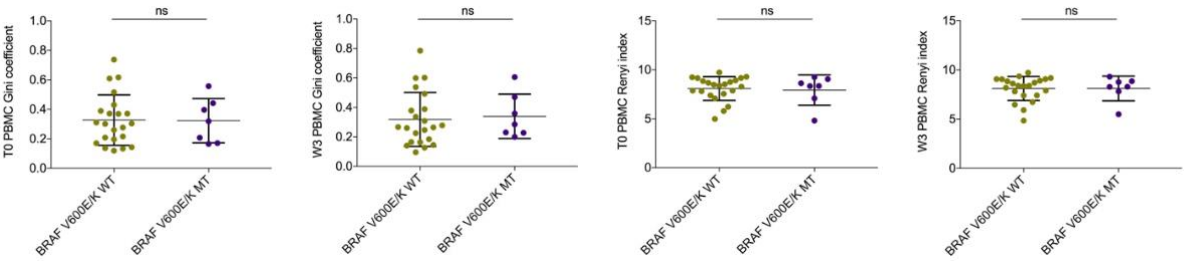
T0 PBMC Gini coefficient
W3 PBMC Gini coefficient
T0 PBMC Renyi index
W3 PBMC Renyi index
ns
BRAF V600E/K WT
BRAF V600E/K MT

C

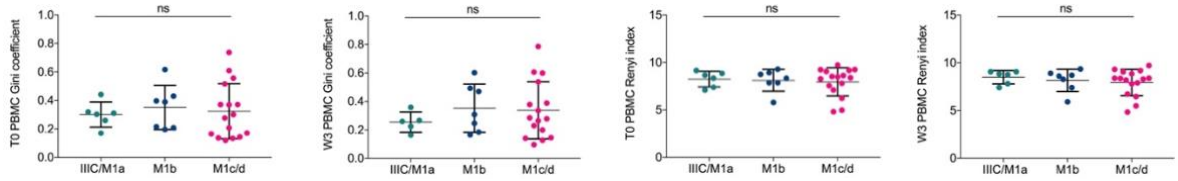
T0 PBMC Gini coefficient
W3 PBMC Gini coefficient
T0 PBMC Renyi index
W3 PBMC Renyi index
ns
IIIC/M1a
M1b
M1c/d

D

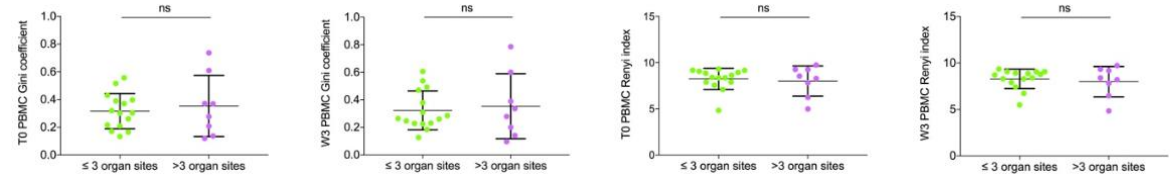
T0 PBMC Gini coefficient
W3 PBMC Gini coefficient
T0 PBMC Renyi index
W3 PBMC Renyi index
ns
≤ 3 organ sites
>3 organ sites

E

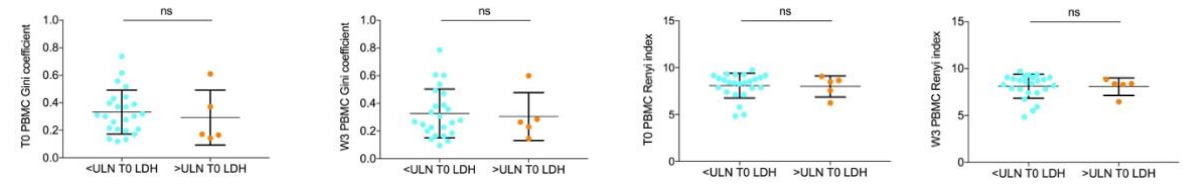
T0 PBMC Gini coefficient
W3 PBMC Gini coefficient
T0 PBMC Renyi index
W3 PBMC Renyi index
ns
<ULN T0 LDH
>ULN T0 LDH

Figure 4.9 Patient cohort clinical variables and their correlation with peripheral TCR clonality (Gini coefficient) and diversity (Renyi index)

A: Correlation between Gini coefficient and gender at T0 (p=0.21) and W3 (p=0.38); Correlation between Renyi index and gender at T0 (p=0.27) and W3 (p=0.38).

B: Correlation between Gini coefficient and *BRAF* V600E/K mutation status at T0 (p=0.82) and W3 (p=0.57); Correlation between Renyi index and *BRAF* V600E/K mutation status at T0 (p=0.90) and W3 (p= 0.94).

C: Correlation between Gini coefficient and disease stage at T0 (p=0.63) and W3 (p=0.78); Correlation between Renyi index and disease stage at T0 (p=0.99) and W3 (p=0.72).

D: Correlation between number of organ sites with metastases and Gini coefficient at T0 (p=0.92) and W3 (p=0.97); Correlation between number of organ sites with metastases and Renyi index at T0 (p=0.97) and W3 (p=0.87).

E: Baseline, T0 LDH values below (<) and above (>) ULN and their correlation with Gini coefficient at T0 (p=0.52), W3 (p=0.89) and Renyi index at T0 (p=0.76), W3 (p=0.72).

Data points represent individual patients**.** n=50 for all analysis with the exception of D; n=39 and E; n=29; error bars show ± SD. Statistical analysis was performed using a Mann-Whitney test two-sided p or non-parametric Analysis of Variance.

ns = not significant, WT = wild-type, MT = mutant, SD = standard deviation.

A

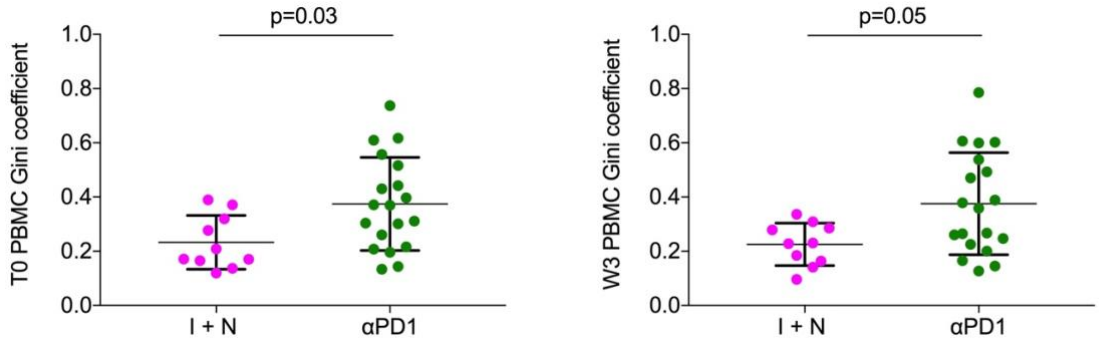

B

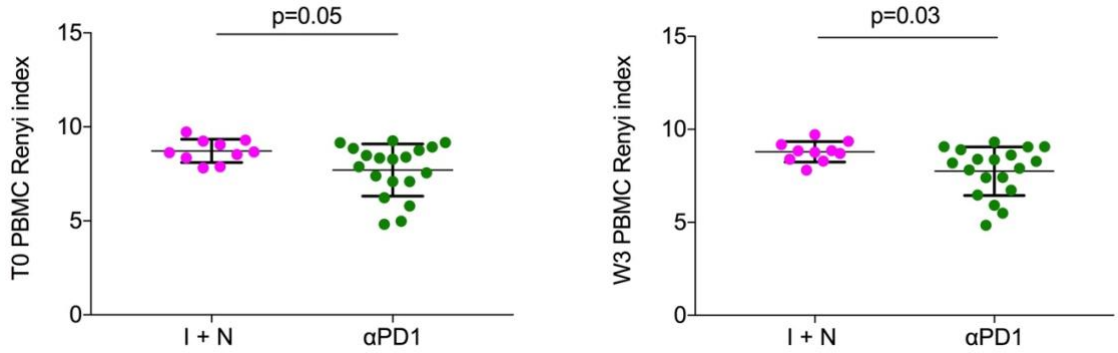

Figure 4.10 Treatment groups and their correlation with peripheral TCR clonality (Gini coefficient) and diversity (Renyi index)

A: Correlation between patients receiving combination anti-CTLA4 plus anti-PD1 drugs (I+N) or single-agent anti-PD1 drugs (αPD1) and Gini coefficient at baseline, T0 (p=0.03) and after first cycle ICB at W3 (p=0.05).

B: Correlation between patients receiving combination anti-CTLA4 plus anti-PD1 drugs (I+N) or single-agent anti-PD1 drugs (αPD1) and Renyi index at baseline T0 (p=0.05) and after first cycle of ICB at W3 (p=0.03).

Data points represent individual patients. I+N; n=21, αPD1; N=29, error bars show ± SD. Statistical analysis was performed using a Mann-Whitney test two-sided p.

I + N = ipilimumab + nivolumab, αPD1=nivolumab or pembrolizumab, SD = standard deviation.

4.4.6 There is a correlation between TCR repertoire and age and TCR evolution in response to ICB is affected by age

In view of the observed association between treatment protocol and clonality and diversity at T0 and W3 (Figure 4.10A, Figure 4.10B), and the preferential allocation of combined therapy to younger patients and single agent therapy to older patients (Figure 4.5), it was important to examine if age impacted clonality and diversity. At T0 it was observed that the Gini coefficient mean was 0.26 (range 0.13-0.44) for patients 69 years and less, and 0.38 (range 0.11-0.73) for patients of 70 years and older (Figure 4.11A). At W3 the mean Gini coefficients were 0.24 (range 0.14-0.38) for patients 69 years and less, and 0.39 (range 0.09-0.78) for patients of 70 years and over (Figure 4.11A). Thus, TCR clonality showed an overall positive correlation with age (r=0.36 and r=0.39 at T0 and W3 respectively), but unlike T_{IE} abundance and TCR RES, the linear regression line did not shift up or down with ICB treatment, but changed in slope, suggesting a trend towards increased clonality in older patients on ICB therapy (Figure 4.11A).

At T0 the mean Renyi index was 8.49 (range 7.09-9.29) for patients of 69 years and less, and 7.64 (range: 4.82-9.73) in patients of 70 years and older (Figure 4.11B). At W3 the mean Renyi index was 8.62 (range 7.42-9.35) in patients 69 years and less, and 7.63 (range 4.84-9.72) in patients of 70 years and older (Figure 4.11B). Thus, TCR diversity showed an inverse relationship with age (r=-0.29 and r=-0.39 at T0 and W3 respectively) and as was observed with clonality, the linear regression line did not shift up or down with ICB treatment, but changed in slope, suggesting a trend towards increased diversity in younger patients on ICB treatment (Figure 4.11B).

A

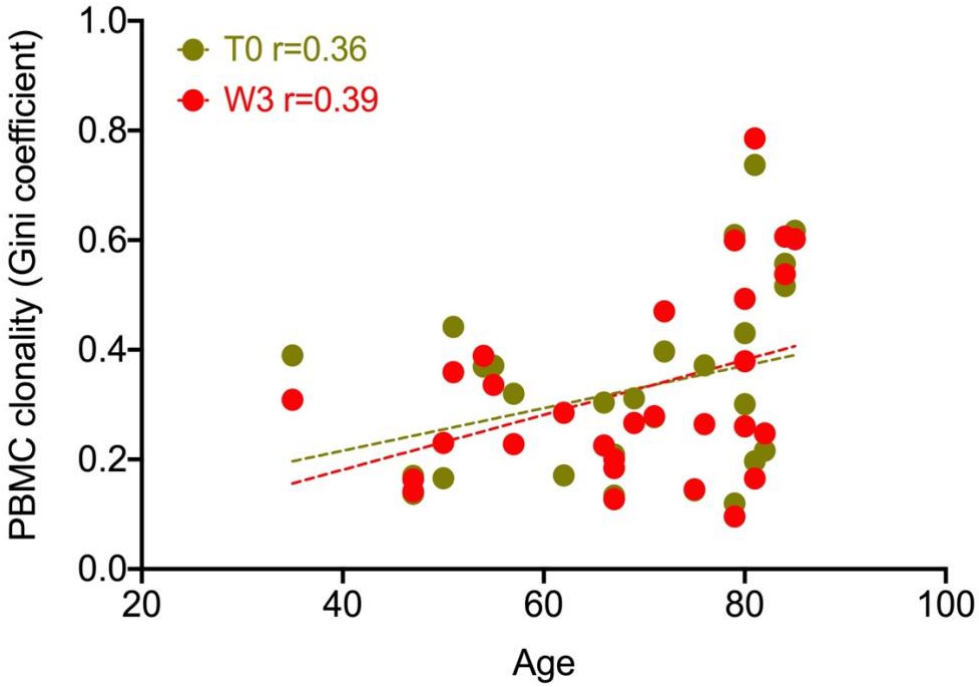

B

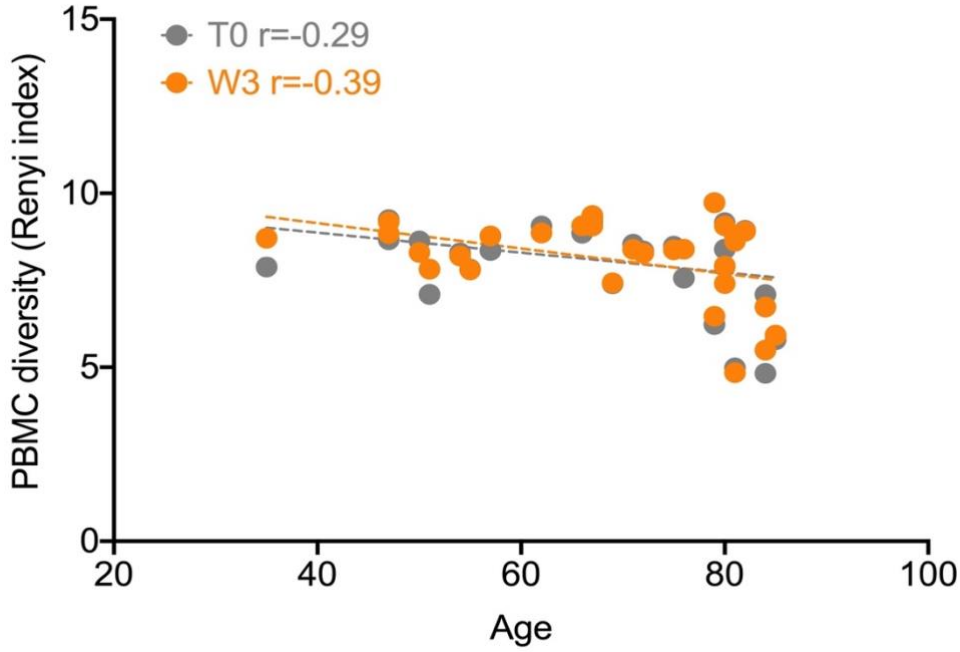

Figure 4.11 Correlation between age and peripheral TCR clonality and diversity
A: Correlation between age (years) and PBMC clonality (Gini coefficient) at baseline (T0, olive, r=0.36; n=29), and after the first cycle of immunotherapy (W3, red, r=0.39; n=29.
B: Correlation between age (years) and PBMC T cell receptor diversity (Renyi index) at baseline (T0, grey, r=-0.29; n=29) and after first cycle of immunotherapy (W3, orange, r=-0.39; n=29).
Data points represent individual patients. Statistical analysis was performed using Spearman test.

4.4.7 Relationship between peripheral TCR repertoire and T_{IE} cells before and after the first cycle of ICB

As the data suggest that peripheral T_{IE} cell abundance and TCR repertoire rearrangements were both influenced by age, the next step was to compare these variables to each other. At T0, the mean T_{IE} cell abundance was 17%, so using this as a cut-off, it was observed that patients with a T_{IE} cell abundance $\leq$17% had a mean TCR Gini coefficient of 0.29 (range: 0.11-0.73), whereas patients with a T_{IE} cell abundance >17% had a mean TCR Gini coefficient of 0.37 (range: 0.14-0.61) (Figure 4.12A). Conversely, patients with a T_{IE} cell abundance $\leq$17% had a mean Renyi index of 8.35 (range: 4.97-9.25), whereas patients with a T_{IE} cell abundance >17% had a mean Renyi index of 7.63 (range: 4.82-9.05) (Figure 4.12A). After one cycle of ICB treatment (W3), the mean T_{IE} cell abundance was 22%, so using this as a cut-off, it was observed that patients with a T_{IE} cell abundance $\leq$22% had a mean TCR Gini coefficient of 0.30 (range: 0.09-0.78), whereas patients with a T_{IE} cell abundance >22% had a mean TCR Gini coefficient of 0.34 (range: 0.14-0.60) (Figure 4.12B). Conversely, patients with a T_{IE} cell abundance $\leq$22% had a mean Renyi index of 8.23 (range: 4.84-9.72), whereas patients with a T_{IE} cell abundance >22% had a mean Renyi index of 7.93 (range: 5.48-9.31) (Figure 4.12B). Thus, both before and after one cycle of ICB treatment, there was a positive correlation between T_{IE} cell abundance and peripheral T cell TCR clonality (r=0.43, r=0.19 respectively), but an inverse correlation between T_{IE} cell abundance and peripheral T cell TCR diversity (r=-0.42, r=-0.17 respectively) (Figure 4.12A, Figure 4.12B).

A

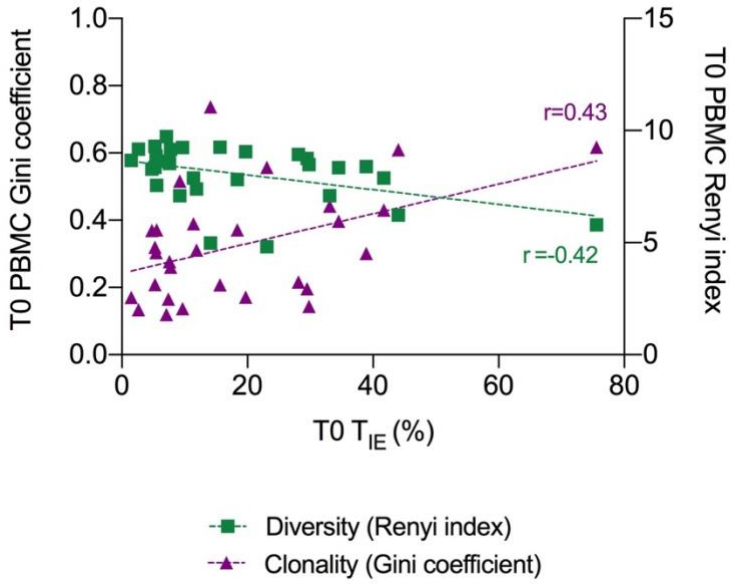

B

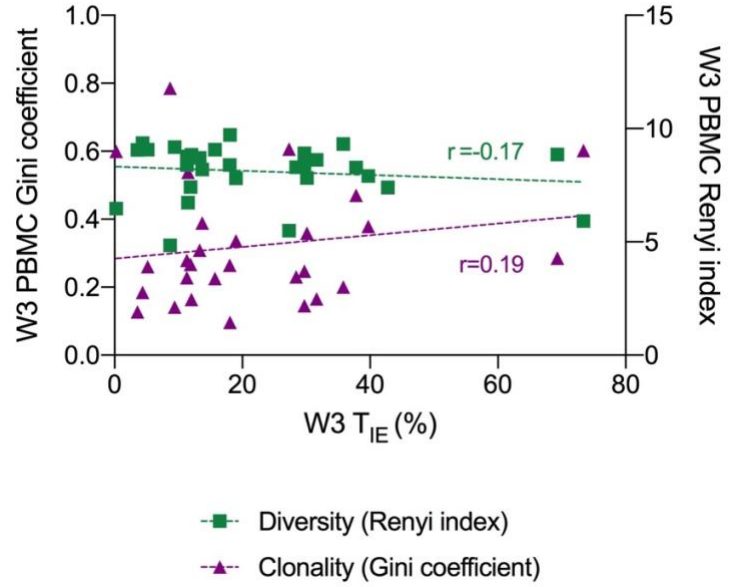

Figure 4.12 Correlation between T_{IE} cells and peripheral TCR repertoire
A: Correlation between T_{IE} cell abundance at baseline T0 and PBMC T cell receptor Renyi index and Gini coefficient at T0 (green squares denote diversity, r=-0.42; purple triangles denote clonality, r=0.43).
B: Correlation between T_{IE} cell abundance after first cycle of immunotherapy W3 and PBMC T cell receptor Renyi index and Gini coefficient at W3 after first cycle of immunotherapy (green squares denote diversity, r=-0.17; purple triangles denote clonality, r=0.19).
Data points represent individual patients. n=29. Statistical analysis was performed using linear regression.

4.4.8 Age is associated with different patterns of T cell repertoire rearrangement

Finally, a comparison of how peripheral T cell clonality and diversity changed at W3 relative to T0 (W3-T0[Gini]=Δ_{W3}Gini; W3-T0 [Renyi]=Δ_{W3}Renyi) and assessment of the impact of age on the pattern of evolution was performed. To separate the TCR repertoire rearrangement at W3 according to evolution pattern (prevalence of increased clonality vs prevalence of increased diversity), a linear classifier algorithm was applied to segregate the changes of clonality and diversity at W3 into predominant clonal evolution (blue hemi-plot in Figure 4.13A) or predominant diversity evolution (pink hemi-plot in Figure 4.13A) for patients <70 years (purple dots in Figure 4.13A) and ≥70 years (green dots in Figure 4.13A). There were 5 patients <70 years and 12 patients ≥70 years who fell into the predominant clonal evolution plot, whereas 9 patients <70 years and 3 patients ≥70 years fell into the predominant diverse evolution plot (Figure 4.13A). Thus, in patients <70 years of age, 5/14 had peripheral T cell TCR clonality dominance and 9/14 had peripheral T cell TCR diversity dominance (Figure 4.13B), whereas in patients ≥70 years of age, 12/15 had peripheral T cell clonality dominance and 3/15 had peripheral T cell diversity dominance (p=0.03, Figure 4.13B). Therefore, in response to ICB therapy, TCR rearrangements trend towards increased diversity in younger patients but increased clonality in older patients.

In a separate external cohort of 11 patients with metastatic melanoma treated with first line anti-PD1 based therapy, evaluation of TCR repertoire pre-treatment, T0 and after the first cycle at W3 was undertaken to validate the findings[80]. Calculating the change in peripheral T cell clonality and diversity from T0 to W3 using Δ_{W3}Gini and Δ_{W3}Renyi and segregating the changes of clonality and diversity at W3 into predominant clonal evolution (blue hemi-plot in Figure 4.14A) or predominant diverse evolution (pink hemi-plot in Figure 4.14A) for patients <70 years (purple dots in Figure 4.14A) and ≥70 years (green dots in Figure 4.14A). There was 1 patient <70 years and 3 patients ≥70 years who fell into the predominant clonal evolution plot, whereas 6 patients <70 years and 1 patient ≥70 years fell into the predominant diverse evolution plot (Figure 4.14A). Thus, in patients <70 years of age, 1/7 had peripheral T cell TCR clonality dominance and 6/7 had peripheral T cell TCR diversity dominance (Figure 4.14B), whereas in patients ≥70 years of age, 3/4 had peripheral T cell clonality dominance and 1/4 had peripheral T cell diversity dominance (p=0.08, Figure 4.14B).

A

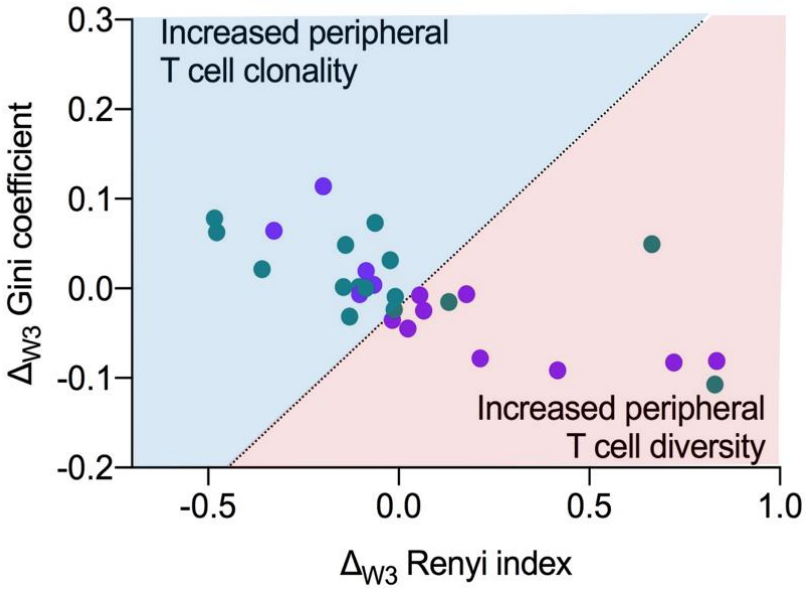

B

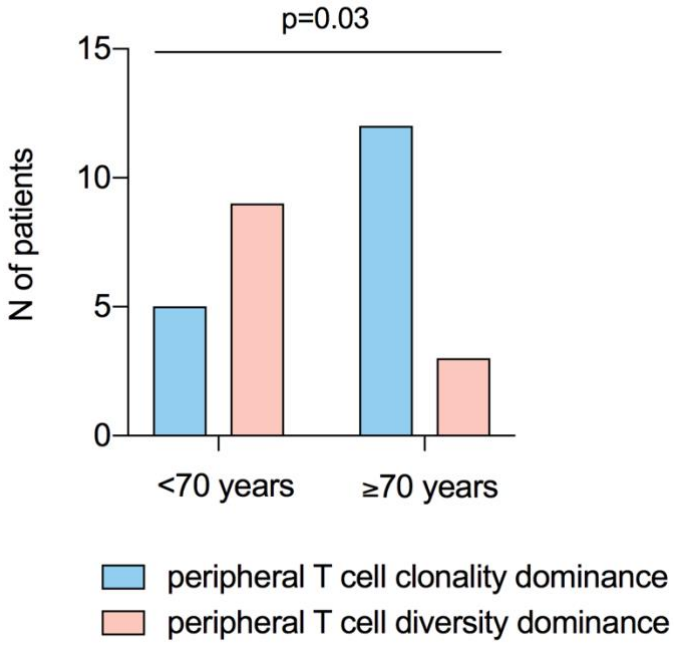

Figure 4.13 Relationship between age and peripheral TCR repertoire re-arrangement
A: Scatter plot showing changes in peripheral TCR clonality (Gini coefficient) and diversity (Renyi index) after one cycle of anti-PD1 based treatment (W3 compared T0: Δ_{W3}) for patients in the age group < 70 years (purple dots) and ≥ 70 years (green dots). The dotted line represents the linear discriminant (X0=0.024, slope=0.4) for TCR re-arrangement with increased peripheral T cell clonality (hemi-plot in blue) vs increased peripheral T cell diversity (hemi-plot in pink). Each dot is a single patient (n=29).
B: Comparison of the number of patients with peripheral T cell re-arrangement pattern towards dominant clonality (blue) or dominant diversity in (pink) from **A**, according to age group (n=29; Fisher test p=0.03). N=number of patients.

A

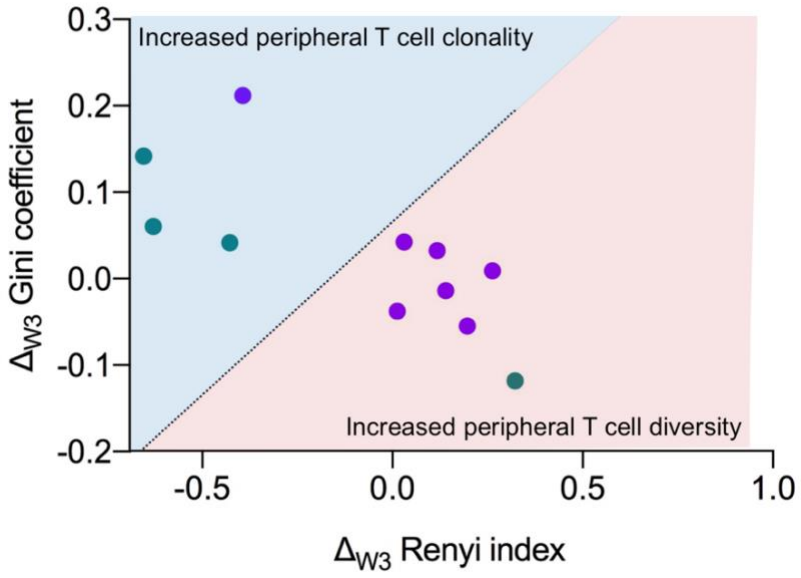

B

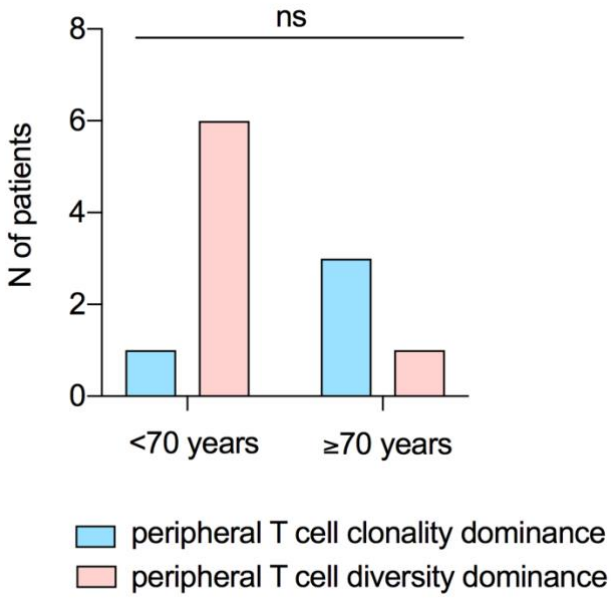

Figure 4.14 External validation cohort of relationship between age and peripheral TCR repertoire re-arrangement

A: Scatter plot showing changes in peripheral TCR clonality (Gini coefficient) and diversity (Renyi index) after one cycle of anti-PD1 based treatment (W3 compared T0: Δ_{W3}) for patients in the age group < 70 years (purple dots) and ≥ 70 years (green dots). The dotted line represents the linear discriminant (X0=0.024, slope=0.4) for TCR re-arrangement with increased peripheral T cell clonality (hemi-plot in blue) vs increased peripheral T cell diversity (hemi-plot in pink). Each dot is a single patient (n=11).

B: Comparison of the number of patients with peripheral T cell re-arrangement pattern towards dominant clonality (blue) or dominant diversity in (pink) from **A**, according to age group (n=11; Fisher test, p=0.08). N=number of patients.

4.5 Discussion

Immunotherapy has revolutionised clinical outcomes in melanoma. However, not all patients will derive clinical benefit or durable responses, highlighting the need to identify reliable predictive biomarkers of response to immunotherapeutic agents. The development of biomarkers with high sensitivity, specificity and accuracy would enable early identification of responders from non-responders and improved tailoring of treatment strategy. This study was undertaken to explore the impact of patient clinical variables on candidate biomarkers identified as predictive of response to ICB in treatment naïve metastatic melanoma patients, specifically, peripheral T_{IE} cell evolution, T cell turnover and TCR repertoire changes prior to and following the first cycle of ICB.

Despite the acknowledged sex-related dimorphism in immune system response[297], little is known about early changes in circulating T cells and their association with gender. However, studies of immunotherapy responses have identified that the magnitude of benefit is sex-dependent as with advanced solid malignancies, males have a better response than females to treatment with ICB[297]. Another widely accepted marker of response to immunotherapy is TMB[97,98]. TMB has been correlated with gender, with higher TMB observed in males compared to females[195,298]. Within this study, limited availability of tumour tissue and unbalanced gender groups with predominantly more males than females in the cohort meant meaningful comparisons could not be made with the immune signature.

Interestingly, no difference was observed in expression of the immune signature and melanoma *BRAF* mutation status, despite the typically different clinical disease courses observed. This finding suggests that the peripheral T cell phenotype is independent of the presence or absence of *BRAF* mutation. Evaluation of disease stage and peripheral T cell and TCR repertoire changes in the context of ICB did not reveal any significant correlations. However, it is important to consider that sites of metastasis such as liver and brain harbour different immune microenvironments[299]. Within the context of this study, it was not possible to evaluate this further by separating the M1c and M1d cohorts as at the time of patient recruitment, routine baseline brain imaging as part of clinical work up was not fully established within the treating organisation. Therefore, not all patients had undergone baseline brain imaging and so the study cohort may have included patients with undiagnosed brain metastasis.

In the advanced disease setting, responses to ICB are heterogeneous depending on the metastatic organ sites involved and the tissue specific immunobiology within the TME which

are known to contribute to differential therapeutic responses[300]. Peripheral T_{IE} expansion at W3 was associated with response to ICB and improved survival[234]. Thus, the significant difference in T_{IE} cell abundance in patients with ≤ 3 organ sites compared to those with > 3 organ sites with metastases at W3 may be due to a deeper interaction between local immune-biological TME and the systemic adaptive immune system response. Patients with ≤ 3 organs affected by metastases had an increase in peripheral T_{IE} cell abundance at W3 after one cycle of ICB, in keeping with the widely accepted concept that those with fewer sites of disease are more likely to respond to ICB therapy[301].

Notably, the LDH assay was modified during the course of the study and a change in the ULN cut off values affected 6 of 50 patients, which could have influenced the relationship between LDH ULN and the T cell biomarkers reported, thus making it difficult to draw any definitive conclusions from the LDH data in this setting.

A significant difference in age between the two treatment groups was observed, which likely reflects selection bias from clinicians in the real-world setting, as patients ≥70 years were preferentially assigned to single agent therapy. This could affect the interpretation of the effect of treatment regimen on the biomarker dynamics, and the small sample size precludes the ability to gain meaningful insight from any intra-group comparisons. However, the absence of any change from pre-treatment in the relationships between treatment regimen and the immune-biomarkers that were measured after treatment initiation suggests a negligible effect of drug schedule in this cohort. Moreover, there was no effect of the clinical variables of gender, BRAF mutation, stage, and LDH status on T_{IE} cell expansion, T cell turnover or peripheral T cell TCR repertoire rearrangements. This supports the importance of T_{IE} cell expansion, T cell turnover and peripheral T cell TCR repertoire rearrangements as biomarkers of response to therapy.

The role of age as a prognostic factor for melanoma is well described[302,303,304,305], but it is unclear if this is a consequence of distinct melanoma biology[306], different patterns of UV-induced DNA damage[9] or immune-senescence[307]. Notably, elderly patients often display greater benefit from ICB than younger patients[308,309], but the mechanisms underlying this observation are unclear[308], and it could be due to a selection bias caused by fitter patients with less advanced disease within the elderly cohort being offered ICB preferentially[309]. Taken together, these observations suggest that age plays an important role in the interactions between melanoma, the immune system and immunotherapy, and are consistent with the findings here that age affects immune-awakening in response to ICB.

Age is associated with different patterns of T cell repertoire rearrangement but has no significant impact on peripheral T_{IE} cell dynamics. However, the increase in peripheral T_{IE} cell abundance with advancing age is in line with previous reports showing that memory T cell pools expand with increasing age[310], but also suggest that peripheral T_{IE} subset responses to ICB therapies are age-independent. It has also been demonstrated that T_{IE} cell abundance inversely correlates with peripheral TCR repertoire diversity and directly correlates with peripheral T cell repertoire clonality, consistent with a repertoire convergence in patients with pre-existing T_{IE} expansion[234]. Moreover, as previously shown[234] this relationship became less apparent as T_{IE} expansion was boosted in patients benefitting from treatment, irrespective of age.

It was demonstrated that although T_{IE} expansion and peripheral T cell turnover are biomarkers of immunotherapy response across all age groups, patients in different age groups present different patterns of peripheral T cell TCR repertoire evolution in response to ICB. Specifically, after one cycle of immunotherapy, in patients ≥70 years immunotherapy leads to a preferential increase in peripheral T cell TCR clonality, whereas in patients <70 years it leads to a preferential increase in peripheral T cell TCR diversity. In a separate external cohort of 11 patients[80], there was no statistically significant difference in TCR repertoire observed between patients aged <70 years and those ≥ 70 years. However, there was a trend towards, patients aged ≥70 years displaying an increase in clonality as measured by the Δ_{W3}Gini coefficient, whereas patients aged <70 years with the exception of one, had an increase in diversity as measured by Δ_{W3}Renyi index. It is therefore likely that statistical significance was not reached due to the small number of patients in the validation cohort. However, the trend is consistent with the observation that in different age groups one cycle of immunotherapy induces different dynamics in peripheral T cell evolution.

These findings are in keeping with the literature observing a differential pattern of response to ICB in older patients[308,309]. A multi-institutional cohort of over 500 patients were studied to analyse the relationship between age and response to anti-PD1 therapy. Older patients were found to respond more efficiently to anti-PD-1 and the likelihood of response increased with age even in the absence of a more complex mutational landscape[308]. A further study using a real-world patient cohort evaluated the efficacy of ICB in older compared to younger patients with metastatic melanoma and a survival benefit was observed in both younger and older patients. Interestingly, there was a statistically significant interaction between age and survival with ICB, where a greater benefit was observed for older patients[309]. These studies highlight

the importance of age as an integral factor in furthering our understanding of tumour response to ICB therapy.

Furthermore, the data are consistent with the observation that age is associated with decreased thymic output[234,311]. Age-related regression of the thymus is accompanied by a decline in naïve T cell output, which is thought to contribute to the reduced T cell diversity in older individuals, and is linked to increased susceptibility to infection, autoimmune disease and cancer[312]. Although widely accepted, this age-associated TCR repertoire constriction has not been widely studied using direct methodologies[313] and has not been analysed in cancer patients treated with immunotherapy. While it is acknowledged that high TCR repertoire diversity is a prerequisite for an effective adaptive immune response against new antigens[314] and that age impacts cancer therapy responses[315], this is a novel finding of age-specific differential immune response patterns induced by immunotherapy in cancer patients. It is posited that these findings reflect age-related thymic involution[316,317] and a consequent reduction of new clonotype output[318] available to recognise and kill cancer cells[319].

Finally, the results of this study support a model whereby age does not affect peripheral T_{IE} subset expansion in response to ICB, but does influence immunotherapy-induced peripheral TCR repertoire evolution. Although limited by the small sample size and these findings requiring validation in larger cohorts that can differentiate responses in younger versus older patients, these exploratory observations highlight the importance of considering age during the development of immunotherapy approaches and biomarker-led strategies. For example, TCR-based biomarkers should consider how age affects TCR repertoire evolution following treatment, and therapies that require more diverse T cell repertoires may be less effective in older patients. Critically, the inconsistent recruitment of older patients into clinical trials has led to the development of treatments largely in younger patients who typically have different biological and physiological responses[320,321]. Future work should focus on specific enrolment of patients ≥70 years of age in immunotherapy clinical trials and the reporting of age-group specific survival outcomes. Refinements in the design of preclinical and clinical trials is necessary to determine how aging impacts the efficacy of different classes of immunotherapy. These results provide testable hypotheses of how age and reduced thymic output influence T cell evolution in response to ICB, potentially providing a molecular explanation of the age-related differences in response to immunotherapy.

Chapter 5: Personalising Immunotherapy in Early Stage Melanoma

5.1 Introduction

For early stage melanoma, surgical excision is the mainstay of treatment and this approach is curative for the majority of patients. Over 90% of patients with stage I melanoma will be alive 5 or more years after diagnosis and in stage II melanoma this figure remains high, with approximately 80% of patients alive 5 or more years after diagnosis[322]. The survival rates begin to drop with more advanced disease stage, approximately 50% of patients with stage III melanoma are alive 5 or more years after diagnosis. This figure declines further in stage IV disease to 30-40% of patients alive 5 or more years from diagnosis[57]. Despite increased risk of death at stage IV, a higher number of patients diagnosed at earlier stages actually progress and succumb to their disease. This is the low risk paradox illustrated in Figure 5.1.

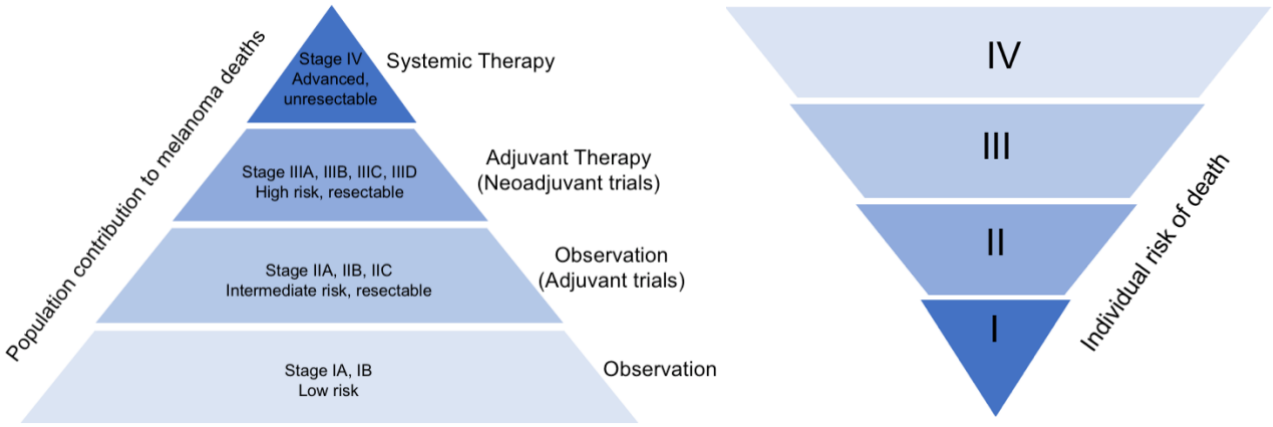

Figure 5.1 Low risk paradox
The individual risk of death increases with stage, however at a population level the number of patients dying from melanoma is highest for those presenting with lower stage of disease (I – III).

Immunotherapy and targeted therapy have revolutionised the outcomes for patients with advanced melanoma, with an increase in expected median survival from 6-9 months to 24 – 36 months[54,55], and more than 60 months in patients treated with combination immunotherapy, with emerging evidence of long-term benefit and potential cure for some patients[56]. Studies to identify the clinical features that are most likely to predict a benefit for treatment consistently show low tumour burden and good performance status to be among the most powerful indicators[323,324]. Over the years, and particularly since the advent of targeted and immunotherapies in melanoma, the main focus of research in the field has been in the stage IV advanced disease setting. However, recent trials have shown that adjuvant treatment of earlier stage disease results in improved survival and thus, focus is shifting towards early detection and intervention to minimise the number of patients that will develop metastatic disease.

5.1.1 Stage II Melanoma

Currently, following resection for stage II melanoma, adjuvant therapy is not approved for use, and current standard of care after resection of stage II melanoma is observation. Follow up of these patients consists of regular clinical examination for stage IIA and IIB patients. For patients with stage IIC disease, follow up includes regular cross-sectional imaging (CT or PET) and MRI brain in addition to clinical examination. The incidence of stage II melanoma is significantly higher than later stages (Figure 5.1 and Table 5.1). For these patients, the individual risk of recurrence is low, yet they account for approximately 30-50% of all those who subsequently develop metastases and succumb to their disease. This is the low risk paradox, thus identifying an effective and economical adjuvant treatment strategy for patients with stage II disease is an important unmet clinical need. Treating all patients with expensive and potentially toxic treatments is impractical, a better approach would be accurate identification of the important minority of patients who will progress to stage IV disease and may therefore benefit from early treatment initiation, and separate them from the majority of patients cured by surgery alone.

Table 5.1 Incidence and survival according to tumour thickness in Queensland Australia, 2005-2009 (adapted from Whiteman et al[325]).

Characteristic (Primary thickness)	Equivalent stage	Incidence proportion (%)	Mortality proportion (%)
≤1mm	I	68	22.7
1.01-2mm	I and II*	13.6	20.8
2.01-4mm	II	8	20.4
>4mm	II	4.7	14.2
metastasis	III and IV	2.8	15.9

*dependent on ulceration

Interestingly, patients with stages IIB/IIC melanoma have a poorer 5 year melanoma specific survival (MSS) compared to patients with stages IIIA/IIIB melanoma (87%/82% vs. 93%/83%)[15]. Therefore, it is suggested that stages IIB/IIC should also be considered for adjuvant therapy[326]. The largest clinical trial to date in the stage II setting, KEYNOTE-716 (NCT03553836) enrolled 954 patients and assessed the safety and efficacy of 1 year of pembrolizumab 200mg 3 weekly compared to placebo in high risk resected stage IIB and IIC melanoma. This phase III study met its primary end point RFS, for the adjuvant treatment of patients with surgically resected high-risk stage II melanoma. At median follow up of 14.4 months, pembrolizumab showed a statistically significant and clinically meaningful improvement in RFS compared with placebo (HR 0.65, 95% CI 0.46-0.92; P=0.00658) and no new safety signals were observed[327].

The challenge for adjuvant therapy in stage II disease is that the majority of patients are cured by surgery. Treating such a large group of unselected patients upfront is likely to result in a significant burden of cost and toxicity to the health service and to patients. There is a need to personalise the approach to treatment to patients that are not cured by surgery alone and will relapse. It has been observed that ctDNA can be used to track melanoma burden in stage IV disease[196,328]. Furthermore, it has recently been shown that melanoma patients who were ctDNA positive after surgical resection of stage II/III melanoma had a very high risk of recurrence and death[204]. A subsequent retrospective study confirmed detection of ctDNA within 12 weeks of surgery was a strong predictor of RFS (HR 12; 95% CI 5.3-29; p<0.001). In addition, longitudinal ctDNA monitoring also identified disease at an early timepoint[203]. Taken together, these data suggest that ctDNA is a measure of micro-metastatic disease activity and is a powerful tool to identify MRD or early molecular relapse not detected by

imaging. The ongoing, phase III open label multicentre ctDNA guided therapy switch for stage IIB/C melanoma after surgical resection (DETECTION) trial (NCT04901988) will test whether ctDNA can identify patients at low risk by conventional staging but who are at very high risk of melanoma recurrence and evaluate whether early treatment of these patients improves outcomes. This approach differs from KEYNOTE-716 (NCT03553836) in that DETECTION enriches for the high-risk patients rather than treating all patients and will provide valuable information on this approach. If positive, this will be one of the first studies to show how ctDNA can be incorporated into improved clinical practice and will provide valuable clinical samples for translational research into predictors of patients at high risk of relapse and into early detection of recurrence in early stage melanoma. Furthermore, if a signal is seen in this study, a further trial in the stage III setting in which standard of care is adjuvant therapy with immune or targeted therapy could be performed. The aim would be to show non-inferiority of selecting patients for adjuvant therapy based on ctDNA, which would reduce the burden of toxicity in this group and also reduce costs for healthcare systems.

5.1.2 Stage III Melanoma

Treatment of stage III melanoma consists of complete surgical resection with curative intent. However, the risk of recurrence following surgery is high and outcomes are heterogeneous, resulting in 5-year OS rates between 30 and 78%. According to sub-stage, 5 year survival rates are; 78% for stage IIIA, 59% for stage IIIB, 40% for stage IIIC and patients with macroscopic lymph node metastasis, stage IIID have the poorest outcome with survival dropping to 30%[62,304]. A significant proportion will suffer loco-regional recurrence or distant relapse with metastatic disease. In stage III melanoma, most recurrences appear within the first 2 years of surgical resection[329].

Landmark clinical trials EORTC 18071 (NCT00636168), CheckMate 238 (NCT02388906), KEYNOTE-054 (NCT02362594) and COMBI-AD (NCT01682083) investigating adjuvant therapy in high risk resected stage III melanoma have reported significant benefits in terms of RFS and OS[72,73,74,75,104,330]. Thus, 12 months of adjuvant therapy has become standard of care in resected stage III melanoma. Intriguingly, KEYNOTE-054 (NCT02362594) showed that 50% of patients do not relapse at 2 years on the placebo arm. This suggests that a potentially toxic treatment is given to a subgroup of patients that may not require it. There is a crucial need to identify the 30% of patients that do benefit and separate them from those cured by surgery alone.

The concept of MRD has traditionally been associated with haematological malignancies[331,332]. MRD is the presence of residual malignant cells even when so few cancer cells are present they cannot be identified by routine means, indicating micro-metastatic disease or molecular relapse that cannot be detected on imaging[333]. The term is used to describe disease detectable only by specific laboratory techniques, such as flow cytometry for the detection of leukaemia cells and PCR to detect specific TCR gene rearrangements such as BCR/ABL in chronic myeloid leukaemia (CML) patients[334]. This residual disease is believed to be minimal, given that it is identified in the absence of clinical signs or symptoms. More recently, it has been suggested that ctDNA enables the detection of MRD and molecular relapse in solid malignancies[335,336]. In stage III melanoma patients treated with surgery, the presence of MRD post operatively indicates that surgery alone has not been curative. Thus, MRD can distinguish those needing intensive and potentially more toxic therapy from those who do not. An important consideration is that MRD may be present and undetectable due to limits in current methodology[335,337,338]. Additionally, not all patients with MRD requiring further therapy will respond and therefore it is also important to identify this subgroup to effectively guide clinical care and treatment choice to increase cure rates. Identifying means of effectively detecting MRD and stratifying patients based on risk of relapse and response is therefore an important and significant challenge. Notably IMvigor010 (NCT02450331), a phase III adjuvant study that compared atezolizumab to observation after surgical resection for urothelial cancer, did not show a significant benefit in DFS in unselected patients[339]. However, exploratory analysis identified that patients with detectable ctDNA postoperatively had improved DFS and OS in the atezolizumab arm[340]. Thus, detecting MRD post operatively could have practice changing implications if validated, in that patients can be selected for adjuvant therapy based on a ctDNA MRD biomarker.

Predictive and prognostic biomarkers of response to ICB have been discussed in section 1.7 and section 1.8. Biomarkers of response to ICB in the adjuvant setting for stage III melanoma have not been widely explored. However, results from biomarker analysis of patients treated with adjuvant nivolumab or ipilimumab in CheckMate 238 found that patients with higher levels of a IFNγ gene expression signature, tumour mutational burden and CD8+ T cell infiltration gained the most clinical benefit with improved RFS for both ipilimumab and nivolumab[341]. Changes in the peripheral T cell compartment pre-treatment and early on treatment is an area of particular interest and remains relatively under studied in this setting. It has recently been demonstrated in the metastatic setting that peripheral blood TCR repertoire changes early on treatment are predictive of response to ICB[234]. In addition, phenotyping immune populations from PBMCs has also been effective in predicting response to ICB[210,216,234,342]. Therefore, an approach that utilises liquid biopsy to combine analysis of peripheral blood TCR repertoire

features and immune cell phenotyping to assess frequencies of T cell subpopulations prior to and longitudinally on treatment could prove to be a strong response predictor for ICB therapy. The encouraging results in the stage IV setting provides the rationale for considering this approach in stage III disease.

5.1.2.1 Potential patient outcomes on adjuvant immunotherapy in stage III melanoma

The different trajectories of the potential patient journey in patients with high risk resected stage III melanoma receiving adjuvant therapy are illustrated in Figure 5.2. Questions that need to be addressed in this setting include, which patients need further intervention after surgery i.e. those with MRD. Which patients are 'cured' by surgery and do not have MRD post operatively (pink line, Figure 5.2). Which patients will benefit from adjuvant therapy (green lines, Figure 5.2). Which patients will progress on adjuvant ICB (primary progression, [blue line] versus acquired 'immune escape', [yellow lines], Figure 5.2).

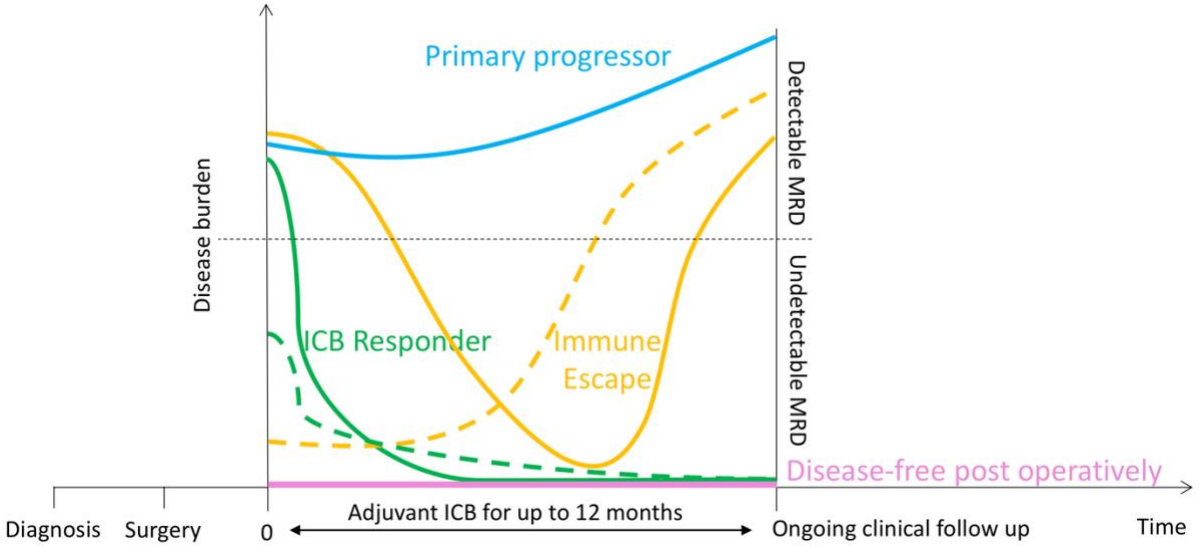

Figure 5.2 Graphical illustration of the potential patient outcomes on adjuvant immunotherapy in stage III melanoma
Pink line: cured by surgery alone, no MRD post operatively and do not relapse (Disease free post operatively). Solid green line: detectable MRD post operatively that responds to treatment with ICB and becomes undetectable with no relapse (ICB responder). Dashed green line undetectable MRD that responds to adjuvant ICB, remains undetectable with no relapse (ICB responder). Blue line: detectable MRD but disease will progress early on adjuvant ICB (primary progressor). Solid yellow line: detectable MRD that becomes undetectable on treatment then relapses during ICB therapy (immune escape). Dashed yellow line: undetectable MRD that becomes detectable during treatment and disease will relapse (immune escape).
X axis represents time, starting at diagnosis of stage III disease, followed by surgery then adjuvant ICB therapy and ongoing clinical follow up. Y axis represents disease burden at start of adjuvant treatment (0). MRD: minimal residual disease; ICB: immune checkpoint blockade with anti-PD-1 therapy.

5.1.2.2 Survival and relapse risk

Clinicopathologic features such as primary tumour thickness, ulceration, number of mitoses in addition to nodal classification and disease stage represent conventional parameters for melanoma staging and prognosis and to date are the most powerful predictors of survival[5]. Gene expression profiling has identified subgroups that are associated with a poor outcome in stage I-III melanoma, but patient numbers were limited and have yet to be confirmed in larger cohorts[343,344]. As described in section 5.1.1, ctDNA has also been shown to be a powerful predictor of disease relapse post operatively in early stage disease, but is yet to be prospectively validated. Early identification of MRD or small volume disease has been shown to improve patient outcomes, with significantly increased likelihood of obtaining and maintaining a complete response[65,67,73,324,345]. Development of biomarkers that identify patients at high risk of relapse and those that will benefit from further treatment post-operatively is essential. Standard methods of predicting risk of relapse are not very precise and the approval of adjuvant therapy in stage III disease has resulted in over-treatment of some patients.

Notably, detection and high levels of ctDNA have also reliably correlated with inferior prognosis in the stage IV setting, despite the new treatment paradigm[197,208,346]. Furthermore, in patients treated with both targeted and ICB therapy, baseline ctDNA levels have been shown to be associated with inferior survival and higher disease burden[208,346]. It is therefore hypothesised that patients with high risk resected stage III disease and detectable ctDNA in the adjuvant setting are less likely to respond or have durable responses to ICB. In addition, parameters such as the peripheral T cell compartment could be evaluated as part of a multifaceted approach to identify MRD and predict relapse and response, which might further improve a liquid biopsy test if combined with ctDNA.

5.2 Hypothesis and Aims

Patients with high-risk stage III resected melanoma commonly develop distant metastases. At present, we cannot differentiate between patients who will recur or those who are cured by surgery. Prior to the introduction of adjuvant ICB therapy, it has been shown that ctDNA is a predictor of relapse and survival in patients with resected stage III melanoma[203,204]. CtDNA has emerged as one of the most promising circulating biomarkers for patient stratification and monitoring response to treatment[335]. It is hypothesised that patient segregation can be achieved using an integrated approach, combining primary tumour analysis with liquid biopsies at early stages of adjuvant treatment (e.g. up to week 12 of treatment). Therefore, I sought to assess whether tumour immunological features in addition to changes in circulating biomarkers such as immune cell repertoire and ctDNA upon adjuvant ICB can be used to predict clinical outcome in stage III melanoma patients. The main question is, can stage III melanoma patients with MRD after primary tumour resection that will benefit from adjuvant therapy be identified. When considering the categories of predicted patient response to adjuvant ICB in the setting of high risk resected stage III disease, the initial step is to identify patients with MRD from those with no MRD, at present the best tool to assess this is ctDNA. The next step is to strengthen ctDNA readout by combining with peripheral T cell changes to assess response to ICB in the adjuvant setting. This will involve segregating a group of patients from those who do not have MRD and those who have MRD but will not respond to adjuvant ICB, with the ultimate goal of utilising these methods to predict response and improve patient stratification.

The following aims were therefore proposed:

1. To identify whether in addition to ctDNA, there are changes in circulating biomarkers such as T_{IE} cells and TCR repertoire early on adjuvant treatment that can be used to predict patient response to therapy.

2. To identify tumour-associated biomarkers predictive of response to adjuvant immunotherapy in stage III melanoma.

3. To investigate whether circulating biomarkers predictive of response (1) correlate with tumour biomarkers (2) and whether this can be used to predict clinical outcome.

5.3 Current study status

I conceived the rationale for the project and led on the design and set up of the study protocol (Appendix D), which took approximately 12 months to develop and gain approval, opening to recruitment in January 2020. Since opening, 7 patients were consented and baseline samples were collected from these patients prior to lockdown in March 2020. The COVID-19 pandemic has had a significant impact on the progress of this study, which was reliant upon the availability of longitudinal prospective clinical samples from stage III melanoma patients prior to, during and post treatment. This has unfortunately not been possible due to the stopping of and subsequent restriction on clinical sample collection over the last 18 month period. Critical research activities have therefore suffered significant delay and the impact cannot be mitigated. The study will re-open to recruitment when COVID-19 restrictions have eased, but will be led by another clinician and will require modifications to the design and protocol given that dosing and scheduling of ICB has changed since the global COVID-19 pandemic and so this study, although still relevant and necessary, would need to be adjusted in light of the changes to timing of administration of treatment cycles.

5.4 Research Protocol

5.4.1 Clinical characteristics

Blood and tumour samples from patients at The Christie NHS Foundation Trust will be collected with written informed consent under the MCRC Biobank (project code: 19_RIMA_08). Patient confidentiality will be maintained by assigning an anonymous patient number to each sample on arrival into the laboratory.

The study population focusses on patients aged 16 or above with high risk resected stage III *BRAF, NRAS* or *TERT* promoter mutant cutaneous melanoma due to commence adjuvant ICB with Pembrolizumab. When considering ctDNA analysis, it is likely that 80% of patients will have either *BRAF, NRAS* or *TERT* mutations, thus capturing the majority of patients with these common mutations. A validated ddPCR assay will be used to track these mutations in circulation longitudinally to monitor for MRD. Up to 20% of patients are likely to be wild type for these mutations and will therefore be ineligible for the study.

Response to treatment will be assessed on CT scan, using RECIST 1.1 response evaluation criteria. Disease control defined as CR, PR, or SD on CT imaging. Baseline tumour tissue will be collected as standard of care at the time of surgery. Optional repeat tissue biopsy are to be performed on consenting patients that experience disease progression to allow study of mechanisms of resistance to therapy with paired biopsies. All blood sampling will be carried out at routine time points before, during and after completion of ICB. Thus, patients do not require additional hospital visits for phlebotomy.

5.4.2 Key inclusion criteria

1. Histological confirmation of cutaneous melanoma.
2. Stage III disease.
3. SLNB or CLND performed within 12 weeks of commencing ICB.
4. Disease free status documented post operatively, both clinically and radiologically.
5. Mutation confirmed in *BRAF* (V600E, V600K and V600R), *NRAS* (Q61R, Q61K, Q61L and G12D) or *TERT* promoter (146 C>T and 124 C>T), which can be tracked in ctDNA.

5.4.3 Exclusion criteria

1. Prior ICB, chemotherapy, vaccine therapy or BRAF/MEK targeted therapy.
2. Active auto-immune disease contra-indicating use of ICB, or subjects with a condition requiring systemic treatment with either corticosteroids (>10mg daily prednisolone equivalent) or other immunosuppressive medications.
3. Any other active malignancy.

5.4.4 Feasibility of recruitment

Patients undergo resection of the primary lesion at the local hospital where the diagnosis of cutaneous melanoma is confirmed. Patients are then referred to The Christie NHS Foundation Trust, Plastic Surgery Department for either SLNB or CLND. The clinical research team identify these patients in the surgical outpatient clinic where they are informed about the study and arrangements made for consenting if appropriate. Approximately 150 patients per year are referred for SLNB to stage their disease. Of those, approximately 50 patients will have a positive SLNB and are subsequently referred to the Medical Oncology team for adjuvant therapy. The remaining 100 patients with negative SLNB are now offered the DETECTION trial (NCT04901988) or continue under clinical follow up, not requiring further active treatment. The initial steps involved in patient recruitment are illustrated in Figure 5.3. Of note, a further approximately 20 patients will undergo CLND for macroscopic disease and will then require adjuvant therapy and approximately 20 patients with satellite or in transit metastases are also eligible. Therefore, a potential total of approximately 90 patients per year treated within the adjuvant setting at The Christie NHS Foundation Trust, equating to approximately 7 patients per month. A proportion of these patients with a BRAFV600 mutation may commence adjuvant targeted therapy. However, only patients starting adjuvant anti-PD-1 monotherapy will be included, the aim is to recruit 60 patients.

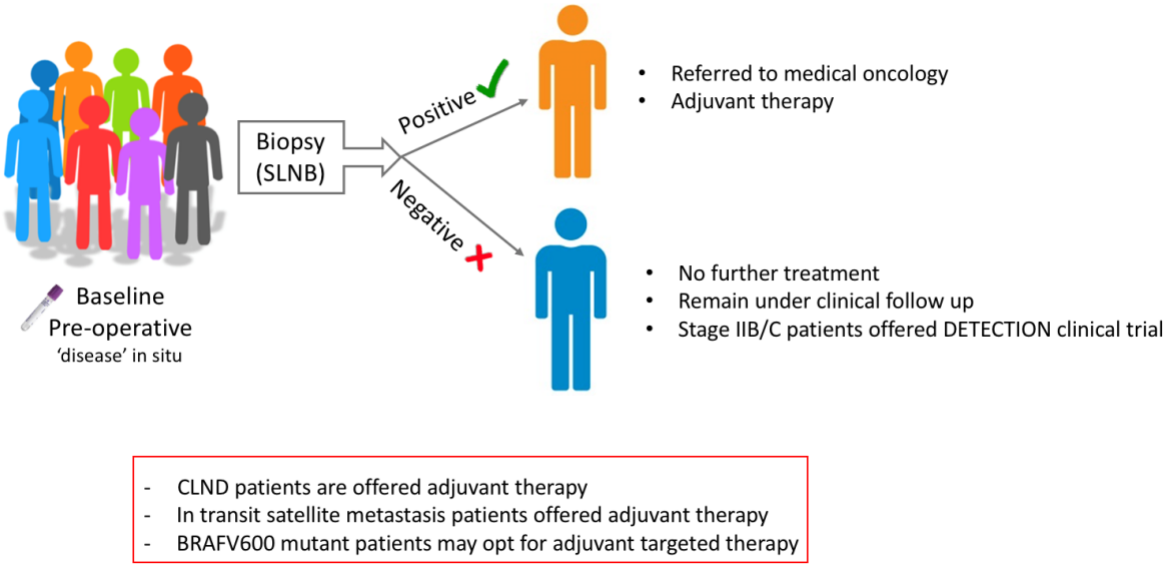

Figure 5.3 Overview of patient recruitment

Of the patients referred for SLNB or CLND, there will be an opportunity for patient blood sample pre-operatively potentially with disease *in situ*. If the SLNB result is positive then the patient is referred for adjuvant therapy. If the SLNB is negative then no further active treatment is required and patients will remain under clinical follow up only. Those with stage IIB/C disease will be offered the DETECTION clinical trial. CLND and in transit satellite metastasis patients will be offered adjuvant therapy.

5.4.5 Patients and clinical samples

Figure 5.4 illustrates the patient journey from surgery to adjuvant ICB treatment and ongoing clinical follow up. The post-operative period before commencing adjuvant ICB can be up to 12 weeks. Patients then complete 12 months of adjuvant treatment with Pembrolizumab 3 weekly cycles, unless discontinued early due to toxicity or disease progression. The routine clinical follow up period is usually 10 years.

The study opened in January 2020 and recruitment was planned to take place over a 12 month period, with a minimum of 12 months follow up for each patient. Blood sampling scheduled to be taken at 6 time points: pre-operatively on the day of surgery, Cycle 1 (C1, usually Week 0), Cycle 2 (C2, usually Week 3), Cycle 3 (C3, usually Week 6), Cycle 4 (C4, usually Week 9), Cycle 5 (C5, usually Week 12). For 60 patients recruited, this equated to 360 blood samples in total (60 patients x 6 timepoints).

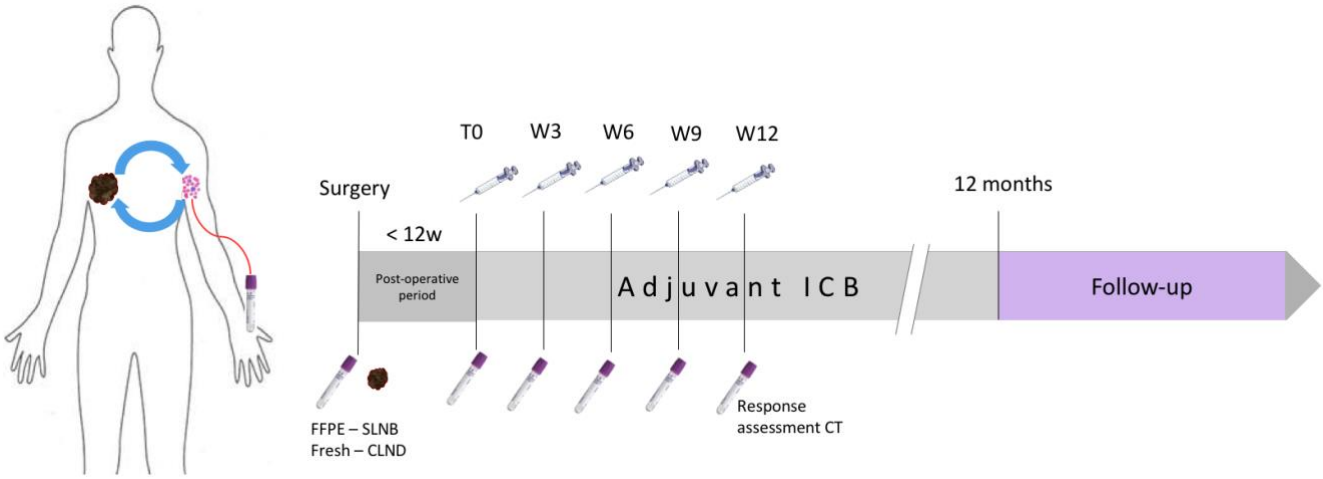

Figure 5.4 Adjuvant ICB patient journey
From surgery i.e. SLNB or CLND, through to the post-operative period, up to 12 weeks, followed by 12 month duration of adjuvant ICB treatment and then the clinical follow up period. SLNB = sentinel lymph node biopsy, CLND = completion lymph node dissection, <12w = less than 12 weeks, T0 = baseline, pre-treatment, W3 = week 3, W6 = week 6, W9 = week 9, W12 = week 12, ICB = immune checkpoint blockade, FFPE = formalin fixed paraffin embedded.

5.5 Experimental Plan

5.5.1 Addressing aim 1: To identify whether in addition to ctDNA, there are changes in circulating biomarkers such as T_{IE} cells and TCR repertoire early on adjuvant ICB treatment that identify patients with MRD and can be used to predict patient response to therapy

Three types of circulating biomarkers will be monitored in all recruited patients at baseline and during the first 12 weeks of treatment prior to each cycle of ICB: ctDNA, circulating immune cells and TCR repertoire. Figure 5.5 illustrates the timepoints for blood sample collection from patients undergoing adjuvant ICB as described above. A total of 60mL blood will be drawn from each patient at each timepoint. Two EDTA tubes (20mL blood) will be used for PBMC isolation. These cells will subsequently be utilised for CyTOF analysis and RNA extracted for TCR sequencing. The remaining 40mL of blood will be collected in 4 STREK tubes for ddPCR ctDNA analysis.

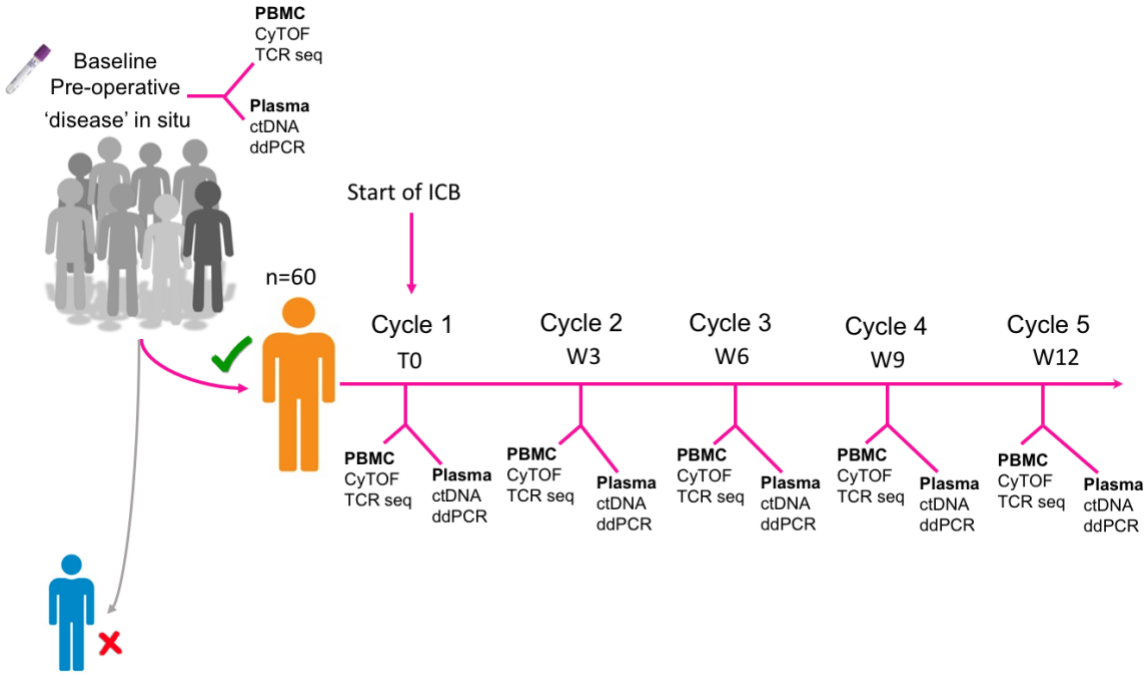

Figure 5.5 Overview of predicted blood sample collection and how they will be utilised
Blood samples from 60 patients will be taken baseline pre-operatively and then again at each of the subsequent 5 time points prior to each cycle of ICB in the first 12 weeks of treatment. Blood samples will be used to isolate PBMCs for CyTOF and TCR sequencing and plasma extracted for ctDNA monitoring. Patients with a negative SLNB will not be included in the study.

5.5.1.1 Multiparametric approach to liquid biopsy

Following surgery, a patient can either harbour MRD or be disease free with no MRD. Currently, our best available tool to detect MRD is ctDNA monitoring, which has its limitations i.e. detection threshold of 1 copy of mutant allele/20mL blood. In view of previous data in stage IV disease, TCR monitoring and T cell repertoire (namely T_{IE} expansion) will be used as a complement to strengthen ctDNA readout as part of the liquid biopsy approach. Clinical outcome will be monitored up to 1 year after completion of adjuvant treatment. The dynamics of immune biomarkers (T cell populations and TCR repertoire) will be correlated with relapse information available on CT scan 12 – 52 weeks after commencing treatment combined with monitoring ctDNA levels during treatment and on follow up. The predicted changes in TCR repertoire, T_{IE} expansion and ctDNA status in the resected stage III setting, when adjuvant ICB therapy is applied is outlined in Figure 5.6.

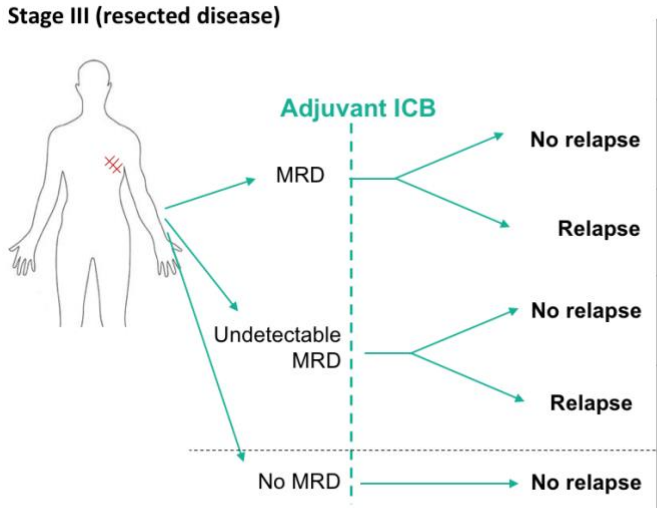

T_{IE} cell expansion	TCR repertoire	ctDNA
✓	↑ diversity and/or clonality	positive → negative
x	No change	positive → positive
✓	↑ diversity and/or clonality	negative
x	No change	negative
x ?	No change?	negative

*Relapse end point only known after 2 year follow up

Figure 5.6 Potential patient outcomes in resected stage III melanoma treated with ICB.
Patients with MRD can be further subdivided into detectable and non-detectable MRD by ctDNA monitoring. Patients with no MRD following surgery are disease free.
The table summarises the possible outcomes for each biomarker potentially detectable at week 3 on adjuvant ICB according to the findings in stage IV disease.

5.5.1.2 ctDNA

Primary excision FFPE tumour blocks will be requested retrospectively from the local hospitals via The Christie NHS Foundation Trust Pathology Department. The blocks will be used to determine baseline mutation status to confirm presence of trackable mutation in circulation for ctDNA monitoring. This will be done using a targeted NGS mutation panel on each patients' primary lesion. The panel and method are described in section 2.11.

The most common mutations (*BRAF*^{V600}, *NRAS*^{G12,Q61} and *TERT* promoter) found in 80% of melanoma patients will be tracked in ctDNA using ddPCR. This approach will allow identification of patients with detectable MRD, which is a crucial step in assessing response to ICB in this setting. Given the low to absent disease burden, ctDNA monitoring will be based on a digital signal (whether the aforementioned mutations can or cannot be detected) and how this signal changes during treatment. Responders will be classified as: ctDNA positive $\rightarrow$ negative. Non-responders will be classified as: ctDNA positive $\rightarrow$ positive and ctDNA negative $\rightarrow$ positive. It is important to note that if ctDNA remains negative throughout, it will not be possible to distinguish responding patients from those that were cured by surgery alone using only ctDNA. Disease evolution will be further monitored beyond the initial 12 weeks on a 3-monthly basis for a total duration of 2 years using the same ctDNA approach. This will equate to potentially a further 7 time points for plasma collection at month 6, month 9, month 12, month 15, month 18, month 21 and month 24. Thereby allowing assessment of the feasibility of monitoring for disease progression and response to therapy using ctDNA in the stage III setting in addition to standard of care CT scans.

5.5.1.3 Circulating immune cells

In the study of stage IV disease where patients present with high disease burden, T_{IE} expansion was defined as >0.8% increase in the cell population. As the percentage increase is small, it has to be considered that in stage III disease, patients harbouring MRD (or disease-free) systemic changes in the T_{IE} subset may be undetectable, due to the minimal signal/background ratio. The specific subset of CD8+ effector memory T cells, T_{IE} cells identified in the stage IV setting will be used as the starting point in this stage III study. The hypothesis is that there will also be early changes in these peripheral T cells on adjuvant therapy that are predictive of response. However, the challenge is whether the signal will be strong enough when disease burden is lower and also whether in the stage III setting clinical response correlates with the same subset of immune cells. To address this, rather than using

the optimised FACS panel employed in Chapter 3, CyTOF will be used as this will include peripheral T_{IE} cells but, in the event that these cells are not identified, the ability to utilise a wider panel of additional markers will increase the likelihood of identifying meaningful changes relevant for immune response. The CyTOF platform to date has not been used to assess response to ICB in early stage disease and there are currently no defined subsets of T cells with potential predictive or prognostic value in this setting. Therefore, there is a need to explore this immune system biology to develop a new set of tools.

CyTOF will be used to incorporate a broad panel of antibodies to identify circulating immune cells in the isolated PBMCs. This panel will include markers of T lymphocytes, monocytes and dendritic cells, comprising 37 antibodies that recognise the respective markers, these are described in section 2.8. Specific cell populations, such as T_{IE} cells will be closely monitored on a longitudinal basis during the first 12 weeks of treatment in order to identify fluctuations in their percentages. t-SNE analysis will be performed on each sample and evolution of different T cell clusters will be followed throughout 12 weeks of adjuvant treatment. This information will then be correlated with patient outcome.

5.5.1.4 TCR sequencing

TCR sequencing will be performed on RNA extracted from PBMCs (Qiagen Immune repertoire RNA library) to assess TCR repertoire changes on treatment. As part of the optimisation phase, RNA was extracted from HD PBMCs using the Qiagen RNeasy plus kit, NanoDrop, HS RNA Qubit kit and Agilent bioanalyser were then used to quality control (QC) check the RNA as described in section 2.10.1. TCR library preparation and sequencing on the MiSeq 2 x 251 base pair will be performed by the Circulating Biomarker Centre Laboratory at Cancer Research UK Manchester Institute. The rationale for RNA based TCR sequencing is described in section 5.5.2.2.

Unlike stage IV disease, in the resected stage III setting, clonal expansion of T cells is less likely to be driven by disease burden, apart from in rapid progressors. Thus, the changes between pre-operative timepoint, T0 and the initial stages of immune response to ICB after the first cycle of treatment, at W3 may elucidate how CDR3 diversity evolves in the absence of metastatic disease. Unless patients become clinically symptomatic, there is likely to be no definitive information about patient response before the response assessment CT scan at week 12. Clonal relatedness analysis will be performed on the obtained TCR sequences and assessment of the potential changes in TCR repertoire on adjuvant ICB during the first 12

weeks of treatment. Peripheral TCR diversity and clonality results from each of the 6 sample timepoints will be analysed and correlated to patient clinical outcome.

5.5.2 Addressing aim 2: To identify tumour-associated biomarkers predictive of response to adjuvant immunotherapy in stage III melanoma

Peripheral biomarker monitoring is appealing given the minimally invasive approach required for sample collection and the ability to monitor activity longitudinally over time, particularly on treatment. When considering predictors of response to ICB, a lot of focus has been placed on analysis of peripheral blood. However, it is important to consider whether these measurements have relevance and reflect anti-tumour immunity. The initial objective of this project is to assess whether there are identifiable systemic changes in the circulation during adjuvant ICB treatment and to establish if these changes are relevant to identify the patients that need adjuvant treatment i.e. patients with MRD that will respond to ICB. To accomplish this, it is important to correlate clinical outcome with peripheral blood markers and the TME.

It is important to consider the possibility that any meaningful circulating immune cell repertoire changes may not be identified in the resected stage III setting as in theory, after surgery there should not be any remaining residual disease and in the case of MRD, the minimal nature of the disease burden may not be enough to illicit significant changes in the immune repertoire early on ICB treatment compared to what has been observed in the stage IV setting. For this reason, tumour tissue will be collected for analysis and correlation with circulating immune repertoire changes and clinical outcome.

One major advantage of studying tumour tissue in early stage melanoma is the relatively low intra-patient heterogeneity compared to advanced stage disease[347]. Given that the surgical sample (e.g. CLND) is likely to represent practically the entirety of that patient's disease[348], it is therefore likely to establish causality relationships with response as well as with circulating biomarkers findings. Immune cell infiltrates, TCR repertoire and tumour gene expression will be analysed in patient resected tissue to identify reliable markers of response to therapy. Tumour sample status (fresh or fixed) will dictate which analysis is the most reliable.

5.5.2.1 Fresh CLND tumour samples

Fresh CLND samples will be collected prospectively and split into 3 pieces: one piece will be flash frozen in liquid nitrogen for storage, one will be lysed for RNA extraction and the third

will be immediately digested into single cell suspension. Tumour digestion is described in section 2.5.

5.5.2.2 TCR sequencing

The Illumina based platform was selected for TCR sequencing as it is the most established technology. An RNA based approach was selected to facilitate potential sequencing of the complete V and J gene whilst also providing information about expression levels. This approach has the ability to identify pairs of the two TCR chains (αβ, γδ) at a single cell level and it is the pair that most closely reflects biological function in vivo.

As discussed in section 1.9.2, the αβ chain of the TCR has three hypervariable loops termed complementary determining regions (CDR1-3) which interact with the MHC complex. CDR1 and CDR2 are encoded by the V genes and influence sensitivity and affinity of the TCR binding to the MHC. The CDR3 region however interacts with the peptide and MHC complex. T cells can express one or more type of α chain but will only express one type of β chain. The CDR3β chain is more diverse than CDR3α because it is additionally coded using the diversity gene. Therefore, sequencing the CDR3β chain enables identification and quantification of unique T cell clones. This is illustrated in Figure 5.7 together with the Illumina TCR sequencing workflow. The QIAseq Immune Repertoire RNA Library Kit is highly optimised and incorporates unique molecular indices (UMIs) to facilitate ultrasensitive and accurate characterisation of the immune repertoire in cells and tissues with an input RNA amount of 10-100ng[349].

TCR sequencing will be performed on RNA extracted from the tumour, which will be achieved using fresh tumour samples from CLND. When considering the approach for TCR sequencing, the Illumina platform offers multiple advantages including, the ability to sequence the alpha, beta, delta and gamma sequences of CDR3, higher sensitivity, that facilitates the detection of rare clonotypes and less bias due to only one annealing temperature. TCR sequences from tumour and peripheral blood will be correlated to identify which circulating TCR sequences are unique to the presence of the tumour. This information will complement circulating TCR repertoire and will be used to assess the relevance of circulating sequences.

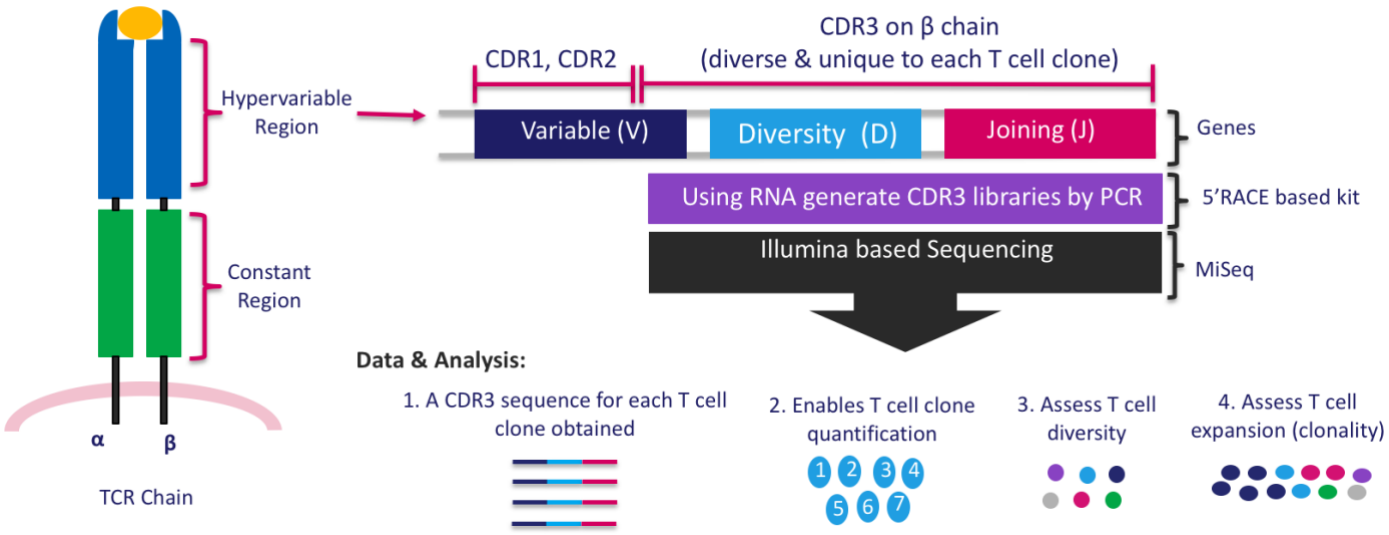

Figure 5.7 TCR sequencing workflow using next generation sequencing Illumina platform

TCR sequencing using Illumina MiSeq will be performed on RNA extracted from PBMCs and fresh tumour from CLND surgery to assess TCR repertoire at baseline and on treatment in the circulation.

CDR = complimentary determining region.

5'RACE based kit uses one annealing temperature for all primers therefore less bias.

5.5.2.3 Tumour cell gene expression

Melanoma is a highly heterogeneous disease, particularly in terms of mutational burden and landscape, aggressiveness, response to treatment, histopathological and inflammatory / immunogenic traits, and metastatic patterns[350,351,352]. The more advanced the disease, the higher the interpatient as well as intrapatient heterogeneity[353]. In order to personalise the immunotherapeutic approach in oncology, there is a reliance upon both cancer and immune profiling. The increasing interest in accurate depiction of the tumour immune environment has highlighted RNA sequencing (RNAseq) as a potential tool in determining the molecular mechanisms underlying responses to ICB. RNAseq is an efficient and cost-effective tool for identifying differentially expressed genes, also known as gene signatures which can be used for whole transcriptome-based biomarker discovery, for diagnosis, prognosis, prediction and as a guide for treatment[354].

Traditional methods such as micro arrays and quantitative PCR have been used to develop clinically validated gene expression signatures such as OncotypeDX for breast cancer and GeneFX for lung and colon cancer which are well established and widely used in clinical practice[354]. The translatability of these panels into RNAseq signature panels has been demonstrated by comparing gene expression signatures using Affymetrix microarray and Illumina RNAseq technology in breast cancer[355]. RNAseq based technology was found to be superior in transcriptome characterisation with similar predictive power for clinical outcomes when compared with microarrays. More recently, RNAseq-based signatures have been developed and validated, such as a diagnostic signature for thyroid cancer[356], prognostic signatures for both Neuroblastoma[357] and Lung Adenocarcinoma[358], and predictive signatures for metastatic melanoma[359,360].

Notably, RNAseq may only provide an average gene expression profile and will lack spatial content[354]. However, RNAseq data will provide a more complete view of cancer-related genetic alterations for clinical applications when compared with DNA based or the other classic methods described. For example, RNAseq identified an alternative breast cancer 1 (*BRCA1*) transcript in a subset of breast cancer patients that was not detected using conventional genomic analysis[361] . The advantages include specific detail regarding base pairs ability to detect splicing variants, allele-specific expression, novel gene fusion, non-coding RNA, and novel RNAs. In addition, RNAseq can be applied to all tumour samples including, fresh, frozen, FFPE and liquid biopsy[354]. This study seeks to identify whether changes in gene expression, as assessed by RNAseq of the bulk fresh tumour, can provide useful information regarding risk of relapse and response to adjuvant ICB therapy.

5.5.2.4 FFPE SLNB tumour samples and CO-Detection by indEXing (CODEX)

CODEX is a novel highly multiplexed tissue imaging platform. A recent meta-analysis of more than 50 studies, with outcome data for over 8,000 patients compared effectiveness of individual diagnostic approaches in predicting patient responses to anti-PD-1/PD-L1 ICB therapy in various different cancer types. Focussing on four main assay types most commonly utilised in immuno-oncology, CODEX had significantly greater diagnostic accuracy compared to TMB, PDL-1 immunohistochemistry (IHC), multiplex IHC and gene expression profiling for multiple tumour types[362].

CODEX has been observed as compatible with lymph node FFPE melanoma samples[363]. FFPE SLNB tumour samples will be collected retrospectively from the patients that have a positive SLNB and go on to receive adjuvant ICB. These FFPE SLNB samples will be used for single cell spatial analysis and multiplexed immunofluorescence using the Akoya Biosciences CODEX platform.

Using a high level of multiplexed marker detection at the single cell level with spatial context, CODEX will enable the study of different cell phenotypes and how they interact in the tissue microenvironment to impact disease pathology and progression. The roles of spatial relationships between infiltrating immune cells and the remodelling of the cellular matrix are key components that define tissue heterogeneity[364]. The ability to characterise the complexities of the TME is a critical element in understanding the molecular and cellular mechanisms driving melanoma as well as therapeutic responses. The key advantage of this technology is the high level of multiplexing using more than 40 protein markers in tissue samples at single cell resolution allowing for greater interrogation of the TME with the potential to accelerate the discovery of better predictive biomarkers using FFPE tumour material which is the most easily accessible in routine clinical practice. Specifically, protein markers identified by CyTOF will be utilised to investigate their spatial expression within the tumour.

5.5.3 Addressing aim 3: To investigate whether circulating biomarkers predictive of response correlate with tumour biomarkers (1 and 2) and whether this can be used to predict clinical outcome

It would be anticipated that early on ICB, those patients who are ctDNA positive with detectable MRD following surgical resection and respond to adjuvant ICB with no evidence of disease relapse, would display peripheral T_{IE} cell expansion and TCR repertoire increase in clonality or diversity. Additionally, over the course of treatment ctDNA would become negative and remain negative on follow up; these patients would not relapse and be classified as ICB responders (solid green line Figure 5.2).

The remaining patients with positive ctDNA and detectable MRD post operatively will go on to relapse on adjuvant ICB with clinical or radiological evidence of disease progression and their ctDNA will remain positive throughout. These patients can be categorised as either primary progressors (blue line Figure 5.2) or immune escapers (solid yellow line Figure 5.2). In patients with primary progression, disease relapses early on treatment, it is expected that there will be no evidence of T_{IE} cell expansion or TCR repertoire changes. In patients with immune escape whereby the disease initially appears to be responding to ICB, ctDNA changes from positive to negative, but later on treatment ctDNA reverts back from negative to positive with clinical or radiological confirmation of disease progression, it is posited that no meaningful peripheral T cell changes will be observed.

In patients that have MRD following surgery, but this is below the threshold of detection and thus ctDNA is negative and MRD undetectable, a proportion will not relapse on adjuvant ICB or follow up; this group are termed ICB responders (dashed green line Figure 5.2) whereby ctDNA remains negative longitudinally. It is anticipated that there may be evidence of peripheral T_{IE} cell expansion and peripheral TCR repertoire convergence with increased clonality or diversity. The remaining group of patients with undetectable MRD are ctDNA negative post operatively, but will relapse during ICB treatment. It is expected that ctDNA will remain negative longitudinally until the detection threshold is exceeded. These patients incorporate a further category of immune escape (dashed yellow line Figure 5.2) in which no meaningful peripheral T cell changes are anticipated.

The final subgroup are those patients that do not have MRD, are ctDNA negative post operatively and remain ctDNA negative throughout the course of ICB treatment and on follow up. These patients are termed disease-free post operatively (pink line Figure 5.2) and are anticipated to have no residual disease following resection, thus cured by surgery alone. Therefore, it is expected that there are no dynamic peripheral T cell changes as there is no

disease present to mount an immune response, however, these patients may mount an immune response to another stimulus and so will act as an important control group. Additionally, it would be anticipated that comparison of the tumour sample and pre-operative peripheral blood T cell repertoire with the longitudinal peripheral T cell findings might identify disease specific changes that were present prior to tumour removal and their dissipation may provide insight into tumour specificity.

Tumour tissue analysis of CLND samples will explore the tumour specificity of any T cell findings identified in the circulation. TCR sequencing aims to identify the presence of tumour resident T cell clones and assess for the presence of shared sequences in the circulation and how these change in response to ICB. Multiparametric imaging technology such as CODEX to interrogate FFPE SLNB positive melanoma tissue will utilise high throughput technology staining multiple markers to gain co-expression information, spatial relationships and proximity information relating to the TME. Unlike conventional immunofluorescence and IHC which are limited to measuring few parameters simultaneously and single cell technology such as CyTOF which provides limited spatial information, it is anticipated that unbiased, hypothesis free biomarker discovery approaches utilising higher resolution of the TME may lead to further insight into patient response to ICB. Gene expression profiling has been successfully implemented in several malignancies such as breast and prostate cancer where it provides personalised treatment[365]. However, in melanoma whilst it is being implemented in a limited capacity to predict sentinel node positivity and studies have supported gene signatures such as IFNγ as both predictive and prognostic, these have not been validated for routine clinical use[93,365,366,]. The applicability of gene expression profiling to other aspects of melanoma care have not been fully explored and therefore its role in determining the utility of adjuvant therapy and surgical management is yet to be elucidated. It is anticipated that differences in gene expression between analysed patients in this study will be observed and that these differences may highlight a gene expression signature of patients at higher risk of relapse, such as those with ctDNA positivity post operatively. Additionally, potential gene expression signatures or trends in responders compared with non-responders to adjuvant ICB may be identified. Together host and tumour information will provide a broader understanding of melanoma response to ICB when correlated with clinical outcome.

When considering tumour analysis in this study, a 60 patient cohort is underpowered to draw meaningful conclusions from specific subgroup analysis, however it is anticipated that trends in tumour and circulatory changes will be observed in each group when correlated with clinical outcome. Notably, relapse and clinical endpoint data will only be known after 2 years of follow up, thus if the initial hypothesis is corroborated and T cell repertoire and ctDNA changes follow

the expected trajectory early on adjuvant ICB in resected stage III melanoma, the preliminary findings from this study may provide the rationale for a larger feasibility study to assess the clinical utility of these findings.

Although the study is in relative infancy, there is undoubtedly significant clinical relevance to the proposal and underlying aim to identify resected stage III melanoma patients with MRD that will benefit from adjuvant therapy and improve stratification and prediction tools for ICB response assessment. Thus, if the potential findings were validated in a future feasibility study, this would provide rationale for a larger scale clinical trial. The potential clinical trial schema for this is illustrated in Figure 5.8. These patient groups would be stratified according to prediction on biomarker analysis to be a responder or non-responder to anti-PD1 therapy or those that do not relapse and do not require adjuvant therapy based on ctDNA and immune cell profiling. These groups would be compared to patients that receive standard of care adjuvant anti-PD1 therapy unstratified. The primary endpoint suggested is PFS at 2 years and the hypothesis is that this would be improved in the stratified groups.

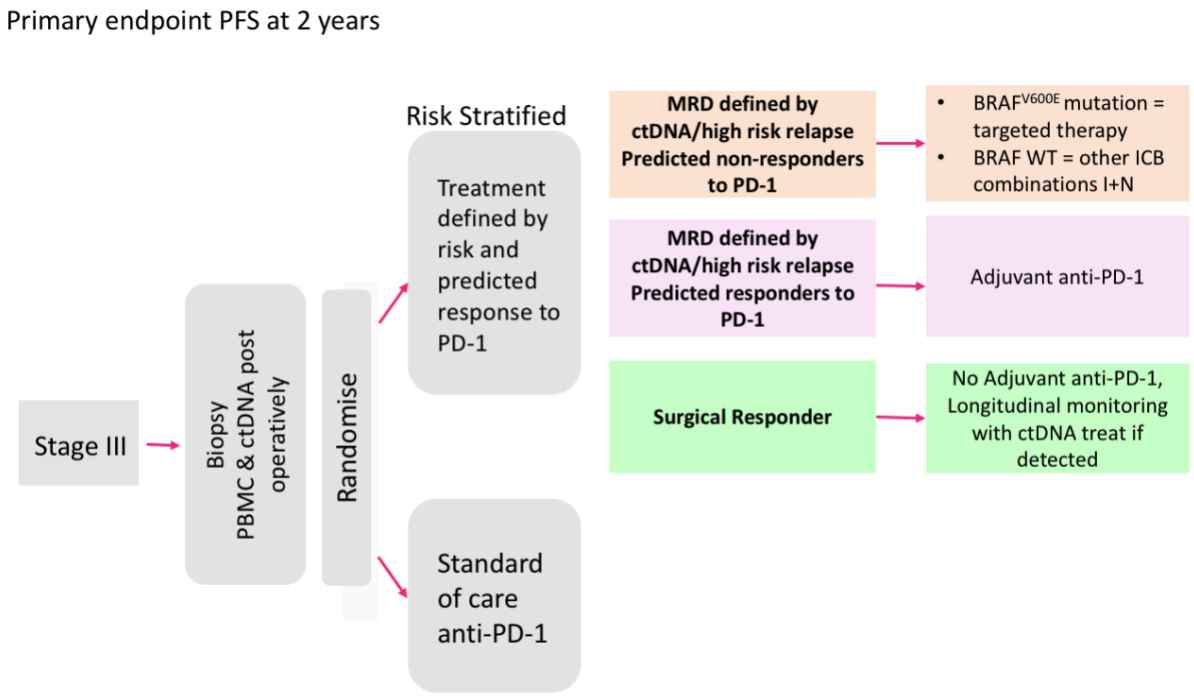

Figure 5.8 Proposed clinical trial schema
Based on the analysis of peripheral blood and tumour samples of stage III patients if the hypothesis is corroborated and biomarkers of response/MRD identified.
Targeted therapy = BRAF/MEK inhibitors, ICB = immune checkpoint blockade, N = nivolumab, I = ipilimumab, surgical responder = no MRD and remains disease free post operatively.

5.6 Optimisation Results

5.6.1 Comparison of SepMate™ and LeucoSep™ PBMC isolation for downstream CyTOF application

The aim here is to understand the effect of the PBMC isolation protocol on cell yield, cell viability and the extent of iodine contamination. It is important to consider iodine contamination of the cells being studied, because metal and non-metal contaminants can generate undesired background interference which can affect the signal generated within the detection channels, iodine (127DA) in particular can be found in some buffers and commercial reagents[367]. For example, Ficoll contains large amounts of iodine and so should be used with particular care. To limit contamination of cells by the iodine contained in Ficoll, it is important to avoid mixing cells with the layer of density gradient medium when using SepMate™ or Leucosep™ to isolate PBMCs[367].

SepMate™ and LeucoSep™ protocols were used to isolate PMBCs according to protocols described in section 2.3.1 and section 2.8.2, from the same HD (n=1). Eight mL of whole blood was taken from 1 HD, the sample was collected in an EDTA tube and split into 2 parts, 4mL of whole blood was used for each of the PBMC isolation protocols. Both 4mL samples were processed fresh and analysed in real-time. The cell yield was higher with LeucoSep™ at 7.5 x 10^6/mL compared to 4.26 x 10^6/mL with SepMate™. Similar cell viability between the two was observed, 95% with SepMate™ (Figure 5.9A) and 98% with LeucoSep™ (Figure 5.9C) when analysed on Helios, but there was a lower level of iodine contamination with SepMate™ at 12% (Figure 5.9B), compared to 16% with LeucoSep™ (Figure 5.9D).

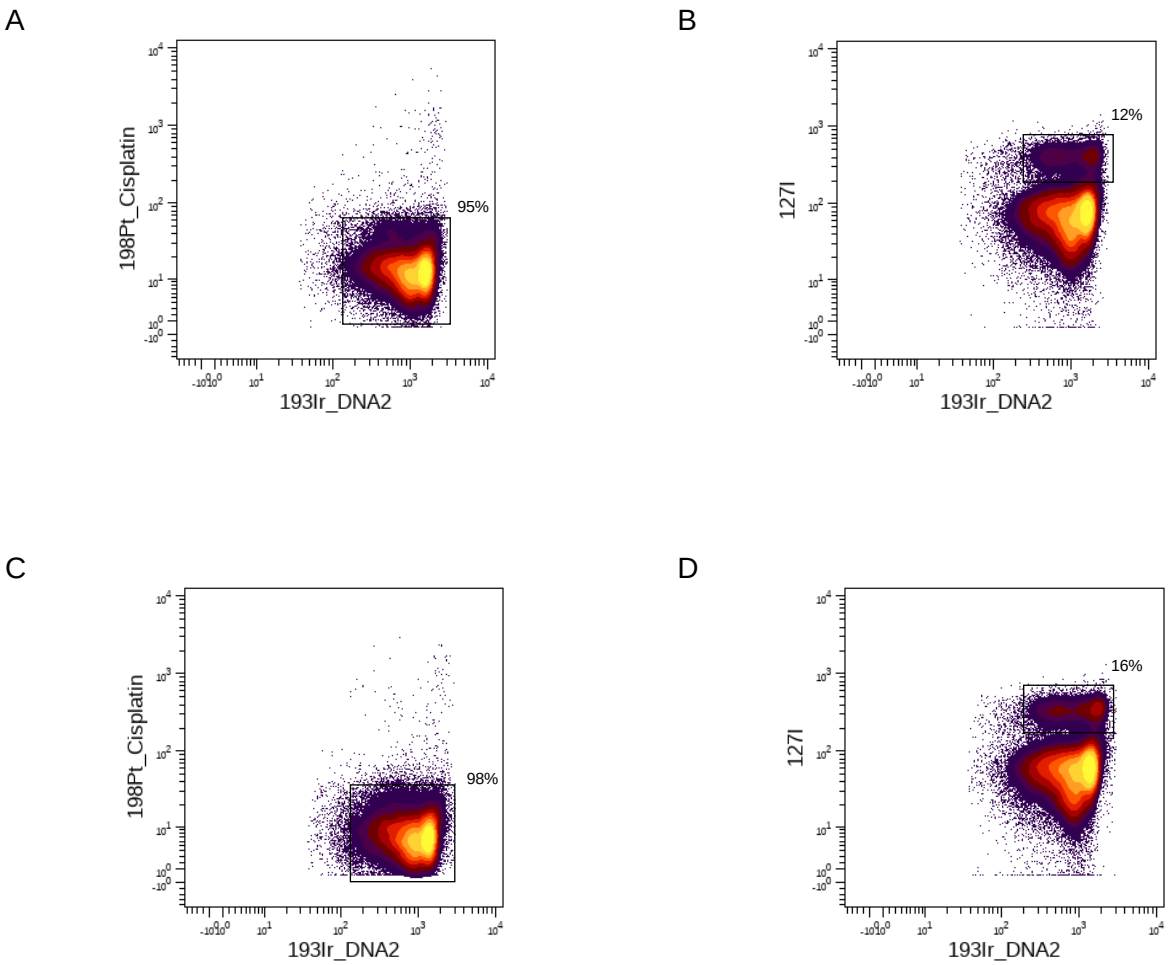

Figure 5.9 Comparison of SepMate™ and LeucoSep™ preparation tubes for PBMC analysis on Helios

PBMCs from a healthy donor were isolated and analysed using Helios to assess cell yield, cell viability and level of iodine contamination using SepMate™ and LeucoSep™ protocols, n=1 example shown. 8mL of whole blood was taken and 4mL was used for each protocol.

A: Dot plot showing the SepMate™ PBMC protocol produced a cell viability of 95%. Gating on cells negative for cisplatin and positive for 193IrDNA2 live/dead cell markers.

B: Dot plot showing the SepMate™ PBMC protocol produced an iodine contamination level of 12%. Gating on cells positive for 127I (iodine channel) and positive for 193IrDNA2.

C: Dot plot showing the LeucoSep™ PBMC protocol produced a cell viability of 98%. Gating on cells negative for cisplatin and positive for 193IrDNA2 live/dead cell markers.

D: Dot plot showing the LeucoSep™ PBMC protocol produced an iodine contamination level of 16%. Gating on cells positive for 127I (iodine channel) and positive for 193IrDNA2.

5.6.2 CyTOF Optimisation: Fresh vs frozen PBMCs

A comparison of fresh and frozen PBMC analysis using the same sample from a HD and run on Helios was required to assess to what extent cryopreservation affects the CyTOF signal. An n=1 experiment was carried out to assess the cell yield and viability of cryopreserved PBMCs from the same HD in section 5.6.1, where the results of fresh PBMC analysis using SepMate™ is described. Four mL of whole blood was processed using the SepMate™ PBMC isolation protocol described in section 2.3.1. Cells were cryopreserved in 1mL aliquot at -80°C for 24 hours, cells were then thawed and counted. The cell yield was lower than fresh PBMCs using SepMate™ at 3.72 x 10^6/mL and cell viability was significantly lower at 67%. Viable and non-viable dead cells are indicated in Figure 5.10.

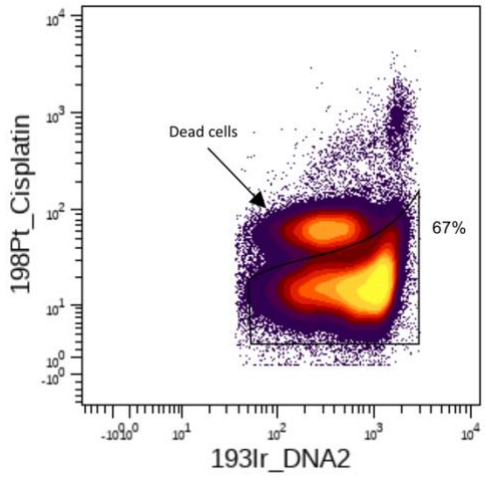

Figure 5.10 Cryopreserved PBMCs isolated using SepMate™ for analysis on Helios
PBMCs from a healthy donor were isolated using the SepMate™ protocol, cryopreserved for 24 hours then thawed and analysed using HELIOS to assess cell viability, n=1 example shown. 4mL of whole blood was used. Dot plot showing the SepMate™ PBMC protocol cryopreserved PBMCs produced a cell viability of 67%.

5.6.3 Optimisation of RNA extraction and quantification

Three HD whole blood samples were used and 20mL of whole blood was taken from each volunteer. Subsequently, 10mL whole blood from each volunteer was used for fresh analysis and 10mL whole blood processed and PBMCs cryopreserved. Comparison of RNA quantity and RNA integrity from fresh and frozen PBMC was undertaken. For both fresh and frozen analysis, PBMCs were isolated using the SepMate^{TM} protocol. RNA extraction, concentration and quantification were performed using the manufacturers protocols as discussed in section 2.10.1. Table 5.2 illustrates the cell count, RNA concentration and RIN values for the 3 HD fresh PBMC samples and the cell count and RNA concentration from the same 3 HD PBMC samples. There was an expected drop in cell count and RNA concentration following cryopreservation and thawing of PBMCs. RNA integrity from fresh PBMCs was high and the bioanalyser profiles of RNA extracted from the fresh PBMCs of each of the 3 HDs is shown in Figure 5.11. It was not possible to perform the assessment of RNA integrity using the frozen samples due to the COVID-19 pandemic and temporary closing of laboratory facilities.

Table 5.2 Optimisation of RNA extraction and quantification: n=3, fresh and frozen HD PBMC samples

PBMC Sample	Cell count (total per 10 mL blood)	RNA concentration (ng/µL)	RIN values
Fresh	8-10 x 10^6	186 - 304	9.5 – 9.8
Frozen	4-6 x 10^6	88 - 165	N/A*

*N/A: not assessed

A

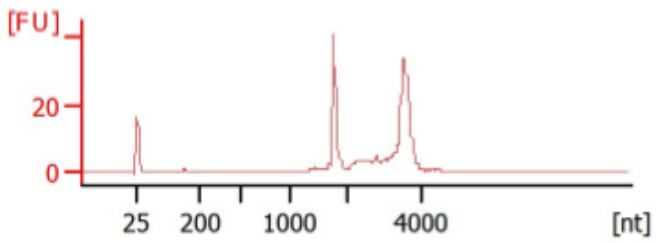

B

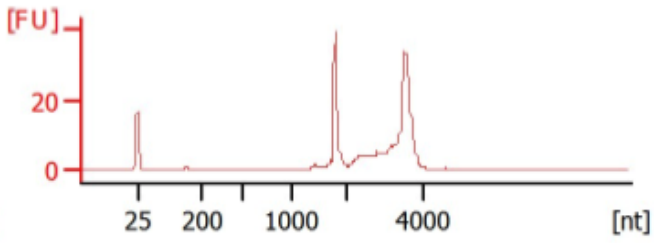

C

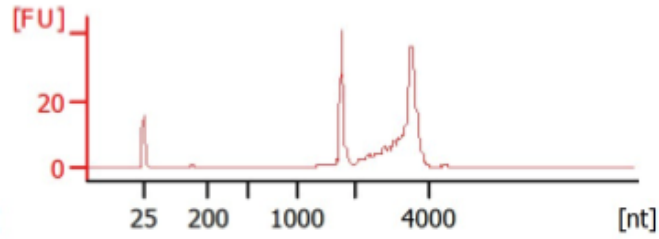

Figure 5.11 Bioanalyser profiles of RNA extracted from fresh HDs (n=3)
A: HD 1 fresh PBMCs: Electropherogram from bioanalyser showing the high integrity of RNA isolated from cells, RIN value 9.80.
B: HD 2 fresh PBMCs: Electropherogram from bioanalyser showing the high integrity of RNA isolated from cells, RIN value 9.50.
C: HD 3 fresh PBMCs: Electropherogram from bioanalyser showing the high integrity of RNA isolated from cells, RIN value 9.70.

5.7 Discussion

There has already been a dramatic paradigm shift in cancer treatment since the advent of immunotherapy, both as single agent and combination therapies. The advances in treatment for patients with metastatic melanoma have been rapidly translated to the high-risk adjuvant setting. However, primary and acquired resistance to ICB remains a challenge. Therefore, biomarkers predictive of response to therapy that can be assessed prior to initiation of treatment and early during the course of therapy are critical. Equally important is on-treatment biomarker monitoring that may predict the likelihood of treatment failure and disease relapse.

The body of work aimed at addressing the issue of response to immunotherapy with the intention of personalising the approach to treatment in melanoma has been focussed to date on the stage IV setting[144,215,216,219,221,228,368,369]. Most of these studies include small sample sizes, address tumour and circulation separately and do not seek to integrate the approaches utilised. There has been very little progress in terms of understanding the biology behind why these drugs are not effective for every individual and how to improve outcomes. This is most likely due to our incomplete understanding of how ICB modifies the already complex immune response to cancer in addition to the contribution of immuno-editing to a dynamic tumour microenvironment.

Establishing predictive biomarkers is likely to be instrumental in achieving effective patient stratification as well as tailoring optimal sequencing and scheduling of therapy. Despite the fact that several candidates discussed in Chapter 1, including circulating (CTCs, ctDNA, microRNAs, cytokines, exosomal PDL-1) and genomic markers (TMB, specific mutated gene pathways such as IFNγ and neoantigen load) have been suggested as predictive of immune response, these are yet to be validated for routine clinical use in a standardised and easily reproducible manner.

The approval of ICB in resected stage III disease and the growing number of clinical trials investigating their efficacy in the stage II and neoadjuvant settings reflects the shift towards early detection and prevention of patients developing metastatic disease[370,371,372]. As the risk of relapse varies in the stage III setting, the development of tools that can identify patients at high risk of recurrence and those that will benefit from further treatment post-operatively remains an important yet considerable challenge. This study will provide a unique opportunity to evaluate the biology of the disease at an early stage, where although still heterogeneous, more amenable to tissue sampling at the time of surgery providing access to the primary or lymph node tissue. The potential findings in blood and/or tumour are more likely to be

representative of the entirety of the patients' disease compared to the stage IV setting where any biopsy is likely to provide limited sample information. Combining peripheral blood circulating candidate biomarkers such as ctDNA and immune cell repertoire may mean that these could be measured by a single validated assay. The development of such a multiparametric assay and use of integrated platforms to reduce the heterogeneity and complexity of the host genomic and immunologic landscape would facilitate a comprehensive predictive system for immune response and clinical efficacy of ICB in cancer patients.

CtDNA has been identified as a candidate liquid biomarker of MRD and molecular relapse and has been utilised within clinical trials to guide treatment decisions. However, there remains a lack of standardised detection assay, thus it has yet to be fully validated for routine clinical use[187]. In the meantime, there are other blood-based modalities that could be explored which might further improve a liquid biopsy test if combined with ctDNA. Peripheral blood T cell immunophenotyping was explored in a proof of principle study in multiple myeloma and NK-T and T cell peripheral immunophenotypes were found to differ in MRD positive and MRD negative patients, providing a distinctive signature for each[373]. This data supports exploration of immune profiling according to MRD defined responses to identify patients that may benefit from maintenance therapy in this setting. Several other studies have also identified peripheral immune cell immunophenotyping as a method of accurately capturing MRD in haematological malignancies[374,375]. However, this has yet to be explored in solid tumours and one approach could be to track peripheral T cell dynamics in combination with ctDNA. A multi-omic approach utilising ctDNA to track MRD and evaluation of peripheral T cell immunophenotyping in addition to assessment of the TCR repertoire may offer new and relevant insights into the impact of anti-PD1 therapy on T cell responses and how this correlates with MRD and the potential patient groups described earlier.

In stage III disease, the tumour excised is of lymph node origin and could prove challenging to apply the CyTOF platform, as it is not possible to differentiate TIL from lymph node resident immune cells. This precludes comparisons with T cell changes identified in the peripheral circulation, so to account for this, CyTOF analysis on lymph node tumour and healthy matched lymph node tissue would be required. As such, CyTOF analysis on tumour tissue in this study would not be feasible. If CyTOF analysis identifies a specific immune cell population in the circulation as being indicative of involvement in response, then the question regarding functionality in the tumour will be raised. In this event, the CLND patients will have dissociated single cell suspension frozen in FBS/DMSO that would be available for analysis. Gene expression analysis may give some preliminary insights that can be further explored in a subsequent study and potentially validated in FFPE tissue. A potential limitation within this

study, is the small number of patients undergoing CLND. Therefore, any gene expression findings will be difficult to correlate with response, particularly given that patients with macroscopic disease at presentation undergoing CLND are at a higher risk of relapse from the outset.

Additionally, the assessment of fresh lymph node tumour tissue for tumour specific T cell responses will be undertaken, it is anticipated that there will be evidence of tumour resident T cell clones that are also present in the periphery and that expansion of these clones will correlate with response to ICB therapy. Recent retrospective studies have shown that high TCR diversity in pre-treatment TIL is prognostic for survival in melanoma patients who did not receive ICB, whereas baseline high tumour TCR clonality was identified as predictive of response to anti-PD1 ICB therapy[305]. Thus, suggesting that high TCR diversity in TIL identifies those patients whose immune system achieves durable tumour control without anti-PD1 ICB, whereas high TIL clonality determines which patients will mount an effective anti-PD1-induced immune response. This is in keeping with studies in which on treatment TIL sampling identified clonality as a predictor of response to ICB in melanoma[369,376].

With adjuvant anti-PD1 based therapy approved for use in high risk resected stage III melanoma and the recent interim results of Keynote-716 suggesting improved PFS (NCT03553836) following surgical resection in stage II melanoma, there is a high likelihood that approval will be imminent for adjuvant ICB in earlier stage disease, thus increasing the population of patients exposed to potentially toxic therapy. Further underscoring the need for predictive and prognostic immunotherapy biomarkers, particularly for patients with intermediate risk disease, where the risk of toxicity may outweigh the benefit of adjuvant ICB therapy. The addition of tumour assessment to peripheral blood T cell repertoire findings has the potential to further strengthen liquid biopsy readout by confirming tumour TCR specificity and ultimately aiding the pursuit for a reliable multiparametric tool for patient selection.

The optimisation work initially sought to assess both PBMC isolation protocols to understand the impact on cell yield and viability, whilst then also considering the degree of iodine contamination which could have downstream effects on sample analysis as discussed in section 5.6.1. Both SepMate™ and LeucoSep™ had similar cell viability however the cell yield was higher with LeucoSep™, although, this was at the cost of higher levels of iodine contamination. The cleaner signal with SepMate™ having a lower level of iodine contamination was a key determinant in the decision to proceed with SepMate™ protocol, despite the lower cell yield, as for CyTOF a minimum of 3 x 10^6/mL cells is required and the SepMate™ protocol provides cell numbers above this threshold. The experiment was limited by the n=1 sample

size, however, only 4mL of blood was used and minimum cell yield was exceeded and within the study protocol blood volumes of 20mL EDTA will be used for PBMC isolation to ensure a high cell yield.

Subsequently, using the SepMate^{TM} protocol for PBMC isolation, the effect of cryopreservation on cell yield and viability was studied. The cell yield was slightly lower compared to fresh analysis, but still within the acceptable threshold for CyTOF analysis. Notably, however, the cell viability was significantly lower compared to the fresh comparison. Thus, if the study went ahead with frozen PBMCs the possibility that small cell populations that could be significant may be lost and not captured by CyTOF should be considered[377]. For this reason, the study protocol is planned to proceed with fresh PBMC labelling in real time. Nevertheless, it is important to consider that assessment of peripheral cell immunophenotyping of any future external validation cohort would likely come from cryopreserved PBMC samples and so it may not be possible to recapitulate potential findings from this study. When evaluating optimisation for downstream peripheral TCR sequencing, RNA concentration and integrity were assessed on both fresh and frozen HD PBMC samples. The drop in RNA concentration following cryopreservation and thawing was expected, however it was not possible to assess the RNA integrity of the cryopreserved PBMCs. It is anticipated that there would not be a significant drop in RIN as cells were frozen immediately after isolation and thus results should be comparable[378], indicating that there is likely to be minimal impact on quality of TCR sequencing from cryopreservation of PBMCs.

Approximately 150 patients are referred to The Christie NHS Foundation Trust per year for SLNB to stage their disease. The pre-operative blood sample will be taken on the day of surgery and processed for all consented and eligible patients. According to available audit data from The Christie NHS Foundation Trust, of those, only approximately 50 patients will have a positive SLNB and will be confirmed as having stage III disease requiring referral to Medical Oncology for adjuvant ICB. The remaining 100 patients are expected to be SLNB negative and will remain under clinical follow up not requiring further treatment (stage IIB/C patients will be offered the DETECTION trial). This will result in 100 stored pre-operative PBMC and plasma samples not required for this study as these patients will be ineligible. It has been observed that up to 25% of SLNB negative patients will relapse[379], therefore this patient cohort will be valuable for future studies exploring whether molecular monitoring in stage II disease could enable early identification of patients with micro-metastatic relapse that may benefit from early therapy initiation compared to standard of care follow up.

A growing number of patients with early stage melanoma are faced with an extremely high risk of recurrence and melanoma specific mortality. Adjuvant therapy has been validated as an efficacious management strategy for stage III melanoma and given that more patients are diagnosed with stage I and stage II melanoma compared to stage III, the role of adjuvant therapy has been evaluated in earlier stage disease. Understanding whether early treatment improves overall survival remains a critically important unanswered question and clinical trials are underway to address this. Melanoma has been a model cancer for immunotherapy and there are already data in the adjuvant and metastatic settings supporting the rationale that early treatment could lead to more durable responses and improvements in chance of cure[69,104]. This study in the surgically resected stage III setting, strives to have a positive clinical impact on the field that translates into a clinically meaningful benefit to patients in terms of the ability to limit adjuvant therapy to patients who have a higher risk of relapse and death and a higher likelihood of deriving benefit.

Validation and clinical implementation of risk-assessment and response tools to enable detection of patients with MRD and appropriate selection of treatments that extend the duration of complete response over current empiric approaches could transform the way adjuvant therapy in stage III disease is utilised. This prospective study in the adjuvant setting has the potential to validate findings from previous work whilst also examining treatment effect of ICB and the ability of ctDNA to capture responses in this population, to establish whether it is also a predictive biomarker for response to ICB[203] . In particular, it has been observed that a single time point of blood sampling post operatively is unlikely to identify all patients that will relapse[203,205], however, longitudinal sampling has identified relapse before radiological imaging in the stage IV setting and thus provides a rationale for this approach in stage III disease[208]. CtDNA detection at a single time point post operatively as a marker of MRD could inform on individual prognosis and adding to AJCC staging information and informing discussion with patients regarding the risks and benefits of adjuvant ICB. This study will enable identification of a subgroup of patients at high risk of early relapse and inferior survival, this coupled with the potential for ctDNA to be combined with peripheral T cell changes as a multiparametric marker of response to ICB would further strengthen the potential readout, thus facilitating stratification of patients to adjuvant therapies associated with significant toxicity, but with greater potential efficacy[67].

Additionally, when considering the issues surrounding the design of a clinical trial that tests the functional assessment of MRD and response biomarkers including peripheral T cell repertoire, surrogate endpoints such as eradication of detectable MRD and definitive endpoints such as PFS must be carefully selected to evaluate for superiority of a rational MRD

and response biomarker targeted treatment approach. Consideration must be given to frequency of liquid biopsy monitoring, threshold for therapeutic actionability and issues of standardisation and generalisability of implementation would need to be addressed, as will the availability of multiple potentially active therapeutics[333].

If ctDNA is validated as a marker of MRD and T cell repertoire changes correlate with response to adjuvant ICB which can also be tracked with ctDNA, the potential findings of this study could result in the development of clinically actionable multi-modality biomarkers for MRD and response to ICB which is a current unmet need in the clinic. Despite numerous candidate biomarkers demonstrating correlations with response in preclinical and clinical studies, no biomarker currently exists which is sufficiently robust to aid in patient selection. A major challenge which this study seeks to address is identifying a biomarker with sufficient negative predictive value to only exclude patients who are very unlikely to benefit, without depriving patients requiring treatment and may respond a chance at a potentially life-extending therapy. Focusing health care resources on patients at the highest risk will enable optimal resource utilisation and spare low-risk patients from the risks and potential toxicities of treatment.

In summary, the key issues to be addressed for the adjuvant approach are the selection of patients, optimising therapeutic outcomes and minimising the number of patients exposed to potentially toxic treatment without gaining clinical benefit. This study strives to tackle these important emerging issues, with the aim to develop a multi-parametric tool facilitating patient stratification, with the ability to anticipate therapeutic responses in real-time. In the future, this study has the potential to aid personalised management and clinical decision making for oncology patients. Comprehensive predictive models developed by integrating different types of data based on different components of tumour-host interactions is the direction of future research and will have a profound impact in the field of precision immuno-oncology.

Chapter 6: Final Discussion

6.1 Immunotherapy and melanoma

Melanoma is a paradigm of how the treatment landscape can be revolutionised over a decade. Prior to this, patients with chemotherapy refractory advanced melanoma had an average life expectancy of three to six months. Today, patients are returning to clinic for their third year of follow up, giving hope where just a decade ago there was little. Behind the transformation in melanoma survival rates are both targeted therapy and checkpoint inhibitor drugs. Figure 6.1 illustrates the timeline of melanoma therapy approval. Targeted therapy for BRAF mutated melanoma offers some extension in PFS and OS, although resistance is common[380]. Since the approval of ICB in 2011, there has been further improvement in the treatment landscape. Notably, in the USA, among all cancer types, cutaneous melanoma had the greatest decline in annual deaths, 6% per year, between 2014-2018[381]. More recently, these advances have been rapidly translated into the high-risk adjuvant setting, with ongoing studies investigating neoadjuvant ICB in high risk resectable melanoma.

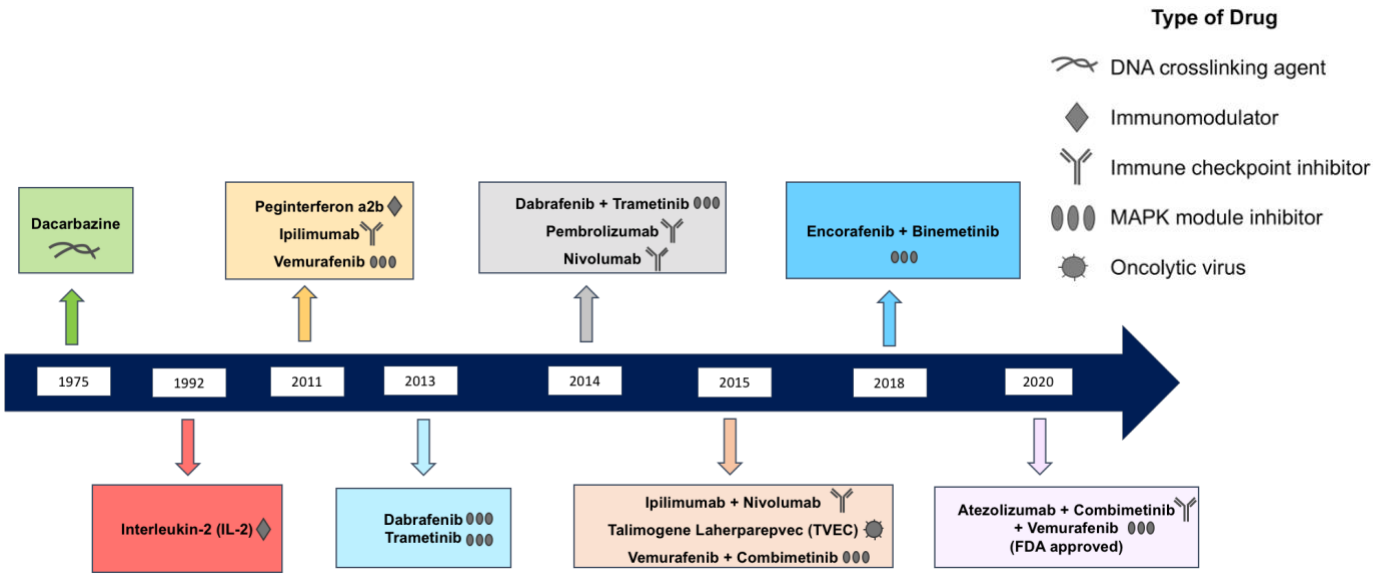

Figure 6.1 Timeline of treatment approvals for advanced melanoma patients
MAPK=mitogen activated protein kinase, FDA=Food and Drug Administration.

Synergistic combinations were developed to heighten potency and duration of immune response. Immunotherapy regimes have evolved from the single agent approach to combination ICB such as anti-CTLA-4 plus anti-PD-1, and recent studies have paired ICB with conventional cancer therapies such as chemotherapy or targeted therapies[382,383,384,385]. At present there are no robust data in support of chemotherapy immunotherapy combinations in melanoma in the first line setting, however these combinations have been approved for PDL-1 positive triple negative breast cancer (TNBC), PDL-1 positive head and neck squamous cell cancer (HNSCC) and all patients in the first-line setting irrespective of PDL-1 status for gastro-oesophageal adenocarcinoma, leading to a paradigm shift in the treatment of these tumour types[386,387,388].

Despite the treatment armamentarium for patients with metastatic melanoma expanding significantly and checkpoint inhibitors having demonstrated unprecedented rates of durable responses, many patients treated do not respond and the burden of potentially serious toxicity exists. Thus, there is a need to discover biomarkers that will aid patient selection and help tailor treatment regimes. The search for robust biomarkers is limited by our incomplete understanding of how ICB modifies the pre-existing complex immune response to cancer. Furthermore, candidate assays are yet to be deployed into large prospective studies, and the lack of standardisation in measurement and interpretation restricts their validity[389].

The current understanding of the clinical response to ICB therapy implies a single biomarker cannot predict patients who will benefit from immunotherapy. Thus, a predictive model that considers the different components that affect tumour–host interactions is needed. The development of a multiparametric assay and use of integrated platforms to compress the heterogeneity and complexity of the host genomic and immunologic landscape would allow a comprehensive predictive system for immune response and clinical efficacy of immunotherapy in melanoma patients. On-treatment biomarker monitoring that could predict likelihood of treatment failure and disease relapse is required and similarly, biomarkers predictive of response to ICB that can be assessed prior to treatment initiation and early during the course of therapy are vital in achieving precision immuno-oncology.

The principal aim of this thesis was to explore liquid biopsy as a tool for effective patient stratification in melanoma immunotherapy. Chapter 3 focussed on utilising an optimised multiparametric flow cytometry panel to identify peripheral blood T cell markers of response to immunotherapy early after treatment initiation in stage IV melanoma and explored the potential to develop a prospective clinical study to test the hypothesis that early on treatment changes in peripheral T cell subsets can predict response to ICB therapy. Subsequently,

Chapter 4 addressed the impact of patient age and other clinical variables on peripheral T cell and TCR repertoire evolution and pattern of response under the selective pressure of ICB in stage IV melanoma. Finally, Chapter 5 sought to investigate the feasibility of translating these findings into the adjuvant setting to identify patients with MRD at high risk of relapse and predict patient response to ICB therapy in stage III melanoma.

6.2 Summary of Key Results

Assessment of peripheral T cell changes that relate to pre-treatment and early on treatment time points was undertaken in metastatic melanoma patients undergoing first line ICB therapy. Flow cytometry revealed expansion of a subset of CD8+ memory immune effector cytotoxic T cells, termed T_{IE} cells in peripheral blood. Changes in T_{IE} cell abundance inversely correlated with changes in the tumour burden as determined by size of RECIST target lesions on patient's W12 CT scan and peripheral T cell pools experienced dynamic turnover proportional to the magnitude of response. At W3 after therapy initiation, expansion of peripheral T_{IE} cells was significantly greater in patients that responded to ICB. An increase of 0.8% in the ratio of T_{IE} cells relative to all CD8+ memory cells at W3 was associated with improved OS and separated 6-month responders from non-responders, this was confirmed in a separate validation cohort. Analysis from later W9 treatment time point revealed the presence of T_{IE} cells, however there was no longer a correlation with response, highlighting the dynamic nature of these immune signatures and indicating that these changes occur early and are transient. T_{IE} cell expansion at W3 was predictive of outcome in patients treated with both single agent anti-PD1 and combination ICB.

Interestingly, when compared with other candidate biomarkers within the literature such as peripheral Ki67/TB or PDL-1 staining in pre-treatment melanoma biopsies, W3 T_{IE} expansion displayed superior accuracy in identifying patients that achieved disease control early on treatment. However, within this study the small sample size limited a statistically meaningful result when comparing increased peripheral Ki67 expression and T_{IE} expansion at W3.

Evaluation of whether changes in W3 T_{IE} cell expansion were associated with immune related adverse events revealed no correlation between T_{IE} expansion and grade of toxicity, suggesting that T_{IE} cells are not a predictive marker of immunotherapy toxicity in this setting. However, expansion of a separate T_{reg} subset characterised by the surface phenotype $CD3^{+}CD4^{+}CD8^{-}CD25^{+}CD127^{-/low}$ did correlate with grade of toxicity.

The follow-on study described in Chapter 4 sought to extend these observations by analyzing the impact of patient clinical variables on peripheral T_{IE} cells and TCR repertoire rearrangement. Although T_{IE} expansion is a biomarker of immunotherapy response across all age groups, patients at different ages present different patterns of peripheral TCR repertoire evolution in response to ICB. Following the first cycle of ICB, in patients ≥70 years treatment resulted in an increase in peripheral TCR clonality, whereas in patients <70 years it led to an increase in peripheral TCR diversity. These findings were replicated in a separate validation cohort, although the patient numbers were too small to reach statistical significance, the trend was consistent with initial findings. There was a significant age difference between the two treatment groups (single agent ICB vs combination ICB), with older patients ≥70 years preferentially assigned to single agent therapy, likely reflecting selection bias from clinicians in a real world setting. This complicated interpretation of the effect of treatment regimen on the biomarker dynamics, but nevertheless there was no correlation identified between other clinical variables such as gender, disease stage, or BRAF mutation status on T_{IE} cell expansion or peripheral TCR repertoire rearrangements supporting their validity as biomarkers of response to therapy.

Although the study described in Chapter 5 could not be carried out, the investigation of these candidate biomarkers in early stage melanoma remains undoubtedly clinically relevant in identifying resected stage III patients with MRD that would benefit from adjuvant therapy and improving stratification and prediction tools for ICB response assessment.

6.3 Significance of Results Presented

ICB therapy works by removing inhibitory signals of T cell activation, allowing tumour reactive T cells to overcome regulatory mechanisms and mount an effective anti-tumour response. Recently, particular focus has been placed upon peripheral T cell changes during ICB therapy as a readout of immunotherapy related changes in melanoma. To date analysis of TIL T cell repertoire has been at the forefront of research into ICB responses in melanoma, but understanding of how T cell repertoire changes in the tumour are then reflected in the circulation has been limited. The work here concentrated on an early, but clinically relevant time point of week 3, following one cycle of ICB therapy. This is in keeping with recent literature which suggests that in cancer immunotherapy, the peak of immune activation is at week 3[213,271]**.** To date, the majority of studies interrogating pharmacodynamic changes in peripheral T cells had focussed on later time points between 3 and 12 weeks of ICB initiation, which may represent different aspects of T cell changes[211,215,216,390,391].

The work presented in this thesis suggests that activation of a common CD8+ immune effector memory cell subset may be relevant for monitoring early on treatment immunotherapy responses and highlights the dynamic changes observed among circulating T cells in peripheral blood. These findings are of particular significance given the correlation with subsequent clinical responses. It has been established that this subset of lymphocytes is involved in cytotoxic response to infections and thus could limit specificity in the immunotherapy setting, necessitating further kinetic analysis and clinical validation[252,257,264]. Future work to delineate the anti-tumour reactivity and specificity of T_{IE} cells is required. However, as far as is known, this is the first report demonstrating the relevance of peripheral T_{IE} cells in cancer immunotherapeutics.

Expanding on observations of the different variation of T_{IE} cells in patients who benefitted from ICB compared to those who did not, the inverse correlation between changes in T_{IE} cell abundance and radiological tumour burden suggest that an increase in T_{IE} abundance 3 weeks after start of ICB therapy is anticipatory of tumour shrinkage at W12. The magnitude of T cell turnover at W3 was proportional to the magnitude of response to ICB which is consistent with the immune signature acting as a reliable early biomarker of response to immunotherapy.

There are differences in the time course of efficacy and toxicity between anti-PD-1 monotherapy and anti-PD-1 plus CTLA-4 combination therapy[109,392]. However, the lack of significant differences observed between single agent and combination therapy suggests the findings described here are independent of treatment modality and reflect the final effects

needed for tumour elimination. The relatively small patient cohort may limit the generalisation of the results, however, W3 T_{IE} cell expansion could segregate patients that would benefit from ICB therapy with superior accuracy compared to standard biopsy PD-L1 staining for which predictive accuracy has already been validated[65,393]. It is likely that this is in part due to most of the immunological compartment being omitted from tumour tissue-based analyses. Thus, minimally invasive liquid biopsy acquired T_{IE} cells hold promise for potential future clinical development.

Checkpoint inhibitors are arguably the most important development in cancer therapy over the past decade. The indications for these agents continue to expand across malignancies and disease settings, reshaping many of the previous standard-of-care approaches. One of the costs of these advances is the emergence of a new spectrum of immune-related adverse events, which are often distinct from classical chemotherapy-related toxicities. Owing to the growing use of ICB in oncology, clinicians are increasingly confronted with common but also rare irAEs that can be irreversible. Thus, it is imperative to anticipate and have a better understanding of such toxicity. A multi-centre study seeking to explore whether irAEs reflected anti-tumour responses identified that the presence and number of irAEs in NSCLC patients was a strong predictor of response and survival outcomes[394]. This suggests a mechanistic association between irAEs and immunotherapy efficacy, therefore it was important to investigate T_{IE} cell expansion at W3 as a potential biomarker of toxicity. Although there was no correlation identified between T_{IE} cell expansion and the presence of $\geq$ G3 toxicity, the potential for an association at another timepoint (prior to or later than week 3) cannot be excluded and remains an important focus for future investigation. Moreover, as the clinical characteristics of irAEs can be insidious and are often difficult to determine in the early stages, the finding of a correlation between T_{reg} expansion at W3 and toxicity severity provides rationale for active surveillance of patients with a rise in peripheral T_{regs} which may facilitate early identification of patients susceptible to irAEs prior to their onset.

An immune biomarker predictive of clinical outcome prior to treatment initiation would be optimal and preferably therapeutic decision making should be based on such patient specific immune markers. This would potentially avoid toxicity risk, have considerable cost benefits and avoid exposing patients to treatment they are unlikely to gain benefit from. In the absence of such clinically validated markers, an early response indicator, such as a biomarker of immune activation consistent with the first dose of ICB at W3, has the potential to facilitate treatment decisions in a clinically actionable time frame.

In response to ICB therapy, the trend of TCR rearrangements towards increased diversity in younger patients, but increased clonality in older patients suggests that at different ages one cycle of immunotherapy induces different dynamics in peripheral T cell evolution. These observations likely reflect the age-related thymic involution[316,317] and the consequent reduction of new clonotype output[318] available to recognise and kill cancer cells[319]. This novel finding is extremely clinically relevant as therapeutic strategies aiming to boost peripheral T cell repertoire diversification to recognise tumour neoantigens might be ineffective in elderly patients where successful new clonotype recruitment would be impaired by thymic involution. Although limited by a small sample size and the biological biases of an unselected population, taken together the data support a model whereby age does not affect peripheral T_{IE} subset expansion in response to ICB, but does influence immunotherapy-induced peripheral TCR repertoire evolution.

6.4 Future Challenges and Opportunities for Melanoma Immunotherapeutics

This work has demonstrated that liquid biopsy is feasible for early on treatment monitoring of ICB therapy response in metastatic melanoma. However, the immune signature identified requires further kinetic analysis and clinical validation.

There are inherent challenges associated with biomarker development in cancer immunotherapy. Unlike targeted therapies, where patients with targetable mutations or genetic alterations, such as *BRAF* mutation in melanoma and *EGFR* mutations or *ALK* translocations in lung cancer are defined as binary (yes or no) assays, candidate biomarkers in onco-immunology are a continuous variable, as is the case with PD-L1 expression, and TMB, both of which can be defined at multiple different biomarker cut offs. This undoubtedly results in challenges in pre-defining a cut off to identify biomarker high versus low populations for prospective clinical trial design[395]. In Chapter 3, where early clinical testing of T_{IE} cells as a biomarker of ICB response was being undertaken, the ROC curve was utilised as a valuable statistical tool in defining the T_{IE} cell cut off as it was unclear whether the endpoint being measured was strongly associated with longer term outcomes. This finding requires validation in a much larger cohort of patients.

Within the body of work described in this thesis, constraints upon availability of patient tumour tissue samples meant that phenotypic analysis of T cells was limited to peripheral blood samples. The study of TIL and tumour immune microenvironment interactions with the peripheral immune system has not been described here and should be considered a priority

for future pre-clinical work as elucidating whether there is cross-talk between the TME and expansion of T_{IE} cells and TCR repertoire in peripheral blood will be important when considering tailoring treatment and design of future clinical trials.

The work presented focused on delineating changes in CD8+ T cell populations in metastatic melanoma. It will be interesting to observe if the findings described within this thesis translate into the early stage setting utilising the study protocol from Chapter 5, as this will have clinically relevant implications on a subset of patients potentially cured by surgery alone. Additionally, exploring the relevance of the findings from this thesis in other solid tumour types such as NSCLC and renal cell carcinoma where immunotherapy is a key therapeutic modality could be considered. Future work should focus on combining biomarkers and streamlining their application to create a more clinically viable and cost-effective model for immune monitoring during ICB therapy as it is likely that immunological changes will depend on the context and timing of patient sampling. Thus, multiplexed, longitudinal analysis will add value to future studies.

The recent phase III study RELATIVITY-047 (NCT03470922) in patients with treatment naïve advanced melanoma demonstrated a statistically significant and clinically meaningful improvement in PFS with anti-LAG3 antibody relatlimab plus nivolumab compared to nivolumab monotherapy with a manageable toxicity profile[396]. In parallel, a further investigator initiated single arm phase II study (NCT02519322) of nivolumab and relatlimab in patients with resectable melanoma demonstrated high pCR rates with a favourable toxicity profile in the neoadjuvant and adjuvant settings[397]. These studies provide potential novel checkpoint inhibitor combination treatment options in both early and advanced stage disease.

The concept of different drug combinations and therapy escalation is intriguing, and early immune-based biomarkers could facilitate more nuanced clinical decision making, as despite the improved clinical outcomes observed with checkpoint inhibitors, approximately 40-60% of patients with advanced melanoma display primary resistance and do not respond to single agent ICB therapy with progression within the first 3 months of therapy and those that do respond, this can be transient with development of acquired resistance over time if progression occurs after a period of stable disease or response on therapy[398]. To overcome resistance and bring clinical benefit to the majority of patients the dissection of melanoma immunobiology will be instrumental in fully understanding the mechanisms that lead to an effective anti-tumour response and tumour cell-intrinsic and extrinsic factors that cause ICB

resistance. Elucidation of these mechanisms is likely to uncover vital clues to the next steps in the endeavour to overcome resistance to ICB therapy and further improve clinical outcomes.

Several studies have explored the role of the gut microbiome in modulating response to ICB. Characterisation of stool samples from melanoma patients treated with anti-PD1 therapy identified a significant association between commensal microbial composition and clinical responses to immunotherapy[399,400]. Within the context of the work described in this thesis, it should be considered that the gut microbiome may also be an important factor that could not be controlled for in the patient cohort. It is unlikely that a favourable response to ICB can be linked to a single bacterium, but it remains unclear whether response could correlate to a distinct combination of species. Nevertheless, the therapeutic potential to improve clinical outcomes by manipulating the microbiome is an exciting one and where possible, should be incorporated into future work.

Understanding the characteristics of the patient populations that will or will not respond to ICB is vital for making informed treatment decisions. This information could spare some patients from receiving treatment and the risk of side effects when they are unlikely to benefit and may also guide alternative more effective therapeutic strategies. Precision medicine in the context of immunotherapy has exciting advances on the horizon, but there remains a fundamental need to rethink how treatment can be optimised when transitioning forward into the next phase of cancer care. Ultimately, an improved understanding of the mechanisms underlying the biology that drives ICB therapy responses will be vital when improving the design of future clinical trials and rational drug combinations. The ability to collect serial peripheral blood samples from patients for T cell repertoire analysis and utilising these samples to inform further studies in a reverse translational manner may yield vital information for the identification of novel biomarkers of response. Identifying markers in the blood predictive of response to immunotherapy has the potential to provide a minimally invasive and early measure of whether treatment is going to benefit an individual patient.

6.5 Conclusion

In summary, this work has identified a peripheral blood early immune signature characterised by turnover of a specific subset of T cells. These changes detected in blood provide the advantages inherent in minimally invasive liquid biopsies. Critically, the magnitude of immune signature changes following the first cycle of ICB therapy anticipated which patients would go on to respond and ultimately correlated with overall survival.

Although T_{IE} cells may act as early prognostic biomarkers irrespective of patients' age, T cell repertoire analysis must be contextualised by the patients' age. Investigation of the clinical correlates associated with the immune signature identified a model whereby age does not affect peripheral T_{IE} subset expansion in response to ICB, but does influence immunotherapy-induced peripheral TCR repertoire evolution. Therapeutic strategies aiming to boost peripheral T cell repertoire diversification to increase tumour neoantigen recognition are likely to be less effective in patients $\geq$70 years. These findings will have important ramifications both in the biomarker development field and for planning future therapeutic strategies.

Further work is necessary to determine the mechanisms underpinning these observations and their specificity for ICB induced responses providing the rationale for a larger study to further investigate these novel findings. Future studies should also incorporate kinetic analysis and if validated, would represent a clinically significant, potentially practice changing result.

References

1. Urban, K., Mehrmal, S., Uppal, P., Giesey, R. L. & Delost, G. R. The global burden of skin cancer: A longitudinal analysis from the Global Burden of Disease Study, 1990–2017. *JAAD Int.* **2**, 98–108 (2021).
2. Mayers, K. What is the scale of the skin cancer problem in the UK? *J. Aesthetic Nurs.* **7**, 230–230 (2018).
3. Schadendorf, D. *et al.* Melanoma. *Lancet* **392**, 971–984 (2018).
4. Cancer Research UK. Melanoma skin cancer statistics. Available at: https://www.cancerresearchuk.org/health-professional/cancer-statistics/statistics-by-cancer-type/melanoma-skin-cancer. (Accessed: 29th June 2019)
5. Dickson, P. V. & Gershenwald, J. E. Staging and prognosis of cutaneous melanoma. *Surg. Oncol. Clin. N. Am.* **20**, 1–17 (2011).
6. Cancer Research UK. Risks and causes of melanoma. Available at: https://www.cancerresearchuk.org/about-cancer/melanoma/risks-causes. (Accessed: 29th June 2019)
7. D'Orazio, J., Jarrett, S., Amaro-Ortiz, A. & Scott, T. UV radiation and the skin. *Int. J. Mol. Sci.* **14**, 12222–12248 (2013).
8. Viros, A. *et al.* Ultraviolet radiation accelerates BRAF-driven melanomagenesis by targeting TP53. *Nature* **511**, 478–482 (2014).
9. Trucco, L. D. *et al.* Ultraviolet radiation–induced DNA damage is prognostic for outcome in melanoma. *Nat. Med.* (2018). doi:10.1038/s41591-018-0265-6
10. Gandini, S., Autier, P. & Boniol, M. Reviews on sun exposure and artificial light and melanoma. *Prog. Biophys. Mol. Biol.* **107**, 362–366 (2011).
11. Rastrelli, M., Tropea, S., Rossi, C. R. & Alaibac, M. Melanoma: epidemiology, risk factors, pathogenesis, diagnosis and classification. *In Vivo* **28**, 1005–11 (2014).
12. Leest, R. J. T., Flohil, S. C., Arends, L. R., Vries, E. & Nijsten, T. Risk of subsequent cutaneous malignancy in patients with prior melanoma: a systematic review and meta-analysis. *J. Eur. Acad. Dermatology Venereol.* **29**, 1053–1062 (2014).
13. Berwick, M., Erdei, E. & Hay, J. Melanoma epidemiology and public health. *Dermatol. Clin.* **27**, 205–viii (2009).
14. Silva, J. H., Sá, B. C. de, Avila, A. L. R. de, Landman, G. & Duprat Neto, J. P. Atypical mole syndrome and dysplastic nevi: identification of populations at risk for developing melanoma - review article. *Clinics (Sao Paulo).* **66**, 493–499 (2011).
15. Gershenwald, J. E. *et al.* Melanoma staging: Evidence-based changes in the American Joint Committee on Cancer eighth edition cancer staging manual. *CA. Cancer J. Clin.* **67**, 472–492 (2017).
16. Weide, B. *et al.* Serum S100B, lactate dehydrogenase and brain metastasis are prognostic factors in patients with distant melanoma metastasis and systemic therapy. *PLoS One* **8**, (2013).
17. Davies, M. A. *et al.* Prognostic factors for survival in melanoma patients with brain metastases. *Cancer* **117**, 1687–1696 (2011).
18. Michielin, O., Van Akkooi, A. C. J., Ascierto, P. A., Dummer, R. & Keilholz, U. Cutaneous melanoma: ESMO Clinical Practice Guidelines for diagnosis, treatment and follow-up. *Ann. Oncol.* **30**, 1884–1901 (2019).
19. Trotter, S. C., Sroa, N., Winkelmann, R. R., Olencki, T. & Bechtel, M. A Global Review of Melanoma Follow-up Guidelines. *J. Clin. Aesthet. Dermatol.* **6**, 18–26 (2013).
20. Morton, D. L. *et al.* Final trial report of sentinel-node biopsy versus nodal observation in melanoma. *N. Engl. J. Med.* **370**, 599–609 (2014).
21. Faries, M. B. *et al.* Completion Dissection or Observation for Sentinel-Node Metastasis in Melanoma. *N. Engl. J. Med.* **376**, 2211–2222 (2017).
22. Leiter, U. *et al.* Complete lymph node dissection versus no dissection in patients with sentinel lymph node biopsy positive melanoma (DeCOG-SLT): a multicentre,

randomised, phase 3 trial. *Lancet Oncol.* **17**, 757–767 (2016).
23. Hayward, N. K. *et al.* Whole-genome landscapes of major melanoma subtypes. *Nat. Publ. Gr.* **545**, 8010 (2017).
24. Ludmil B. Alexandrov, Serena Nik-Zainal, D. C. W. *et al.* Signatures of mutational processes in human cancer. *Nature* (2013). doi:10.1038/nature12477
25. Pfeifer, G. P. Environmental exposures and mutational patterns of cancer genomes. *Genome Med.* **2**, 54 (2010).
26. TCGA. Genomic Classification of Cutaneous Melanoma The Cancer Genome Atlas Network. *Cell* **161**, 1681–1696 (2015).
27. Cheng, L., Lopez-Beltran, A., Massari, F., MacLennan, G. T. & Montironi, R. Molecular testing for BRAF mutations to inform melanoma treatment decisions: a move toward precision medicine. *Mod. Pathol.* **31**, 24–38 (2018).
28. Network, C. G. A. Genomic Classification of Cutaneous Melanoma. *Cell* **161**, 1681–1696 (2015).
29. Hodis, E. *et al.* A Landscape of Driver Mutations in Melanoma. *Cell* **150**, 251–263 (2012).
30. Burnet, M. Cancer: a biological approach. III. Viruses associated with neoplastic conditions. IV. Practical applications. *Br. Med. J.* **1**, 841–847 (1957).
31. Swann, J. B. & Smyth, M. J. Immune surveillance of tumors. *J. Clin. Invest.* **117**, (2007).
32. Thomas, L. Cellular and humoral aspects of the hypersensitive states. *Acta Med. Scand.* **170**, 128 (1961).
33. Smyth, M. J., Dunn, G. P. & Schreiber, R. D. Cancer Immunosurveillance and Immunoediting: The Roles of Immunity in Suppressing Tumor Development and Shaping Tumor Immunogenicity. in 1–50 (2006). doi:10.1016/S0065-2776(06)90001-7
34. Chaplin, D. D. Overview of the Immune Response. **845**, 35294–2170
35. Chaffey, N. Alberts, B., Johnson, A., Lewis, J., Raff, M., Roberts, K. and Walter, P. Molecular biology of the cell. 4th edn. *Ann. Bot.* **91**, 401 (2003).
36. Janeway CA Jr, Travers P, Walport M, et al. *Immunobiology: The Immune System in Health and Disease*. (Garland science, 2001).
37. Waldman, A. D., Fritz, J. M. & Lenardo, M. J. A guide to cancer immunotherapy: from T cell basic science to clinical practice. *Nat. Rev. Immunol.* doi:10.1038/s41577-020-0306-5
38. Finn, O. J. Immuno-oncology: Understanding the function and dysfunction of the immune system in cancer. *Ann. Oncol.* **23**, viii6–viii9 (2012).
39. Sansom, D. M. *CD28, CTLA-4 and their ligands: who does what and to whom?*
40. Chen, L. & Flies, D. B. Molecular mechanisms of T cell co-stimulation and co-inhibition. *Nat Rev Immunol* **13**, 227–242 (2013).
41. Bell, R. B., Fox, B. A. & Oncology, N. Cytotoxic T Lymphocyte Antigen 4 Learn more about Cytotoxic T Lymphocyte Antigen Second Signals for Lymphocyte Activa- tion. (2018).
42. Buchbinder, E. I. & Desai, A. CTLA-4 and PD-1 Pathways Similarities, Differences, and Implications of Their Inhibition. (2015). doi:10.1097/COC.0000000000000239
43. Hodi, F. S. *et al.* Improved Survival with Ipilimumab in Patients with Metastatic Melanoma. *N. Engl. J. Med.* **363**, 711–723 (2010).
44. Pardoll, D. M. The blockade of immune checkpoints in cancer immunotherapy. *Nat. Rev. Cancer* **12**, 252–264 (2012).
45. Herbst, R. S. *et al.* Predictive correlates of response to the anti-PD-L1 antibody MPDL3280A in cancer patients HHS Public Access. *Nature* **515**, 563–567 (2014).
46. Riley, J. L. PD-1 signaling in primary T cells. doi:10.1111/j.1600-065X.2009.00767.x
47. Rotte, A. Combination of CTLA-4 and PD-1 blockers for treatment of cancer. *J. Exp. Clin. Cancer Res.* **38**, 1–12 (2019).
48. Middleton, M. R. *et al.* Randomized Phase III Study of Temozolomide Versus Dacarbazine in the Treatment of Patients With Advanced Metastatic Malignant Melanoma. *J. Clin. Oncol.* **18**, 158 (2000).
49. Bedikian, A. Y. *et al.* Bcl-2 Antisense (oblimersen sodium) Plus Dacarbazine in Patients

With Advanced Melanoma: The Oblimersen Melanoma Study Group. *J. Clin. Oncol.* **24**, 4738–4745 (2006).
50. Long, G. V. *et al.* Dabrafenib and trametinib versus dabrafenib and placebo for Val600 BRAF-mutant melanoma: A multicentre, double-blind, phase 3 randomised controlled trial. *Lancet* **386**, 444–451 (2015).
51. Robert, C. *et al.* Improved Overall Survival in Melanoma with Combined Dabrafenib and Trametinib. *N. Engl. J. Med.* **372**, 30–39 (2015).
52. Dummer, R. *et al.* Encorafenib plus binimetinib versus vemurafenib or encorafenib in patients with BRAF-mutant melanoma (COLUMBUS): a multicentre, open-label, randomised phase 3 trial. *Lancet. Oncol.* **19**, 603–615 (2018).
53. Gogas, H. J., Kirkwood, J. M. & Sondak, V. K. Chemotherapy for metastatic melanoma. *Cancer* **109**, 455–464 (2007).
54. Robert, C. *et al.* Five-Year Outcomes with Dabrafenib plus Trametinib in Metastatic Melanoma. *N. Engl. J. Med.* **381**, 626–636 (2019).
55. Ascierto, P. A. *et al.* Update on tolerability and overall survival in COLUMBUS: landmark analysis of a randomised phase 3 trial of encorafenib plus binimetinib vs vemurafenib or encorafenib in patients with BRAF V600–mutant melanoma. *Eur. J. Cancer* **126**, 33–44 (2020).
56. Larkin, J. *et al.* Five-Year Survival with Combined Nivolumab and Ipilimumab in Advanced Melanoma. *N. Engl. J. Med.* **381**, 1535–1546 (2019).
57. Ugurel, S. *et al.* Survival of patients with advanced metastatic melanoma: The impact of MAP kinase pathway inhibition and immune checkpoint inhibition - Update 2019. *Eur. J. Cancer* **130**, 126–138 (2020).
58. Ugurel, S. *et al.* Survival of patients with advanced metastatic melanoma: the impact of novel therapies–update 2017. *Eur. J. Cancer* **83**, 247–257 (2017).
59. Ascierto, P. A. *et al.* LBA45 First report of efficacy and safety from the phase II study SECOMBIT (SEquential COMBo Immuno and Targeted therapy study). *Ann. Oncol.* **31**, S1173–S1174 (2020).
60. ClinicalTrials.gov. Immunotherapy With Ipilimumab and Nivolumab Preceded or Not by a Targeted Therapy With Encorafenib and Binimetinib (EBIN). Available at: https://clinicaltrials.gov/ct2/show/NCT03235245. (Accessed: 20th June 2021)
61. ClinicalTrials.gov. Dabrafenib and Trametinib Followed by Ipilimumab and Nivolumab or Ipilimumab and Nivolumab Followed by Dabrafenib and Trametinib in Treating Patients With Stage III-IV BRAFV600 Melanoma. Available at: https://www.clinicaltrials.gov/ct2/show/NCT02224781. (Accessed: 20th May 2021)
62. Balch, C. M. *et al.* Final version of 2009 AJCC melanoma staging and classification. *J. Clin. Oncol.* **27**, 6199–6206 (2009).
63. Schadendorf, D. *et al.* Three-year pooled analysis of factors associated with clinical outcomes across dabrafenib and trametinib combination therapy phase 3 randomised trials. *Eur. J. Cancer* **82**, 45–55 (2017).
64. Weide, B. *et al.* Baseline Biomarkers for Outcome of Melanoma Patients Treated with Pembrolizumab. *Clin. Cancer Res.* **22**, 5487–5496 (2016).
65. Robert, C. *et al.* Nivolumab in Previously Untreated Melanoma without BRAF Mutation. *N. Engl. J. Med.* **372**, 320–330 (2015).
66. Robert, C. *et al.* Pembrolizumab versus Ipilimumab in Advanced Melanoma. *N. Engl. J. Med.* **26**, 2521–2553 (2015).
67. Larkin, J. *et al.* Combined Nivolumab and Ipilimumab or Monotherapy in Untreated Melanoma. *N. Engl. J. Med.* **373**, 23–34 (2015).
68. Hodi, F. S. *et al.* Nivolumab plus ipilimumab or nivolumab alone versus ipilimumab alone in advanced melanoma (CheckMate 067): 4-year outcomes of a multicentre, randomised, phase 3 trial. *Lancet. Oncol.* **19**, 1480–1492 (2018).
69. Wolchok, J. D. *et al.* CheckMate 067: 6.5-year outcomes in patients (pts) with advanced melanoma. *J. Clin. Oncol.* **39**, 9506 (2021).
70. Czarnecka, A. M., Bartnik, E., Fiedorowicz, M. & Rutkowski, P. Targeted therapy in melanoma and mechanisms of resistance. *Int. J. Mol. Sci.* **21**, 1–21 (2020).

71. Leonardi, G. C., Candido, S., Falzone, L., Spandidos, D. A. & Libra, M. Cutaneous melanoma and the immunotherapy revolution (Review). *Int. J. Oncol.* **57**, 609–618 (2020).
72. M Eggermont, A. M. *et al.* Adjuvant ipilimumab versus placebo after complete resection of high-risk stage III melanoma (EORTC 18071): a randomised, double-blind, phase 3 trial. *Lancet Oncol* **16**, 522–552 (2015).
73. Weber et al. Adjuvant Nivolumab versus Ipilumimab in resected stage 3 or 4 melanoma. *NEJM* (2017). doi:10.1056/NEJMoa1709030
74. Eggermont, A. M. M. *et al.* Adjuvant Pembrolizumab versus Placebo in Resected Stage III Melanoma. *N. Engl. J. Med.* **378**, 1789–1801 (2018).
75. Ascierto, P. A. *et al.* Adjuvant nivolumab versus ipilimumab in resected stage IIIB-C and stage IV melanoma (CheckMate 238): 4-year results from a multicentre, double-blind, randomised, controlled, phase 3 trial. *Lancet. Oncol.* **21**, 1465–1477 (2020).
76. Sullivan, R. J. Adjuvant nivolumab plus ipilimumab for resected stage IV melanoma. *Lancet* **395**, 1524–1525 (2020).
77. Masood, S. Neoadjuvant chemotherapy in breast cancers. *Women's Heal.* **12**, 480–491 (2016).
78. Versluis, J. M., Thommen, D. S. & Blank, C. U. Rationalizing the pathway to personalized neoadjuvant immunotherapy: The Lombard Street Approach. *J. Immunother. Cancer* **8**, 1–8 (2020).
79. Blank, C. U. *et al.* Neoadjuvant versus adjuvant ipilimumab plus nivolumab in macroscopic stage III melanoma. *Nat. Med.* 1 (2018). doi:10.1038/s41591-018-0198-0
80. Amaria, R. N. *et al.* Neoadjuvant immune checkpoint blockade in high-risk resectable melanoma. *Nat. Med.* 1 (2018). doi:10.1038/s41591-018-0197-1
81. Blank, C. U. *et al.* 3-year relapse-free survival (RFS), overall survival (OS) and long-term toxicity of (neo)adjuvant ipilimumab (IPI) + nivolumab (NIVO) in macroscopic stage III melanoma (OpACIN trial). *Ann. Oncol.* **30**, v535 (2019).
82. Rozeman, E. A. *et al.* Identification of the optimal combination dosing schedule of neoadjuvant ipilimumab plus nivolumab in macroscopic stage III melanoma (OpACIN-neo): a multicentre, phase 2, randomised, controlled trial. *Lancet Oncol.* **20**, 948–960 (2019).
83. Pons-Tostivint, E. *et al.* Comparative Analysis of Durable Responses on Immune Checkpoint Inhibitors Versus Other Systemic Therapies: A Pooled Analysis of Phase III Trials. *JCO Precis. Oncol.* 1–10 (2019). doi:10.1200/po.18.00114
84. Redman, J. M., Gibney, G. T. & Atkins, M. B. Advances in immunotherapy for melanoma. *BMC Med.* **14**, 1–11 (2016).
85. Davis, A. A. & Patel, V. G. The role of PD-L1 expression as a predictive biomarker: An analysis of all US food and drug administration (FDA) approvals of immune checkpoint inhibitors. *J. Immunother. Cancer* **7**, 1–8 (2019).
86. Mahoney, K. M. & Atkins, M. B. Prognostic and predictive markers for the new immunotherapies. *Oncology (Williston Park).* **28**, 39–48 (2014).
87. Borghaei, H. *et al.* Nivolumab versus Docetaxel in Advanced Nonsquamous Non-Small-Cell Lung Cancer. *N. Engl. J. Med.* **373**, 1627–1639 (2015).
88. Garon, E. B. *et al.* Pembrolizumab for the treatment of non-small-cell lung cancer. *N. Engl. J. Med.* **372**, 2018–2028 (2015).
89. Mansfield, A. S. *et al.* Heterogeneity of Programmed Cell Death Ligand 1 Expression in Multifocal Lung Cancer. *Clin. Cancer Res.* **22**, 2177–2182 (2016).
90. Gibney, G. T., Weiner, L. M. & Atkins, M. B. Predictive biomarkers for checkpoint inhibitor-based immunotherapy. *Lancet. Oncol.* **17**, e542–e551 (2016).
91. Patel, S. P. & Kurzrock, R. PD-L1 Expression as a Predictive Biomarker in Cancer Immunotherapy. *Mol. Cancer Ther.* **14**, 847–856 (2015).
92. Johnson, D. B. *et al.* Melanoma-specific MHC-II expression represents a tumour-autonomous phenotype and predicts response to anti-PD-1/PD-L1 therapy. *Nat. Commun.* **7**, (2016).
93. Ribas, A. *et al.* Association of response to programmed death receptor 1 (PD-1)

blockade with pembrolizumab (MK-3475) with an interferon-inflammatory immune gene signature. *J. Clin. Oncol.* **33**, 3001 (2015).
94. Papadopoulos, K. P. *et al.* Phase I Study of MK-4166, an Anti-human Glucocorticoid-Induced TNF Receptor Antibody, Alone or with Pembrolizumab in Advanced Solid Tumors. *Clin. Cancer Res.* **27**, 1904 LP – 1911 (2021).
95. Chen, D. S. & Mellman, I. Elements of cancer immunity and the cancer-immune set point. *Nature* **541**, 321–330 (2017).
96. Hamid, O. *et al.* A prospective phase II trial exploring the association between tumor microenvironment biomarkers and clinical activity of ipilimumab in advanced melanoma. *J. Transl. Med.* **9**, 204 (2011).
97. Snyder, A. *et al.* Genetic basis for clinical response to CTLA-4 blockade in melanoma. *N. Engl. J. Med.* **371**, 2189–2199 (2014).
98. Goodman, A. M. *et al.* Tumor Mutational Burden as an Independent Predictor of Response to Immunotherapy in Diverse Cancers. *Mol. Cancer Ther.* **16**, 2598–2608 (2017).
99. Samstein, R. M. *et al.* Tumor mutational load predicts survival after immunotherapy across multiple cancer types. *Nat. Genet.* **51**, 202–206 (2019).
100. Chalmers, Z. R. *et al.* Analysis of 100,000 human cancer genomes reveals the landscape of tumor mutational burden. *Genome Med.* **9**, 1–14 (2017).
101. Addeo, A., Friedlaender, A., Banna, G. L. & Weiss, G. J. TMB or not TMB as a biomarker: That is the question. *Crit. Rev. Oncol. Hematol.* **163**, 103374 (2021).
102. Wu, Y. *et al.* The Predictive Value of Tumor Mutation Burden on Efficacy of Immune Checkpoint Inhibitors in Cancers: A Systematic Review and Meta-Analysis. *Frontiers in oncology* **9**, 1161 (2019).
103. Testori, A. A. E., Chiellino, S. & van Akkooi, A. C. J. Adjuvant Therapy for Melanoma: Past, Current, and Future Developments. *Cancers (Basel).* **12**, (2020).
104. Eggermont, A. M. M. *et al.* Adjuvant pembrolizumab versus placebo in resected stage III melanoma (EORTC 1325-MG/KEYNOTE-054): distant metastasis-free survival results from a double-blind, randomised, controlled, phase 3 trial. *Lancet Oncol.* **22**, 643–654 (2021).
105. Postow, M. A. Managing immune checkpoint-blocking antibody side effects. *Am. Soc. Clin. Oncol. Educ. book. Am. Soc. Clin. Oncol. Annu. Meet.* 76–83 (2015). doi:10.14694/EdBook_AM.2015.35.76
106. Topalian, S. L. *et al.* Survival, durable tumor remission, and long-term safety in patients with advanced melanoma receiving nivolumab. *J. Clin. Oncol. Off. J. Am. Soc. Clin. Oncol.* **32**, 1020–1030 (2014).
107. Hommes, J. W., Verheijden, R. J., Suijkerbuijk, K. P. M. & Hamann, D. Biomarkers of Checkpoint Inhibitor Induced Immune-Related Adverse Events—A Comprehensive Review. *Front. Oncol.* **10**, 1–16 (2021).
108. Martins, F. *et al.* Adverse effects of immune-checkpoint inhibitors: epidemiology, management and surveillance. *Nat. Rev. Clin. Oncol.* **16**, 563–580 (2019).
109. Haanen, J. B. A. G. *et al.* Management of toxicities from immunotherapy: ESMO Clinical Practice Guidelines for diagnosis, treatment and follow-up. *Ann. Oncol.* **28**, iv119–iv142 (2017).
110. Khoja, L., Day, D., Wei-Wu Chen, T., Siu, L. L. & Hansen, A. R. Tumour- and class-specific patterns of immune-related adverse events of immune checkpoint inhibitors: a systematic review. *Ann. Oncol. Off. J. Eur. Soc. Med. Oncol.* **28**, 2377–2385 (2017).
111. Abdel-Rahman, O., ElHalawani, H. & Fouad, M. Risk of endocrine complications in cancer patients treated with immune check point inhibitors: a meta-analysis. *Future Oncol.* **12**, 413–425 (2016).
112. Naidoo, J. *et al.* Pneumonitis in Patients Treated With Anti-Programmed Death-1/Programmed Death Ligand 1 Therapy. *J. Clin. Oncol. Off. J. Am. Soc. Clin. Oncol.* **35**, 709–717 (2017).
113. Morganstein, D. L. *et al.* Thyroid abnormalities following the use of cytotoxic T-lymphocyte antigen-4 and programmed death receptor protein-1 inhibitors in the

treatment of melanoma. *Clin. Endocrinol. (Oxf).* **86**, 614–620 (2017).
114. Osorio, J. C. *et al.* Antibody-mediated thyroid dysfunction during T-cell checkpoint blockade in patients with non-small-cell lung cancer. *Ann. Oncol. Off. J. Eur. Soc. Med. Oncol.* **28**, 583–589 (2017).
115. Iwama, S. *et al.* Pituitary expression of CTLA-4 mediates hypophysitis secondary to administration of CTLA-4 blocking antibody. *Sci. Transl. Med.* **6**, 230ra45 (2014).
116. Caturegli, P. *et al.* Hypophysitis Secondary to Cytotoxic T-Lymphocyte-Associated Protein 4 Blockade: Insights into Pathogenesis from an Autopsy Series. *Am. J. Pathol.* **186**, 3225–3235 (2016).
117. Francisco, L. M., Sage, P. T. & Sharpe, A. H. The PD-1 pathway in tolerance and autoimmunity. *Immunol. Rev.* **236**, 219–242 (2010).
118. Tarhini, A. A. *et al.* Baseline circulating IL-17 predicts toxicity while TGF-β1 and IL-10 are prognostic of relapse in ipilimumab neoadjuvant therapy of melanoma. *J. Immunother. cancer* **3**, 39 (2015).
119. Johnson, D. *et al.* IL17A Blockade Successfully Treated Psoriasiform Dermatologic Toxicity from Immunotherapy. *Cancer Immunol. Res.* **7**, 860–865 (2019).
120. Postow, M. A., Sidlow, R. & Hellmann, M. D. Immune-Related Adverse Events Associated with Immune Checkpoint Blockade. *N. Engl. J. Med.* **378**, 158–168 (2018).
121. Horvat, T. Z. *et al.* Immune-Related Adverse Events, Need for Systemic Immunosuppression, and Effects on Survival and Time to Treatment Failure in Patients With Melanoma Treated With Ipilimumab at Memorial Sloan Kettering Cancer Center. *J. Clin. Oncol. Off. J. Am. Soc. Clin. Oncol.* **33**, 3193–3198 (2015).
122. Weber, J. S. *et al.* Safety Profile of Nivolumab Monotherapy: A Pooled Analysis of Patients With Advanced Melanoma. *J. Clin. Oncol. Off. J. Am. Soc. Clin. Oncol.* **35**, 785–792 (2017).
123. Esfahani, K. & Miller, W. H. J. Reversal of Autoimmune Toxicity and Loss of Tumor Response by Interleukin-17 Blockade. *The New England journal of medicine* **376**, 1989–1991 (2017).
124. Sato, K. *et al.* Correlation between immune-related adverse events and efficacy in non-small cell lung cancer treated with nivolumab. *Lung Cancer* **115**, 71–74 (2018).
125. Elias, R. *et al.* Immune-related adverse events are associated with improved outcomes in ICI-treated renal cell carcinoma patients. *J. Clin. Oncol.* **37**, 645 (2019).
126. Riudavets, M. *et al.* Correlation between immune-related adverse events (irAEs) and efficacy in patients with solid tumors treated with immune-checkpoints inhibitors (ICIs). *J. Clin. Oncol.* **36**, 3064 (2018).
127. Rogado, J. *et al.* Immune-related adverse events predict the therapeutic efficacy of anti-PD-1 antibodies in cancer patients. *Eur. J. Cancer* **109**, 21–27 (2019).
128. Okada, N. *et al.* Association Between Immune-Related Adverse Events and Clinical Efficacy in Patients with Melanoma Treated With Nivolumab: A Multicenter Retrospective Study. *Clin. Ther.* **41**, 59–67 (2019).
129. Robert, C. *et al.* Long-term safety of pembrolizumab monotherapy and relationship with clinical outcome: A landmark analysis in patients with advanced melanoma. *Eur. J. Cancer* **144**, 182–191 (2021).
130. Hua, C. *et al.* Association of Vitiligo With Tumor Response in Patients With Metastatic Melanoma Treated With Pembrolizumab. *JAMA dermatology* **152**, 45–51 (2016).
131. Teulings, H.-E. *et al.* Vitiligo-like depigmentation in patients with stage III-IV melanoma receiving immunotherapy and its association with survival: a systematic review and meta-analysis. *J. Clin. Oncol. Off. J. Am. Soc. Clin. Oncol.* **33**, 773–781 (2015).
132. Das, S. & Johnson, D. B. Immune-related adverse events and anti-tumor efficacy of immune checkpoint inhibitors. *J. Immunother. Cancer* **7**, 1–11 (2019).
133. Jia, X. H. *et al.* The biomarkers related to immune related adverse events caused by immune checkpoint inhibitors. *J. Exp. Clin. Cancer Res.* **39**, 1–17 (2020).
134. Abolhassani, A. R., Schuler, G., Kirchberger, M. C. & Heinzerling, L. C-reactive protein as an early marker of immune-related adverse events. *J. Cancer Res. Clin. Oncol.* **145**, 2625–2631 (2019).

135. Valpione, S. *et al.* Sex and interleukin-6 are prognostic factors for autoimmune toxicity following treatment with anti-CTLA4 blockade. *J. Transl. Med.* **16**, 94 (2018).
136. Fujisawa, Y. *et al.* Fluctuations in routine blood count might signal severe immune-related adverse events in melanoma patients treated with nivolumab. *J. Dermatol. Sci.* **88**, 225–231 (2017).
137. Diehl, A., Yarchoan, M., Hopkins, A., Jaffee, E. & Grossman, S. A. Relationships between lymphocyte counts and treatmentrelated toxicities and clinical responses in patients with solid tumors treated with PD-1 checkpoint inhibitors. *Oncotarget* **8**, 114268–114280 (2017).
138. Khan, S. *et al.* Immune dysregulation in cancer patients developing immune-related adverse events. *Br. J. Cancer* **120**, 63–68 (2019).
139. Lim, S. Y. *et al.* Circulating cytokines predict immune-related toxicity in melanoma patients receiving anti-PD-1–based immunotherapy. *Clin. Cancer Res.* **25**, 1557–1563 (2019).
140. Bomze, D., Hasan Ali, O., Bate, A. & Flatz, L. Association Between Immune-Related Adverse Events During Anti–PD-1 Therapy and Tumor Mutational Burden. *JAMA Oncol.* **5**, 1633–1635 (2019).
141. Pistillo, M. P. *et al.* Soluble CTLA-4 as a favorable predictive biomarker in metastatic melanoma patients treated with ipilimumab: an Italian melanoma intergroup study. *Cancer Immunol. Immunother.* **68**, 97–107 (2019).
142. Chaput, N. *et al.* Baseline gut microbiota predicts clinical response and colitis in metastatic melanoma patients treated with ipilimumab. *Ann. Oncol.* **28**, 1368–1379 (2017).
143. Shahabi, V. *et al.* Gene expression profiling of whole blood in ipilimumab-treated patients for identification of potential biomarkers of immune-related gastrointestinal adverse events. *J. Transl. Med.* **11**, 75 (2013).
144. Friedlander, P. *et al.* A whole-blood RNA transcript-based gene signature is associated with the development of CTLA-4 blockade-related diarrhea in patients with advanced melanoma treated with the checkpoint inhibitor tremelimumab. *J. Immunother. Cancer* **6**, 90 (2018).
145. Hasan Ali, O. *et al.* Human leukocyte antigen variation is associated with adverse events of checkpoint inhibitors. *Eur. J. Cancer* **107**, 8–14 (2019).
146. Tahir, S. A. *et al.* Autoimmune antibodies correlate with immune checkpoint therapy-induced toxicities. *Proc. Natl. Acad. Sci.* **116**, 22246 LP – 22251 (2019).
147. Toi, Y. *et al.* Profiling Preexisting Antibodies in Patients Treated With Anti–PD-1 Therapy for Advanced Non–Small Cell Lung Cancer. *JAMA Oncol.* **5**, 376–383 (2019).
148. Weinstein, D., Leininger, J., Hamby, C. & Safai, B. Diagnostic and prognostic biomarkers in melanoma. *J. Clin. Aesthet. Dermatol.* **7**, 13–24 (2014).
149. Petrelli, F. *et al.* Prognostic and predictive role of elevated lactate dehydrogenase in patients with melanoma treated with immunotherapy and BRAF inhibitors: a systematic review and meta-analysis. *Melanoma Res.* **29**, 1–12 (2019).
150. Petrelli, F. *et al.* Prognostic role of lactate dehydrogenase in solid tumors: A systematic review and meta-analysis of 76 studies. *Acta Oncol. (Madr).* **54**, 961–970 (2015).
151. Gogas, H. *et al.* Biomarkers in melanoma. *Ann. Oncol. Off. J. Eur. Soc. Med. Oncol.* **20 Suppl 6**, vi8–vi13 (2009).
152. Ascierto, P. A. *et al.* Prognostic value of serum VEGF in melanoma patients: A pilot study. *Anticancer Res.* **24**, 4255–4258 (2004).
153. Robert, C. *et al.* Five-year outcomes with nivolumab in patients with wild-type BRAF advanced melanoma. *J. Clin. Oncol.* **38**, 3937–3946 (2020).
154. Van Wilpe, S. *et al.* Lactate dehydrogenase: a marker of diminished antitumor immunity. *Oncoimmunology* **9**, 1–11 (2020).
155. Kelderman, S. *et al.* Lactate dehydrogenase as a selection criterion for ipilimumab treatment in metastatic melanoma. *Cancer Immunol. Immunother.* **63**, 449–458 (2014).
156. Simeone, E. *et al.* Immunological and biological changes during ipilimumab treatment and their potential correlation with clinical response and survival in patients with

advanced melanoma. *Cancer Immunol Immunother* **3**, 675–683 (2014).
157. Diem, S. *et al.* Serum lactate dehydrogenase as an early marker for outcome in patients treated with anti-PD-1 therapy in metastatic melanoma. (2016). doi:10.1038/bjc.2015.467
158. Felix, J. *et al.* Relevance of serum biomarkers associated with melanoma during follow-up of anti-CTLA-4 immunotherapy. *Int. Immunopharmacol.* **40**, 466–473 (2016).
159. Damuzzo, V. *et al.* Clinical implication of tumor-associated and immunological parameters in melanoma patients treated with ipilimumab. *Oncoimmunology* **5**, e1249559 (2016).
160. Gambichler, T. *et al.* Baseline laboratory parameters predicting clinical outcome in melanoma patients treated with ipilimumab: a single-centre analysis. *J. Eur. Acad. Dermatol. Venereol.* **32**, 972–977 (2018).
161. Wagner, N. B., Forschner, A., Leiter, U., Garbe, C. & Eigentler, T. K. S100B and LDH as early prognostic markers for response and overall survival in melanoma patients treated with anti-PD-1 or combined anti-PD-1 plus anti-CTLA-4 antibodies. *Br. J. Cancer* **119**, 339–346 (2018).
162. Yuan, J. *et al.* Pretreatment serum VEGF is associated with clinical response and overall survival in advanced melanoma patients treated with ipilimumab. *Cancer Immunol. Res.* **2**, 127–132 (2014).
163. Itatani, Y., Kawada, K., Yamamoto, T. & Sakai, Y. Resistance to Anti-Angiogenic Therapy in Cancer-Alterations to Anti-VEGF Pathway. *Int. J. Mol. Sci.* **19**, 1232 (2018).
164. Wu, X. *et al.* Angiopoietin-2 as a Biomarker and Target for Immune Checkpoint Therapy. *Cancer Immunol. Res.* **5**, 17–28 (2017).
165. Phan, G. Q., Attia, P., Steinberg, S. M., White, D. E. & Rosenberg, S. A. Factors associated with response to high-dose interleukin-2 in patients with metastatic melanoma. *J. Clin. Oncol.* **19**, 3477–3482 (2001).
166. Berman, D. M. *et al.* Association of peripheral blood absolute lymphocyte count (ALC) and clinical activity in patients (pts) with advanced melanoma treated with ipilimumab. *J. Clin. Oncol.* **27**, 3020 (2009).
167. Ku, G. Y. *et al.* Single-Institution Experience With Ipilimumab in Advanced Melanoma Patients in the Compassionate Use Setting Lymphocyte Count After 2 Doses Correlates With Survival. doi:10.1002/cncr.24951
168. Delyon, J. *et al.* Experience in daily practice with ipilimumab for the treatment of patients with metastatic melanoma: an early increase in lymphocyte and eosinophil counts is associated with improved survival. *Ann. Oncol.* **24**, 1697–1703 (2013).
169. Postow, M. A. *et al.* Pharmacodynamic effect of ipilimumab on absolute lymphocyte count (ALC) and association with overall survival in patients with advanced melanoma. *J. Clin. Oncol.* **31**, 9052–9052 (2013).
170. Di Giacomo, A. M. *et al.* Long-term survival and immunological parameters in metastatic melanoma patients who responded to ipilimumab 10 mg/kg within an expanded access programme. *Cancer Immunol. Immunother.* **62**, 1021–1028 (2013).
171. Ferrucci, P. F. *et al.* Baseline neutrophils and derived neutrophilto-lymphocyte ratio: Prognostic relevance in metastatic melanoma patients receiving ipilimumab. *Ann. Oncol.* **27**, 732–738 (2016).
172. Kitano, S. *et al.* Computational algorithm-driven evaluation of monocytic myeloid-derived suppressor cell frequency for prediction of clinical outcomes. *Cancer Immunol. Res.* **2**, 812–821 (2014).
173. Meyer, C. *et al.* Frequencies of circulating MDSC correlate with clinical outcome of melanoma patients treated with ipilimumab. *Cancer Immunol. Immunother.* **63**, 247–257 (2014).
174. Martens, A. *et al.* Baseline Peripheral Blood Biomarkers Associated with Clinical Outcome of Advanced Melanoma Patients Treated with Ipilimumab. *Clin. cancer Res. an Off. J. Am. Assoc. Cancer Res.* **22**, 2908–2918 (2016).
175. Mitchell, P. S. *et al.* Circulating microRNAs as stable blood-based markers for cancer detection. *Proc. Natl. Acad. Sci. U. S. A.* **105**, 10513–10518 (2008).

176. Rajakumar, T. *et al.* A blood-based miRNA signature predicts immunotherapy efficacy in advanced stage non-small cell lung cancer. *medRxiv* 2021.10.31.21265722 (2021). doi:10.1101/2021.10.31.21265722
177. Incorvaia, L. *et al.* A 'Lymphocyte MicroRNA Signature' as Predictive Biomarker of Immunotherapy Response and Plasma PD-1/PD-L1 Expression Levels in Patients with Metastatic Renal Cell Carcinoma: Pointing towards Epigenetic Reprogramming. *Cancers (Basel).* **12**, 3396 (2020).
178. Wang, Z., Han, J., Cui, Y., Fan, K. & Zhou, X. Circulating microRNA-21 as noninvasive predictive biomarker for response in cancer immunotherapy. *Med. Hypotheses* **81**, 41–43 (2013).
179. Huber, V. *et al.* Tumor-derived microRNAs induce myeloid suppressor cells and predict immunotherapy resistance in melanoma. *J. Clin. Invest.* **128**, 5505–5516 (2018).
180. Sunshine, J. C. *et al.* PD-L1 Expression in Melanoma: A Quantitative Immunohistochemical Antibody Comparison. *Clin. Cancer Res.* **23**, 4938–4944 (2017).
181. Vilain, R. E. *et al.* Dynamic Changes in PD-L1 Expression and Immune Infiltrates Early During Treatment Predict Response to PD-1 Blockade in Melanoma. *Clin. Cancer Res.* **23**, 5024 LP – 5033 (2017).
182. Kitano, S., Nakayama, T. & Yamashita, M. Biomarkers for Immune Checkpoint Inhibitors in Melanoma. *Front. Oncol.* **8**, 270 (2018).
183. Chen, G. *et al.* Exosomal PD-L1 contributes to immunosuppression and is associated with anti-PD-1 response. *Nature* **560**, 382–386 (2018).
184. Del Re, M. *et al.* PD-L1 mRNA expression in plasma-derived exosomes is associated with response to anti-PD-1 antibodies in melanoma and NSCLC. *Br. J. Cancer* **118**, 820–824 (2018).
185. Hong, X. *et al.* Molecular signatures of circulating melanoma cells for monitoring early response to immune checkpoint therapy. *Proc. Natl. Acad. Sci. U. S. A.* **115**, 2467–2472 (2018).
186. Lin, S. Y. *et al.* Prospective molecular profiling of circulating tumor cells from patients with melanoma receiving combinatorial immunotherapy. *Clin. Chem.* **66**, 169–177 (2020).
187. Kilgour, E., Rothwell, D. G., Brady, G. & Dive, C. Liquid Biopsy-Based Biomarkers of Treatment Response and Resistance. *Cancer Cell* **37**, 485–495 (2020).
188. Schwarzenbach, H., B Hoon, D. S. & Pantel, K. Cell-free nucleic acids as biomarkers in cancer patients. *Nat. Publ. Gr.* **11**, (2011).
189. Valpione, S. *et al.* Plasma total cell-free DNA (cfDNA) is a surrogate biomarker for tumour burden and a prognostic biomarker for survival in metastatic melanoma patients. (2018). doi:10.1016/j.ejca.2017.10.029
190. Bronkhorst, A. J., Ungerer, V. & Holdenrieder, S. The emerging role of cell-free DNA as a molecular marker for cancer management. *Biomol. Detect. Quantif.* **17**, 100087 (2019).
191. Ossandon, M. R. *et al.* Circulating Tumor DNA Assays in Clinical Cancer Research. *J. Natl. Cancer Inst.* **110**, 929–934 (2018).
192. Calapre, L., Warburton, L., Millward, M., Ziman, M. & Gray, E. S. Circulating tumour DNA (ctDNA) as a liquid biopsy for melanoma. *Cancer Lett.* **404**, 62–69 (2017).
193. Seremet, T. *et al.* Illustrative cases for monitoring by quantitative analysis of BRAF/NRAS ctDNA mutations in liquid biopsies of metastatic melanoma patients who gained clinical benefits from anti-PD1 antibody therapy. *Melanoma Res.* **28**, 65–70 (2018).
194. Johnson, D. B. *et al.* Impact of NRAS mutations for patients with advanced melanoma treated with immune therapies. *Cancer Immunol. Res.* **3**, 288–295 (2015).
195. Forschner, A. *et al.* Tumor mutation burden and circulating tumor DNA in combined CTLA-4 and PD-1 antibody therapy in metastatic melanoma – results of a prospective biomarker study. *J. Immunother. Cancer* **7**, 180 (2019).
196. Seremet, T. *et al.* Undetectable circulating tumor DNA (ctDNA) levels correlate with favorable outcome in metastatic melanoma patients treated with anti-PD1 therapy. *J.*

Transl. Med. **17**, (2019).
197. Lipson, E. J. *et al.* Circulating tumor DNA analysis as a real-time method for monitoring tumor burden in melanoma patients undergoing treatment with immune checkpoint blockade. *J. Immunother. Cancer* **2**, 42 (2014).
198. Lee, J. H. *et al.* Circulating tumour DNA predicts response to anti-PD1 antibodies in metastatic melanoma. *Ann. Oncol. Off. J. Eur. Soc. Med. Oncol.* **28**, 1130–1136 (2017).
199. Bratman, S. V *et al.* Personalized circulating tumor DNA analysis as a predictive biomarker in solid tumor patients treated with pembrolizumab. 1–9 (2020). doi:10.1038/s43018-020-0096-5
200. Ashida, A., Sakaizawa, K., Uhara, H. & Okuyama, R. Circulating tumour DNA for monitoring treatment response to anti-PD-1 immunotherapy in melanoma patients. *Acta Derm. Venereol.* **97**, 1212–1218 (2017).
201. Gremel, G. *et al.* Distinct subclonal tumour responses to therapy revealed by circulating cell-free DNA. *Ann. Oncol.* **27**, 1959–1965 (2016).
202. Marsavela, G. *et al.* Circulating tumor DNA predicts outcome from first-, but not second-line treatment and identifies melanoma patients who may benefit from combination immunotherapy. *Clin. Cancer Res.* **26**, 5926–5933 (2020).
203. Lee, R. J. *et al.* Circulating tumor DNA predicts survival in patients with resected high-risk stage II/III melanoma. *Ann. Oncol.* **29**, 490–496 (2018).
204. Tan, L. *et al.* Prediction and monitoring of relapse in stage III melanoma using circulating tumor DNA. doi:10.1093/annonc/mdz048
205. Garcia-Murillas, I. *et al.* Mutation tracking in circulating tumor DNA predicts relapse in early breast cancer. *Sci. Transl. Med.* **7**, 302ra133 (2015).
206. Chen, Y.-H. *et al.* Next-generation sequencing of circulating tumor DNA to predict recurrence in triple-negative breast cancer patients with residual disease after neoadjuvant chemotherapy. *npj Breast Cancer* **3**, 24 (2017).
207. Tie, J. *et al.* Circulating tumor DNA analysis detects minimal residual disease and predicts recurrence in patients with stage II colon cancer. *Sci. Transl. Med.* **8**, 346ra92 LP-346ra92 (2016).
208. Gray, E. S. *et al.* Circulating tumor DNA to monitor treatment response and detect acquired resistance in patients with metastatic melanoma. *Oncotarget* **6**, 42008–42018 (2015).
209. Schreuer, M. *et al.* Quantitative assessment of BRAF V600 mutant circulating cell-free tumor DNA as a tool for therapeutic monitoring in metastatic melanoma patients treated with BRAF/MEK inhibitors. *J. Transl. Med.* **14**, 95 (2016).
210. Nixon, A. B. *et al.* Peripheral immune-based biomarkers in cancer immunotherapy: can we realize their predictive potential? *Journal for ImmunoTherapy of Cancer* **7**, 325 (2019).
211. Wistuba-Hamprecht, K. *et al.* Peripheral CD8 effector-memory type 1 T-cells correlate with outcome in ipilimumab-treated stage IV melanoma patients. *Eur. J. Cancer* **73**, 61–70 (2017).
212. Tietze, J. K. *et al.* The proportion of circulating CD45RO+CD8+ memory T cells is correlated with clinical response in melanoma patients treated with ipilimumab. *Eur. J. Cancer* **75**, 268–279 (2017).
213. Huang, A. *et al.* T-cell invigoration to tumour burden ratio associated with anti-PD-1 response. *Nat. Publ. Gr.* **545**, (2017).
214. Jacquelot, N. *et al.* Predictors of responses to immune checkpoint blockade in advanced melanoma. *Nat. Commun.* **8**, 592 (2017).
215. Takeuchi, Y. *et al.* Clinical response to PD-1 blockade correlates with a sub-fraction of peripheral central memory CD4+ T cells in patients with malignant melanoma. *Int. Immunol.* **30**, 13–22 (2018).
216. Krieg C, Nowicka M, Guglietta S, et al. High-dimensional single-cell analysis predicts response to anti-PD-1 immunotherapy. *Nat. Med.* **24**, 144–153 (2018).
217. Martens, A. *et al.* Increases in absolute lymphocytes and circulating CD4+ and CD8+ T cells are associated with positive clinical outcome of melanoma patients treated with

ipilimumab. *Clin. Cancer Res.* **22**, 4848–4858 (2016).
218. Subrahmanyam, P. B. *et al.* Distinct predictive biomarker candidates for response to anti-CTLA-4 and anti-PD-1 immunotherapy in melanoma patients. *J. Immunother. Cancer* **6**, 1–14 (2018).
219. Robert, L. *et al.* CTLA4 blockade broadens the peripheral T-cell receptor repertoire. *Clin. Cancer Res.* **20**, 2424–2432 (2014).
220. Cha, E. *et al.* Improved survival with T cell clonotype stability after anti-CTLA-4 treatment in cancer patients. *Sci. Transl. Med.* **6**, 238ra70 (2014).
221. Postow, M. A. *et al.* Peripheral T cell receptor diversity is associated with clinical outcomes following ipilimumab treatment in metastatic melanoma. *J. Immunother. Cancer* **3**, 23 (2015).
222. Hogan, S. A. *et al.* Peripheral Blood TCR Repertoire Profiling May Facilitate Patient Stratification for Immunotherapy against Melanoma. (2019). doi:10.1158/2326-6066.CIR-18-0136
223. Hopkins, A. C. *et al.* T cell receptor repertoire features associated with survival in immunotherapy-treated pancreatic ductal adenocarcinoma. *JCI insight* **3**, (2018).
224. Liu, Y.-Y. *et al.* Characteristics and prognostic significance of profiling the peripheral blood T-cell receptor repertoire in patients with advanced lung cancer. *Int. J. Cancer* **145**, 1423–1431 (2019).
225. Akyüz, N. *et al.* T-cell diversification reflects antigen selection in the blood of patients on immune checkpoint inhibition and may be exploited as liquid biopsy biomarker. *Int. J. Cancer* **140**, 2535–2544 (2017).
226. Han, J. *et al.* TCR repertoire diversity of peripheral PD-1þCD8þ T cells predicts clinical outcomes after immunotherapy in patients with non–small cell lung cancer. *Cancer Immunol. Res.* **8**, 146–154 (2020).
227. Snyder, A. *et al.* Contribution of systemic and somatic factors to clinical response and resistance to PD-L1 blockade in urothelial cancer: An exploratory multi-omic analysis. (2017). doi:10.1371/journal.pmed.1002309
228. Tumeh, P. C. *et al.* PD-1 blockade induces responses by inhibiting adaptive immune resistance. (2014). doi:10.1038/nature13954
229. Cheng, H., Zheng, Z. & Cheng, T. New paradigms on hematopoietic stem cell differentiation. *Protein Cell* **11**, 34–44 (2020).
230. Pearse, G. Normal Structure, Function and Histology of the Thymus. *Toxicol. Pathol.* **34**, 504–514 (2006).
231. Pellicci, D. G., Koay, H. F. & Berzins, S. P. Thymic development of unconventional T cells: how NKT cells, MAIT cells and γδ T cells emerge. *Nat. Rev. Immunol.* **20**, 756–770 (2020).
232. Ceredig, R. & Rolink, T. A positive look at double-negative thymocytes. *Nat. Rev. Immunol.* **2**, 888–896 (2002).
233. Bhandoola, A., Sambandam, A., Allman, D., Meraz, A. & Schwarz, B. Early T Lineage Progenitors: New Insights, but Old Questions Remain. *J. Immunol.* **171**, 5653–5658 (2003).
234. Valpione, S. *et al.* Immune awakening revealed by peripheral T cell dynamics after one cycle of immunotherapy. *Nat. Cancer* **1**, 210–221 (2020).
235. Dutta, A. & Venkataganesh, H. New Insights into Epigenetic Regulation of T Cell Differentiation. **31**, 1–18 (2021).
236. Kurd, N. & Robey, E. A. T-cell selection in the thymus: a spatial and temporal perspective. *Immunol. Rev.* **271**, 114–126 (2016).
237. Alberts B, Johnson A, Lewis J, et al. T Cells and MHC Proteins. in *Molecular Biology of the Cell* (Garland Science, 2002).
238. Kasper, I. R., Apostolidis, S. A., Sharabi, A. & Tsokos, G. C. Empowering Regulatory T Cells in Autoimmunity. *Trends Mol. Med.* **22**, 784–797 (2016).
239. Ruddle, N. H. & Akirav, E. M. Secondary lymphoid organs: responding to genetic and environmental cues in ontogeny and the immune response. *J. Immunol.* **183**, 2205–2212 (2009).

240. Prabhakar M, Ershler WB, L. D. Bone marrow, thymus and blood: changes across the lifespan. *Aging health* **5**, 385–393 (2009).
241. Tak W. Mak, M. E. S. and B. D. J. Chapter 8 - The T Cell Receptor: Proteins and Genes. in *Primer to the Immune Response* (eds. Mak, T. W., Saunders, M. E. & Jett, B. D. B. T.-P. to the I. R. (Second E.) 181–196 (Academic Cell, 2014). doi:https://doi.org/10.1016/B978-0-12-385245-8.00008-X
242. Wang, C. Y. *et al.* αβ T-cell receptor bias in disease and therapy (Review). *Int. J. Oncol.* **48**, 2247–2256 (2016).
243. Yannoutsos, N. *et al.* The role of recombination activating gene (RAG) reinduction in thymocyte development in vivo. *J. Exp. Med.* **194**, 471–480 (2001).
244. Nishana, M. & Raghavan, S. C. Role of recombination activating genes in the generation of antigen receptor diversity and beyond. *Immunology* **137**, 271–281 (2012).
245. Bio-rad. Mini-Review: An Overview of T cell Receptors. Available at: https://www.bio-rad-antibodies.com/t-cell-receptor-minireview.html. (Accessed: 29th June 2021)
246. Lescale, C. & Deriano, L. V(D)J Recombination: Orchestrating Diversity without Damage. *Encycl. Cell Biol.* **3**, 550–566 (2016).
247. Sewell, A. K. Why must T cells be cross-reactive? *Nat. Rev. Immunol.* **12**, 669–677 (2012).
248. Hale, J. S. & Fink, P. J. T-cell receptor revision: friend or foe? *Immunology* **129**, 467–473 (2010).
249. Oh-hora, M. & Rao, A. Calcium signaling in lymphocytes. *Curr. Opin. Immunol.* **20**, 250–258 (2008).
250. Zhang, Q. & Vignali, D. A. A. Co-stimulatory and co-inhibitory pathways in autoimmunity. doi:10.1016/j.immuni.2016.04.017
251. Butt, A. Q. & Mills, K. H. G. Immunosuppressive networks and checkpoints controlling antitumor immunity and their blockade in the development of cancer immunotherapeutics and vaccines. *Oncogene* **33**, 4623–4631 (2014).
252. Mahnke, Y. D., Brodie, T. M., Sallusto, F., Roederer, M. & Lugli, E. The who's who of T-cell differentiation: Human memory T-cell subsets. *European Journal of Immunology* **43**, 2797–2809 (2013).
253. Fagnoni, F. F. *et al.* Shortage of circulating naive CD8(+) T cells provides new insights on immunodeficiency in aging. *Blood* **95**, 2860–2868 (2000).
254. Lugli, E. *et al.* Subject classification obtained by cluster analysis and principal component analysis applied to flow cytometric data. *Cytometry. A* **71**, 334–344 (2007).
255. Hamann, D. *et al.* Phenotypic and functional separation of memory and effector human CD8+ T cells. *J. Exp. Med.* **186**, 1407–1418 (1997).
256. Sallusto, F., Lenig, D., Förster, R., Lipp, M. & Lanzavecchia, A. Two subsets of memory T lymphocytes with distinct homing potentials and effector functions. *Nature* **401**, 708–712 (1999).
257. Martin, M. D. & Badovinac, V. P. Defining memory CD8 T cell. *Front. Immunol.* **9**, 1–10 (2018).
258. Zhu, J., Yamane, H. & Paul, W. E. Differentiation of effector CD4 T cell populations. *Annu. Rev. Immunol.* **28**, 445–489 (2010).
259. Kishton, R. J., Sukumar, M. & Restifo, N. P. Metabolic Regulation of T Cell Longevity and Function in Tumor Immunotherapy. *Cell Metab.* **26**, 94–109 (2017).
260. Thapa, D. R. *et al.* Longitudinal analysis of peripheral blood T cell receptor diversity in patients with systemic lupus erythematosus by next-generation sequencing. *Arthritis Res. Ther.* **17**, 1–12 (2015).
261. Spreafico, R. *et al.* A circulating reservoir of pathogenic-like CD4+ T cells shares a genetic and phenotypic signature with the inflamed synovial micro-environment. *Ann. Rheum. Dis.* **75**, 459–465 (2016).
262. McKinnon, K. M. Flow Cytometry: An Overview. *Curr. Protoc. Immunol.* **120**, 5.1.1-5.1.11 (2018).
263. Wong, S. Q. *et al.* Circulating Tumor DNA Analysis and Functional Imaging Provide Complementary Approaches for Comprehensive Disease Monitoring in Metastatic

Melanoma. *JCO Precis. Oncol.* 1–14 (2017). doi:10.1200/PO.16.00009
264. Radziewicz, H., Uelbelhoer, L., Bengsch, B. & Grakoui, A. Memory CD8+ T cell differentiation in viral infection: A cell for all seasons. *World J. Gastroenterol.* **13**, 4848–4857 (2007).
265. Seder, R. A. & Ahmed, R. Similarities and differences in CD4+ and CD8+ effector and memory T cell generation. *Nat. Immunol.* **4**, 835–842 (2003).
266. Ribas, A. *et al.* PD-1 blockade expands intratumoral memory T cells. *Cancer Immunol. Res.* **4**, 194–203 (2016).
267. Wykes, M. N. & Lewin, S. R. Immune checkpoint blockade in infectious diseases. *Nat. Rev. Immunol.* **18**, 91–104 (2018).
268. Goldszmid, R. S., Dzutsev, A. & Trinchieri, G. Host immune response to infection and cancer: Unexpected commonalities. *Cell Host Microbe* **15**, 295–305 (2014).
269. Vance, R. E., Eichberg, M. J., Portnoy, D. A. & Raulet, D. H. Listening to each other: Infectious disease and cancer immunology. *Sci. Immunol.* **2**, 1–6 (2017).
270. Dunn, G. P., Old, L. J. & Schreiber, R. D. The Three Es of Cancer Immunoediting. *Annu. Rev. Immunol.* **22**, 329–360 (2004).
271. Huang, A. C. *et al.* A single dose of neoadjuvant PD-1 blockade predicts clinical outcomes in resectable melanoma. *Nat. Med.* **25**, 454–461 (2019).
272. Salih, Z. *et al.* T cell immune awakening in response to immunotherapy is age-dependent. *Eur. J. Cancer* **162**, 11–21 (2022).
273. Eisenhauer, E. A. *et al.* New response evaluation criteria in solid tumours: Revised RECIST guideline (version 1.1). *Eur. J. Cancer* **45**, 228–247 (2009).
274. Prasad, S. R. & Saini, S. Radiological evaluation of oncologic treatment response: Current update. *Cancer Imaging* **3**, 93–95 (2003).
275. Gangadhar, T. C. *et al.* Feasibility of monitoring advanced melanoma patients using cell-free DNA from plasma. *Pigment Cell Melanoma Res* **31**, 73–81 (2019).
276. Yarchoan, M. *et al.* PD-L1 expression and tumor mutational burden are independent biomarkers in most cancers. *JCI Insight* **4**, 1–10 (2019).
277. Wang, W. *et al.* Biomarkers on melanoma patient T Cells associated with ipilimumab treatment. *J. Transl. Med.* **10**, 1–12 (2012).
278. Wherry, E. J. & Kurachi, M. Molecular and cellular insights into T cell exhaustion. *Nat. Rev. Immunol.* **15**, 486–499 (2015).
279. Wolchok JD, Chiarion-Sileni V, Gonzalez R, et al. Overall survival with combined nivolumab and ipilimumab in advanced melanoma. *N. Engl. J. Med.* **5;377**, 1345–1356 (2017).
280. Rossi, J. F., Céballos, P. & Lu, Z. Y. Immune precision medicine for cancer: A novel insight based on the efficiency of immune effector cells. *Cancer Commun.* **39**, 1–16 (2019).
281. Fritsch, R. D. *et al.* Stepwise Differentiation of CD4 Memory T Cells Defined by Expression of CCR7 and CD27. *J. Immunol.* **175**, 6489–6497 (2005).
282. Hendriks, J., Xiao, Y. & Borst, J. CD27 Promotes Survival of Activated T Cells and Complements CD28 in Generation and Establishment of the Effector T Cell Pool. *J. Exp. Med.* **198**, 1369–1380 (2003).
283. Britschgi, M. R., Link, A., Lissandrin, T. K. A. & Luther, S. A. Dynamic Modulation of CCR7 Expression and Function on Naive T Lymphocytes In Vivo. *J. Immunol.* **181**, 7681–7688 (2008).
284. Larbi, A. & Fulop, T. From 'truly naïve' to 'exhausted senescent' T cells: When markers predict functionality. *Cytom. Part A* **85**, 25–35 (2014).
285. Cortes, J. *et al.* Comparison of unidimensional and bidimensional measurements in metastatic non-small cell lung cancer. *Br. J. Cancer* **87**, 158–160 (2002).
286. Hauth, E. A. M., Stattaus, J. & Forsting, M. [Comparison of unidimensional and bidimensional measurement to assess therapeutic response in the treatment of solid tumors]. *Radiologe* **47**, 628,630-634 (2007).
287. James, K. *et al.* Measuring response in solid tumors: unidimensional versus bidimensional measurement. *J. Natl. Cancer Inst.* **91**, 523–528 (1999).

288. Hopper, K. D. *et al.* The impact of 2D versus 3D quantitation of tumor bulk determination on current methods of assessing response to treatment. *J. Comput. Assist. Tomogr.* **20**, 930–937 (1996).
289. Marten, K. *et al.* Inadequacy of manual measurements compared to automated CT volumetry in assessment of treatment response of pulmonary metastases using RECIST criteria. *Eur. Radiol.* **16**, 781–790 (2006).
290. Greenplate, A. R. *et al.* Computational immune monitoring reveals abnormal double-negative T cells present across human tumor types. *Cancer Immunol. Res.* **7**, 86–99 (2019).
291. Kim, K. H. *et al.* Immune-related adverse events are clustered into distinct subtypes by T-cell profiling before and early after anti-PD-1 treatment. *Oncoimmunology* **9**, 1–12 (2020).
292. Fairfax, B. P. *et al.* Peripheral CD8+ T cell characteristics associated with durable responses to immune checkpoint blockade in patients with metastatic melanoma. *Nat. Med.* **26**, 193–199 (2020).
293. Long, G. V *et al.* 1141 Impact of baseline serum lactate dehydrogenase concentration on the efficacy of pembrolizumab and ipilimumab in patients with advanced melanoma: data from KEYNOTE-006. *Eur. J. Cancer* **72**, s122–s123 (2017).
294. Tarhini, A. & Kudchadkar, R. R. Predictive and on-treatment monitoring biomarkers in advanced melanoma: Moving toward personalized medicine. *Cancer Treat. Rev.* **71**, 8–18 (2018).
295. Robert, C. *et al.* Pembrolizumab versus ipilimumab in advanced melanoma (KEYNOTE-006): post-hoc 5-year results from an open-label, multicentre, randomised, controlled, phase 3 study. *Lancet Oncol.* **20**, 1239–1251 (2019).
296. Owusu, C. & Berger, N. A. Comprehensive geriatric assessment in the older cancer patient: Coming of age in clinical cancer care. *Clin. Pract.* **11**, 749–762 (2014).
297. Conforti, F. *et al.* Cancer immunotherapy efficacy and patients' sex: a systematic review and meta-analysis. *Lancet Oncol.* **19**, 737–746 (2018).
298. Gupta, S., Artomov, M., Goggins, W., Daly, M. & Tsao, H. Gender Disparity and Mutation Burden in Metastatic Melanoma. *JNCI J. Natl. Cancer Inst.* **107**, djv221 (2015).
299. Damsky, W. E., Rosenbaum, L. E. & Bosenberg, M. Decoding Melanoma Metastasis. *Cancers (Basel).* **3**, 126–163 (2011).
300. Zhang, C. & Yu, D. Suppressing immunotherapy by organ-specific tumor microenvironments: What is in the brain? *Cell Biosci.* **9**, 1–8 (2019).
301. Rauwerdink, D. J. W. *et al.* Mixed Response to Immunotherapy in Patients with Metastatic Melanoma. *Ann. Surg. Oncol.* **27**, 3488–3497 (2020).
302. Austin, P. F. *et al.* Age as a prognostic factor in the malignant melanoma population. *Ann. Surg. Oncol.* **1**, 487–494 (1994).
303. Balch, C. M. *et al.* Age as a Prognostic Factor in Patients with Localized Melanoma and Regional Metastases. *Ann. Surg. Oncol.* **20**, 3961–3968 (2013).
304. Balch, C. M. *et al.* Prognostic Factors Analysis of 17,600 Melanoma Patients: Validation of the American Joint Committee on Cancer Melanoma Staging System. *J. Clin. Oncol.* **19**, 3622–3634 (2001).
305. Valpione, S. *et al.* The T cell receptor repertoire of tumor infiltrating T cells is predictive and prognostic for cancer survival. *Nat. Commun.* **12**, 4098 (2021).
306. Bauer, J., Büttner, P., Murali, R., Okamoto, I. & Nicholas, A. BRAF mutations in cutaneous melanoma are independently associated with age, anatomic site of the primary tumor and the degree of solar elastosis at the primary tumor site. *Pigment Cell Melanoma Res.* **24**, 345–351 (2011).
307. Lian, J., Yue, Y., Yu, W. & Zhang, Y. Immunosenescence: a key player in cancer development. *J. Hematol. Oncol.* **13**, 151 (2020).
308. Kugel, C. H. *et al.* Age Correlates with Response to Anti-PD1, Reflecting AgeRelated Differences in Intratumoral Effector and Regulatory TCell Populations. **24**, 5347–5356 (2019).
309. Jain, V. *et al.* Association of Age with Ef fi cacy of Immunotherapy in Metastatic

Melanoma. *Oncologist* **25,2**, (2020).
310. Nikolich-Žugich, J. Ageing and life-long maintenance of T-cell subsets in the face of latent persistent infections. *Nat. Rev. Immunol.* **8**, 512–522 (2008).
311. Falci, C. *et al.* Immune senescence and cancer in elderly patients: Results from an exploratory study. *Exp. Gerontol.* **48**, 1436–1442 (2013).
312. Palmer, D. B. The effect of age on thymic function. *Front. Immunol.* **4**, 1–6 (2013).
313. Britanova, O. V. *et al.* Age-Related Decrease in TCR Repertoire Diversity Measured with Deep and Normalized Sequence Profiling. *J. Immunol.* **192**, 2689–2698 (2014).
314. Nikolich-Žugich, J., Slifka, M. K. & Messaoudi, I. The many important facets of T-cell repertoire diversity. *Nat. Rev. Immunol.* **4**, 123–132 (2004).
315. Shah, S. & Boucai, L. Effect of Age on Response to Therapy and Mortality in Patients With Thyroid Cancer at High Risk of Recurrence. *J. Clin. Endocrinol. Metab.* **103**, 689–697 (2018).
316. Mitchell, W. A., Lang, P. O. & Aspinall, R. Tracing thymic output in older individuals. *Clin. Exp. Immunol.* **161**, 497–503 (2010).
317. Daste, A. *et al.* Immune checkpoint inhibitors and elderly people: A review. *Eur. J. Cancer* **82**, 155–166 (2017).
318. Qi, Q., Zhang, D. W., Weyand, C. M. & Goronzy, J. J. Mechanisms shaping the naïve T cell repertoire in the elderly — Thymic involution or peripheral homeostatic proliferation? *Exp. Gerontol.* 71–74 (2014). doi:doi:10.1016/j.exger.2014.01.005
319. He, Q., Jiang, X., Zhou, X. & Weng, J. Targeting cancers through TCR-peptide/MHC interactions. *J. Hematol. Oncol.* **12**, 1–17 (2019).
320. Hurez, V., Padrón, S., Svatek, R. S. & Curiel, T. J. Considerations for successful cancer immunotherapy in aged hosts. *Clinical and Experimental Immunology* **187**, 53–63 (2017).
321. Hamilton, J. A. G. & Henry, C. J. Aging and immunotherapies: New horizons for the golden ages. *Aging and Cancer* **1**, 30–44 (2020).
322. Cancer Research UK. Melanoma Survival. (2020). Available at: https://www.cancerresearchuk.org/about-cancer/melanoma/survival. (Accessed: 12th December 2020)
323. Luke, J. J., Flaherty, K. T., Ribas, A. & Long, G. V. Targeted agents and immunotherapies: Optimizing outcomes in melanoma. *Nat. Rev. Clin. Oncol.* **14**, 463–482 (2017).
324. Robert, C. *et al.* Durable complete response after discontinuation of pembrolizumab in patients with metastatic melanoma. *J. Clin. Oncol.* **36**, 1668–1674 (2018).
325. Whiteman, D. C., Baade, P. D. & Olsen, C. M. More People Die from Thin Melanomas (≤1 mm) than from Thick Melanomas (>4 mm) in Queensland, Australia. *J. Invest. Dermatol.* **135**, 1190–1193 (2015).
326. Kanaki, T. *et al.* Impact of American Joint Committee on Cancer 8th edition classification on staging and survival of patients with melanoma. *Eur. J. Cancer* **119**, 18–29 (2019).
327. J.J. Luke, P. Rutkowski, P. Queirolo, M. et al. LBA3_PR - Pembrolizumab versus placebo after complete resection of high-risk stage II melanoma: Efficacy and safety results from the KEYNOTE-716 double-blind phase III trial. *Ann. Oncol.* **32**, **Supple**, (2021).
328. Marczynski, G. T., Laus, A. C., dos Reis, M. B., Reis, R. M. & Vazquez, V. de L. Circulating tumor DNA (ctDNA) detection is associated with shorter progression-free survival in advanced melanoma patients. *Sci. Rep.* **10**, 1–11 (2020).
329. Romano, E. *et al.* Site and Timing of First Relapse in Stage III Melanoma Patients: Implications for Follow-Up Guidelines. *J Clin Oncol* **28**, 3042–3047 (2010).
330. Long, G. V *et al.* Adjuvant Dabrafenib plus Trametinib in Stage III BRAF-Mutated Melanoma. *N. Engl. J. Med.* **377**, 1813–1823 (2017).
331. van Dongen, J. J. M., van der Velden, V. H. J., Brüggemann, M. & Orfao, A. Minimal residual disease diagnostics in acute lymphoblastic leukemia: need for sensitive, fast, and standardized technologies. *Blood* **125**, 3996–4009 (2015).

332. Paietta, E. Assessing minimal residual disease (MRD) in leukemia: A changing definition and concept? *Bone Marrow Transplant.* **29**, 459–465 (2002).
333. Luskin, M. R., Murakami, M. A., Manalis, S. R. & Weinstock, D. M. Targeting minimal residual disease: A path to cure? *Nat. Rev. Cancer* **18**, 255–263 (2018).
334. Béné, M. C. & Kaeda, J. S. How and why minimal residual disease studies are necessary in leukemia: A review from WP10 and WP12 of the European LeukaemiaNet. *Haematologica* **94**, 1135–1150 (2009).
335. Peng, Y., Mei, W., Ma, K. & Zeng, C. Circulating Tumor DNA and Minimal Residual Disease (MRD) in Solid Tumors: Current Horizons and Future Perspectives. *Front. Oncol.* **11**, 1–14 (2021).
336. Testa, U., Castelli, G. & Pelosi, E. Detection of Circulating Tumor DNA in Solid Tumors. *OBM Genet.* **4**, 1–40 (2020).
337. McGuire, A. L. *et al.* Optimizing molecular residual disease detection using liquid biopsy postoperatively in early stage lung cancer. *Lung Cancer Manag.* **9**, LMT24 (2020).
338. Cabel, L. *et al.* Clinical potential of circulating tumour DNA in patients receiving anticancer immunotherapy. doi:10.1038/s41571-018-0074-3
339. Bellmunt, J. *et al.* Adjuvant atezolizumab versus observation in muscle-invasive urothelial carcinoma (IMvigor010): a multicentre, open-label, randomised, phase 3 trial. *Lancet. Oncol.* **22**, 525–537 (2021).
340. Powles, T. *et al.* ctDNA guiding adjuvant immunotherapy in urothelial carcinoma. *Nature* **595**, 432–437 (2021).
341. Weber, J. S. *et al.* Adjuvant nivolumab (NIVO) versus ipilimumab (IPI) in resected stage III/IV melanoma: 3-year efficacy and biomarker results from the phase III CheckMate 238 trial. *Ann. Oncol.* **30**, v533–v534 (2019).
342. Hogan, S. A., Levesque, M. P. & Cheng, P. F. Melanoma immunotherapy: Next-generation biomarkers. *Frontiers in Oncology* **8**, 178 (2018).
343. Gerami, P. *et al.* Gene expression profiling for molecular staging of cutaneous melanoma in patients undergoing sentinel lymph node biopsy. *J. Am. Acad. Dermatol.* **72**, 780-785.e3 (2015).
344. John, T. *et al.* Predicting clinical outcome through molecular profiling in stage III melanoma. *Clin. Cancer Res.* **14**, 5173–5180 (2008).
345. Eggermont, A. M. M. *et al.* Prolonged Survival in Stage III Melanoma with Ipilimumab Adjuvant Therapy. *N. Engl. J. Med.* **375**, 1845–1855 (2016).
346. Santiago-Walker, A. *et al.* Correlation of BRAF Mutation Status in Circulating-Free DNA and Tumor and Association with Clinical Outcome across Four BRAFi and MEKi Clinical Trials. *Clin. Cancer Res.* **22**, 567–574 (2016).
347. Grzywa, T. M., Paskal, W. & Włodarski, P. K. Intratumor and Intertumor Heterogeneity in Melanoma. *Transl. Oncol.* **10**, 956–975 (2017).
348. Da Cunha Cosme, M. L., Liuzzi Samaterra, J. F., Siso Cardenas, S. A. & Chaviano Hernández, J. I. Lymphadenectomy after a positive sentinel node biopsy in patients with cutaneous melanoma. A systematic review. *Surg. Exp. Pathol.* **4**, (2021).
349. Rosati, E. *et al.* Overview of methodologies for T-cell receptor repertoire analysis. *BMC Biotechnol.* **17**, 61 (2017).
350. Jackett, L. A. & Scolyer, R. A. A review of key biological and molecular events underpinning transformation of melanocytes to primary and metastatic melanoma. *Cancers (Basel).* **11**, (2019).
351. Leonardi, G. C. *et al.* Cutaneous melanoma: From pathogenesis to therapy (Review). *International Journal of Oncology* (2018). doi:10.3892/ijo.2018.4287
352. Chan, T. A. *et al.* Development of tumor mutation burden as an immunotherapy biomarker: Utility for the oncology clinic. *Ann. Oncol.* **30**, 44–56 (2019).
353. Bedard, P. L., Hansen, A. R., Ratain, M. J. & Siu, L. L. Tumour heterogeneity in the clinic. *Nature* **501**, 355–364 (2013).
354. Wang, Y. *et al.* Changing Technologies of RNA Sequencing and Their Applications in Clinical Oncology. *Front. Oncol.* **10**, 1–11 (2020).
355. Fumagalli, D. *et al.* Transfer of clinically relevant gene expression signatures in breast

cancer: From Affymetrix microarray to Illumina RNA-Sequencing technology. *BMC Genomics* **15**, 1–12 (2014).
356. Han, L. O., Li, X. Y., Cao, M. M., Cao, Y. & Zhou, L. H. Development and validation of an individualized diagnostic signature in thyroid cancer. *Cancer Med.* **7**, 1135–1140 (2018).
357. Zhou, J. G. *et al.* Development and Validation of an RNA-Seq-Based Prognostic Signature in Neuroblastoma. *Front. Oncol.* **9**, 1–12 (2019).
358. Shukla, S. *et al.* Development of a RNA-seq based prognostic signature in lung adenocarcinoma. *J. Natl. Cancer Inst.* **109**, 1–9 (2017).
359. Chen, P. L. *et al.* Analysis of immune signatures in longitudinal tumor samples yields insight into biomarkers of response and mechanisms of resistance to immune checkpoint blockade. *Cancer Discov.* **6**, 827–837 (2016).
360. Van Allen, E. M. *et al.* Genomic correlates of response to CTLA-4 blockade in metastatic melanoma. *Science* **350**, 207–211 (2015).
361. Gambino, G., Tancredi, M., Falaschi, E., Aretini, P. & Caligo, M. A. Characterization of three alternative transcripts of the BRCA1 gene in patients with breast cancer and a family history of breast and/or ovarian cancer who tested negative for pathogenic mutations. *Int. J. Mol. Med.* **35**, 950–956 (2015).
362. Lu, S. *et al.* Comparison of Biomarker Modalities for Predicting Response to PD-1/PD-L1 Checkpoint Blockade: A Systematic Review and Meta-analysis. *JAMA Oncol.* **5**, 1195–1204 (2019).
363. Gallina, M. E. *et al.* Abstract A074: Spatially resolved deep antigen profiling of single cells in FFPE tissue samples through CODEXTM. *Cancer Immunol. Res.* **7**, A074 LP-A074 (2019).
364. Kennedy-Darling, J. *et al.* PO-281 Automated multiparametric tissue imaging platform using existing microscope hardware for the detection of spatially resolved single-cell resolution data. *ESMO Open* **3**, A337–A338 (2018).
365. Bollard, S. M., Casalou, C. & Potter, S. M. Gene expression profiling in melanoma: A view from the clinic. *Cancer Treat. Res. Commun.* **29**, 100447 (2021).
366. Ayers, M., Ribas, A. & Mcclanahan, T. K. IFN-g g-related mRNA profile predicts clinical response to PD-1 blockade The Journal of Clinical Investigation. *J Clin Invest* **127**, (2017).
367. Maby, P., Corneau, A. & Galon, J. Phenotyping of tumor infiltrating immune cells using mass-cytometry (CyTOF). *Methods Enzymol.* **632**, 339–368 (2020).
368. Riaz, N. *et al.* Tumor and Microenvironment Evolution during Immunotherapy with Nivolumab. (2017). doi:10.1016/j.cell.2017.09.028
369. Roh, W. *et al.* Integrated molecular analysis of tumor biopsies on sequential CTLA-4 and PD-1 blockade reveals markers of response and resistance. *Sci. Transl. Med.* **9**, eaah3560 (2017).
370. ClinicalTrials.gov. Neoadjuvant PD-1 Blockade in Patients With Stage IIB/C Melanoma (NCT03757689). Available at: https://clinicaltrials.gov/ct2/show/NCT03757689. (Accessed: 19th May 2021)
371. ClinicalTrials.gov. Adjuvant Nivolumab Treatment in Stage II (IIA, IIB, IIC) High-risk Melanoma (NivoMela). Available at: https://clinicaltrials.gov/ct2/show/NCT04309409. (Accessed: 19th May 2021)
372. ClinicalTrials.gov. Tiragolumab Plus Atezolizumab Versus Atezolizumab in the Treatment of Stage II Melanoma Patients Who Are ctDNA-positive Following Resection. Available at: https://clinicaltrials.gov/ct2/show/NCT05060003. (Accessed: 19th May 2021)
373. Bhutani, M. *et al.* Peripheral Immunotype Correlates with Minimal Residual Disease Status and Is Modulated by Immunomodulatory Drugs in Multiple Myeloma. *Biol. Blood Marrow Transplant.* **25**, 459–465 (2019).
374. Shao, H. *et al.* Minimal residual disease detection by flow cytometry in adult T-cell leukemia/lymphoma. *Am. J. Clin. Pathol.* **133**, 592–601 (2010).
375. Chatterjee, T., Mallhi, R. S. & Venkatesan, S. Minimal residual disease detection using

flow cytometry: Applications in acute leukemia. *Med. journal, Armed Forces India* **72**, 152–156 (2016).
376. Amaria, R. N. *et al.* Neoadjuvant plus adjuvant dabrafenib and trametinib versus standard of care in patients with high-risk, surgically resectable melanoma: a single-centre, open-label, randomised, phase 2 trial. *Artic. Lancet Oncol* **19**, 181–93 (2018).
377. Kadić, E., Moniz, R. J., Huo, Y., Chi, A. & Kariv, I. Effect of cryopreservation on delineation of immune cell subpopulations in tumor specimens as determinated by multiparametric single cell mass cytometry analysis. *BMC Immunol.* **18**, 6 (2017).
378. Rodríguez, A. *et al.* Comparison of procedures for RNA-extraction from peripheral blood mononuclear cells. *PLoS One* **15**, 1–17 (2020).
379. Adler, N. R. *et al.* Tumour mutation status and melanoma recurrence following a negative sentinel lymph node biopsy. *Br. J. Cancer* **118**, 1289–1295 (2018).
380. Schummer, P., Schilling, B. & Gesierich, A. Long-Term Outcomes in BRAF-Mutated Melanoma Treated with Combined Targeted Therapy or Immune Checkpoint Blockade: Are We Approaching a True Cure? *Am. J. Clin. Dermatol.* **21**, 493–504 (2020).
381. Islami, F. *et al.* Annual Report to the Nation on the Status of Cancer, Part 1: National Cancer Statistics. *JNCI J. Natl. Cancer Inst.* **113**, 1648–1669 (2021).
382. Vera Aguilera, J. *et al.* Chemo-immunotherapy combination after PD-1 inhibitor failure improves clinical outcomes in metastatic melanoma patients. *Melanoma Res.* 364–375 (2020). doi:10.1097/CMR.0000000000000669
383. Di Giacomo, A. M. *et al.* Guadecitabine plus ipilimumab in unresectable melanoma: The NIBIT-M4 clinical trial. *Clin. Cancer Res.* **25**, 7351–7362 (2019).
384. Yu, C. *et al.* Combination of immunotherapy with targeted therapy: Theory and practice in metastatic melanoma. *Front. Immunol.* **10**, (2019).
385. Pelster, M. S. & Amaria, R. N. Combined targeted therapy and immunotherapy in melanoma: a review of the impact on the tumor microenvironment and outcomes of early clinical trials. *Ther. Adv. Med. Oncol.* **11**, 1–11 (2019).
386. Schmid, P. *et al.* Atezolizumab and Nab-Paclitaxel in Advanced Triple-Negative Breast Cancer. *N. Engl. J. Med.* **379**, 2108–2121 (2018).
387. Burtness, B. *et al.* Pembrolizumab alone or with chemotherapy versus cetuximab with chemotherapy for recurrent or metastatic squamous cell carcinoma of the head and neck (KEYNOTE-048): a randomised, open-label, phase 3 study. *Lancet* **394**, 1915–1928 (2019).
388. Janjigian, Y. Y. *et al.* First-line nivolumab plus chemotherapy versus chemotherapy alone for advanced gastric, gastro-oesophageal junction, and oesophageal adenocarcinoma (CheckMate 649): a randomised, open-label, phase 3 trial. *Lancet* **398**, 27–40 (2021).
389. Spencer, K. R. *et al. Biomarkers for Immunotherapy: Current Developments and Challenges*. (2016).
390. Dronca, R. S. *et al.* Bim as a predictive T-cell biomarker for response to anti-PD-1 therapy in metastatic melanoma (MM). *J. Clin. Oncol.* **33**, 9013 (2015).
391. Tarhini, A. A. *et al.* Immune monitoring of the circulation and the tumor microenvironment in patients with regionally advanced melanoma receiving neoadjuvant ipilimumab. *PLoS One* **9**, (2014).
392. Hao, C. *et al.* Ef fi cacy and safety of anti-PD-1 and anti-PD-1 combined with anti-CTLA-4 immunotherapy to advanced melanoma. **26**, (2017).
393. Masucci, G. V. *et al.* Validation of biomarkers to predict response to immunotherapy in cancer: Volume I - pre-analytical and analytical validation. *J. Immunother. Cancer* **4**, 1–25 (2016).
394. Ricciuti, B. *et al.* Impact of immune-related adverse events on survival in patients with advanced non-small cell lung cancer treated with nivolumab: long-term outcomes from a multi-institutional analysis. *J. Cancer Res. Clin. Oncol.* **145**, 479–485 (2019).
395. Hegde, P. S. & Chen, D. S. Top 10 Challenges in Cancer Immunotherapy. *Immunity* **52**, 17–35 (2020).
396. Lipson, E. J. *et al.* Relatlimab (RELA) plus nivolumab (NIVO) versus NIVO in first-line

advanced melanoma: Primary phase III results from RELATIVITY-047 (CA224-047). *J. Clin. Oncol.* **39**, 9503 (2021).
397. Amaria, R. N. *et al.* Neoadjuvant and adjuvant nivolumab (nivo) with anti-LAG3 antibody relatlimab (rela) for patients (pts) with resectable clinical stage III melanoma. *J. Clin. Oncol.* **39**, 9502 (2021).
398. Gide, T. N., Wilmott, J. S., Scolyer, R. A. & Long, G. V. Primary and acquired resistance to immune checkpoint inhibitors in metastatic melanoma. *Clin. Cancer Res.* **24**, 1260–1270 (2018).
399. Gopalakrishnan, V. *et al.* Gut microbiome modulates response to anti-PD-1 immunotherapy in melanoma patients. *Science* **359**, 97–103 (2017).
400. Matson, V. *et al. The commensal microbiome is associated with anti-PD-1 efficacy in metastatic melanoma patients*. *Science* **359**, (2018).

Appendices

Appendix A: AJCC 8th edition cutaneous melanoma staging

AJCC Melanoma of the Skin Staging 8th Edition

Definitions

Primary Tumor (T)

- **TX** Primary tumor cannot be assessed (for example, curettaged or severely regressed melanoma)
- **T0** No evidence of primary tumor
- **Tis** Melanoma in situ
- **T1** Melanomas 1.0 mm or less in thickness
- **T2** Melanomas 1.1 - 2.0 mm
- **T3** Melanomas 2.1 - 4.0 mm
- **T4** Melanomas more than 4.0 mm

NOTE: a and b subcategories of T are assigned based on ulceration and thickness as shown belowt:

T CLASSIFICATION	THICKNESS (mm)	ULCERATION STATUS
T1	≤1.0	a: Breslow < 0.8 mm w/o ulceration b: Breslow 0.8-1.0 mm w/o ulceration or ≤ 1.0 mm w/ ulceration.
T2	1.1-2.0	a: w/o ulceration b: w/ ulceration
T3	2.1-4.0	a: w/o ulceration b: w/ ulceration
T4	>4.0	a: w/o ulceration b: w/ ulceration

Regional Lymph Nodes (N)

- **NX** Patients in whom the regional nodes cannot be assessed (for example previously removed for another reason)
- **N0** No regional metastases detected
- **N1-3** Regional metastases based on the number of metastatic nodes, number of palpable metastatic nodes on clinical exam, and presence or absence of MSI[2]

NOTE: N1-3 and a-c subcategories assigned as shown below:

N CLASSIFICATION	# NODES	CLINICAL DETECTABILITY/MSI STATUS
N1	0-1 node	a: clinically occult[1], no MSI[2] b: clinically detected[1], no MSI[2] c: 0 nodes, MSI present[2]
N2	1-3 nodes	a: 2-3 nodes clinically occult[1], no MSI[2] b: 2-3 nodes clinically detected[1], no MSI[2] c: 1 node clinical or occult[1], MSI present[2]
N3	>1 nodes	a: >3 nodes, all clinically occult[1], no MSI[2] b: >3 nodes, ≥1 clinically detected[1] or matted, no MSI[2] c: >1 nodes clinical or occult[1], MSI present[2]

Distant Metastasis (M)

- **M0** No detectable evidence of distant metastases
- **M1a** Metastases to skin, sub cutaneous, or distant lymph nodes
- **M1b** Metastases to lung
- **M1c** Metastases to all other visceral sites
- **M1d** Metastases to brain

NOTE: Serum LDH is incorporated into the M category as shown below:

M CLASSIFICATION	SITE	Serum LDH
M1a-d	Skin/subcutaneous/nodule (a), lung (b) other visceral (c), brain (d)	Not assessed
M1a-d(0)	Skin/subcutaneous/nodule (a), lung (b) other visceral (c), brain (d)	Normal
M1a-d(1)	Skin/subcutaneous/nodule (a), lung (b) other visceral (c), brain (d)	Elevated

ANATOMIC STAGE/PROGNOSTIC GROUPS

	Clinical Staging[3]				Pathologic Staging[4]		
Stage 0	Tis	N0	M0	0	Tis	N0	M0
Stage IA	T1a	N0	M0	IA	T1a	N0	M0
Stage IB	T1b	..	..		T1b	..	..
	T2a	..	..	IB	T2a	..	..
Stage IIA	T2b	N0	M0	IIA	T2b	M0	M0
	T3a	..	..		T2a	..	..
Stage IIB	T3b	..	..	IIB	T3b	..	..
	T4a	..	..		T4a	..	..
Stage IIC	T4b	..	..	IIC	T4b	..	..
Stage III	Any T	≥N1	M0	IIIA	T1-2a	N1a	M0
	..	..	..		T1-2a	N2a	..
	..	..	..	IIIB	T0	N1b-c	M0
	..	..	..		T1-2a	N1b-c	..
	..	..	..		T1-2a	N2b	..
	..	..	..		T2b-3a	N1a-2b	..
	..	..	..	IIIC	T0	N2b-c	M0
	..	..	..		T0	N3b-c	..
	..	..	..		T1a-3a	N2c-3c	..
	..	..	..		T3b-4a	Any N	..
	..	..	..		T4b	N1a-2c	..
	..	..	..	IIID	T4b	N3a-c	M0
Stage IV	Any N	Any N	M1	IV	Any T	Any N	M1

Baseline survival after Stage III diagnosis[5]

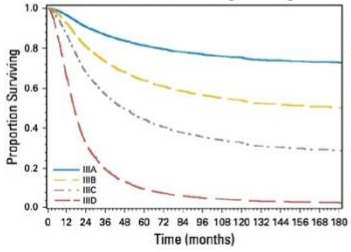

Conditional, 5-year survival (%)[5]

Stage	Baseline	3y survivors
IIIA	81.4	83.1
IIIB	64.0	76.0
IIIC	44.5	66.7
IIID	9.8	40.6

Notes

[1]Nodes are designated as 'clinically detectable' if they can be palpated on physical exam and are confirmed melanoma by pathology following excision/biopsy.

[2]MSI comprise any satellite, locally recurrent, or in transit lesions.

[3]Clinical staging includes microstaging of the primary melanoma and clinical/radiologic evaluation for metastases. By convention it should be used after complete excision of the primary melanoma with clinical assessment for regional and distant metastases.

[4]Pathologic staging includes microstaging of the primary melanoma and pathologic information about the regional lymph nodes after partial or complete lymphadenectomy. Pathologic Stage 0 and I patients are the exceptions; they do not necessarily require pathologic evaluation of their lymph nodes. Physicians should "discuss and consider" SLNB for patients with T1b Stage IA disease; physicians should "discuss and offer" SLNB for patients with Stage IB disease.

[5]From Haydu et al., Journal of Clinical Oncology, 2017.

Produced following the 8th Ed. AJCC guidlines released January 1, 2017. Contact Dr. M. Gormally (mvgg07@gmail.com) for reprint.

Appendix B: Nature Cancer Publication

ARTICLES
https://doi.org/10.1038/s43018-019-0022-x
nature cancer

Immune awakening revealed by peripheral T cell dynamics after one cycle of immunotherapy

Sara Valpione[1,2], Elena Galvani[1], Joshua Tweedy[1], Piyushkumar A. Mundra[1], Antonia Banyard[3], Philippa Middlehurst[4], Jeff Barry[3], Sarah Mills[4], Zena Salih[2], John Weightman[5], Avinash Gupta[2], Gabriela Gremel[1,6], Franziska Baenke[1,7,8], Nathalie Dhomen[1], Paul C. Lorigan[2*] and Richard Marais[1*]

Our understanding of how checkpoint inhibitors (CPIs) affect T cell evolution is incomplete, limiting our ability to achieve full clinical benefit from these drugs. Here, we analyzed peripheral T cell populations after one cycle of CPI treatment and identified a dynamic awakening of the immune system, as revealed by T cell evolution in response to treatment. We sequenced T cell receptors in plasma cell-free DNA and peripheral blood mononuclear cells and performed phenotypic analysis of peripheral T cell subsets from patients with metastatic melanoma treated with CPIs. We found that early peripheral T cell turnover and T cell receptor repertoire dynamics identified which patients would respond to treatment. Additionally, the expansion of a subset of immune effector peripheral T cells we call T_{IE} cells correlated with response. These events are prognostic and occur within 3 weeks of starting immunotherapy, raising the potential for monitoring patients' responses by using minimally invasive liquid biopsies.

T cell maturation begins when pro-T cells enter the thymus and attempt to generate a functional T cell receptor (TCR). Cells that fail to do so are eliminated through β selection, but those that succeed must still pass positive and negative selection for human leukocyte antigen binding and the absence of reactivity to self-antigen in order to survive (Extended Data Fig. 1a,b). Successful naïve T cells enter the circulation as early thymic emigrants (ETEs) and, if stimulated by antigen-presenting cells in the lymphatic system, they expand and migrate to sites of inflammation to combat harmful agents—a process that resolves through clonal contraction and more T cell death[1] (Extended Data Fig. 1c–e).

Checkpoint inhibitor (CPI) drugs awaken the immune system so that it attacks tumors. CPIs have revolutionized cancer care and, over the past decade, have contributed to a fourfold improvement in the survival of patients with metastatic melanoma[2]. Despite these remarkable advances, our understanding of T cell evolution under the selective pressure of CPI is still incomplete and this limits our ability to derive full clinical benefit from these drugs. Consequently, most patients with advanced-stage melanoma still die of the disease. Sharing features with responses to infectious diseases[3–5], tumor control by the immune system requires coordination between systemic and intratumoral immunity[6], and although several studies have investigated intratumoral responses to immunotherapy[7–9], few have focused on how CPIs affect the peripheral immune system, or whether changes in peripheral T cells are associated with patient responses[7,8,10].

We hypothesized that because immune responses to tumors mirror normal defensive responses to pathogens, it would be possible to study patient responses to CPI by monitoring peripheral T cell evolution during treatment. TCRs are generated by error-prone recombination of the *TCR* locus[11,12], creating the enormous diversity needed for effective immune function. This process is ~80% efficient, so most peripheral T cells carry only productive *TCR* sequences. However, in ~20% of peripheral T cells, the first attempts at *TCR* locus rearrangement failed due to acquisition of stop codons or because the protein-coding region was out of frame, so these T cells carry both productive and non-productive *TCR* sequences[13]. The complementarity-determining region 3 (CDR3) of the TCR in particular is highly variable and the sequences are unique to individual T cell clones, so both the productive and non-productive *TCR* sequences serve as a 'fingerprints' for individual T cell clones.

We posited that by sequencing peripheral T cell *CDR3* regions, we could track T cell responses to CPI, and because dying cells release their DNA into the circulation, we could also sequence *CDR3* regions in cell-free DNA (cfDNA) in the blood to monitor T cell turnover in patients receiving CPIs. We found an increase in productive TCR sequences in the plasma cfDNA of patients who responded to CPIs, and this correlated with response. These events were accompanied by evolution of the peripheral T cell repertoire in a manner that mimicked changes induced by antiviral vaccines. The dynamics of T cell turnover revealed by the cfDNA analysis also correlated with expansion of a specific subset of cytotoxic memory effector peripheral T cells we call immune effector cells (or T_{IE} cells). Importantly, T_{IE} cell expansion after one cycle of CPIs enabled us to anticipate which patients would go on to respond to treatment. Our data reveal an awakening of the immune system that occurs within 3 weeks of initiating CPI treatment and anticipates clinical response to first-line therapy. These changes are dynamic and quantifiable

[1]Molecular Oncology Group, Cancer Research UK Manchester Institute, The University of Manchester, Alderley Park, UK. [2]The Christie NHS Foundation Trust, Manchester, UK. [3]Advanced Imaging and Flow Cytometry, Cancer Research UK Manchester Institute, The University of Manchester, Alderley Park, UK. [4]Manchester Cancer Research Centre Biobank, The Christie NHS Foundation Trust, Manchester, UK. [5]Molecular Biology Core Facility, Cancer Research UK Manchester Institute, The University of Manchester, Alderley Park, UK. [6]Present address: Boehringer Ingelheim, Vienna, Austria. [7]Present address: German Cancer Consortium (DKTK), German Cancer Research Centre (DKFZ), Heidelberg, Germany. [8]Present address: Department of Visceral, Thoracic and Vascular Surgery, University Hospital Carl Gustav Carus, Technical University Dresden, Dresden, Germany. *e-mail: paul.lorigan@christie.nhs.uk; richard.marais@cruk.manchester.ac.uk

and can be monitored with minimally invasive liquid biopsies—features that could be used to identify which patients will benefit from CPIs early during their treatment, allowing the delivery of more precise treatment planning.

Results

Immunotherapy does not alter thymic output. First, we examined the effects of CPIs on thymic function. We used fluorescence-activated cell sorting (FACS; Extended Data Fig. 2) to quantify the ETEs ($CD3^+CD45RA^+CD45RO^-CCR7^+CD27^+CD31^+$ T cells[14]) in peripheral blood mononuclear cells (PBMCs) from 50 patients with metastatic melanoma (patients 1–50) receiving first-line anti-programmed cell death protein 1 (anti-PD1) or anti-PD1/anti-cytotoxic T lymphocyte-associated protein 4 (anti-CTLA4) treatment (Extended Data Fig. 2i). As expected[15], we observed an age-related decrease in ETE levels in pre-treatment (t_0) patient blood (Fig. 1a), but we also found that one cycle of CPIs did not affect ETE levels measured at week 3 ($P=0.274$; Fig. 1b). Next, we examined the TCR excision circle (TREC) in the peripheral T cells of 16 of our patients (1, 10–13, 22, 24–27, 30, 42 and 51–54). The TREC—a by-product of *TCR* locus rearrangements—is a non-replicating episome that is diluted when T cells divide[16] (Extended Data Fig. 1a–d). We found that the TREC-to-genome ratio in T cells was not affected by CPIs ($P=0.129$; Fig. 1c).

CPIs induce TCR repertoire divergence in peripheral T cells. The observations above indicate that CPIs did not affect thymic output in patients with melanoma, so to monitor how CPIs affected post-thymic T cell evolution, we analyzed the TCR in peripheral PBMCs and melanoma metastases. For patient 12, we obtained a fresh tumor biopsy at t_0, as well as whole blood at t_0 and after the first cycle of CPI at week 3. Using ImReP[17], we identified 16 unique *CDR3* DNA sequences from the biopsy and found that six of these were also present in the PBMCs and cfDNA (Fig. 1d and Fig. 2). Thus, about one-third of the sequences in the tumor were also in the periphery: four in pre-treatment PBMCs (sequences $CDR3_{DNA1.1}$, $CDR3_{DNA1.2}$, $CDR3_{DNA2.1}$ and $CDR3_{DNA3}$), three in week-3 PBMCs ($CDR3_{DNA1.1}$, $CDR3_{DNA2.1}$ and $CDR3_{DNA2.2}$) and one in week-3 cfDNA ($CDR3_{DNA4}$) (Fig. 2). Intriguingly, $CDR3_{DNA1.1}$ and $CDR3_{DNA1.2}$ both encoded TCR $CDR3_{prot1}$ (Fig. 2), and $CDR3_{DNA2.1}$ and $CDR3_{DNA2.2}$ both encoded $CDR3_{prot2}$ (Fig. 2), suggesting convergence by these TCRs on dominant tumor antigens. We also analyzed *CDR3* sequences in 18 paired PBMCs and tumor-infiltrating lymphocytes (TILs) from a published melanoma cohort[18]. As an example, at t_0, patient 1 presented 123,981 unique *CDR3* sequences in bulk PBMCs, 21,052 in TILs and 3,741 shared sequences (Fig. 1e), and comparable patterns were seen in the other patients (Supplementary Table 1).

These data established that tumor-resident T cell clones were also present in the periphery, so we called these cells tumor-emigrant PBMCs (tePBMCs). We compared the clonal relatedness[19,20] of the CDR3 regions from the tePBMCs with the PBMC-private and TIL-private pools. At t_0, the tePBMCs and TIL-private TCR pools displayed more clonal relatedness than the PBMC-private CDR3 regions (Fig. 1f), suggesting more TCR convergence in tumor-associated T cells than in the bulk PBMC population. At week 3, we did not observe differences in clonal relatedness in the PBMC-private or TIL-private TCRs when we compared patients who achieved disease control at week 12 with those who developed progressive disease (Extended Data Fig. 3a). Similarly, when we compared clonal relatedness in the PBMC-private TCRs at t_0 and week 3, we did not observe differences between patients with disease control or progressive disease, whereas in the tePBMC pool, there was a significant reduction in TCR clonal relatedness in patients who achieved disease control, but not in patients who had progressive disease (Fig. 1g). This suggests there was recruitment of T cells with a broader TCR repertoire from the periphery to the tumors of patients who responded, but not to the tumors of patients who did not respond.

CPIs induce peripheral T cell turnover. Next, we compared the CDR3 clonal relatedness in PBMCs and cfDNA of 28 CPI-treated patients with metastatic melanoma (11–27 and 29–39). In t_0 blood from patient 27, we observed 14,112 unique *CDR3* sequences in bulk PBMCs, 844 in cfDNA and 193 shared sequences (Fig. 3a). Comparable patterns were seen in the other 27 patients (Supplementary Table 2). Intriguingly, the numbers of unique PBMC/cfDNA-shared CDR3 sequences increased after one cycle of CPIs (Fig. 3b), so we investigated how CPIs affected the immune-recognition landscape in these pools. At t_0, the PBMC-private CDR3 clonal relatedness was ~0, but this was significantly higher in both the cfDNA-private and PBMC/cfDNA-shared pools (Fig. 3c). Critically, clonal relatedness in the PBMC/cfDNA-shared pool decreased significantly in patients who achieved disease control at week 12, but not in patients with progressive disease (Fig. 3d), suggesting there is repertoire divergence in the T cells that turnover in responding patients.

The cfDNA *CDR3* sequences come from T cell turnover in the thymus and periphery and contain both productive and non-productive sequences (Extended Data Fig. 1). We used ImmunoSeq to quantify productive (reading frame intact) and non-productive (out-of-frame or stop codon) *CDR3* sequences and to calculate a rearrangement efficiency score (RES; productive/(productive+non-productive)). In healthy donors, the PBMC RES was ~0.8, as expected[13], but in cfDNA, the RES was 0.44 ($P<0.001$; Fig. 3e), presumably from non-productive *TCR* sequences released by T cells failing β selection in the thymus. The t_0 PBMC and cfDNA RES (RES_{t_0}) values were similar in healthy donors and patients (Fig. 3e), suggesting that melanoma does not overtly affect the

Fig. 1 | CPI treatment induced peripheral TCR repertoire divergence. a, Graph showing ETEs in pre-treated patients' blood (% ETE_{t_0} relative to total naïve T cells; determined by FACS) relative to age ($P=0.002$; linear regression, $R^2=-0.17$; $n=50$). **b**, Levels of ETE in paired patient samples pre-treatment (t_0) and at week 3 (W3) of CPI treatment ($P=0.274$; $n=50$). **c**, The TREC concentration relative to genomic DNA was measured by ddPCR in sorted $CD3^+$ peripheral T cells at t_0 (median: 0.5×10^{-3}) and week 3 (median: 0.1×10^{-2}) ($P=0.129$; $n=17$). **d**, TIL *CDR3* sequences also present in peripheral PBMC DNA and cfDNA for one patient at t_0 and week 3 (see Fig. 2 for specific DNA sequences); tot, total. **e**, Venn diagram showing unique predicted productive *CDR3* sequences in PBMCs and TILs for patient 1 at t_0 (Supplementary Table 1)[21]. Numbers show unique nucleotide sequence counts for PBMC-private (pink), TIL-private (brown) and tePBMC pools (intersection; orange). **f**, Clonal relatedness (the proportion of amino acid sequences that were related by a maximum edit distance of 3) for CDR3 in the PBMC-private, tePBMC and TIL-private pools at t_0. ***$P=0.003$; ****$P<0.0001$ ($n=18$; median $=0.4\times10^{-6}$ for PBMC-private; 0.2×10^{-2} for tePBMC; and 0.4×10^{-3} for TIL-private). **g**, Clonal relatedness (maximum edit distance = 3 amino acids) for CDR3 sequence in PBMC TCR pools at t_0 and week 3. Comparisons were made between the clonal relatedness of PBMC-private TCRs of patients with progressive disease (PD; orange; $n=11$; median $=4.3\times10^{-5}$ and 5.6×10^{-5}, respectively) or disease control (DC; green; $n=7$; median $=4.0\times10^{-5}$ and 8.0×10^{-5}, respectively) after 12 weeks of treatment ($P=0.413$ and $P=0.999$, respectively) and between the clonal relatedness of tePBMC TCRs of patients with progressive disease ($n=11$; median = 0.002 and 0.0008, respectively) or disease control ($n=7$; median = 0.0017 and 0.0007, respectively) ($P=0.638$ and *$P=0.031$, respectively). All statistical comparisons in **b**, **c**, **f** and **g** were made by two-sided Wilcoxon test. NS, not significant. Each dot represents one patient, lines represent median values, error bars show s.d., connecting lines show paired samples and *n* values represent the number of patients.

efficiency of T cell rearrangements in the thymus and also that it does not affect bulk T cell turnover in the periphery. We therefore compared the RES in PBMCs and cfDNA at t_0 and week 3 to generate difference scores (Δ_{W3}RES) and measure how CPIs affect T cell rearrangement and turnover during the first cycle of immunotherapy. The PBMC Δ_{W3}RES measured changes in *TCR* rearrangement efficiency and was ~0 irrespective of whether the patients responded or not (Fig. 3f). Thus, CPI treatment did not affect *TCR* rearrangement efficiency in the thymus, meaning that the cfDNA Δ_{W3}RES measured changes in the peripheral T cell turnover alone. Notably, the cfDNA Δ_{W3}RES was ~0 in patients with progressive disease but rose to 0.09 (P=0.037) in patients who achieved disease control at 12 weeks (Fig. 3f). Thus, CPI increased peripheral T cell turnover in responding patients, but not in non-responding patients.

CPIs stimulate expansion of specific peripheral T cell subsets. Our data reveal that there is dynamic TCR repertoire reorganization during T cell expansion/contraction in responding patients, so we

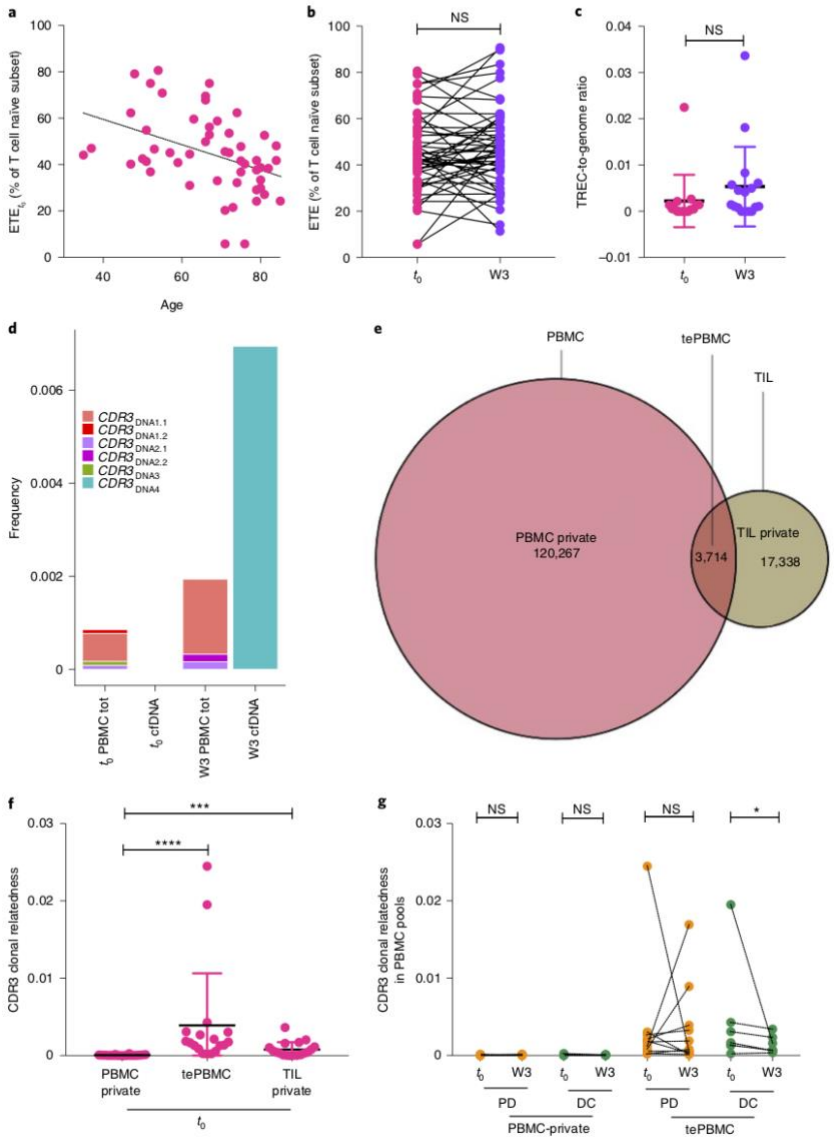

Peripheral sample	Sequence		Count[a]	Frequency[b]	V gene name	D gene name	J gene name
t_0 PBMCs	$CDR3_{prot1}$	L E S P S P N Q T S L Y F C A S S L Q G A N Y E Q Y F G P G T R L					
	$CDR3_{DNA1.1}$	CTGGAGTCGCCCAGCCCCAACCAGACCTCTCTGTACTTCTGTGCCAGCAGCCTACAGGGGGCGAACTACGAGCAGTACTTCGGGCCGGGCACCAGGCTC	7	0.000599	TCRBV27-01	TCRBD01-01	TCRBJ02-07
	$CDR3_{DNA1.2}$	CTGGAGTCGCCCAGCCCCAACCAGACCTCTCTGTACTTCTGTGCCAGCAGCCTACAGGGGGCGAACTACGAGCAGTACTTCGGGCCAGGCACGCGGCTC	1	8.56×10^{-6}	TCRBV27-01	TCRBD01-01	TCRBJ02-05
	$CDR3_{prot2}$	L T V T S A H P E D S S F Y I C S A R G P E E T Q Y F G P G T R L					
	$CDR3_{DNA2.1}$	CTGACAGTGACCAGTGCCCATCCTGAAGACAGCAGCTTCTACATCTGCAGTGCCCGGGGTCCGGAAGAGACCCAGTACTTCGGGCCAGGCACGCGGCTC	1	8.56×10^{-6}	TCRBV20	TCRBD02-01	TCRBJ02-05
	$CDR3_{prot3}$	S D L E L G D S A L Y F C A S S V G R S S Y N E Q F F G P G T R L					
	$CDR3_{DNA3}$	AGCTCTCTGGAGCTGGGGGACTCAGCTTTGTATTTCTGTGCCAGCAGCGTAGGGAGAAGCTCCTACAATGAGCAGTTCTTCGGGCCAGGGACACGGCTC	1	8.56×10^{-6}	TCRBV09-01	TCRBD02-01	TCRBJ02-01
Week-3 cfDNA	$CDR3_{prot4}$	S A H P E D S S F Y I C S A R D W L A G D T G E L F F G E G S R L					
	$CDR3_{DNA4}$	AGTGCCCATCCTGAAGACAGCAGCTTCTACATCTGCAGTGCTAGAGATTGGCTAGCGGGAGACACCGGGGAGCTGTTTTTTGGAGAAGGCTCTAGGCTG	2	0.0069444	TCRBV20	TCRBD02-01	TCRBJ02-02
Week-3 PBMCs	$CDR3_{prot1}$	L E S P S P N Q T S L Y F C A S S L Q G A N Y E Q Y F G P G T R L					
	$CDR3_{DNA1.1}$	CTGGAGTCGCCCAGCCCCAACCAGACCTCTCTGTACTTCTGTGCCAGCAGCCTACAGGGGGCGAACTACGAGCAGTACTTCGGGCCGGGCACCAGGCTC	10	0.0016176	TCRBV27-01	TCRBD01-01	TCRBJ02-07
	$CDR3_{prot2}$	L T E T S A H P E D S S F Y I C S A R G P E E T Q Y F G P G T R L					
	$CDR3_{DNA2.1}$	CTGACAGTGACCAGTGCCCATCCTGAAGACAGCAGCTTCTACATCTGCAGTGCCCGGGGTCCGGAAGAGACCCAGTACTTCGGGCCAGGCACGCGGCTC	1	0.000162		TCRBD02-01	TCRBJ02-05
	$CDR3_{DNA2.2}$	CTGACAGTGACCAGTGCCCATCCTGAAGACAGCAGCTTCTACATCTGCAGTGCCCGGGGTCCGGAAGAGACTCAGTACTTCGGGCCAGGCACGCGGCTC	1	0.000162	TCRBV20	TCRBD02-01	TCRBJ02-05

Fig. 2 | TIL CDR3 sequences also present in peripheral PBMCs and cfDNA for patient 12 at t0 and week 3. Displayed are the DNA sequences (CDR3DNA1.1–4) and their paired predicted protein sequences (CDR3prot1–4) for the TCRs that were identified in the pre-treatment tumor biopsy and also in the periphery, either in t0 or week-3 PBMCs or in week-3 cfDNA. For the proteins, the different CDR3 sequences are color coded, with CDR3prot1 in red, CDR3prot2 in purple, CDR3prot3 in green and CDR3prot4 in blue. The black text is the flanking TCR protein sequence. The red underlined bases in CDR3DNA1.2 highlight that CDR3DNA1.1 and CDR3DNA1.2 encode the same protein. Similarly, the red underlined base in CDR3DNA2.2 highlights that CDR3DNA2.1 and CDR3DNA2.2 encode the same protein. [a]CDR3 sequence count in the biopsy. [b]CDR3 sequence frequency in the sample.

used high dimensional FACS to characterize peripheral T cell subsets and monitor T cell evolution under CPI treatment (Extended Data Fig. 2). We found that a $CD8^+$ memory effector cytotoxic T cell subset (T_{IE} cells) expanded proportionally to the cfDNA Δ_{W3}RES (Fig. 4a). T_{IE} cells are characterized by the surface phenotype $CD3^+CD4^-CD8^+CD45RA^-CD45RO^{high}CD27^-CCR7^-$ (Extended Data Fig. 1k) and have been shown to be associated with response to infections[21,22].

To study cytotoxic T cell turnover, we sequenced the *TCR* in t_0 and week-3 purified $CD8^+$ peripheral memory and naïve T cells from three patients with progressive disease and three patients with disease control (12, 16–19 and 29). More than other peripheral T cell subsets, the T_{IE} cells had the highest similarity to cfDNA *CDR3* sequences (Fig. 4b) and presented the highest clonality (Fig. 4c). This suggests that T_{IE} cells are actively turning over, but with convergence towards dominant clones. Moreover, although it is not yet possible to establish whether the T_{IE} cell CDR3 regions recognized neo-epitopes, largely these cells did not express TCRs known to recognize public epitopes such as Melan-A or viral proteins (Supplementary Table 3). In patient 12, from whom we obtained a biopsy, we identified identical CDR3 sequences in the tumor and the peripheral T_{IE} cells (Fig. 4d), showing that individual T_{IE} clones coexisted in the tumor and periphery. Moreover, expansion of intratumoral cells with the T_{IE} phenotype has been reported to be associated with responses to CPIs[23], and we used published cytometry by time-of-flight mass spectrometry (CyTOF) data[24] to confirm that T_{IE} cells were resident in melanoma and renal cell carcinoma (immune-responsive tumors), but were negligible in glioblastoma (immune-refractory tumor) and tonsils (Fig. 5a–d).

Next, we analyzed PBMCs from 30 CPI-treated patients with metastatic melanoma from our cohort (1–30) and show that the T_{IE} cells expanded at week 3 in patients who achieved disease control, including late responders, but not patients with progressive disease ($P=0.0007$; Fig. 6a), irrespective of the therapy protocol ($P=0.200$; Fig. 6b). Notably, despite a week-3 T_{IE} expansion of ~20%, the week-12 computed tomography scan revealed that patient 20 was progressing (Fig. 6a). Unfortunately, the patient died of complications so a late response could not be measured, but from day 40 we observed a steady decline in this patient's $NRAS^{Q61R}$ circulating tumor DNA[25] (Fig. 6c), revealing that consistent with the observed expansion in T_{IE} cells, the patient achieved a biochemical response (Fig. 6c). An increase of >0.8% in the T_{IE} ratio relative to all $CD8^+$ memory T cells at week 3 was associated with increased overall survival and segregated disease control (including late responders) from patients with progressive disease, with a sensitivity of 0.94 and a specificity of 0.79 (accuracy = 0.87; area under the curve = 0.85) (Fig. 6d). The hazard ratio for patients without week-3 T_{IE} expansion was 3.7 (95% confidence interval: 1.12–11.9; $P=0.032$) (Fig. 6e). We confirmed these observations in an independent cohort of 20 CPI-treated patients (31–50; Fig. 6f,g), with a sensitivity of 0.82 and a specificity of 1 (accuracy = 0.90; area under the curve = 0.92). By week 9, T_{IE} cells no longer discriminated patients with disease control from patients with progressive disease (Extended Data Fig. 4a). Accordingly, when we analyzed published CyTOF data[3], we confirmed T_{IE} to be a distinct T cell subset in PBMCs of patients with metastatic melanoma (Extended Data Fig. 4b,c), but consistent with our findings, the T_{IE} levels at week 12 did not distinguish patients with disease control from patients with progressive disease (Extended Data Fig. 4d). Thus, changes at week 3 were prognostic for melanoma responses to CPI, but were no longer prognostic by week 9 or week 12, showing the dynamic nature of these responses, and consistent with a previous study showing that the peak of immune activation is at week 3 (refs. [7,10]).

We note that the week-3 T_{IE} expansion identified patients who achieved disease control early during treatment with superior accuracy to the week-3 peripheral T lymphocyte invigoration-to-tumor burden ratio (Ki67/TB), where the accuracy was 0.64 (16/24 patients with Ki67/TB > 1.94 had an objective response compared with 3/17 patients with Ki67/TB < 1.94)[7]. We also note that the week-3 T_{IE} expansion also had greater accuracy than programmed death-ligand 1 (PD-L1) staining in pre-treatment melanoma biopsies where the accuracy in a phase III clinical trial was 0.67 (78/148 patients with $PD\text{-}L1^+$ biopsy had an objective response compared with 89/270 patients with $PD\text{-}L1^-$ biopsy)[26].

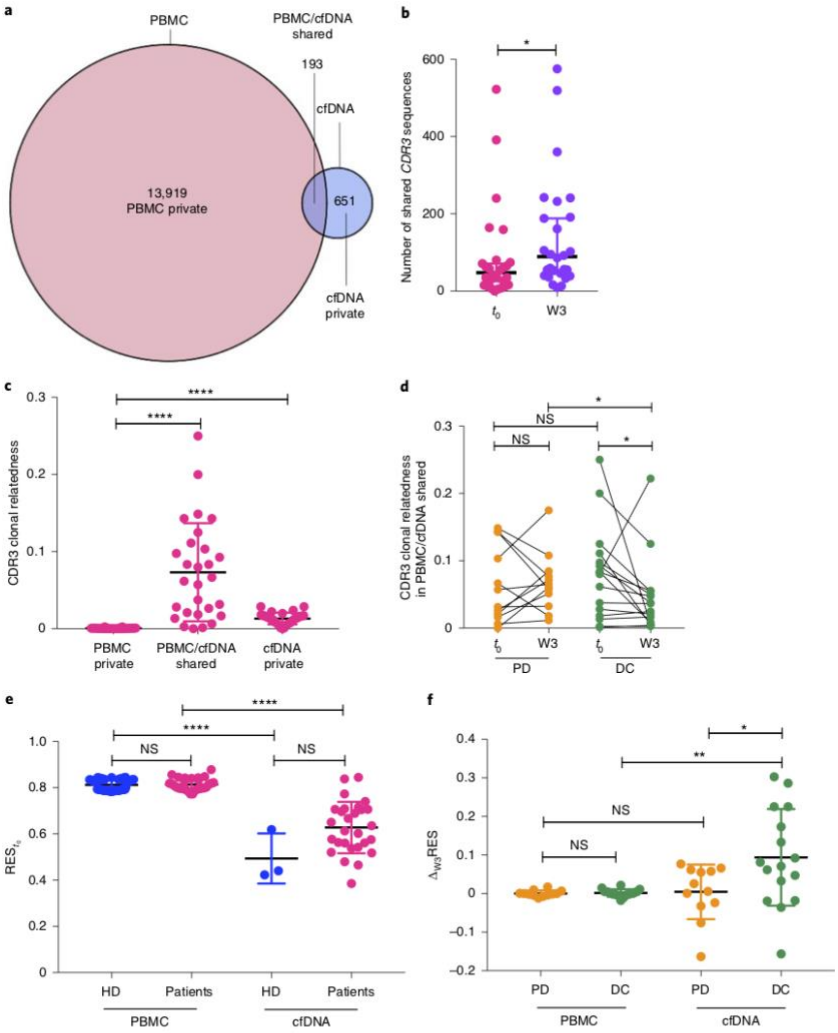

Fig. 3 | CPI treatment induced peripheral T cell turnover. a, Venn diagram showing unique predicted productive *CDR3* sequences in PBMC (pink), PBMC/cfDNA-shared (intersection; purple) and cfDNA pools (blue) for patient 27 at t_0 (Supplementary Table 2). **b**, Total number of *CDR3* clones at t_0 (pink) and week 3 (purple) in the PBMC/cfDNA-shared pool (*$P = 0.010$; two-sided Wilcoxon test). **c**, Clonal relatedness (maximum edit distance = 3 amino acids) for CDR3 in the PBMC-private, PBMC/cfDNA-shared and cfDNA-private pools at t_0. ****$P < 0.0001$ for both comparisons (two-sided Wilcoxon test; median = 0.3×10^{-3} for PBMC-private; 0.01 for cfDNA-private; and 0.06 for PBMC/cfDNA-shared). **d**, Clonal relatedness of CDR3 sequence in the PBMC/cfDNA-shared pool at t_0 and week 3 for patients with progressive disease ($n = 12$; orange) or disease control ($n = 16$; green) at week 12. For patients with progressive disease versus those with disease control, $P = 0.623$ at t_0 (median = 0.04 and 0.08, respectively) and *$P = 0.026$ at week 3 (median = 0.06 and 0.03, respectively) (both two-sided Mann–Whitney *U*-test). For t_0 versus week 3, $P = 0.733$ for patients with progressive disease and *$P = 0.039$ for patients with disease control (both two-sided Wilcoxon test). **e**, Pre-treatment *TCR* RES (RES_{t_0}) of rearranged *CDR3* in healthy donors (HD) and patients on CPI treatment, in PBMC DNA and cfDNA. For healthy donors versus patients, $P = 0.445$ for PBMC DNA (median = 0.83 and 0.81, respectively; $n = 77$ replicates from 4 healthy donors; $n = 29$ patients) and $P = 0.09$ for cfDNA (median = 0.44 and 0.62, respectively; $n = 3$ healthy donors; $n = 28$ patients) (both two-sided Mann–Whitney *U*-test). For PBMC DNA versus cfDNA, $P < 0.0001$ for healthy donors (two-sided Mann–Whitney *U*-test) and $P < 0.0001$ for patients (two-sided Wilcoxon test). **f**, Δ_{W3}RES according to response group at week 12. **$P = 0.008$ (two-sided Wilcoxon test; median = 0.001 and 0.08, respectively, for PBMC and cfDNA). *$P = 0.037$ (two-sided Mann–Whitney *U*-test; median = 0.02 and 0.08, respectively, for progressive disease and disease control). The total number of patients with melanoma was 28. Each dot represents one patient, error bars show s.d., connecting lines show paired samples and horizontal lines represent median values.

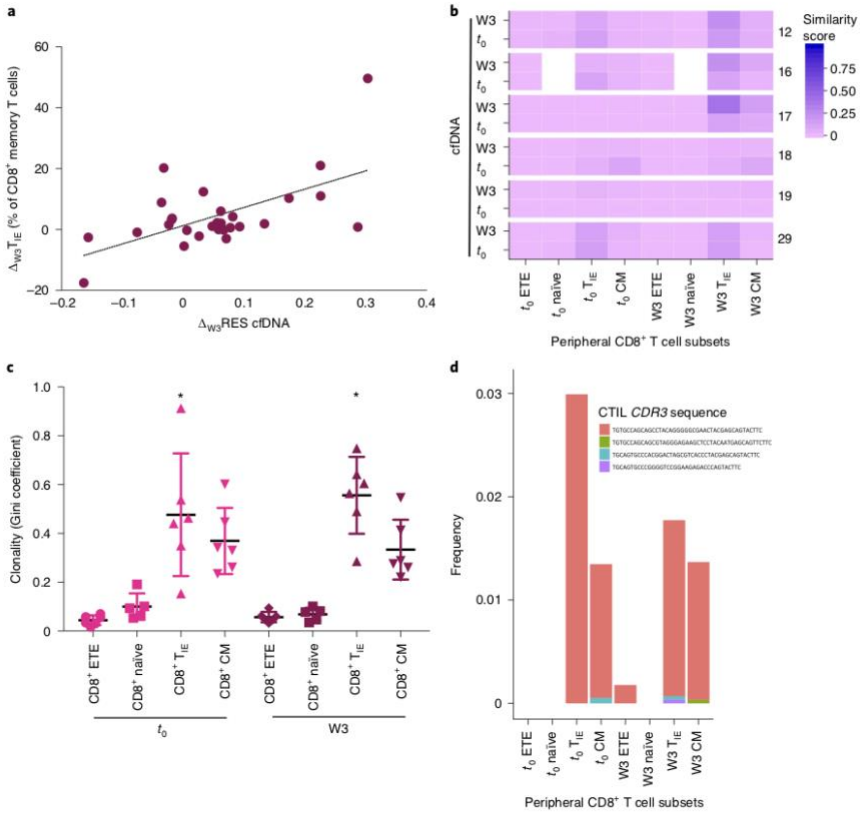

Fig. 4 | Identification of T_{IE} cells. a, Correlation between T_{IE} cell abundance ($\Delta_{W3}T_{IE}$) and cfDNA Δ_{W3}RES ($P = 0.001$; linear regression, $R^2 = 0.34$; $n = 28$ patients). The dotted line is the linear regression line. **b**, Similarity matrix of *TCR* sequences in cfDNA and peripheral CD8+ T cell subsets in six patients. Median similarity scores for central memory (CM) cells, T_{IE} cells, naïve cells and ETEs at t_0 were 0.026, 0.045, 0.004 and 0.003, respectively ($P = 0.0013$; Friedman analysis of variance; Friedman statistic = 15.64). Median similarity scores at week 3 were 0.043, 0.136, 0 and 0.003, respectively ($P < 0.0001$; Friedman analysis of variance; Friedman statistic = 23.05). The naïve subset was not assessed for patient 16 at either time point. **c**, Clonality (Gini coefficient) in peripheral CD8+ T cell subsets. The median T_{IE} subset clonality relative to the other subsets was 0.46 at t_0 and 0.61 at week 3 (after the first cycle of CPI) in six matched patient samples (*$P = 0.0006$ and *$P = 0.0002$, respectively; Friedman analysis of variance; Friedman statistics = 12.6 and 13.08, respectivley). Again, the naïve subset not assessed in patient 16. Horizontal lines show median values and error bars represent s.d. The small sample size did not allow for comparison between responders (patients 16–18) and those whose disease progressed (patients 12, 19 and 29). **d**, Graph showing the frequency of pre-treatment TIL *CDR3* sequences in sorted peripheral CD8+ T cell subsets of patient 12 at t_0 and week 3. Data points in **a** and **c** represent individual patients.

Next, we analyzed published single-cell RNA expression and protein sequencing (REAP-Seq) data from healthy donors[27] and found that T_{IE} cells have the additional surface phenotype CD69$^+$PD1$^{low/dim}$TIGIT$^+$CD25$^{+/-}$CD155$^+$CD40$^{med/high}$CD154$^{med/high}$CD357$^{med/high}$ and a distinct transcriptome signature including immune activation genes (cluster 9 in Extended Data Fig. 5a,b and Supplementary Table 4). Our analysis of these data also showed that T_{IE} cells expanded from healthy donor CD8+ naïve PBMCs following in vitro stimulation, and that they expressed genes associated with immune effector function (Extended Data Fig. 5c,d). Using FACS analysis of five patients' PBMCs (1, 24, 29, 42 and 54), we observed a trend for T_{IE} reinvigoration (increased Ki67+ expression) after one cycle of CPI treatment (Extended Data Fig. 6a), although the limited sample size could not support robust conclusions. Note that the week-3 T_{IE} expansion was not associated with toxicity, but expansion of a separate T regulatory (T_{reg}) subset characterized by the surface phenotype CD3$^+$CD4$^+$CD8$^-$CD25$^+$CD127$^{-/low}$ (ref. [28]) correlated with toxicity grade (Fig. 7a,b).

CPIs induce peripheral T cell repertoire rearrangements. Our findings revealed intriguing parallels between immune responses to infection[21,22] and CPI treatment, and we hypothesized that immune responses to CPIs mirror the defense against pathogens. To test this, we compared T cell repertoire rearrangements in people receiving vaccination or CPIs. Using published data[29,30], we calculated T cell clonality (measures clone dominance) and diversity (indicates heterogeneity) and note that 1–2 weeks after antiviral vaccines were administered, healthy donor TCR repertoires presented bifurcated

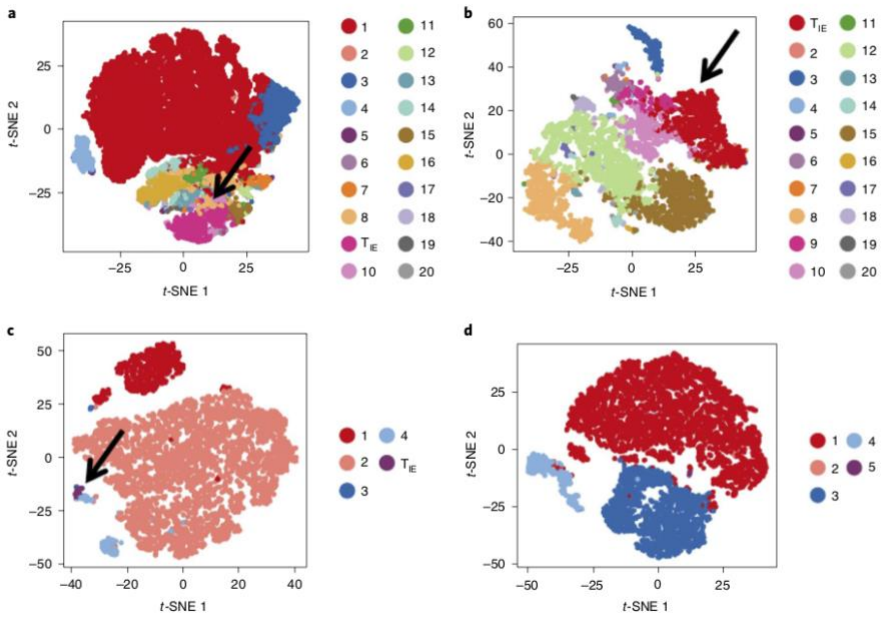

Fig. 5 | T_{IE} cells infiltrate tumors that respond to immunotherapy. a–d, *t*-distributed stochastic neighbor embedding (*t*-SNE) plots of biopsy cell clusters (numbered and color coded) according to T cell surface markers in: (**a**) melanoma ($n=18$ patient samples); (**b**) renal cell carcinoma ($n=3$ patient samples); (**c**) glioblastoma ($n=3$ patient samples); and (**d**) non-cancerous tonsils ($n=4$ patient samples). Samples for this analysis were from ref. [24]. Black arrows highlight the clusters with the T_{IE} phenotype.

reorganization with either increased clonality or increased diversity (Fig. 8a). Next, we compared clonality (Δ_{W3}clonality) and diversity (Δ_{W3}diversity) in t_0 and week-3 PBMCs from 17 CPI-treated patients with metastatic melanoma (11–27). In patients who went on to achieve disease control at week 12, we observed bifurcated reorganization of the TCR repertoire, with substantially increased clonality or diversity, whereas no such response occurred in patients with progressive disease (Fig. 8b). Using our training cohort, we developed a linear discriminant analysis (LDA) algorithm that at week 3 classified patients according to response (assessed at week 12) with an accuracy of 0.9 (specificity = 1; sensitivity = 0.8). We validated these findings in an independent cohort of 27 patients with advanced melanoma[7,18], and again found a bifurcated TCR repertoire reorganization in patients with disease control, but not patients with progressive disease (Fig. 8c). Our LDA accuracy for response prediction was 0.77 in this validation cohort.

Discussion

We examined how the selective pressure of a single cycle of CPIs affects peripheral T cell evolution in patients with previously untreated metastatic melanoma. We found that CPIs induced immune awakening that was revealed by increased levels of productive *CDR3* sequences released into the blood, and dynamic changes in the TCR repertoire. CPIs did not affect thymic output but did induce peripheral T cell turnover, and this correlated with the expansion of a $CD8^+$ cytotoxic memory effector subset that was $CCR7^-CD27^-$. This subset of lymphocytes is involved in cytotoxic response to infections[31,32] and we have now established that they are also associated with CPI responses. Immune effector cells are the cells of the immune system that support anticancer immune surveillance[33], and since our data identified a specific T cell subset involved in this network, we called them T_{IE} cells.

It was recently shown that following CPI treatment, the expansion of tumor-infiltrating T cell clones did not come from pre-existing TILs[34], but rather from novel clonotypes, most probably in the peripheral compartment. Those observations are consistent with a model in which the tumor is an open compartment with active cross-talk with the peripheral immune system; accordingly, in responding patients, we observed a significant early T cell repertoire rearrangement in the fraction of TILs circulating in the blood, which we call tePBMCs.

Clonotype modulation by checkpoint blockade has been described previously (largely in the tumor microenvironment[7,35–37]), but we determined that the pattern of peripheral turnover and overall repertoire rearrangement of T cells in blood identify the patients with an effective immune awakening who will go on to respond to CPI treatment. It has also been shown in animal models that anti-CTLA4 and anti-PD1 drugs induce distinct cellular reactions[38]. That we did not observe significant differences between single-agent and anti-PD1/CTLA4 combined therapy supports that our observations reflect the final effects needed for tumor elimination, and importantly we showed that these changes could be detected in the periphery. Although we could not determine whether the T cell clones driving these changes were melanoma specific, or whether this reflected a general, off-target immune activation, our results nonetheless contribute to our understanding of the dynamics of immune system evolution after one cycle of CPI treatment. That these responses also occur with infection could limit specificity in the CPI setting, necessitating further kinetic analysis and clinical validation, but our results have established that these responses

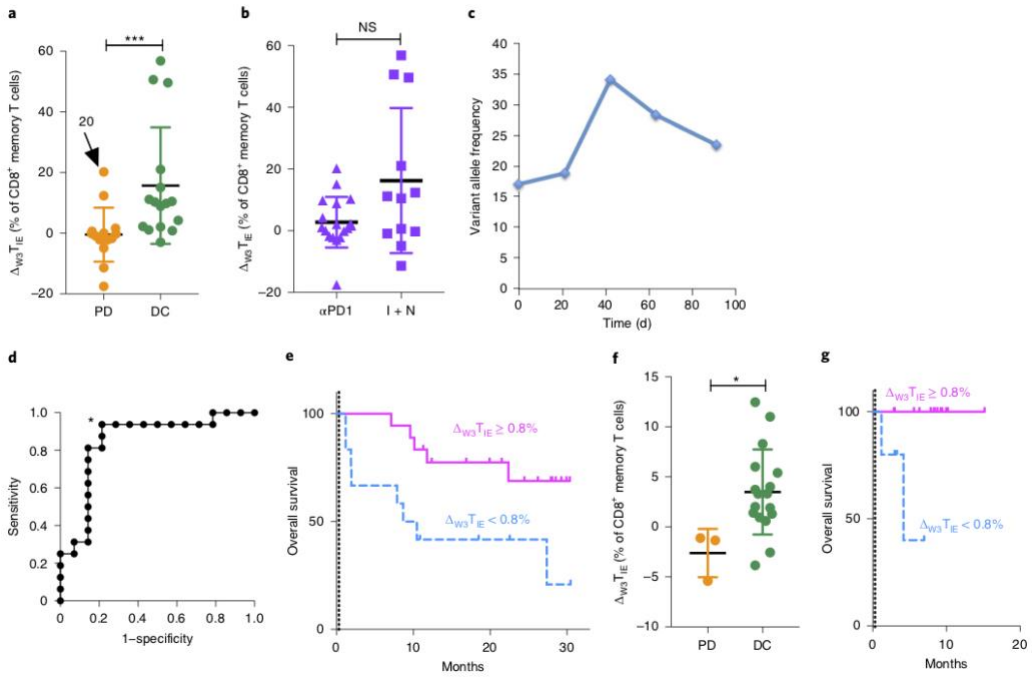

Fig. 6 | Peripheral T_{IE} cell expansion in response to first-line CPI treatment. a, $\Delta_{W3}T_{IE}$ in patients with best-response progressive disease (orange; $n=14$; median = −0.58%) or best-response disease control (green; $n=16$; median = 10.04%) in the training set. ***$P=0.0007$ (two-sided Mann–Whitney *U*-test). The arrow points to patient 20. **b**, $\Delta_{W3}T_{IE}$ in patients receiving anti-PD1 monotherapy (αPD1; $n=18$; median = 1.35%) or a combination of ipilimumab and nivolumab (I + N; $n=12$; median = 10.84%). $P=0.2$ (two-sided Mann–Whitney *U*-test). **c**, Variations over time (days from treatment initiation) in the variant allele frequency of mutant *NRAS*^{Q61R}, as measured in circulating tumor DNA by ddPCR over the course of CPI treatment for patient 20 (arrow in **a**). Blood collection ceased after day 90 due to patient complications leading to patient death. **d**, Receiver operating curve showing the sensitivity and false positive rate (1 − specificity) of $\Delta_{W3}T_{IE}$ values in identifying the patients that would achieve disease control. The asterisk indicates maximum accuracy (cut-off = +0.8%). **e**, Kaplan–Meier survival curves for patients with T_{IE} expansion ≥ 0.8% (pink; $n=12$; median survival not reached) at week 3 compared with patients with T_{IE} expansion < 0.8% (blue; $n=18$; median survival = 9.6 months) in the training set. $P=0.013$ (log-rank test). **f**, $\Delta_{W3}T_{IE}$ in patients with best-response progressive disease (orange; $n=3$; median = −1.3%) or best-response disease control (green; $n=17$; median = 3.3%) in the validation set. *$P=0.019$ (two-sided Mann–Whitney *U*-test). **g**, Kaplan–Meier survival curves for patients with T_{IE} expansion ≥ 0.8% (pink; $n=15$; median survival not reached) at week 3 compared with patients with T_{IE} expansion < 0.8% (blue; $n=5$; median survival = 4.2 months) in the validation set. $P=0.003$ (two-sided log-rank test). Dots represents individual patients, *n* represents the number of patients, horizontal lines show median values and error bars represent s.d. In **e** and **g**, dotted vertical line is landmark at week 3.

could provide tractable tools for the delivery of precision immunotherapy. Moreover, our hypothesis-generating results contribute to improved understanding of immune system biology and could have broader implications beyond the oncoimmunology field.

Note that CCR7 and CD27 were downregulated in T_{IE} cells and that phenotype has been associated with differentiated effector T cell release from lymph nodes to the periphery[39–42]. Also, in line with previous observations that in vitro stimulation of CD8$^+$ T cells induced downregulation of CD27 and CCR7 (refs. [43,44]), our analysis of previous data showed that T_{IE} cells expanded following in vitro stimulation. Our data also showed that the expansion of these cells after one cycle of CPI identified the patients for whom therapy overcame melanoma-induced immune suppression. Within the scope of this study, we have not analyzed the antitumor reactivity of T_{IE} cells, but our data show that peripheral T_{IE} clones infiltrated melanoma and represent an abundant fraction of tumor-infiltrating lymphocytes with high repertoire clonality. The T_{IE} cells were also in active turnover. The relatively small size of our sample could limit the generalization of our results, but both T_{IE} cell and TCR peripheral repertoire reorganization could identify which patients will benefit from CPI treatment with greater accuracy than standard biopsy PD-L1 staining or Ki67/TB. Future research will investigate the antitumor cytotoxicity and specificity of these cells, and their potential for clinical development.

In summary, here we identified a peripheral blood early immune signature characterized by significant rearrangements of the peripheral T cell repertoire and by turnover of specific T cell subsets. Critically, the magnitude of the immune signature changes after the first cycle of therapy anticipated which patients would go on to respond, and were detected in the blood, providing the advantages inherent in minimally invasive liquid biopsies. Although further studies are required to determine the mechanisms underpinning our observations and their specificity for CPI-induced responses, our research provides a strategy to analyze immune cell evolution under the selective pressure of CPIs. Our findings advance our knowledge of immune system responses to immunotherapy and,

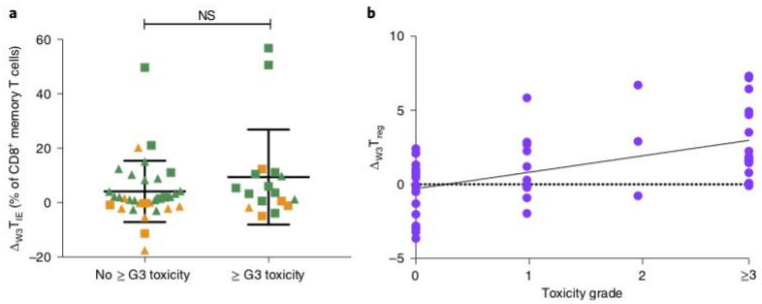

Fig. 7 | Expansion of a peripheral regulatory T cell subset associated with toxicity. a, Graph showing $\Delta_{W3}T_{IE}$ in patients without (median = 1.6; $n = 33$) or with greater than or equal to grade 3 (G3) toxicity (median = 3.72; $n = 17$). $P = 0.347$ (two-sided Mann–Whitney U-test). Lines show median values, error bars represent s.d. and data points represent individual patients (orange: progressive disease; green: disease control; triangles: single-agent anti-PD1; squares: combination ipilimumab + nivolumab). **b**, Expansion of $CD3^+CD4^+CD8^-CD25^+CD127^{-/low}$ T_{reg} cells (Extended Data Fig. 2g) at week 3 ($\Delta_{W3}T_{reg}$) according to toxicity at any time between 2 weeks and 6 months ($P < 0.0001$; $n = 50$; two-sided linear regression analysis, $R^2 = 0.29$). The dotted line is the linear regression line. In **a** and **b**, n represents the number of patients.

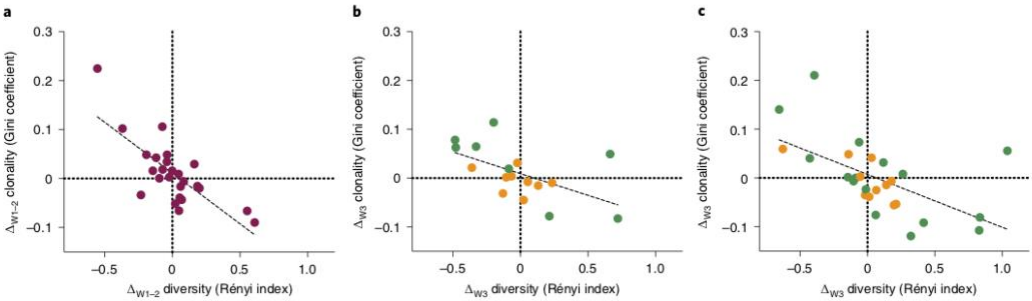

Fig. 8 | TCR repertoire evolution after immune stimulation. a, Changes in *CDR3* clonality (Δ_{W1-2}clonality; Gini coefficient) and diversity (Δ_{W1-2}diversity; Rényi index; $\alpha = 1$) in peripheral T cells from t_0 to weeks 1 and 2 in healthy donors who received antiviral vaccination ($n = 25$ healthy donor samples). **b**, Changes in *CDR3* clonality (Δ_{W3}clonality; Gini coefficient) and diversity (Δ_{W3}diversity; Rényi index; $\alpha = 1$) in peripheral T cells from t_0 to week 3 in the training cohort (The Christie NHS Foundation Trust) of patients with advanced melanoma receiving first-line anti-PD1-based immunotherapy ($n = 17$ patients) who progressed ($n = 9$ patients) or responded ($n = 8$ patients) at week 12. **c**, Changes in *CDR3* clonality (Δ_{W3}clonality; Gini coefficient) and Δ_{W3}diversity (Rényi index; $\alpha = 1$) in peripheral T cells from t_0 to week 3 in the validation cohort (The Christie NHS Foundation Trust, Huang et al.[7] and Amaria et al.[38]; $n = 12$, $n = 4$ and $n = 11$ patients, respectively) of patients with advanced melanoma who progressed ($n = 11$ patients) or responded ($n = 16$ patients) at week 12 of anti-PD1-based treatment. Each dot represents one healthy donor or patient sample (orange: patients who progressed after 12 weeks of immunotherapy; green: patients who achieved disease control after 12 weeks of immunotherapy). Dotted lines are linear regression lines.

critically, they provide a potentially tractable tool to identify which patients will benefit from CPIs early during treatment. This could help clinicians to stratify their patients more effectively to thereby improve personalization of therapeutic planning.

Methods

Patient samples. Blood samples from patients and healthy donors were collected under Manchester Cancer Research Centre (MCRC) Biobank ethics application 07/H1003/161+5 with written informed consent from the patients at The Christie NHS Foundation Trust. The study was approved by MCRC Biobank Access Committee application 13_RIMA_01. All clinical investigations were conducted according to the principles expressed in the Declaration of Helsinki and good clinical practice guidelines. A total of 54 patients with metastatic melanoma, treated with either pembrolizumab or nivolumab plus ipilimumab as first-line therapy, as per the standard of care, were included in the study. The inclusion criterion was a diagnosis of metastatic melanoma. Exclusion criteria were previous systemic oncological treatment in the neoadjuvant, adjuvant or metastatic setting for melanoma or other cancers, concomitant therapy with immunosuppressant drugs at enrollment and synchronous other active malignancies. With the exception of two patients who had rapid, severe unequivocal clinical disease progression (patient 11, who then died, and patient 3, who was switched to BRAF targeted therapy) before the scheduled re-evaluation, response to treatment was assessed at 12 weeks after the first cycle infusion by radiographic imaging using RECIST 1.1 (week 12 response). For late response evaluation, progression was confirmed or excluded after an additional 12 weeks of treatment (best response). Disease control was defined as complete response, partial response or stable disease. Toxicity was measured according to the Common Terminology Criteria for Adverse Events version 4.0.

PBMC and plasma extraction. PBMCs were isolated from blood samples using Lymphoprep (STEMCELL Technologies) and SepMate tubes (STEMCELL Technologies) as per the manufacturer's instructions. Red cell lysis was performed with RBC Lysis Buffer (BioLegend) as per the manufacturer's instructions. The DNA of PBMCs and sorted $CD3^+$ T cell subsets was extracted using QIAamp DNA Blood Mini kits (Qiagen) as per the manufacturer's instructions.

cfDNA analyses. Extraction and quantification of cfDNA was carried out as described previously[45] for patients 11–27 and 29–39.

FACS analysis. Following isolation, PBMCs from patients 1–50 were kept at 4 °C in phosphate buffered saline plus 2% fetal bovine serum (FBS) and analyzed within 24 h. PBMCs were suspended in FACS buffer (phosphate buffered saline containing 2% FBS, 2 mM EDTA and 0.02% sodium azide) plus 50 µl Brilliant Stain Buffer (BD Biosciences) and Human TruStain FcX (BioLegend) as per the manufacturers' instructions, and incubated at room temperature for 40 min with T_{reg} and $T_{maturation}$ panels of fluorochrome-labeled antibodies. The T_{reg} panel consisted of CD3 (1:100; catalog number 317336), CD4 (1:100; catalog number 317438), CD8a (1:40; catalog number 300914), CD25 (1:10; catalog number 302610) and CD127 (1:40; catalog number 351304), whereas the $T_{maturation}$ panel consisted of CD3 (1:100; catalog number 317337), CD4 (1:100; catalog number 317438), CD8a (1:40; catalog number 300906), CD45RA (1:100; catalog number 304130), CD45RO (1:200; catalog number 304228), CD31 (1:40; catalog number 303118), CD27 (1:200; catalog number 356410) (all from BioLegend) and CCR7 (1:20; catalog number 560765; BD Pharmingen). LIVE/DEAD Fixable Blue Dead Cell Stain (Thermo Fisher Scientific) was added to the final suspension to exclude dead cells. Stained PBMCs were washed once at 300*g* for 7 min in FACS buffer and analyzed using LSR II, LSRFortessa, Aria II or Aria III (Special Order Research Product) (BD Biosciences) cytometers and FlowJo software (version 10; Tree Star). $CD8^+$ T cell subsets were live sorted with Aria III and frozen before DNA extraction.

For $T_{reinvigoration}$ staining (performed for patients 1, 24, 29, 42 and 54), PBMCs previously frozen in FBS + 10% dimethyl sulfoxide were thawed in cold RPMI and washed twice. Then, PBMCs were suspended in FACS buffer and Human TruStain FcX (BioLegend), as per the manufacturer's instructions, and incubated at room temperature for 40 min with antibodies targeting CD3 (1:100; catalog number 317337), CD4 (1:100; catalog number 317438), CD8a (1:40; catalog number 300906), CD45RA (1:100; catalog number 304130), CD45RO (1:200; catalog number 304228), CD27 (1:200; catalog number 356410), PD1 (1:40; catalog number 329939) (all from BioLegend), CCR7 (1:20; catalog number 560765; BD Pharmingen) and LIVE/DEAD Fixable Blue Dead Cell Stain (Thermo Fisher Scientific). Stained PBMCs were then fixed and permeabilized with a Cytofix/Cytoperm kit (BD, catalog number 554714) according to the manufacturer's instructions, and stained for Ki67 (1:20; catalog number 350507; BioLegend) for 30 min at room temperature. Stained cells were resuspended in FACS buffer and analyzed using the LSRFortessa (BD Biosciences) cytometer and FlowJo software (version 10; Tree Star).

In patients 1, 10, 11, 12, 13, 22, 24, 25, 26, 27, 30, 42 and 51–54, an aliquot of PBMCs was frozen in FBS + 10% dimethyl sulfoxide immediately after separation and then thawed and stained with CD3 fluorescent antibody as above; $CD3^+$ cells were sorted with an Aria III (BD Biosciences) and used for TREC quantification.

T_{IE} cells were quantified as the percentage of $CD27^-CCR7^-$ cells in the $CD3^+CD8^+CD45RO^+CD45^-$ gate (Extended Data Extended Data Fig. 1). The gating strategy is shown in Extended Data Fig. 1.

TREC. TREC analysis was performed using frozen PBMCs for patients 1, 10, 11, 12, 13, 22, 24, 25, 26, 27, 30, 42 and 51–54. TREC quantification was performed with droplet digital PCR (ddPCR) using a custom TREC assay (TREC forward primer 5′-CACATCCCTTTCAACCATGCT-3′ at a final concentration of 450 nM, TREC reverse primer 5′-GCCAGCTGCAGGGTTTAGG-3′ at a final concentration of 450 nM and HEX-Black Hole probe 5′-ACACCTCTGGTTTTTGTAAAGGTGCCCACT-3′ at a final concentration of 250 nM, as per Falci et al.[46]; Sigma–Aldrich). For ddPCR, the TREC assay was added to 20 ng DNA from sorted $CD3^+$ peripheral T cells, 11 µl ddPCR Supermix for Probes (NodUTP) (Bio-Rad) and 1.1 µl TERT TaqMan Copy Number Reference Assay (Thermo Fisher Scientific) in a total volume of 22 µl. Droplets were generated and analyzed using the QX200 AutoDG ddPCR system according to the manufacturer's instructions (Bio-Rad). Cycling conditions were 95 °C for 10 min, followed by 40 cycles of 95 °C for 15 s, then 55 °C for 1 min and 50 °C for 2 min. To set up and optimize the assay, we used a TREC-plasmid positive control, which was designed as follows: TREC-plasmid forward primer 5′-AAAGAGGGCAGCCCTCTCCAAGGCAAA-3′ and TREC-plasmid reverse primer 5′-AGGCTGATCTTGTCTGACATTTGCTCCG-3′, as per Richardson et al.[47] (Sigma–Aldrich), were used to amplify the 376-base pair TREC junction from healthy donor PBMC DNA. PCR amplification was performed using Quick-Load Taq 2× Master Mix (NEB) on a Mastercycler Nexus Gradient thermal cycler (Eppendorf). Cycling conditions were 95 °C for 30 s, followed by 30 cycles of 95 °C for 15 s, 60 °C for 30 s, 68 °C for 30 s and 68 °C for 5 min. The resulting amplicon was purified using the QIAquick PCR Purification Kit (Qiagen), TA cloned into the pGEM-T Easy plasmid (Promega) and transformed into competent *Escherichia coli* strain JM109 cells prepared using the Mix & Go *E. coli* Transformation Kit (Zymo Research). Plasmid DNA was purified using the QIAprep Spin Miniprep Kit (Qiagen), and Sanger sequencing using the T7 5′-TAATACGACTCACTCTAGGG-3′ and SP6 5′-ATTTAGGTGACACTATAG-3′ primers was used to confirm correct insert identity. The final plasmid was designated TREC-plasmid.

RNA sequencing. RNA was extracted from a pre-treatment human fresh frozen tumor sample for one patient with available tissue (patient 12) using an AllPrep DNA/RNA kit (Qiagen) according to the manufacturer's instructions. Indexed poly(A) libraries were prepared using 200 ng total RNA and 14 cycles of amplification with the Agilent SureSelect Strand-Specific RNA Library Preparation Kit for Illumina Sequencing (Agilent; G9691B). Libraries were quantified by quantitative PCR using the KAPA Library Quantification Kit for Illumina platforms (Kapa Biosystems; KK4873). Paired-end 100-base pair sequencing was carried out by clustering 15 pM of pooled libraries on the cBot and sequenced on the Illumina HiSeq 2500 in high output mode using TruSeq SBS version 3 chemistry (Illumina). After removing adapters using Cutadapt (version 1.14) and trimming poor-quality base calls using Trimmomatic (version 0.36)[48], the human reads were aligned to GRCh37 (release 75) using STAR (version 2.5.1) aligner[49].

TCR analysis. TCR sequences were inferred from RNA sequencing data from one patient for whom we had a frozen pre-treatment metastasis biopsy sample using ImReP[17].

An immunoSEQ TCRB Assay kit (Adaptive Biotechnologies) was used to amplify and sequence TCR sequences in cfDNA and the DNA of PBMCs as per the manufacturer's instructions. We loaded the same DNA input for all PBMC (350 ng; patients 11–39) and cfDNA samples (40 ng; patients 11–27 and 29–39), while for the sorted T cell subsets (for patients 12, 16, 17, 18, 19 and 29), we loaded all of the DNA extracted from the sorted cells. A metafile is available with each single sample and anonymous patient information from https://gitlab.com/cruk-mi/tcell-immune-awakening. Pooled libraries were quantified by quantitative PCR using the KAPA Library Quantification Kit for Illumina platforms (Kapa Biosystems; KK4873). Sequencing was carried out by clustering 0.6–1.1 pM of pooled libraries on the Illumina NextSeq 500 according to instructions from Adaptive Biotechnologies. Healthy donor PBMC TCR control data were downloaded from the immune ACCESS repository immunoSEQ (Adaptive Biotechnologies; https://doi.org/10.21417/ADPT2017TR). TCR sequencing data were analyzed using immunoSEQ Analyzer (Adaptive Biotechnologies) and the R LymphoSeq package (version 3.4.1; R Foundation for Statistical Computing). Matched paired pre-treatment and week-3 melanoma biopsy and PBMC samples of patients with locally advanced melanoma were downloaded from the referenced accession linked to Amaria et al.[18] (TCR sequencing data were downloaded from the European Genome-phenome Archive (EGA) with the identifier EGAS00001003178 (EGA study accession dataset EGAD00010001608) and the patient clinical history metadata file was downloaded using the identifier EGAD00001004352). Consecutive patients 11–27 from The Christie NHS Foundation Trust constituted the training cohort. The external validation data were pooled from an independent cohort of patients from The Christie NHS Foundation Trust (patients 28–39), a cohort of patients with metastatic melanoma from Huang et al.[7] (PBMC $CD38^+$ plus PBMC $CD38^-$ merged populations from patients 12288, 13471, 14746 and 14835; TCR sequencing data were made available by the authors) and the cohort of patients with locally advanced treatment-naïve melanoma from the referenced accession linked to Amaria et al.[18] (patients 1, 2, 4, 5, 6, 7, 8, 10, 11, 13 and 15; TCR sequencing data were downloaded from EGAS00001003178 (EGA study accession dataset EGAD00010001608); the patient clinical history metadata file was downloaded from EGAD00001004352). The Gini coefficient was used as a measure of clonality[50] and calculated using the function clonality from the LymphoSeq R package. Clonal relatedness was calculated by setting an edit distance of 3, using the clonalRelatedness LymphoSeq function, and similarity was assessed by means of the Bhattacharyya coefficient using the bhattacharyyaMatrix LymphoSeq function. Diversity was calculated using Rényi index ($\alpha = 1$) as per Spreafico et al.[51], with time-point pairwise analysis for each individual patient. LDA (coefficient of linear discriminants LD1: $[\Delta_{W3}\text{Rényi index}]^2 = 5.2$; LD2: $[\Delta_{W3}\text{Gini coefficient}]^2 = 261.3$) and validation to calculate balanced accuracy were performed using the packages MASS and caret in R (version 3.4.1, R Foundation for Statistical Computing). For further details, refer to the extended R scripts available on GitLab (https://gitlab.com/cruk-mi/tcell-immune-awakening).

CyTOF surface phenotype analysis. Differential marker expression analysis was performed on CyTOF data from Krieg et al.[8] and Greenplate et al.[24] downloaded from a publicly available repository (referenced accessions https://flowrepository.org/experiments/1124 and http://flowrepository.org/id/FR-FCM-ZZMC) using the custom workflow described by Nowicka et al.[52]. All analyses on CyTOF data were performed after arcsinh (with a cofactor of 5) transformation of marker expression and correction for the batch effect (function removeBatchEffect; limma R package). The T_{IE} subset was identified by differential expression of the T lymphocytic markers CD3, CD8a, CD45RA, CD45RO, CCR7 and CD27. Cell population clustering was obtained with the R package FlowSOM after the metaclustering step (ConsensusClusterPlus R package).

REAP-Seq single-cell analysis. Differential proteomic and RNA expression analysis was performed on REAP-Seq data from Peterson et al.[27] downloaded from a publicly available repository (referenced accession GSE100501) using the R package Seurat (version 2.4.0)[53]. The single cells with the T_{IE} phenotype were identified based on the expression levels of the antibody-derived tags CD8a, CD45RA, CD45RO, CD27 and CD197 (CCR7) (FetchData command with set conditions based on the expression level; cut-offs for positive/negative and high/low were set based on the normalized data), and the cell identities were used to

define the T_{IE} cluster (SetIdent command). The cell differential expression analysis in the T_{IE} cells from PBMCs versus after in vitro stimulation was performed with the function FindMarkers in the combined Seurat object (RunCCA). The antibody-derived tag data Seurat matrices were imported in Cytobank[54] to analyze the differential representation of the $CD8^+$ subsets under different experimental conditions (Extended Data Fig. 5c).

Statistics and reproducibility. Unless otherwise stated, all statistical tests were two tailed. The statistical differences between two groups for numerical variables were assessed using a two-tailed Mann–Whitney *U*-test (unpaired comparisons) or Wilcoxon test (paired comparisons). The statistical differences between multiple, paired measures were assessed using the Friedman test. Delta values were calculated as the difference between week-3 and t_0 values. The statistical differences of categorical variables between groups were assessed using two-tailed chi-squared or Fisher's exact tests, according to group dimensions. Correlation between continuous variables was assessed with Spearman's test (independent variables) or linear regression (dependent variables). Kaplan–Meier plots with the log-rank test (3-week landmark analysis) were used to analyze survival data. Univariate Cox regression was used to calculate the hazard of death. $P < 0.05$ was considered significant. Cox–Snell residuals were used to verify the proportional hazard hypothesis ($P = 0.141$, with $P > 0.05$ confirming the hypothesis). Sample size calculation was performed using G*Power software[55,56], using the effect size and standard deviation. For the comparison of ΔRES in PBMCs versus cfDNA in patients with disease response, the sample size was $n = 14$ for $\alpha = 0.05$ and $1 - \beta = 0.8$. For the LDA, we used the power and sample size calculation for linear regression with two covariates and an effect size of $f^2 = 0.55$, and the total sample size was calculated as $n = 17$ for $\alpha = 0.05$ and $1 - \beta = 0.8$. For the T cell subset analyses for the T_{IE} cells in patients with progression versus disease control, the total sample size was $n = 32$ for $\alpha = 0.05$ and $1 - \beta = 0.8$. No data were excluded from the analyses. The investigators were blinded during the experiments and outcome assessment was performed after the experiments. Analyses were performed with GraphPad Prism version 7 (GraphPad Software) or R (version 3.4.1; R Foundation for Statistical Computing).

Reporting Summary. Further information on research design is available in the Nature Research Reporting Summary linked to this article.

Data availability

Sample metadata files and custom scripts are available from GitLab (https://gitlab.com/cruk-mi/tcell-immune-awakening). The data from all TCR sequencing performed in this study are deposited in the immuneACCESS repository immunoSEQ (https://doi.org/10.21417/SV2020NM). The RNA sequencing data for patient 12 can be downloaded from EGA (accession code EGAS00001004043). TCR sequencing data for matched pre-treatment and week-3 melanoma biopsy and PBMC samples of patients with locally advanced melanoma[18] re-analyzed here were downloaded from referenced accession EGAS00001003178 (EGA study accession dataset EGAD00010001608). TCR sequencing data of matched pre-treatment and week-3 PBMCs of patients with melanoma from Huang et al.[7] re-analyzed here were made available by the authors. TCR sequencing data of matched pre-treatment and week-3 PBMCs for the cohort of patients with locally advanced treatment-naïve melanoma from referenced accession Amaria et al.[18] re-analyzed here were downloaded from the EGA (accession code EGAS00001003178 (EGA study accession dataset EGAD00010001608)) and the patient clinical history metadata file was downloaded from the EGA via accession dataset EGAD00001004352. PBMC and biopsy CyTOF data from Krieg et al.[8] and Greenplate et al.[24] re-analyzed here were downloaded from referenced accessions https://flowrepository.org/experiments/1124 and http://flowrepository.org/id/FR-FCM-ZZMC, respectively. PBMC REAP-Seq data from Peterson et al.[27] re-analyzed here were downloaded from referenced Gene Expression Omnibus accession GSE100501. The authors confirm that for approved reasons (UK Data Protection Act 2018), some access restrictions apply to the data containing patient medical records (specifically, dates of birth). Source data for Figs. 1–7 and Extended Data Figs. 3–6 are provided with the paper. Additional data that support the findings of this study are available from the corresponding author upon reasonable request.

Code availability

ImmunoSEQ Analyzer (Adaptive Biotechnologies), FlowJo (version 10; Tree Star), Cytobank[54], Trimmomatic (version 0.36)[48] and STAR (version 2.5.1) aligner[49] are published or commercial codes and software programs. Diversity was calculated using the Rényi index ($\alpha = 1$) as per Spreafico et al.[51]. Differential marker expression analysis was performed on CyTOF data using the custom workflow described by Nowicka et al.[52]. Custom R scripts are available from GitLab (https://gitlab.com/cruk-mi/tcell-immune-awakening).

Received: 29 November 2019; Accepted: 17 December 2019;
Published online: 10 February 2020

References

1. Badovinac, V. P., Porter, B. B. & Harty, J. T. Programmed contraction of $CD8^+$ T cells after infection. *Nat. Immunol.* **3**, 619–626 (2002).
2. Ugurel, S. et al. Survival of patients with advanced metastatic melanoma: the impact of novel therapies—update 2017. *Eur. J. Cancer* **83**, 247–257 (2017).
3. Wykes, M. N. & Lewin, S. R. Immune checkpoint blockade in infectious diseases. *Nat. Rev. Immunol.* **18**, 91–104 (2018).
4. Goldszmid, R. S., Dzutsev, A. & Trinchieri, G. Host immune response to infection and cancer: unexpected commonalities. *Cell Host Microbe* **15**, 295–305 (2014).
5. Vance, R. E., Eichberg, M. J., Portnoy, D. A. & Raulet, D. H. Listening to each other: infectious disease and cancer immunology. *Sci. Immunol.* **2**, eaai9339 (2017).
6. Dunn, G. P., Old, L. J. & Schreiber, R. D. The three Es of cancer immunoediting. *Annu. Rev. Immunol.* **22**, 329–360 (2004).
7. Huang, A. C. et al. T-cell invigoration to tumour burden ratio associated with anti-PD-1 response. *Nature* **545**, 60–65 (2017).
8. Krieg, C. et al. High-dimensional single-cell analysis predicts response to anti-PD-1 immunotherapy. *Nat. Med.* **24**, 144–153 (2018).
9. Jacquelot, N. et al. Predictors of responses to immune checkpoint blockade in advanced melanoma. *Nat. Commun.* **8**, 592 (2017).
10. Huang, A. C. et al. A single dose of neoadjuvant PD-1 blockade predicts clinical outcomes in resectable melanoma. *Nat. Med.* **25**, 454–461 (2019).
11. Hozumi, N. & Tonegawa, S. Evidence for somatic rearrangement of immunoglobulin genes coding for variable and constant regions. *Proc. Natl Acad. Sci. USA* **73**, 3628–3632 (1976).
12. Schatz, D. G. & Baltimore, D. Uncovering the V(D)J recombinase. *Cell* **116**, S103–S106 (2004).
13. Janeway C. A. Jr et al. *Immunobiology: The Immune System in Health and Disease* 5th edn (Garland Science, 2001).
14. Kohler, S. & Thiel, A. Life after the thymus: $CD31^+$ and $CD31^-$ human naive $CD4^+$ T-cell subsets. *Blood* **113**, 769–774 (2009).
15. Steinmann, G. G., Klaus, B. & Muller-Hermelink, H. K. The involution of the ageing human thymic epithelium is independent of puberty. A morphometric study. *Scand. J. Immunol.* **22**, 563–575 (1985).
16. Geenen, V. et al. Quantification of T cell receptor rearrangement excision circles to estimate thymic function: an important new tool for endocrine-immune physiology. *J. Endocrinol.* **176**, 305–311 (2003).
17. Mangul, S. M. I. et al. Profiling adaptive immune repertoires across multiple human tissues by RNA sequencing. Preprint at *bioRxiv* https://doi.org/10.1101/089235 (2016).
18. Amaria, R. N. et al. Neoadjuvant immune checkpoint blockade in high-risk resectable melanoma. *Nat. Med.* **24**, 1649–1654 (2018).
19. Coffey, D. LymphoSeq: Analyze high-throughput sequencing of T and B cell receptors. R package version 1.4.1 (2017).
20. Alves Sousa, A. P. et al. Comprehensive analysis of TCR-β repertoire in patients with neurological immune-mediated disorders. *Sci. Rep.* **9**, 344 (2019).
21. Radziewicz, H., Uebelhoer, L., Bengsch, B. & Grakoui, A. Memory $CD8^+$ T cell differentiation in viral infection: a cell for all seasons. *World J. Gastroenterol.* **13**, 4848–4857 (2007).
22. Mahnke, Y. D., Brodie, T. M., Sallusto, F., Roederer, M. & Lugli, E. The who's who of T-cell differentiation: human memory T-cell subsets. *Eur. J. Immunol.* **43**, 2797–2809 (2013).
23. Ribas, A. et al. PD-1 blockade expands intratumoral memory T cells. *Cancer Immunol. Res.* **4**, 194–203 (2016).
24. Greenplate, A. R. et al. Computational immune monitoring reveals abnormal double-negative T cells present across human tumor types. *Cancer Immunol. Res.* **7**, 86–99 (2019).
25. Gremel, G. et al. Distinct subclonal tumour responses to therapy revealed by circulating cell-free DNA. *Ann. Oncol.* **27**, 1959–1965 (2016).
26. Robert, C. et al. Nivolumab in previously untreated melanoma without BRAF mutation. *N. Engl. J. Med.* **372**, 320–330 (2015).
27. Peterson, V. M. et al. Multiplexed quantification of proteins and transcripts in single cells. *Nat. Biotechnol.* **35**, 936–939 (2017).
28. Venken, K. et al. Natural naive $CD4^+CD25^+CD127^{low}$ regulatory T cell (T_{reg}) development and function are disturbed in multiple sclerosis patients: recovery of memory T_{reg} homeostasis during disease progression. *J. Immunol.* **180**, 6411–6420 (2008).
29. Herati, R. S. et al. Successive annual influenza vaccination induces a recurrent oligoclonotypic memory response in circulating T follicular helper cells. *Sci. Immunol.* **2**, eaag2152 (2017).
30. DeWitt, W. S. et al. Dynamics of the cytotoxic T cell response to a model of acute viral infection. *J. Virol.* **89**, 4517–4526 (2015).
31. Martin, M. D. & Badovinac, V. P. Defining memory CD8 T cell. *Front. Immunol.* **9**, 2692 (2018).
32. Tomiyama, H., Takata, H., Matsuda, T. & Takiguchi, M. Phenotypic classification of human $CD8^+$ T cells reflecting their function: inverse correlation between quantitative expression of CD27 and cytotoxic effector function. *Eur. J. Immunol.* **34**, 999–1010 (2004).

33. Rossi, J. F., Ceballos, P. & Lu, Z. Y. Immune precision medicine for cancer: a novel insight based on the efficiency of immune effector cells. *Cancer Commun. (Lond.)* **39**, 34 (2019).
34. Yost, K. E. et al. Clonal replacement of tumor-specific T cells following PD-1 blockade. *Nat. Med.* **25**, 1251–1259 (2019).
35. Cha, E. et al. Improved survival with T cell clonotype stability after anti-CTLA-4 treatment in cancer patients. *Sci. Transl. Med.* **6**, 238ra270 (2014).
36. Robert, L. et al. CTLA4 blockade broadens the peripheral T-cell receptor repertoire. *Clin. Cancer Res.* **20**, 2424–2432 (2014).
37. Wieland, A. et al. T cell receptor sequencing of activated CD8 T cells in the blood identifies tumor-infiltrating clones that expand after PD-1 therapy and radiation in a melanoma patient. *Cancer Immunol. Immunother.* **67**, 1767–1776 (2018).
38. Wei, S. C. et al. Distinct cellular mechanisms underlie anti-CTLA-4 and anti-PD-1 checkpoint blockade. *Cell* **170**, 1120–1133.e17 (2017).
39. Fritsch, R. D. et al. Stepwise differentiation of CD4 memory T cells defined by expression of CCR7 and CD27. *J. Immunol.* **175**, 6489–6497 (2005).
40. Hendriks, J., Xiao, Y. & Borst, J. CD27 promotes survival of activated T cells and complements CD28 in generation and establishment of the effector T cell pool. *J. Exp. Med.* **198**, 1369–1380 (2003).
41. Britschgi, M. R., Link, A., Lissandrin, T. K. & Luther, S. A. Dynamic modulation of CCR7 expression and function on naive T lymphocytes in vivo. *J. Immunol.* **181**, 7681–7688 (2008).
42. Larbi, A. & Fulop, T. From "truly naïve" to "exhausted senescent" T cells: when markers predict functionality. *Cytometry A* **85**, 25–35 (2014).
43. Sallusto, F. et al. Switch in chemokine receptor expression upon TCR stimulation reveals novel homing potential for recently activated T cells. *Eur. J. Immunol.* **29**, 2037–2045 (1999).
44. Geginat, J., Lanzavecchia, A. & Sallusto, F. Proliferation and differentiation potential of human CD8$^+$ memory T-cell subsets in response to antigen or homeostatic cytokines. *Blood* **101**, 4260–4266 (2003).
45. Valpione, S. et al. Plasma total cell-free DNA (cfDNA) is a surrogate biomarker for tumour burden and a prognostic biomarker for survival in metastatic melanoma patients. *Eur. J. Cancer* **88**, 1–9 (2018).
46. Falci, C. et al. Immune senescence and cancer in elderly patients: results from an exploratory study. *Exp. Gerontol.* **48**, 1436–1442 (2013).
47. Richardson, M. W. et al. Analysis of telomere length and thymic output in fast and slow/non-progressors with HIV infection. *Biomed. Pharmacother.* **54**, 21–31 (2000).
48. Bolger, A. M., Lohse, M. & Usadel, B. Trimmomatic: a flexible trimmer for Illumina sequence data. *Bioinformatics* **30**, 2114–2120 (2014).
49. Dobin, A. et al. STAR: ultrafast universal RNA-Seq aligner. *Bioinformatics* **29**, 15–21 (2013).
50. Thapa, D. R. et al. Longitudinal analysis of peripheral blood T cell receptor diversity in patients with systemic lupus erythematosus by next-generation sequencing. *Arthritis Res. Ther.* **17**, 132 (2015).
51. Spreafico, R. et al. A circulating reservoir of pathogenic-like CD4$^+$ T cells shares a genetic and phenotypic signature with the inflamed synovial micro-environment. *Ann. Rheum. Dis.* **75**, 459–465 (2016).
52. Nowicka, M. et al. CyTOF workflow: differential discovery in high-throughput high-dimensional cytometry datasets. *F1000Res* **6**, 748 (2017).
53. Gribov, A. et al. SEURAT: visual analytics for the integrated analysis of microarray data. *BMC Med. Genomics* **3**, 21 (2010).
54. Kotecha, N., Krutzik, P. O. & Irish, J. M. Web-based analysis and publication of flow cytometry experiments. *Curr. Protoc. Cytom.* **53**, 10.17.1–10.17.24 (2010).
55. Faul, F., Erdfelder, E., Lang, A.-G. & Buchner, A. G*Power 3: a flexible statistical power analysis program for the social, behavioral, and biomedical sciences. *Behav. Res. Methods* **39**, 175–191 (2007).
56. Faul, F., Erdfelder, E., Buchner, A. & Lang, A.-G. Statistical power analyses using G*Power 3.1: tests for correlation and regression analyses. *Behav. Res. Methods* **41**, 1149–1160 (2009).

Acknowledgements

We are grateful to the patients who participated to this study and their families. We thank P. Serra-Bellver for help with the collection of patient samples, R. Cox for assistance with preparing the figures, and J. Allen, S. Zelenay and the Molecular Oncology Group for advice. We thank G. Williams for assistance during the TCR sequencing. This work was supported by CRUK (A27412 and A22902), the Harry J. Lloyd Charitable Trust (Career Development Award to S.V.) and the Wellcome Trust (100282/Z/12/Z). The role of the MCRC Biobank is to distribute samples; therefore, it cannot endorse the studies performed or assist in interpretation of the results.

Author contributions

S.V. and R.M. conceived of and designed the study. S.V., N.D. and R.M. developed the methodology. S.V., E.G., P.A.M., A.B., P.M., J.B., J.T., G.G., A.G., S.M., Z.S., F.B., J.W., N.D., P.C.L. and R.M. acquired the data (managed the patients, provided facilities, provided bioinformatics supervision, performed the experiments and so on). S.V., P.A.M., N.D. and R.M. analyzed and interpreted the data (for example, they performed statistical analysis, biostatistics and computational analysis). S.V. and A.B. prepared the figures. S.V., N.D. and R.M. wrote the manuscript with input and final approval from all authors.

Competing interests

R.M. is a consultant for Pfizer and has a drug discovery program with Basilea Pharmaceutica. P.L. serves as a paid advisor/speaker for Bristol-Myers Squibb, Merck Sharp and Dohme, Roche, Novartis, Amgen, Pierre Fabre, Nektar and MelaGenix. P.L. reports travel support from Bristol-Myers Squibb and Merck Sharp and Dohme, and receives research support from Bristol-Myers Squibb. A.G. received honoraria and consultancy fees from Bristol-Myers Squibb and Novartis. The other authors declare no competing interests.

Additional information

Extended data is available for this paper at https://doi.org/10.1038/s43018-019-0022-x.

Supplementary information is available for this paper at https://doi.org/10.1038/s43018-019-0022-x.

Correspondence and requests for materials should be addressed to P.C.L. or R.M.

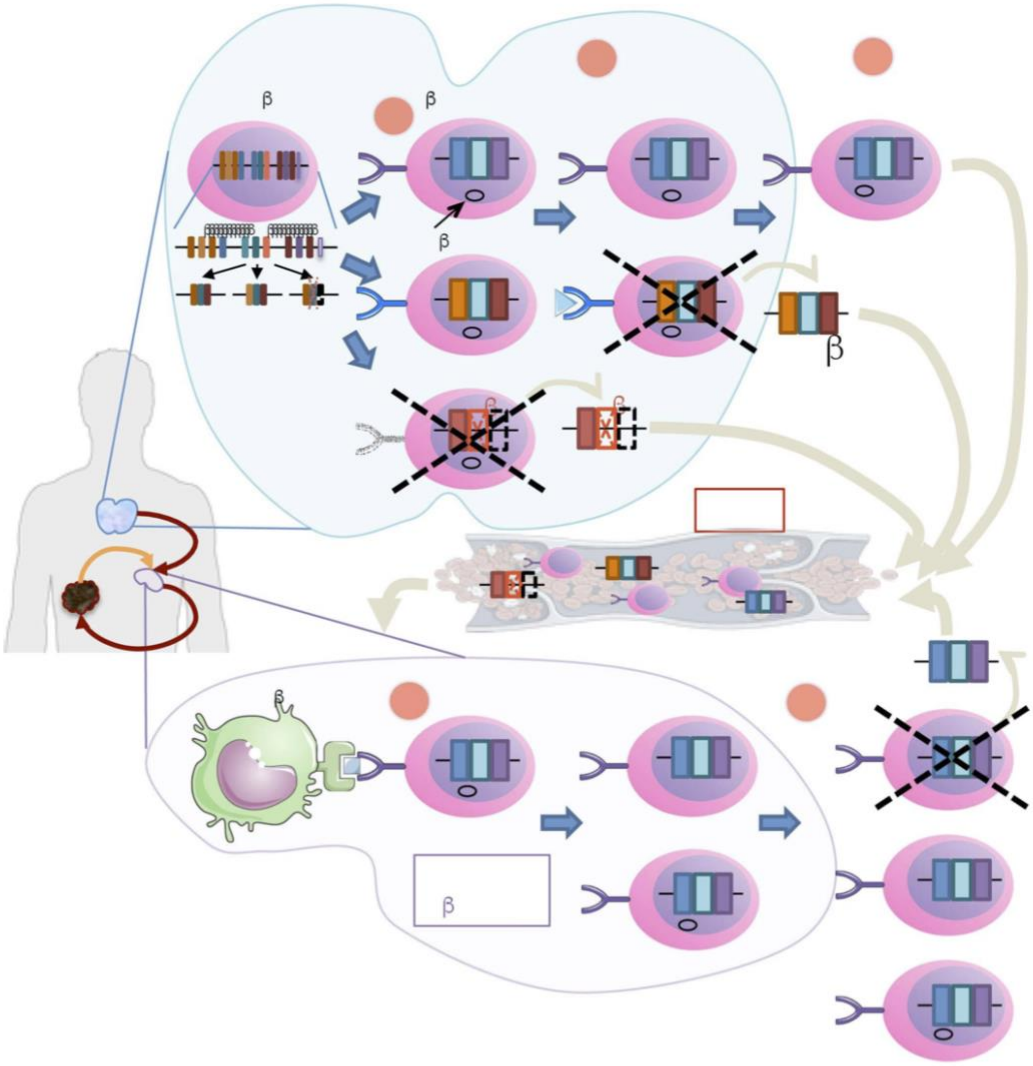

Extended Data Fig. 1 | Schematic summarizing T cell maturation and life-cycle. a Pro-T cells undergo sequential somatic recombination of their T cell Receptor β (*TCR*) loci in attempts to generate functional TCR with unique CDR3 antigen binding regions. Cells that fail to generate a functional TCRβ at the first attempt can recombine their second *TCR* allele, but cells which fail to produce a functional TCR at the end of the process (crossed red box) are eliminated (β-selection) and their DNA, which encodes the *CDR3* unique regions, enters the blood as circulating cell-free DNA (cfDNA). Surviving cells retain the T cell receptor excision circle (TREC) generated during *TCR* locus rearrangement as an episome in the nucleus. The TREC does not replicate so is diluted during subsequent cell divisions. **b** T cells with a functional TCR undergo positive and negative selection (± selection) for HLA and self-antigen recognition. The *CDR3* DNA from T cells eliminated during this step is released into the blood. **c** Naive T cells enter the circulation as early thymic emigrants (ETE). **d** T cells primed by antigen presenting cells (APC) in the lymphatic system undergo clonal expansion, which dilutes the TREC amongst the daughter cells. **e** T cell homeostasis is maintained by subsequent contraction (turnover cycles), releasing further *CDR3* DNA into the blood.

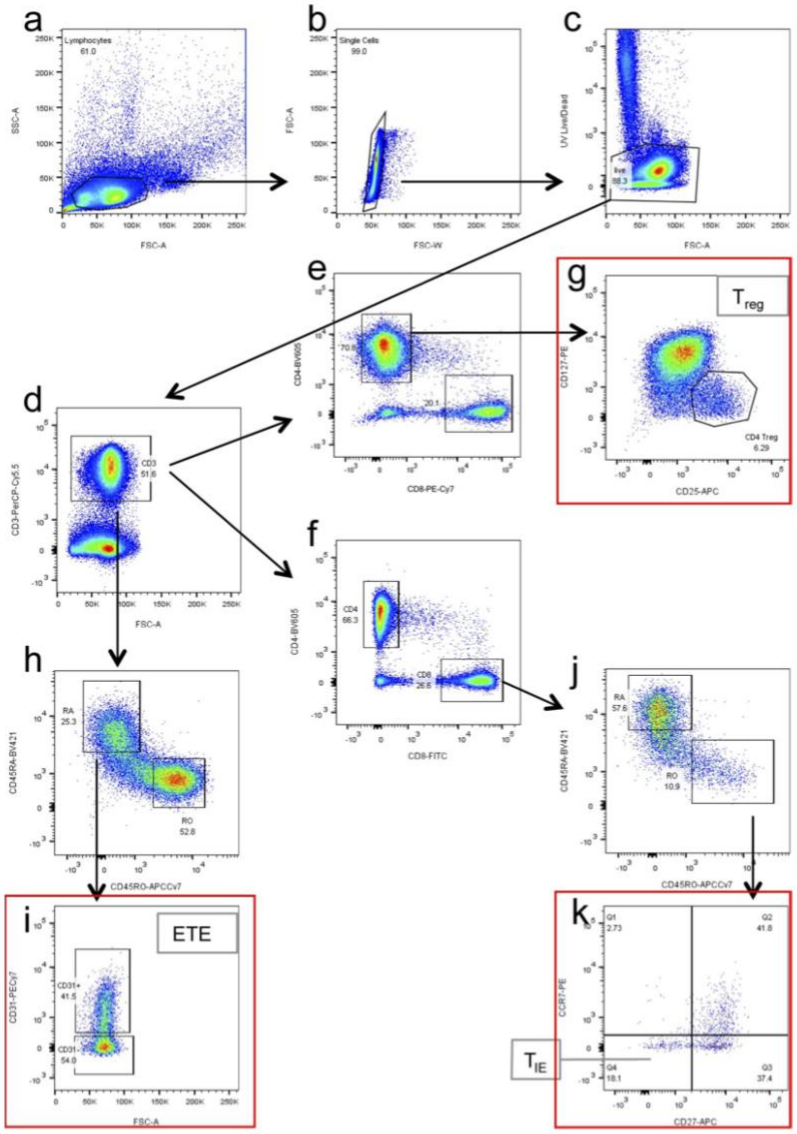

Extended Data Fig. 2 | Gating strategy for the identification of T cell subsets in peripheral blood of melanoma patients. Multiparametric fluorescence activated cell sorting analysis using the indicated gates. **a** Lymphocyte gate on side scatter/forward scatter; **b** single cell gate to exclude doublets; **c** live gating to exclude dead cells from subsequent gates; **d** $CD3^+$ gate for T cells; **e,f** $CD4^+$ and CD8+ gates for "helper" and "killer" T cell subsets, CD8 was detected with a PE-Cy7 labelled antibody for the T_{reg} panel (**e**) and with a FITC labelled antibody for the T maturation panel (**f**); **g** $CD4^+/CD25^+/CD127^{-/low}$ regulatory T cells (T_{reg}); **h** naive (top left) and memory (bottom right) gates total T cells; **i** ETE (top) and $CD31^-$ naive (bottom) gates for naive T cells; **j** naive (top left) and memory (bottom right) gates for $CD8^+$ T cells; **k** $CD8^+$ memory T cell subsets, the left bottom subset ($CCR7^-/CD27^-$) represents the T_{IE} cells.

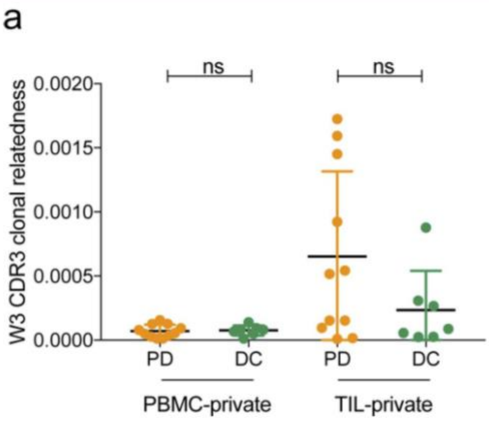

Extended Data Fig. 3 | Clonal relatedness in tumor infiltrating T cells and PBMC. a Clonal relatedness changes in PBMC-private and TIL-private *TCR* pools; comparison of week 3 (W3) *CDR3* clonal relatedness in patients with progressive disease (PD, n=11 patients) and disease control at week 12 (DC, n=7 patients) in the PBMC-private (P=0.724, median=$0.6x10^{-6}$ and $0.6x10^{-6}$, respectively; two-sided Mann-Whitney U test) and TIL-private pools (P=0.246, median= $0.5x10^{-4}$ and $0.8x10^{-5}$, respectively; two-sided Mann-Whitney U test). Dot represents one patient; green indicates DC; orange indicates PD; error bar is standard deviation.

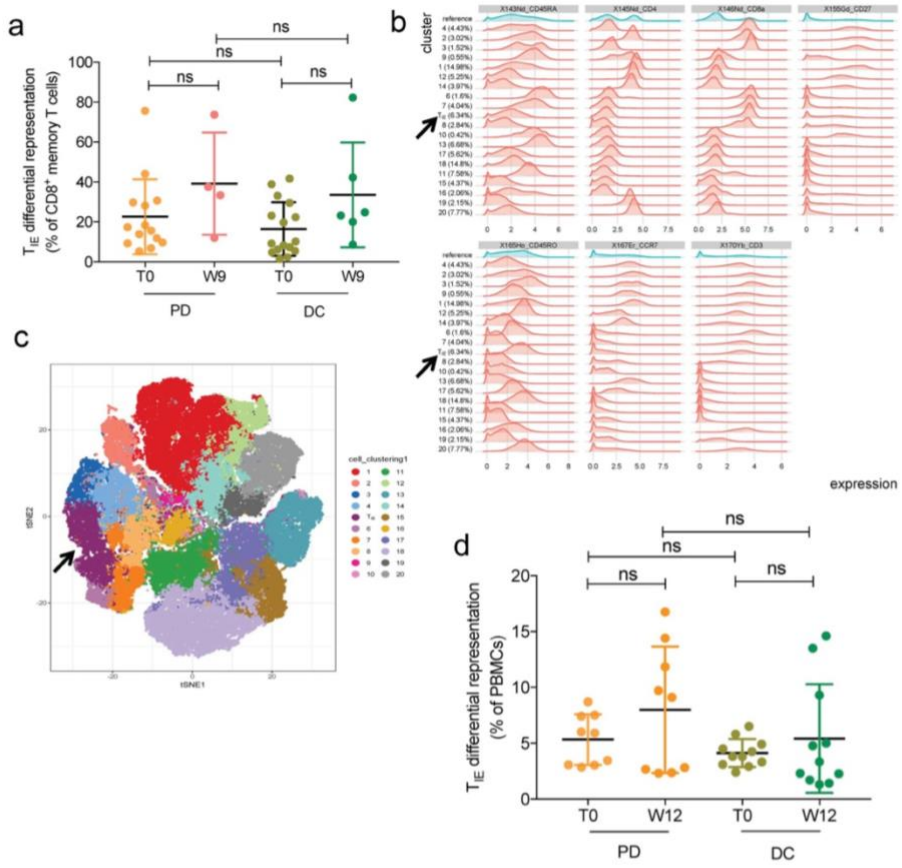

Extended Data Fig. 4 | Identification of T_{IE} in CPI-treated patient PBMC. a Comparison of differential abundance of T_{IE} in $CD8^+$ memory T cells in the PBMC of The Christie NHS Foundation Trust patients with best response progressive disease (PD, orange, n=14) and disease control (DC, green, n=16) at T0 (n=30, light shade) and week 9 (W9; n=10, dark shade; PD, n=4, DC, n=6). Differences over time were not significant for PD (median=15.2 and 35.5; P=0.375; two-sided Wilcoxon test) or DC (median=7.9 and 24; P=0.219; two-sided Wilcoxon test); PD vs DC patient values did not differ at T0 (P=0.275; two-sided Mann-Whitney U test) or W9 (P=0.762; two-sided Mann-Whitney U test). **b** Distributions of marker intensities of the T cell surface markers in the 20 cell populations (clusters) for PBMC from a published cohort[1] (n=20 patients). Cluster 5 was identified as the T_{IE} subset. Blue densities are calculated over all the cells and serve as a reference and red densities represent marker expression for cells in a given cluster. Arrows highlight the T_{IE} subset. **c** T-stochastic neighbor embedding of single cell profiles (dots) performed in an external cohort[1] using the T cell surface markers CD3, CD4, CD8, CD45RA, CD45RO, CCR7 and CD27; different colors are attributed by clustering. Arrow highlights the T_{IE} subset. **d** Comparison of the differential abundance of the T_{IE} cluster in the PBMC from a published cohort[1] of patients with PD (orange, n=9) or DC (green, n=11) at pre-treatment (light shade, n=20; PD, n=9; DC, n=11) and at week 12 (W12, dark shade, n=20) on treatment with pembrolizumab or nivolumab in the external cohort. Horizontal bars indicate the differences over time for the PD (median at T0=5.9 and W12=9.1; P=0.164; two-sided Wilcoxon test) or DC patients (median at T0=3.8 and W12=3.3; P=0.831; two-sided Wilcoxon test), and difference in the two response groups at T0 or W12 (P=0.37 and P=0.201, respectively; two-sided Mann-Whitney U test). Light and dark orange indicate PD for T0 and W9-W12, respectively, light and dark green indicate DC for T0 and W9-W12, respectively; n represents patients; ns means not significant P values; error bars are standard deviation.

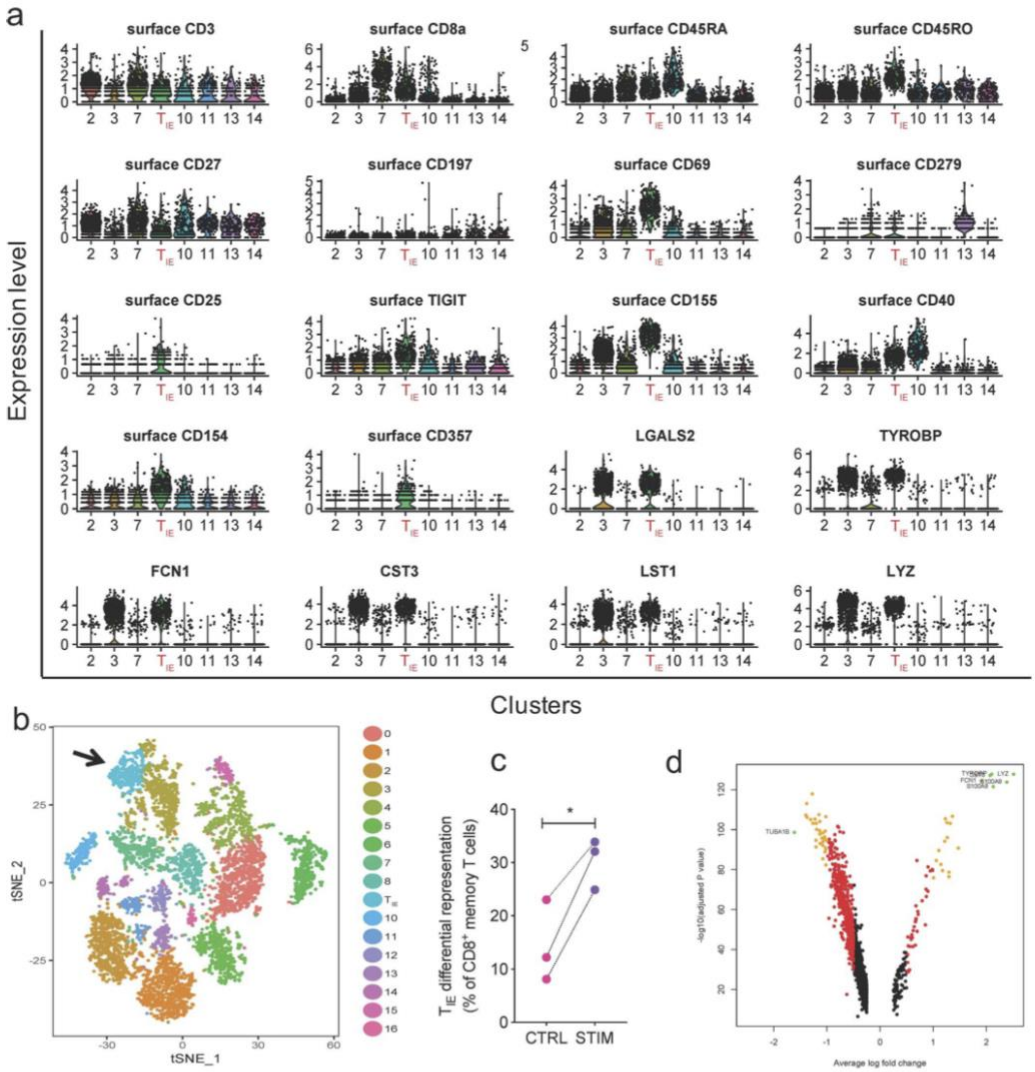

Extended Data Fig. 5 | Characterization of T_{IE} in PBMC. Analysis of published cohort of PBMC single cell data from reference #27. **a** Violin plots of the expression level of selected phenotypic and transcriptomic features of the clusters identifying peripheral T cell subsets (n=7488 single cells), the cluster with T_{IE} phenotype is indicated in red; the plots represent the density probability, the area shapes reflect the data distribution; horizontal lines represent the minima and maxima values; central dots represent the medians. Overall minima, mean and maxima values: surface CD3=0, 0.3785, 4.1396; surface CD8a=0, 0.96327, 6.21476; surface CD45RA=0, 0.8161, 4.8508; surface CD45RO=0, 0.6628, 4.6468; surface CD197/CCR7=0, 0.8961, 5.7975; surface CD69=0, 0.5219, 4.2200; surface CD279=0, 0.09787, 3.84886; surface CD25=0, 0.08653, 4.00428; surface TIGIT=0, 0.4663, 4.2381; surface CD155=0, 0.4850, 4.6679; surface CD40=0, 0.6003, 5.5083; surface CD154=0, 0.4062, 3.8159; surface CD357=0, 0.1193, 4.0316; LGALS2=0, 0.561, 6.089; TYROBP=0, 1.337, 6.662; FCN1=0, 1.290, 6.789; CST3=0, 1.404, 6.504; LST1=0, 1.042, 6.097; LYZ=0, 1.775, 6.859. **b** T-SNE plot showing the clusters identified by means of the antibody derived tags (ADT) targeted to surface markers (n=7488 single cells); the black arrow indicates the cluster with T_{IE} phenotype. **c** Plot showing the proportion of cells with the T_{IE} phenotype from the same published cohort after standard *in vitro* culture (CTRL, n=3 sorted healthy donor peripheral blood $CD8^+$ naïve T cell samples in standard culture) or following stimulation with anti-CD3/anti-CD27 Dynabeads[23] (STIM, n=3 sorted healthy donor peripheral blood $CD8^+$ naïve T cell samples after stimulation) (P=0.0267, two-sided paired t test, two degrees of freedom) and **d** Volcano plot representing the transcriptomic differential expression of the cells with the T_{IE} phenotype in PBMC presented in **a** (n=7488 single cells) or expanded from naive $CD8^+$ T cells from the experiment presented in **c**[22] (n=12217 single cells; two-sided Wilcoxon test with Bonferroni correction for multiple comparisons).

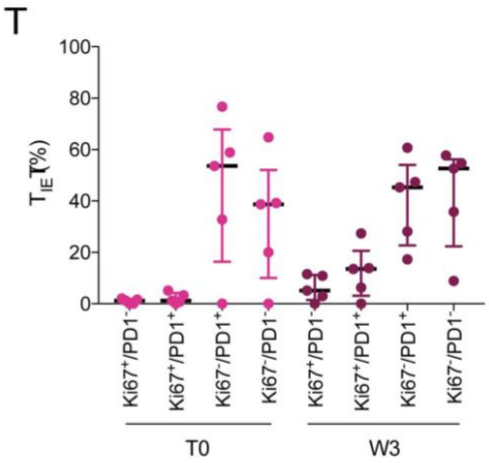

Extended Data Fig. 6 | Expression of Ki-67 and PD-1 in peripheral T_{IE} cells before and after 1 cycle of CPI. a Expression of Ki67 and PD1 in the T_{IE} subset as measured by FACS in n=5 frozen samples of PBMC from The Christie NHS Foundation Trust metastatic melanoma patients treated with CPI, at pre-treatment (T0) and after 1 cycle of CPI (W3); horizontal line indicates median; error bar indicates standard deviation. The small sample size did not allow statistical comparison of the outcome groups.

Appendix C: European Journal of Cancer Publication

European Journal of Cancer 162 (2022) 11–21

Available online at www.sciencedirect.com

ScienceDirect

journal homepage: www.ejcancer.com

Original Research

T cell immune awakening in response to immunotherapy is age-dependent

Zena Salih [a,b], Antonia Banyard [c], Joshua Tweedy [a], Elena Galvani [a], Philippa Middlehurst [d], Sarah Mills [d], John Weightman [e], Avinash Gupta [b], Paul C. Lorigan [b,f], Cong Zhou [g], Nathalie Dhomen [a], Sara Valpione [a,b,1], Richard Marais [a,*,1]

[a] *Molecular Oncology Group, Cancer Research UK Manchester Institute, The University of Manchester, Alderley Park, Macclesfield, Cheshire SK10 4TG, United Kingdom*
[b] *The Christie NHS Foundation Trust, 550 Wilmslow Road, Manchester M20 4BX, United Kingdom*
[c] *Flow Cytometry, Cancer Research UK Manchester Institute, the University of Manchester, Alderley Park, Macclesfield, Cheshire SK10 4TG, United Kingdom*
[d] *Manchester Cancer Research Centre Biobank, The Christie NHS Foundation Trust, 550 Wilmslow Road, Manchester M20 4BX, United Kingdom*
[e] *Molecular Biology Core Facility, Cancer Research UK Manchester Institute, the University of Manchester, Alderley Park, Macclesfield, Cheshire SK10 4TG, United Kingdom*
[f] *Division of Cancer Sciences, The University of Manchester, Oxford Road, Manchester M13 9PL, United Kingdom*
[g] *Cancer Biomarker Centre, Cancer Research UK Manchester Institute, The University of Manchester, Alderley Park, Macclesfield, Cheshire SK10 4TG, United Kingdom*

Received 10 August 2021; received in revised form 29 October 2021; accepted 8 November 2021
Available online 21 December 2021

KEYWORDS
Immunotherapy;
Immune-checkpoint blockade;
Age;
Melanoma;
T cell receptor;
T cell

Abstract ***Background:*** Precision immuno-oncology approaches are needed to improve cancer care. We recently demonstrated that in patients with metastatic melanoma, an increase of clonality or diversity of the T cell receptor (TCR) repertoire of peripheral T cells following one cycle of immunotherapy is coincident with response to immune-checkpoint blockade (ICB). We also identified a subset of peripheral $CD8^+$ immune-effector memory T cells (T_{IE} cells) whose expansion was associated with response to ICB and increased overall survival. To improve our understanding of peripheral T cell dynamics, we examined the clinical correlates associated with these immune signatures.
Methods: Fifty patients with metastatic melanoma treated with first-line anti-PD-1 ICB were included. We analysed TCR repertoire and peripheral T_{IE} cell dynamics by age before

* *Corresponding author*: Molecular Oncology Group, CRUK Manchester Institute, The University of Manchester Alderley Park, Macclesfield, Cheshire SK10 4TG, United Kingdom.
E-mail address: richard.marais@cruk.manchester.ac.uk (R. Marais).
[1] Contributed equally.

https://doi.org/10.1016/j.ejca.2021.11.015

treatment (T0) and after the first cycle of treatment at week 3 (W3).
Results: We observed a correlation between T_{IE} abundance and age at T0 ($r = 0.40$), which reduced following treatment at W3 ($r = 0.07$). However, at W3, we observed two significantly opposing patterns ($p = 0.03$) of TCR repertoire rearrangement in patients who responded to treatment, with patients ≥70 years of age showing an increase in TCR clonality and patients <70 years of age showing an increase in TCR diversity.
Conclusions: We demonstrate that immunotherapy-induced immune-awakening patterns in patients with melanoma are age-related and may impact patient response to ICB, and thus have implications for biomarker development and planning of personalised therapeutic strategies.

1. Introduction

To facilitate the identification of new therapeutic strategies and personalised treatments for patients with melanoma, we need to understand the biological mechanisms that underpin why some patients benefit from immune-checkpoint blockade (ICB) therapies, whereas others do not. Ideally, therapy decisions are based on patient-specific cancer or immunological biomarkers, but many factors are known to influence how patients respond to ICB (stage, lactate dehydrogenase [LDH] level, organ system involved). Furthermore, age-related thymic atrophy reduces naïve T cell output, which could affect T cell diversity and cause age-related immunodepression, leading to different patterns of response to ICB [1–5]. Thus, to deliver effective precision immune-oncology, a variety of clinical variables need to be considered for clinical decision making.

We recently analysed peripheral blood from patients with melanoma before treatment and after the first cycle of ICB [6]. We reported that patients who went on to respond to ICB therapy presented an increase either in the clonality or diversity of the T cell receptors (TCRs) on their circulating T cells. Patients who failed to respond to treatment did not develop this dichotomised response in their TCR. We also reported that after their first cycle of treatment, patients who responded to ICB presented an expansion of a subset of peripheral $CD8^+$ memory T cells that were characterised as $CD27^-$/$CCR7^-$, bore the characteristics of cytotoxic T cells and are known to infiltrate tumours. Because this T cell subset was associated with response to ICB therapy, we called them T immune effector or T_{IE} cells.

Here, we examined the clinical characteristics in patients with melanoma treated with first-line anti-PD-1 ICB. We observed age-related effects on TCR repertoire evolution and T_{IE} cell expansion that are consistent with age-related changes that occur in the human immune system. Our data show that age influences T cell awakening by ICB therapy and, therefore, that age must be incorporated into the development of biomarkers to monitor responses to immunotherapy.

2. Patients and methods

Patient samples. Blood samples from patients and healthy donors were collected under the Manchester Cancer Research Centre (MCRC) Biobank ethics application #07/H1003/161+5, ethics code 18/NW/0092, with written informed consent from the patients at The Christie NHS Foundation Trust. The study was approved by MCRC Biobank Access Committee application 13_RIMA_01. All clinical investigations were conducted according to the principles expressed in the Declaration of Helsinki and good clinical practice guidelines. In the present study, we re-analysed the data from our previously reported cohort [6], which included a total of 50 patients with metastatic melanoma, treated with either single-agent pembrolizumab or combination nivolumab plus ipilimumab as first-line therapy. Inclusion criteria included treatment naïve, inoperable locally advanced or metastatic melanoma. Patients were excluded if they had received any systemic oncological treatment in the neoadjuvant, adjuvant or metastatic setting for melanoma or other cancers, concomitant therapy with immunosuppressant drugs at enrolment or had synchronous other active malignancies. As a surrogate measure of tumour burden, the sum of target lesions on baseline and week 12 (W12) radiographic CT scans were calculated using RECIST 1.1. Measurements were available for 36 patients; the different number of patients included in the sub-studies reflects the availability of detailed target metastatic lesion measurements in the scan reports.

2.1. Peripheral T cell, T cell receptor and cell-free DNA analysis

Data from our previously reported cohort [6] were analysed. Sample collection and processing were performed

as previously described [6]. TCR sequence data were retrieved for 29 (peripheral blood mononuclear cell, PBMC) and 28 (cell-free DNA, cfDNA) of the 50 patients.

2.2. Statistical analyses

Correlation between continuous variables was performed with the Spearman test; the Spearman r was reported as a measure of the correlation magnitude. Linear discriminant analysis was used to separate the Δ_{W3} Renyi index and Δ_{W3} Gini coefficient and categorise the values in classes as indicated in the Fig. 3 legend. Mann–Whitney U test (two-sided) was used for comparison between continuous variables. Comparison between categorical variables was performed with Fisher's exact test. All tests were two-sided, and p-values <0.05 were considered significant. Analyses were performed using Prism version 7.0.

3. Results

3.1. Patient cohort

We recruited 50 predominantly male (32 male, 18 female) patients with treatment-naïve metastatic melanoma attending The Christie Hospital NHS Foundation Trust for first-line immunotherapy [6]. Just over half of the patients (54%) had stage M1c disease, 16% of patients (8/50) had baseline LDH > ULN (upper limit normal), the median age was 70 years (range: 35–85), and 68% of patients (34/50) were *BRAF*-wild type (Table 1). The number of metastatic sites ranged from 1 to 7, and of the 27 patients with stage M1c or M1d disease (Table 1), 15 patients had hepatic metastases, 2 patients in combination with cerebral metastases. Patients received first-line single-agent anti-PD1 drugs (200 mg pembrolizumab 3 weekly, or 480 mg nivolumab 4 weekly, 29 patients) or combination anti-PD1 plus anti-CTLA4 (1 mg/kg nivolumab plus 3 mg/kg ipilimumab 3 weekly for 4 doses, followed by 3 mg/kg nivolumab 2 weekly; 21 patients) as per standard of care. Assessment of tumour response was performed by computed tomography (CT) scans at week 12 (W12).

Table 1
Clinical characteristics of the patient cohort. The table summarises the clinical characteristics of the patient cohort. LDH = lactate dehydrogenase, RECIST = radiologic evaluation criteria for solid tumours; W12 RECIST 1.1 = CT scan lesion measurements of metastatic sites at week 12 from treatment start. * The different number of patients included in the sub-study reflects the availability of detailed target metastatic lesion measurements in the scan reports.

Clinical variable	Number (%)	Median (range)	Total number of patients evaluated
Gender			50
Male	32 (64%)		
Female	18 (36%)		
Stage			50
IIIC – M1a	10 (20%)		
M1b	13 (26%)		
M1c – M1d	27 (54%)		
BRAF V600E/K			50
Mutated	16 (32%)		
Wild type	34 (68%)		
Age (years)		70 (35–85)	50
Baseline LDH (IU/L)		371 (165–2987)	50
<ULN	42 (84%)		
>ULN	8 (16%)		
Treatment			50
Single agent αPD1	29 (58%)		
Combination αPD1 + αCTLA4	21 (42%)		
Sum of RECIST 1.1 marker lesion diameters at Baseline (cm)		4.9 (1.1–21.5)	37*
Sum of RECIST 1.1 marker lesion diameters at W12 (cm)		4.5 (0–31.1)	36*
Number of organ sites with metastases		2 (1–7)	39*

3.2. Patient response to ICB correlates with an expansion in peripheral T_{IE} cells

First, we used flow cytometry to quantify the percentage of T_{IE} cells in the patients' circulating cytotoxic memory T cells from PBMC [6] before treatment (T0) and after one cycle of ICB at week 3 (W3). From this, we calculated the change in T_{IE} abundance at W3 compared with T0 ($W3[T_{IE}]-T0[T_{IE}] = \Delta_{W3}T_{IE}$). As a surrogate of tumour burden, we calculated the sum of the measured target RECIST lesions from the patients' scans at T0 (T0[RECIST]) and week 12 (W12[RECIST]) and then calculated the change at W12 compared with T0 (W12 [RECIST]–T0[RECIST] = Δ_{W12} RECIST) [7, 8]. Notably, patients with a Δ_{W12}RECIST of ≤ 0 (tumour shrinkage) had a mean $\Delta_{W3}T_{IE}$ of 9.57% (range: −2.55–50.62%), whereas patients with a Δ_{W12}RECIST of >0 (tumour growth) had a mean $\Delta_{W3}T_{IE}$ of 0.4% (range: −17.5–20.2%) (Fig. 1A), indicating a negative correlation between T_{IE} cell subset expansion and tumour burden changes (r = −0.35).

To evaluate T cell turnover (death), we determined the TCR rearrangement efficiency score (RES) in cfDNA from the patients' blood. The RES measures the proportion of functional TCR sequences as a product of all TCR sequences, and we recently demonstrated that the change in cfDNA TCR RES at W3 compared with T0 (W3[RES]–T0[RES] = Δ_{W3} RES) is a surrogate for T cell turnover [6]. We show here that patients with an average Δ_{W3}RES of 0.02 (−0.16–0.17) had a Δ_{W12}RECIST > 0, whereas patients with an average Δ_{W3}RES of

0.1 (−0.15–0.30) had a Δ_{W12} RECIST ≤ 0 (Fig. 1B), indicating a negative correlation between peripheral T cell turnover and changes in tumour size (r = −0.50).

Thus, we extend our previous observations by showing that the magnitude of the peripheral T_{IE} cell expansion and the magnitude of T cell turnover at W3 are both inversely proportional to the change in tumour burden at W12 (r = −0.35, r = −0.50, respectively) (Fig. 1A and B).

3.3. T cell kinetics in response to ICB are not affected by age

We next investigated how other clinical factors affected T_{IE} cell expansion and T cell turnover by comparing T_{IE} cell abundance and TCR RES at T0 and W3 across established clinical parameters. We did not find significant association between T_{IE} cell abundance at T0 or W3, or TCR RES at T0 or W3, and gender (p = 0.76, p = 0.93, p = 0.49, p = 0.75), American Joint Committee on Cancer [AJCC] 8th edition stage of disease (p = 0.07, p = 0.09, p = 0.81, p = 0.80), BRAF V600E/K mutation status (p = 0.68, p = 0.1, p = 0.92, p = 0.19), or LDH (p = 0.65, p = 0.27, p = 0.29, p = 0.91) (Table 2). We were, however, intrigued to find an apparent association between treatment group and both T_{IE} cell abundance at T0 (p = 0.02) and TCR RES at W3 (p = 0.01) (Table 2) because connected to this was a significant selection bias of preferential allocation of combined therapy to younger (mean age 58 years; range: 35–79) and single-agent therapy to older patients (mean age 73 years; range: 51–85) (p < 0.0001; Supplementary Fig. 1).

Using the accepted geriatric oncology definition for the elderly population of 70 years of age [9], we show that at T0, the mean T_{IE} cell abundance was 11.2% (range: 1.2%–33.1%) of the circulating CD8+ memory in patients of 69 years and less but 22% (range: 2.54%–75.6%) in patients who were 70 years and older (Fig. 2A). Thus, as a proportion of the memory T cell pool, the T_{IE} cell subset increased with age (r = 0.4), consistent with our observed association between treatment group and T_{IE} cells abundance at T0 (Table 2). At W3, we observed a similar pattern, with a mean T_{IE} cell abundance of 21% (range: 3.47%–79.2%) of the circulating CD8+ memory T cells in patients of 69 years and less and 24% (range: 0.23%–73.4%) in patients of 70 years and older (Fig. 2A). Consistent with an increase in T_{IE} cell abundance associated with clinical response to immunotherapy [6], across all ages, we observe an upward shift of the regression line at W3 compared with T0 (Fig. 2A).

We also show that at T0, the mean RES was 0.62 (range: 0.47–0.74) in patients of 69 years and less, and 0.62 (range: 0.38–0.84) in patients of 70 years and older, while at W3, the mean RES was 0.71 (range: 0.58–0.80) in patients of 69 years and less, but 0.65 (range: 0.51–0.84) in patients of 70 years and older (Fig. 2B). Again, consistent with an increase in RES in responding patients [6] at all ages, we observe an upward shift of the line of regression at W3 compared with T0. Although the inverse relationship between RES and age appears to be rather weak (r = −0.12 to −0.32), the slight increase in correlation between RES and age after treatment is consistent with the observed association between treatment protocol and TCR RES at W3 (Table 2).

3.4. TCR repertoire evolution in response to ICB is affected by age

We next examined if peripheral T cell TCR repertoire rearrangements in response to ICB therapy, another feature of immune awakening [6], was affected by established patient and tumour factors. We reconstructed PBMC TCR sequences using ImmunoSeq and applied our algorithm [6] to calculate clonality (Gini coefficient) and diversity (Renyi index). We did not find an association between Gini coefficient, at T0 and W3,

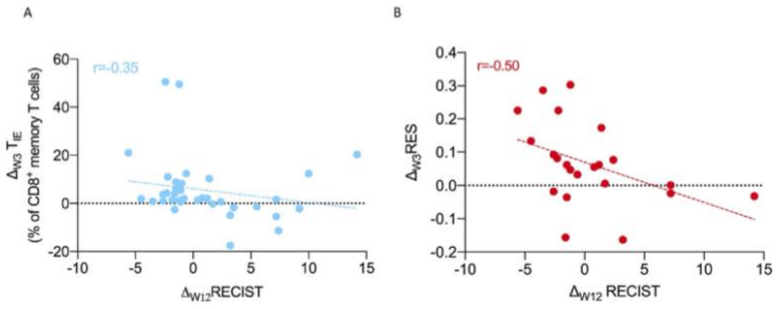

Fig. 1. **Correlation between radiological response and peripheral biomarkers**. **A**: Correlation (r = −0.35) between Δ_{W12}RECIST and $\Delta_{W3}T_{IE}$ in the melanoma patient cohort (n = 36). **B**: Correlation (r = −0.50) between Δ_{W3}RES and Δ_{W12}RECIST in the melanoma patient cohort (n = 22 patients with both measurements available). Data points represent individual patients. Dotted line: linear regression line.

Table 2
Patient cohort clinical variables and their correlation with peripheral T_{IE} cells and RES at T0 and W3. The table summarises the values of T immune effector (T_{IE}) cell percental abundance in the peripheral $CD8^+$ memory T cells and rearrangement efficiency score (RES) in cell-free DNA before treatment (T0) and after 3 weeks on treatment (W3) across the clinical factors. αPD1 = anti-PD1 therapy (pembrolizumab or nivolumab); αCTLA4 = anti-CTLA4 therapy (ipilimumab); ULN = upper limit normal; n = number of patients (total number = 50 for the T_{IE} analyses and 28 for RES analyses due to sample availability); p is Mann–Whitney U test two-sided p or non-parametric Analysis of Variance, values in brackets indicate the variable value range.

	Gender			BRAF V600E/K			Stage				Baseline LDH			Treatment		
	Female n = 18	Male n = 32	p value	Mutant n = 16	wild type n = 34	p value	IIIC/M1a n = 10	M1b n = 13	M1c/d n = 27	p value	<ULN N = 42	>ULN n = 8	p value	αPD1 n = 21	αPD1 + αCTLA4 n = 29	p value
T0 T_{IE} mean (range)	15.19 (1.2–41.7)	17.53 (1.48–75.6)	0.76	16.37 (2.38–39.8)	16.84 (1.2–75.6)	0.68	9.06 (1.2–33.1)	24.58 (2.38–75.6)	15.72 (2.54–44)	0.07	16.94 (1.2–75.6)	15.36 (2.54–44)	0.65	20.83 (2.54–75.6)	10.97 (1.2–38.1)	0.02
W3 T_{IE} mean (range)	21.83 (3.58–79.2)	23.06 (1.2–73.4)	0.93	27.71 (8.97–69.3)	20.22 (1.2–79.2)	0.10	13.75 (4.52–30.1)	33.61 (4.37–79.2)	20.60 (1.2–69.3)	0.09	22.55 (3.58–79.2)	19.68 (0.23–69.3)	0.27	23.30 (1.2–73.4)	21.67 (4.37–79.2)	0.30
	Female n = 11	**Male n = 17**	**P value**	**Mutant n = 7**	**Wild type n = 21**	**p value**	**IIIC/M1a n = 5**	**M1b n = 7**	**M1c/d n = 16**	**p value**	**<ULN n = 23**	**>ULN n = 5**	**p value**	**αPD1 n = 19**	**αPD1 + αCTLA4 n = 9**	**p value**
T0 RES mean (range)	0.61 (0.47–0.71)	0.64 (0.38–0.84)	0.49	0.63 (0.47–0.77)	0.62 (0.38–0.84)	0.92	0.64 (0.51–0.71)	0.65 (0.53–0.78)	0.62 (0.38–0.85)	0.81	0.64 (0.39–0.84)	0.57 (0.48–0.71)	0.29	0.61 (0.38–0.84)	0.65 (0.47–0.84)	0.53
W3 RES mean (range)	0.70 (0.51–0.80)	0.68 (0.52–0.85)	0.75	0.73 (0.58–0.80)	0.67 (0.51–0.84)	0.19	0.68 (0.53–0.77)	0.67 (0.51–0.78)	0.69 (0.52–0.84)	0.80	0.69 (0.51–0.85)	0.66 (0.55–0.80)	0.91	0.65 (0.51–0.85)	0.75 (0.61–0.82)	0.01

Table 3
Patient cohort clinical variables and their correlation with peripheral TCR repertoire at T0 and W3. The table summarises the value of peripheral T cell clonality (Gini coefficient) and diversity (Renyi index) before treatment (T0) and after 3 weeks (W3) on treatment across the clinical factors. αPD1 = anti-PD1 therapy (pembrolizumab or nivolumab); αCTLA4 = anti-CTLA4 therapy (ipilimumab); ULN = upper limit normal; n = number of patients; p is Mann–Whitney U test two-sided p or non-parametric analysis of variance; values in brackets are the variable range.

	Gender			BRAF V600E/K			Stage				Baseline LDH			Treatment		
	Female n = 10	Male n = 19	p value	Mutant n = 7	wild type n = 22	p value	III/M1a n = 6	M1b n = 7	M1c/d n = 16	p value	<ULN n = 24	>ULN n = 5	p value	αPD1 n = 19	αPD1 + αCTLA4 n = 10	p value
T0 clonality mean (range)	0.37 (0.13–0.73)	0.30 (0.11–0.61)	0.21	0.32 (0.16–0.55)	0.32 (0.11–0.73)	0.82	0.30 (0.17–0.44)	0.35 (0.19–0.61)	0.32 (0.11–0.73)	0.63	0.33 (0.12–0.74)	0.29 (0.14–0.61)	0.52	0.37 (0.13–0.73)	0.23 (0.11–0.38)	0.03
W3 clonality mean (range)	0.35 (0.12–0.78)	0.30 (0.09–0.60)	0.38	0.33 (0.20–0.60)	0.31 (0.09–0.78)	0.57	0.25 (0.16–0.35)	0.35 (0.16–0.60)	0.33 (0.09–0.78)	0.78	0.33 (0.10–0.79)	0.31 (0.15–0.60)	0.89	0.37 (0.12–0.78)	0.22 (0.09–0.33)	0.05
T0 diversity mean (range)	7.82 (4.98–9.16)	8.17 (4.82–9.73)	0.27	7.93 (4.82–9.25)	8.09 (4.98–9.73)	0.90	8.25 (7.09–9.15)	8.12 (5.78–9.29	7.95 (4.82–9.73)	0.99	8.07 (4.83–9.74)	7.99 (6.23–9.06)	0.76	7.70 (4.82–9.25)	8.72 (7.81–9.73)	0.05
W3 diversity mean (range)	7.92 (4.84–9.06)	8.20 (5.48–9.72)	0.38	8.11 (5.48–9.31)	8.11 (5.48–9.31)	0.94	8.49 (7.42–9.06)	8.17 (5.92–9.35)	7.93 (4.84–9.72)	0.72	8.12 (4.84–9.72)	8.08 (6.47–8.86)	0.72	7.75 (4.84–9.31)	8.79 (7.80–9.72)	0.03

or Renyi index, at T0 and W3 and gender ($p = 0.21$, $p = 0.38$, $p = 0.27$, $p = 0.38$), AJCC stage of disease ($p = 0.63$, $p = 0.78$, $p = 0.99$, $p = 0.72$), BRAF V600E/K mutation status ($p = 0.82$, $p = 0.57$, $p = 0.90$, $p = 0.94$) or LDH levels ($p = 0.52$, $p = 0.89$, $p = 0.76$, $p = 0.72$) (Table 3).

We did however observe an association between treatment protocol and Gini coefficient at T0 ($p = 0.03$) and W3 ($p = 0.05$) and between treatment protocol and Renyi index at T0 ($p = 0.05$) and W3 ($p = 0.03$) (Table 3). Noting the age-dependent selection bias for treatment protocol, we examined if age impacted clonality and diversity. We show that at T0, the Gini coefficient mean was 0.26 (range: 0.13–0.44) for patients 69 years and less and 0.38 (range: 0.11–0.73) for patients of 70 years and older (Fig. 2C). At W3, the mean Gini coefficients were 0.24 (range: 0.14–0.38) for patients 69 years and less and 0.39 (range: 0.09–0.78) for patients of 70 years and older (Fig. 2C). Thus, TCR clonality showed an overall positive correlation with age ($r = 0.36$ and $r = 0.39$ at T0 and W3, respectively), but unlike T_{IE} abundance and TCR RES, the linear regression line did not shift up or down with ICB treatment but changed in slope, suggesting a trend towards increased clonality in older patients on ICB therapy (Fig. 2C).

At T0, the mean Renyi index was 8.49 (range: 7.09–9.29) for patients of 69 years and less and 7.64 (range: 4.82–9.73) in patients of 70 years and older (Fig. 2D). At W3, the mean Renyi index was 8.62 (range: 7.42–9.35) in patients 69 years and less and 7.63 (range: 4.84–9.72) in patients of 70 years and older (Fig. 2D). Thus, TCR diversity showed an inverse relationship with age ($r = -0.29$ and $r = -0.39$ at T0 and W3, respectively) and, as was observed with clonality, the linear regression line did not shift up or down with ICB treatment but changed in slope, suggesting a trend towards increased diversity in younger patients on ICB treatment (Fig. 2D).

Since our data show that peripheral T_{IE} cell expansion and TCR repertoire rearrangements were both influenced by age, we compared these variables to each other. At T0, the mean T_{IE} cell abundance was 17%, so using this as a cut-off, we show that patients with a T_{IE} cell abundance $\leq$17% had a mean TCR Gini coefficient of 0.29 (range: 0.11–0.73), whereas patients with a T_{IE} cell abundance >17% had a mean TCR Gini coefficient of 0.37 (range: 0.14–0.61) (Supplementary Fig. 2A). Conversely, patients with a T_{IE} cell abundance $\leq$17% had a mean Renyi index of 8.35 (range: 4.97–9.25), whereas patients with a T_{IE} cell abundance >17% had a mean Renyi index of 7.63 (range: 4.82–9.05)

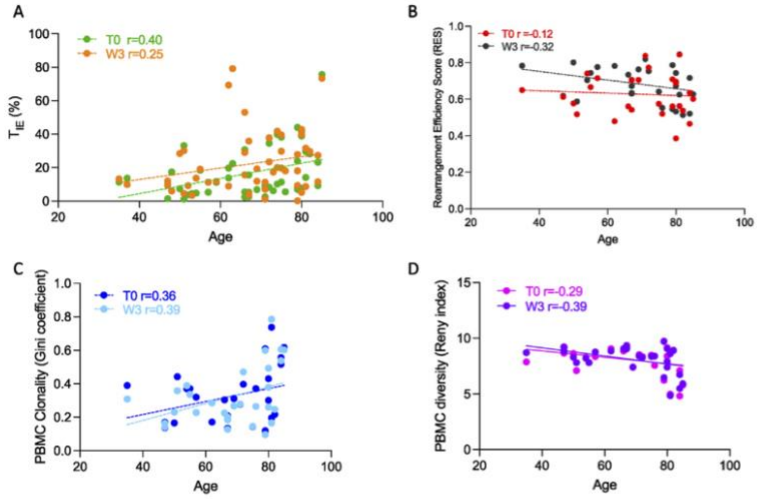

Fig. 2. **Correlation between age and peripheral T cell biomarkers**. **A**: Correlation between age (years) and T_{IE} cell abundance at baseline (T0, green, $r = 0.40$; $n = 50$) and after first cycle of immunotherapy (W3, amber, $r = 0.25$; $n = 50$). **B**: Correlation between age (years) and TCR receptor rearrangement efficiency score (RES) at baseline (T0, red, $r = -0.12$; $n = 28$) and after the first cycle of immunotherapy (W3, black, $r = -0.32$; $n = 28$). **C**: Correlation between age (years) and PBMC clonality (Gini coefficient) at baseline (T0, navy, $r = 0.36$; $n = 29$), and after the first cycle of immunotherapy (W3, light blue, $r = 0.39$; $n = 29$). **D**: Correlation between age (years) and PBMC T cell receptor diversity (Renyi index) at baseline (T0, pink, $r = -0.29$; $n = 29$) and after first cycle of immunotherapy (W3, purple, $r = -0.39$; $n = 29$). T_{IE}, immune-effector T cells; PBMC, peripheral blood mononuclear cell.

(Supplementary Fig. 2A). After one cycle of ICB treatment (W3), the mean T_{IE} cell abundance was 22%, so using this as a cut-off, we show that patients with a T_{IE} cell abundance ≤22% had a mean TCR Gini coefficient of 0.30 (range: 0.09–0.78), whereas patients with a T_{IE} cell abundance >22% had a mean TCR Gini coefficient of 0.34 (range: 0.14–0.60) (Supplementary Fig. 2B). Conversely, patients with a T_{IE} cell abundance ≤22% had a mean Renyi index of 8.23 (range: 4.84–9.72), whereas patients with a T_{IE} cell abundance >22% had a mean Renyi index of 7.93 (range: 5.48–9.31) (Supplementary Fig. 2B). Thus, both before and after one cycle of ICB treatment, there was a positive correlation between T_{IE} cell abundance and peripheral T cell TCR clonality ($r = 0.43$, $r = 0.19$, respectively), but an inverse correlation between T_{IE} cell abundance and peripheral T cell TCR diversity ($r = -0.42$, $r = -0.17$, respectively) (Supplementary Fig. 2A, B). Note however, that both relationships became weaker after one cycle of therapy because the T_{IE} cell population expanded in an inverse proportion to tumour burden changes (Fig. 1A).

We previously showed that treatment induces a bifurcated outcome in peripheral T cell TCR repertoire [6], so we compared how peripheral T cell clonality and diversity changed at W3 relative to T0 (W3–T0 [Gini] = Δ_{W3} Gini; W3–T0[Renyi] = Δ_{W3} Renyi). To separate the T cell TCR repertoire rearrangement at W3 according to evolution pattern (prevalence of increased clonality versus prevalence of increased diversity), we applied a linear classifier algorithm to segregate the changes of clonality and diversity at W3 into predominant clonal evolution (blue hemi-plot in Fig. 3A) or predominant diverse evolution (pink hemi-plot in Fig. 3A) for patients <70 years (purple dots in Fig. 3A) and ≥70 years (green dots in Fig. 3A). There are 5 patients <70 years and 12 patients ≥70 years who fell into the predominant clonal evolution plot, whereas 9 patients <70 years and 3 patients ≥70 years fell into the predominant diverse evolution plot (Fig. 3A). Thus, in patients <70 years of age, 5/14 had peripheral T cell TCR clonality dominance and 9/14 had peripheral T cell TCR diversity dominance (Fig. 3B), whereas in patients ≥70 years of age, 12/15 had peripheral T cell clonality dominance and 3/15 had peripheral T cell diversity dominance ($p = 0.03$, Fig. 3B). Thus, in response to ICB therapy, TCR rearrangements trend towards increased diversity in younger patients but increased clonality in older patients.

4. Discussion and conclusions

The role of age as a prognostic factor for melanoma is well described [10], but it is unclear if this is a consequence of distinct melanoma biology [11], different patterns of UV-induced DNA damage [12] or immunesenescence [13]. Notably, elderly patients often display greater benefit from ICB than younger patients [14, 15], and although the mechanisms underlying this observation are unclear [14], this could be due to selection bias caused by fitter patients with less advanced disease within the elderly cohort being offered ICB preferentially [15]. Taken together, these observations suggest that age plays an important role in the interactions between melanoma, the immune system and immunotherapy and are consistent with our findings

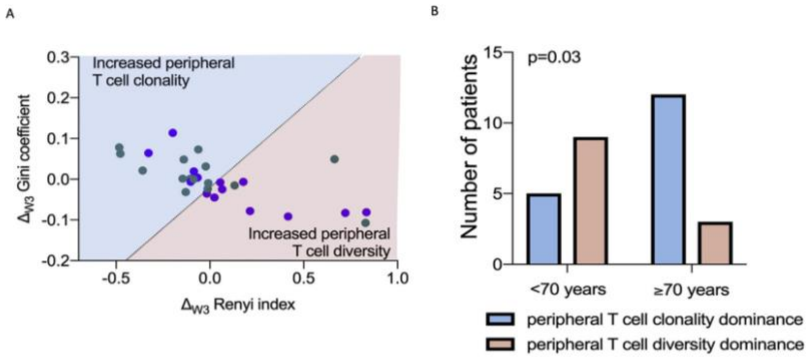

Fig. 3. **Relationship between age and peripheral T cell TCR repertoire re-arrangement**. **A**: Scatter plot showing changes in peripheral TCR clonality (Gini coefficient) and diversity (Renyi index) after one cycle of anti-PD1-based treatment (W3 compared T0: Δ_{W3}) for patients in the age group <70 years (purple dots) and ≥70 years (green dots). The dotted line represents the linear discriminant (X0 = 0.024, slope = 0.4) for TCR re-arrangement with increased peripheral T cell clonality (hemiplot in blue) versus increased peripheral T cell diversity (hemiplot in pink). Each dot is a single patient (n = 29). **B**: Comparison of the number of patients with peripheral T cell rearrangement pattern towards dominant clonality (blue) or dominant diversity in (pink) from A, according to age group (n = 29; Fisher test p = 0.03). TCR, T cell receptor.

here that age affects immune-awakening in response to ICB.

We previously reported that changes in T_{IE} abundance and the RES after the first cycle of immunotherapy identify which patients will achieve disease control at W12 [6]. Here, we extend those findings by showing that in a cohort of 50 melanoma patients receiving ICB, changes in T_{IE} cell abundance inversely correlated with changes in tumour burden determined by RECIST target lesion size in patients' CT scans. This suggests that an increase in T_{IE} abundance 3 weeks after the start of ICB therapy predicts tumour shrinkage at the W12 assessment. Similarly, we show that peripheral T cell pools undergo dynamic turnover proportional to the magnitude of response confirming that the immune signature that we have previously described [6] is a reliable early biomarker of response to ICB.

We next demonstrate that although T_{IE} expansion and peripheral T cell turnover are biomarkers of immunotherapy response across all age groups, patients in different age groups present different patterns of peripheral T cell TCR repertoire evolution in response to ICB. Specifically, after one cycle of immunotherapy, in patients $\geq$70 years immunotherapy tends to a preferential increase in peripheral T cell TCR clonality, whereas in patients $<$70 years, it tends to a preferential increase in peripheral T cell TCR diversity. In addition, we show that T_{IE} cell abundance inversely correlates with peripheral TCR repertoire diversity and directly correlates with peripheral T cell repertoire clonality, consistent with repertoire convergence in patients with pre-existing T_{IE} expansion [6]. Moreover, this relationship became less apparent as T_{IE} expansion was boosted in patients benefitting from treatment, as we previously showed [6], irrespective of age.

Our data are consistent with the observation that age is associated with decreased thymic output [6–16]. Age-related regression of the thymus is accompanied by a decline in naïve T cell output, which is thought to contribute to the reduced T cell diversity in older individuals and is linked to increased susceptibility to infection, autoimmune disease and cancer [2]. Although widely accepted, this age-associated TCR repertoire constriction has not been widely studied using direct methodologies [1] and has not been analysed in patients with cancer treated on immunotherapy. While it is acknowledged that high TCR repertoire diversity is a prerequisite for an effective adaptive immune response against new antigens [17] and that age impacts cancer therapy responses [18], this is the first report of age-specific differential immune-awakening patterns induced by immunotherapy in patients with cancer. We posit that our findings reflect age-related thymic involution [19, 20] and a consequent reduction of new clonotype output [21] available to recognise and kill cancer cells [22].

We observed a significant difference in age between the two treatment groups, which likely reflects selection bias in the real-world clinical setting, as we observed that patients $\geq$70 years were preferentially assigned to single-agent therapy (Supplementary Fig. 1). This could affect the interpretation of the effect of treatment regimen on the biomarker dynamics, and the modest size of our cohort precludes the prospect of meaningful insight from any intra-group comparisons. However, the absence of any change from pre-treatment in the relationships between treatment regimen and the immune-biomarkers we measured after treatment initiation, suggests a negligible effect of drug schedule on the T cell biomarkers we studied in our cohort. Moreover, we saw no effect of the clinical variables of gender, stage, BRAF mutation and LDH status on T_{IE} cell expansion, T cell turnover or peripheral T cell TCR repertoire rearrangements. This supports the importance of T_{IE} cell expansion, T cell turnover and peripheral T cell TCR repertoire rearrangements as biomarkers of response to therapy. Note that the LDH assay was modified during the course of this study and a change in the upper limit of normal (ULN) cut off values affected 6 of our 50 patients, which could have influenced the relationship between LDH ULN and the T cell biomarkers we report. Although limited by a small sample size and the biological biases of an unselected population, together our results support a model whereby age does not affect peripheral T_{IE} subset expansion in response to ICB but does influence immunotherapy-induced peripheral TCR repertoire evolution.

Our findings need validation in larger, randomised cohorts that can differentiate responses in younger versus older patients, controlling for the other clinical variables, but they highlight the importance of considering age during the development of immunotherapy approaches and biomarker-led strategies. For example, TCR-based biomarkers need to consider how age affects TCR repertoire evolution following treatment and therapies that require more diverse T cell repertoires may be less effective in older patients. Critically, the inconsistent recruitment of older patients into clinical trials has led to the development of treatments largely in younger patients who typically have different biological and physiological responses [23, 24]. As our data highlight, future work should focus on ensuring the inclusion of patients $\geq$70 years of age in immunotherapy clinical trials and the reporting of age-group specific survival outcomes. Refinements in the design of preclinical and clinical trials are necessary to determine how ageing impacts the efficacy of different classes of immunotherapy. Finally, the hypothesis deriving from our results, that new clonotype thymic output reduces with age, potentially provides a biological explanation of the bifurcated reorganisation of

the TCR repertoire we have previously observed in response to immunotherapy [6].

Although our sample size is relatively small and our observations require further validation and qualification before these biomarkers could be introduced into clinical practice, our exploratory findings have potentially relevant implications for biomarker development and therapy planning. In particular, although T_{IE} cells may act as early prognostic biomarkers independent of patient age, TCR repertoire analysis must be contextualised by patient age. Moreover, therapeutic strategies that aim to boost peripheral T cell repertoire diversification to increase tumour neoantigen recognition are likely to be less effective in patients $\geq$70 years because successful new clonotype recruitment would be ineffective due to thymic involution.

Author contribution

Conceptualisation: SV and ZS. Data curation: ZS. Formal analysis: ZS, SV, JT, EG; Funding acquisition: RM, SV; Investigation: ZS, SV, JT, EG, PM, SM, JW, AG, PL, ND, RM; Methodology: ZS, SV, JT, EG, PM, SM, JW, AG, PL, CZ, ND, RM; Resources; Software; Supervision: ND, SV, RM; Writing – original draft: ZS, ND, SV, RM; Writing – review & editing: all authors.

Funding

This work was supported by the NIHR Manchester Biomedical Research Centre, CRUK (A27412 and A22902), the Harry J Lloyd Charitable Trust (Career Development Award for SV) and the Wellcome Trust (100282/Z/12/Z).

Conflict of interest statement

RM is an expert witness for Pfizer. RM may benefit from drug discovery programmes that are commercialized. PL serves as a paid advisor/speaker for Bristol-Myers Squibb, Merck Sharp and Dohme, Roche, Novartis, Amgen, Pierre Fabre, Nektar, Melagenix. PL reports travel support from Bristol-Myers Squibb and Merck Sharp and Dohme, and receives research support from Bristol-Myers Squibb. AG received honoraria and consultancy fees from BMS and Novartis. All remaining authors have declared no conflicts of interest.

Acknowledgements

The authors are grateful to the patients who participated to this study and to their families. We thank Dr. Patricio Serra-Bellver for his help in the collection of the patient samples, and Prof. Judi Allen and the Molecular Oncology Group for their advice. Research samples were obtained from the Manchester Cancer Research Centre (MCRC) Biobank, UK. The MCRC Biobank holds a generic ethics approval, which can confer this approval to users of banked samples via the MCRC Biobank Access Policy. The role of the MCRC Biobank is to distribute samples and, therefore, cannot endorse studies performed or the interpretation of results.

Appendix A. Supplementary data

Supplementary data to this article can be found online at https://doi.org/10.1016/j.ejca.2021.11.015.

References

[1] Britanova OV, Putintseva EV, Shugay M, Merzlyak EM, Turchaninova MA, Staroverov DB, et al. Age-related decrease in TCR repertoire diversity measured with deep and normalized sequence profiling. J Immunol 2014;192:2689–98. https://doi.org/10.4049/jimmunol.1302064.

[2] Palmer DB. The effect of age on thymic function. Front Immunol 2013;4:1–6. https://doi.org/10.3389/fimmu.2013.00316.

[3] Fuentes E, Fuentes M, Alarcón M, Palomo I. Immune system dysfunction in the elderly. An Acad Bras Cienc 2017;89:285–99. https://doi.org/10.1590/0001-3765201720160487.

[4] Thomas-vaslin V, Six A, Pham H, Dansokho C, Chaara W, Gouritin B, et al. Immunodepression and immunosuppression during aging. Suman Kapur and Maristela Barbosa Portela. Immunosuppression role in health and diseases. Intech 2012: 125–46. https://doi.org/10.5772/29549.hal-01637377.

[5] Zhang X, Meng X, Chen Y, Leng SX, Zhang H. The biology of aging and cancer: frailty, inflammation, and immunity. Cancer J 2017;23:201–5. https://doi.org/10.1097/PPO.0000000000000270.

[6] Valpione S, Galvani E, Tweedy J, Mundra PA, Banyard A, Middlehurst P, et al. Immune awakening revealed by peripheral T cell dynamics after one cycle of immunotherapy. Nat Cancer 2020;1:210–21. https://doi.org/10.1038/s43018-019-0022-x.

[7] Prasad SR, Saini S. Radiological evaluation of oncologic treatment response: current update. Cancer Imag 2003;3:93–5. https://doi.org/10.1102/1470-7330.2003.0013.

[8] Gangadhar TC, Savitch SL, Yee SS, Xu W, Alexander C, Harmon S, et al. Feasibility of monitoring advanced melanoma patients using cell-free DNA from plasma. Pigment Cell Melanoma Res 2019;31:73–81. https://doi.org/10.1111/pcmr.12623.Feasibility.

[9] Owusu C, Berger NA. Comprehensive geriatric assessment in the older cancer patient: coming of age in clinical cancer care. Clin Pract 2014;11:749–62. https://doi.org/10.2217/cpr.14.72.

[10] Valpione S, Mundra PA, Galvani E, Campana LG, Lorigan P, Rosa F De, et al. The T cell receptor repertoire of tumor infiltrating T cells is predictive and prognostic for cancer survival. Nat Commun 2021;12:4098. https://doi.org/10.1038/s41467-021-24343-x. n.d.

[11] Bauer J, Büttner P, Murali R, Okamoto I, Nicholas A. BRAF mutations in cutaneous melanoma are independently associated with age, anatomic site of the primary tumor and the degree of solar elastosis at the primary tumor site. Pigment Cell Melanoma Res 2011;24:345–51. https://doi.org/10.1111/j.1755-148X.2011.00837.x.BRAF.

[12] Trucco LD, Mundra PA, Hogan K, Garcia-Martinez P, Viros A, Mandal AK, et al. Ultraviolet radiation–induced DNA damage is prognostic for outcome in melanoma. Nat Med 2018;1. https://doi.org/10.1038/s41591-018-0265-6.

[13] Hematol J, Lian J, Yue Y, Yu W, Zhang Y. Immunosenescence : a key player in cancer development. J Hematol Oncol 2020:1–18. https://doi.org/10.1186/s13045-020-00986-z.

[14] Kugel CH, Douglass SM, Webster MR, Kaur A, Liu Q, Yin X, et al. Age correlates with response to anti-PD1, reflecting age related differences in intratumoral effector and regulatory T cell populations. Clin Cancer Res 2019;24:5347–56. https://doi.org/10.1158/1078-0432.CCR-18-1116.Age.
[15] Jain V, Hwang W-T, Venigalla S, Nead KT, Lukens JN, Mitchell TC, et al. Association of age with Ef fi cacy of immunotherapy in metastatic melanoma. Oncologist 2020;25:2. https://doi.org/10.1634/theoncologist.2019-0377.
[16] Falci C, Gianesin K, Sergi G, Giunco S, De Ronch I, Valpione S, et al. Immune senescence and cancer in elderly patients: results from an exploratory study. EXG 2013;48:1436–42. https://doi.org/10.1016/j.exger.2013.09.011.
[17] Nikolich-Žugich J, Slifka MK, Messaoudi I. The many important facets of T-cell repertoire diversity. Nat Rev Immunol 2004;4:123–32. https://doi.org/10.1038/nri1292.
[18] Shah S, Boucai L. Effect of age on response to therapy and Mortality in patients with thyroid cancer at high risk of recurrence. J Clin Endocrinol Metab 2018;103:689–97. https://doi.org/10.1210/jc.2017-02255.
[19] Mitchell WA, Lang PO, Aspinall R. Tracing thymic output in older individuals. Clin Exp Immunol 2010;161:497–503. https://doi.org/10.1111/j.1365-2249.2010.04209.x.
[20] Daste A, Domblides C, Gross-goupil M, Chakiba C, Quivy A, Cochin V, et al. Immune checkpoint inhibitors and elderly people: a review. Eur J Cancer 2017;82:155–66. https://doi.org/10.1016/j.ejca.2017.05.044.
[21] Qi Q, Zhang DW, Weyand CM, Goronzy JJ. Mechanisms shaping the naïve T cell repertoire in the elderly — thymic involution or peripheral homeostatic proliferation? Exp Gerontol 2014:71–4. https://doi.org/10.1016/j.exger.2014.01.005.
[22] He Q, Jiang X, Zhou X, Weng J. Targeting cancers through TCR-peptide/MHC interactions. J Hematol Oncol 2019;12:1–17. https://doi.org/10.1186/s13045-019-0812-8.
[23] Hurez V, Padrón S, Svatek RS, Curiel TJ. Considerations for successful cancer immunotherapy in aged hosts. Clin Exp Immunol 2017;187:53–63. https://doi.org/10.1111/cei.12875.
[24] Hamilton JAG, Henry CJ. Aging and immunotherapies: new horizons for the golden ages. Aging and Cancer 2020;1:30–44. https://doi.org/10.1002/AAC2.12014.

Supplementary Fig. 1

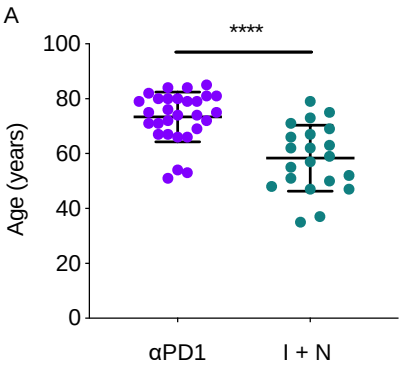

Supplementary Fig. 2A & 2B

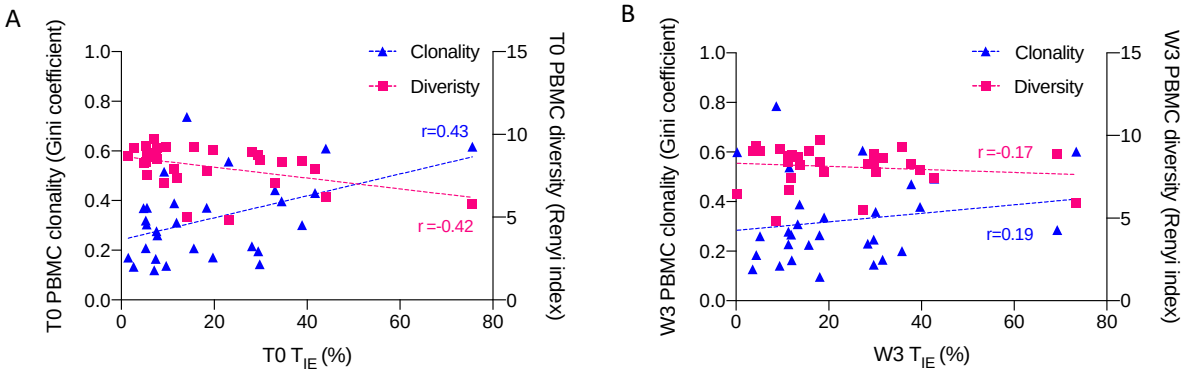

Appendix D: Early stage melanoma project study protocol

Project Plan

Project Long Title:

Personalising Immunotherapy in Early Stage Melanoma

Author	Owner
Zena Salih	Nicola Overton

A record of all approvers, revision history and active date is maintained within Q-Pulse and can be accessed from the document record.

1. Project Details

Project Type	Method Development ☐ Method Validation ☐ Equipment Evaluation ☐ Other ☒ Specify: Research
Validation Level (If Applicable)	Proof of principle ☐ Fit for purpose ☐ Fully Qualified ☐ 3º Endpoint ☐ 2º Endpoint ☐ 1º Endpoint ☐
Biomarker or Equipment to be assessed	Peripheral blood biomarkers: TCR sequencing, CyTOF, and ctDNA. Tumour microenvironment biomarkers TCR sequencing (TIL) and tumour gene expression.
Introduction	The incidence of stage III melanoma is significantly higher than stage IV disease, resulting in a higher overall burden of mortality. Though surgical excision is the mainstay of treatment and this approach can be curative, approximately half of patients will suffer loco-regional recurrence or distant relapse with metastatic disease. Recent practice changing studies have shown that adjuvant immunotherapy is likely to have a positive impact on overall survival, reducing the recurrence rate by destroying minimal residual disease (MRD). However, there are no established biomarkers to predict likelihood of recurrence or response to therapy. As the risk of relapse varies greatly, the development of tools that can identify patients at high risk of recurrence and those that will benefit from further treatment post-operatively remains a considerable challenge. Standard methods of predicting risk of relapse are not very precise and the approval of adjuvant therapy has resulted in over-treatment of some patients. Treating all patients with expensive and potentially toxic treatment is not in every patient's best interest nor is it the most economical approach. Therefore, it is imperative to identify and treat efficiently high-risk stage III patients. The main question underlying this project is: can we identify stage III melanoma patients with MRD after primary tumour resection that will benefit from adjuvant therapy. This also involves segregating this group of patients from those who don't have MRD and those who have MRD but will not respond to adjuvant immunotherapy.
Introduction (continued)	We hypothesise that this patient segregation can be achieved using an integrated approach, combining primary tumour analysis with liquid biopsies at early stages of adjuvant treatment (e.g. up to week 12 of treatment). Therefore, we seek to assess whether tumour molecular features (tumour gene expression profile, ctDNA) can be used in tandem with the assessment of the patient immune response to predict clinical outcome in stage III melanoma patients treated with adjuvant immunotherapy.

Project Objectives	More specifically these are the aims of the project: 1. To identify whether in addition to ctDNA, there are changes in circulating biomarkers such as T_{IE} cells and TCR repertoire, early on adjuvant treatment that can be used to predict patient response to therapy. 2. To identify tumour-associated biomarkers predictive of response to adjuvant immunotherapy in stage III melanoma. 3. To investigate whether circulating biomarkers predictive of response (1) correlate with tumour biomarkers (2) and whether this can be used to predict clinical outcome
Brief Overview of Equipment	Equipment to be used will include that required for the following methods: • Targeted NGS panel of known melanoma mutations • CyTOF • Illumina MiSeq • DETECTION assay (ctDNA by ddPCR) • Potentially CODEX platform and Nanostring on FFPE tissue • RNA sequencing of fresh tumour

Brief Overview of Methods	1. Number of patients to recruit: 160: o Approx. 100 will not proceed to immunotherapy. Baseline (pre-op) blood samples will be collected from these patients, but samples from later time points will not be collected. PBMCs will be stored from these patients and potentially used as controls – but still need surface labelling for cyTOF as this must be done prior to freezing PBMCs. o We expect 7 patients per month to commence adjuvant CPI (anti-PD1 Pembro) (approx. 60 patients during the length of the project). These patients will have blood samples collected at all time points 2. Blood sampling: pre-op and during first 5 cycles of CPI o 6 time points for sampling: Pre-op, Cycle 1 (C1, usually Week 0), Cycle 2 (C2, usually Week 3), Cycle 3 (C3, usually Week 6), Cycle 4 (C4, usually Week 9), Cycle 5 (C5, usually Week 12) o Follow up: 3 monthly blood sampling to monitor MRD with ctDNA (up to 24 months) 3. Blood samples will be used as follows:: o To monitor MRD using ctDNA (ddPCR for $BRAF^{V600}$, $NRAS^{G12,Q61}$ and TERT promoter) o To monitor immune cell populations identified using cyTOF (T cell focussed antibody panel of 36 markers) o For TCR sequencing. This will be performed on RNA extracted from PBMCs (Qiagen Immune repertoire RNA library) to assess TCR repertoire changes on treatment. 4. Primary excision FFPE tumour blocks: o Requested retrospectively from local hospital (via Christie pathology dept) o Used to determine baseline mutation status to confirm if trackable mutation in circulation for ctDNA monitoring o This will be done using a targeted NGS mutation panel 5. Tumour tissue collected prospectively during the study will be used to: o Assess TCR repertoire, using RNA from fresh tumour and correlate the TCR sequences with those identified in circulation. o Assess differential gene expression of tumour cells between patients in order to correlate this information with clinical outcome (are there specific genes/pathways associated with response to therapy? – single cell RNAseq) o Assess immune cell infiltrates using immune fluorescence on fixed tissue (CODEX platform).

2. Timelines and Personnel

Projected start date	01 January 2020
Projected end date	30 September 2022
Project Deadline Date (Date work MUST be completed by to facilitate other work or sample analysis)	N/A
Project Manager	Nicola Overton
Deputy Project Manager	Zena Salih
Analyst(s)	Any trained analyst
QA Representative	N/A. This is a research project; therefore QA input is not required.

3. Related Documents

RSPs will be generated for:

- PBMC isolation
- RNA extraction/quantification
- CyTOF antibody surface labelling
- DETECTION ddPCR assay ctDNA isolation/quantification
- Miltenyi Biotec Gentle MACS tumour dissociation protocol
- Generation of TCR sequencing libraries / quantification

4. Samples Used During Study

If clinical samples from other projects have been used as part of this project, please list the project codes and title under which the samples were collected. Please ensure both consent and ethics are in place for the work to be conducted, and appropriate permission is granted. Evidence of permission to use the samples should be retained.

Project Code	Project Title
CEP-0274	Healthy normal volunteer

5. Kits, Reagents and consumables

- EDTA tubes
- STREK tubes
- Miltenyi Biotec Gentle MACS columns
- CyTOF antibodies and reagents (Helios PBS needed for PBMC processing)
- Reagents for PBMC processing
- Qiagen RNeasy kits
- Reagents for TCR library prep and analysis

6. Detailed Experimental Plan

HNV blood:

HNV blood will be used to assess the performance of SepMate and Leucosep tubes and for other method development work that may be required in order to develop a method of PBMC and RNA extraction for use in CyTOF and TCR sequencing experiments.

Patient Blood: Pre-op, Cycle 1 (C1, usually Week 0), Cycle 2 (C2, usually Week 3), Cycle 3 (C3, usually Week 6), Cycle 4 (C4, usually Week 9), Cycle 5 (C5, usually Week 12 time points):

60ml i.e. 6 tubes (2 EDTA and 4 STREK) will be collected from each patient at each time point

- 2 EDTA blood tubes will be processed in real time to isolate PBMCs using Sepmate tubes

- PBMCs will then be quantified and separated into aliquots:
    - One aliquot will be used to isolate/quantify RNA which will then be frozen for future TCR sequencing/library prep
    - One aliquot will require surface antibody labelling and then once labelled to be frozen in CSM/DMSO and stored for future cyTOF.
    - Additional aliquots may be stored in liquid nitrogen for future use

- 4 STREK tubes (40ml blood) will be used for future ctDNA analysis using the ddPCR DETECTION assay (plasma will be processed to double spun plasma at The Christie and stored in biobank until requested to be transferred to CEP at Alderley Park for future cfDNA isolation and quantification).

Patient Blood (3 monthly follow up time points - up to 24 months, therefore up to 8 follow ups per patient):

40ml i.e. 4 tubes (STREK) will be collected from each patient at each time point

- 4 STREK tubes (40ml blood) will be used for future ctDNA analysis using the ddPCR DETECTION assay (plasma will be processed to double spun plasma at The Christie and stored in biobank until requested to be transferred to CEP at Alderley Park for future cfDNA isolation and quantification).

Tumour:

- Fresh tumour tissue will be enzymatically digested to a single cell suspension in the MolOnc lab. Single cell suspensions will be transferred to the CEP lab, logged into LIMS and stored. Immune infiltrates will be assessed using TCR sequencing. Tumour cell gene expression will be assessed using bulk RNA sequencing. Samples will also be snap frozen in the MolOnc lab. These frozen tumour samples will be transferred to CEP, logged into LIMS and stored.

- FFPE tumour will be requested at a later date to assess immune infiltrates using immunofluorescence CODEX platform and/or targeted sequencing of tumour cells using Nanostring to validate data generated from fresh tissue analysis. Currently, the exact sample type is unknown as discussions with pathologists are ongoing.

7. Performance Criteria

Applicable ☐ Not Applicable ☒

If Applicable, list the criteria to be met in order to progress to additional phases of work or to consider an assay fit-for-purpose. This could include comparison to current laboratory standard procedures, or a set of performance requirements that must be met, as detailed in current policies or SOPs.

Appendix 1: Project Summary

Visit Name*	Alternative Visit ID 1*	Alternative Visit ID 2*
Pre-op	Pre-op	Pre-op
C1	Cycle 1	Week 0
C2	Cycle 2	Week 3
C3	Cycle 3	Week 6
C4	Cycle 4	Week 9
C5	Cycle 5	Week 12
FU1	Follow up 1	3 Month
FU2	Follow up 2	6 Month
FU3	Follow up 3	9 Month
FU4	Follow up 4	12 Month
FU5	Follow up 5	15 Month
FU6	Follow up 6	18 Month
FU7	Follow up 7	21 Month
FU8	Follow up 8	24 Month

Name of site*	Country	City	Site identifier code* *(if available)*
The Christie	UK	Manchester	

What is the patient identifier?*	Patient will be given a unique patient identifier allocated by the Biobank team.
External Identifier* (if applicable)	N/A

Sample storage Instructions (if applicable)	Store samples in locations listed here: \\filestore-01\Clinical_and_Experimental_Pharmacology\Operations\Resourcing and Requests\Allocated Freezer Space for Projects.xlsx

Sample processing Information	Samples can be logged by any trained GCP analyst, then passed to the appropriate analysts for processing and storage as detailed below.
	
	2x 10ml EDTA (PBMC extraction)
	
	• Processing should begin within **4 hours** of blood draw. If the sample arrives outside of this window process immediately and notify the PM as soon as possible.
	• Combine all of the EDTA tubes (create composite sample in LIMS), and then process to PBMCs and create child samples.
	• Follow RSP-50 and include the optional RBC lysis step.
	• Create aliquots of the PBMCs as follows:
	  • Aliquot 1: $4x10^6$ cells for RNA extraction
	  • Aliquot 2: $5\ x10^6$ cells for CyTOF (if required – confirm with PM/DPM prior to creating this aliquot)
	  • Aliquots 3 & 4: two equal aliquots of the remaining PBMCs, for freezing
	• Freeze aliquots 3 & 4 at -80oC overnight according to RSP-50. Transfer to liquid nitrogen within 7 days (location above)
	• Pass aliquot 2 to Zena Salih for surface staining and storage (location above). If Zena is unavailable, an alternative trained analyst may complete this staining if they are available. However, if no trained analyst is available, this staining will not be completed.
	• Extract RNA from aliquot 1 (follow RSP-82), and store extracted RNA (location above).
	
	Plasma samples (store)
	• Store plasma samples (location above)
	
	Dissociated tumour cells (store):
	• Store dissociated tumour cells samples (location above)
	
	Frozen tumour (store):
	• Store frozen tumour samples (location above)
	
	FFPE tumour tissue (store):
	• Store FFPE tumour samples (location above)

* N.B. Entry format needs to be consistent with that used in LIMS.